In-vitro and In-vivo spectrometric investigations on the behavior of lactate under conditions emulating septic shock

Nystha Baishya
Supervisor: Professor Panicos Kyriacou
Research Centre for Biomedical Engineering

This dissertation is submitted for the degree of
Doctor of Philosophy

City, University of London
September 2020

Dedicated to all the healthcare professionals involved in the COVID-19 pandemic.

Abstract

Lactate is an inter- and intra-cellular product in the human body. In patients with life threatening illnesses, the secretion and excretion of lactate is impaired, which might cause the pH of blood to shift to be either acidic or basic. Lactic acidosis can be regarded as a useful biomarker for the onset of haemodynamic shock in patients. Lactate concentration levels are measured and monitored frequently in critical care by utilizing invasive blood sampling techniques. Such techniques, apart from their invasive nature, which is not desirable, are intermittent, time consuming and do not allow the continuous monitoring of lactate. Hence, there is a need for new innovative approaches in research which could lead to the development of non-invasive and continuous monitoring technologies for lactate. The motivation of this research is to explore rigorously the capability and potential of absorption spectroscopy as a technique which could enable the development of non-invasive lactate sensors.

The focus of the research lies in unravelling the basic light-lactate molecular interactions in different media, both *in-vitro* and *in-vivo*, utilizing a wide range of spectrometers. The research investigated lactate "signature peaks" in solution samples, including different concentrations of lactate, in various media (buffer, human serum and whole blood) across the UltraViolet (UV), Visible (Vis), Near Infrared (NIR) and Mid Infrared (MIR) parts of the EM. The results have shown that lactate has limited presence in the UV and Vis parts of the EM spectrum. For the first time, 'signature peaks' for lactate in the NIR and MIR spectral regions have been identified, suggesting that these spectral regions could be used for lactate concentration predictions with 90 % accuracy. More uniquely, it has been shown that these 'signature peaks' for lactate in the NIR spectral region are influenced by the change in physiological conditions and media; these are therefore, not consistent. Nevertheless, in the 'fingerprint region' of the MIR spectral region, these 'signature peaks' for lactate are not only consistent but they could be used inter changeably for different physiological conditions and media for lactate concentration prediction. The results from this suggests that the 'fingerprint region' of the MIR spectral region is most preferred for lactate concentration determination *in-vitro*, for accuracy needed in critical care.

Despite being the most preferred spectral region, the major disadvantage of MIR is the penetration depth and hence, it might not be suitable for *in-vivo* lactate measurements in blood through skin. Therefore, a pilot *in-vivo* study utilizing, a portable NIR spectrometer was conducted in order to evaluate the feasibility of measuring lactate concentrations in this region. The results from this study have shown for the first time that the NIR region could be suitable for measuring lactate concentrations using Absorption/Reflectance portable Spectroscopy accurately and non-invasively. The output from this research could pave the way for the development of optical sensing point-of-care technologies for the continuous and non-invasive monitoring of lactate in critical care.

Table of contents

List of figures

List of tables

Nomenclature

Chemical Symbols

H_2O_2	Hydrogen Peroxide
Ag	Silver
AgCl	Silver Chloride
Au	Gold
C	Carbon
H	Hydrogen
InGaAs	Indium Gallium Arsenide
M	Molar
Na	Sodium
O	Oxygen
PbS	Lead Sulphide
Pt	Platinum

Greek Symbols

ε	Extinction Coefficient of the substance
δ_s	Symmetrical In-Plane Bending
δ_{as}	Asymmetrical In-Plane Bending
ε_r	Permittivity
γ_s	Symmetrical Out-of-Plane Bending
γ_{as}	Asymmetrical Out-of-Plane Bending
λ	Wavelength

λ	Wavelength
μ	Reduced Mass
ν	Frequency
ν_s	Symmetrical Stretching
ν_{as}	Asymmetrical Stretching
σ	Conductivity
υ_r	Quantum number of vibrational mode r
ε	Molar Absorbance of an analyte at an excitation wavelength
ϕ	Luminescence Quantum Yield
E_ν	Discrete Energy Levels

List of Abbreviations

(SmO_2)	Muscle Oxygen Saturation
$(V_{O_{2max}})$	Maximum Oxygen Consumption
$[HbO_2]$	Oxyhemoglobin concentration
I_0	Intensity of reference light beam
[C]	Concentration of the desired analyte
[HbR]	Deoxyhemoglobin concentration
[HbT]	Total Hemoglobin concentration
A	Absorbance
ABG	Arterial Blood Gas
AG	Anion Gap
ATP	Adinosine Tri Phosphate
BE	Base Excess
BGA	Blood Gas Analyser
c	Molar Concentration of the solutions
CHF	Congestive Heart Failure

CI	Cardiac Index
CME	Chemically Modified Electrode
DOF	Degree of Freedom
DPF	Differential Path Length factor
EM	Electro Magnetic
EMP	Emben Meyerhof Parnas
FT-NIR	Fourier Transform Near-Infrared
GI	Gastro-Intestinal
HOMO	Highest Occupied Molecular Orbital
I	Intensity of sample light beam
ICU	Intensive Care Unit
ISE	Ion-Selective Electrode
IUPAC	International Union of Pure and Applied Chemistry
L	Luminescence Intensity
l	Path Length of light through the solution
LDH	Lactate Dehydrogenase
LED	Light Emitting Diode
LOD	Lactate Oxidase
LUMO	Lowest Unoccupied Molecular Orbital
MCT	Monocarboxylate Transporter
MIR	Mid Infrared
NADH	Nicotinamide Adenine Dinucleotide
NIR	Near Infrared
PCR	Polymerase Chain Reaction
PMT	Photo Multiplier
POC	Point-of-Care

R	Reflectence
RBC	Red Blood Cells
SID_a	Strong Base Ions
SID_e	Weak Acid and Proteins
SIG	Strong Ion Gap
SNR	Signal-to-Noise Ratio
SvO_2	Mixed Venous Oxygen Saturation
SVR	Systemic Vascular Resistance
T	Transmittance
TCA	TriCarboxylic Acid
TOI	Tissue Oxygenation Index
UV	Ultra Violet
V	Potential Energy
v	velocity
WABS	Water Absorbance Bands
WAMACS	Water Matrix Absorbance Coordinates
WAPS	Water Absorbance Spectral Pattern

Physics Constants

c	Speed of light
h	Planck's constant

Statistical Abbreviations

2DCoS	2 Dimensional Correlation
a	slope
b	intercept
EMSC	Extended Multiplicative Scatter Correction
LV	Latent Variable

PLS	Partial Least Square
PRESS	Prediction Error Sum of Squares
R^2	Coefficient of Determination
RMSECV	Root Mean Squared Error of Cross Validation
SG	Savitzky-Golay
x	Explanatory Variable
y	Dependent Variable

List of publications

Journal Papers

- N. Baishya, M. Mamouei, K. Budidha, M. Qassem, P. Vadgama and P. A. Kyriacou, 2020, March. Near infrared spectrometric investigation of lactate in a varying pH buffer, *Journal of Near Infrared Spectroscopy*, Volume 28, Issue 5-6 doi:10.1177/0967033520905374.
- N. Baishya, M. Mamouei, K. Budidha, M. Qassem, P. Vadgama and P. A. Kyriacou, 2020, July. Investigations into the effects of pH on quantitative measurements of lactate in biological media using ATR-FTIR spectroscopy, *Molecules*, 25(16), 3695 doi:10.3390/molecules25163695.
- N. Baishya, M. Mamouei, K. Budidha, M. Qassem, P. Vadgama and P. A. Kyriacou, 2020, November. In-vitro Spectrometric analysis of hyperlactatemia and lactic acidosis in relation to Sepsis, *Journal of Near Infrared Spectroscopy*, doi:10.1177/0967033520968951 (available online).
- K. Budidha, M. Mamouei, N. Baishya, M. Qassem, P. Vadgama and P. A. Kyriacou, 2020, July Identification and quantitative determination of lactate using optical spectroscopy - Towards a non-invasive tool for early recognition of sepsis, *Sensors (Special Issue) Optical Sensors in Health and Wellbeing*, 20(18), 5402 doi:10.3390/s20185402.
- M. Mamouei, K. Budidha, N. Baishya, M. Qassem and P. A. Kyriacou, 2020, October. Comparison of wavelength selection methods for in-vitro estimation of lactate: A new unconstrained, genetic algorithm-based wavelength selection, *Scientific Reports*, 10(1), 16905, doi:10.1038/s41598-020-73406-4.
- N. Baishya, M. Mamouei, K. Budidha, M. Qassem, P. Vadgama and P. A. Kyriacou, 2020, October, Comparison of dual beam dispersive and FTNIR spectroscopy for lactate detection, *Spectrochimica Analytica Acta* (submitted for review).

Conference Proceedings

- N. Baishya, K. Budidha, M. Mamouei, M. Qassem, P. Vadgama and P. A. Kyriacou, 2019, July. Near Infrared Spectrometric Investigations on the behaviour of

Lactate. In 2019 41st Annual International Conference of the IEEE Engineering in Medicine and Biology Society (EMBC) (pp. 5769-5772). IEEE. doi:10.1109/EMBC.2019.8857833.

- N. Baishya, K. Budidha, M. Mamouei, M. Qassem, P. Vadgama and P. A. Kyriacou, 2020, July. Near Infrared and Aquaphotomic Analysis of Water Absorption in Lactate Containing Media. In 2020 42nd Annual International Conference of the IEEE Engineering in Medicine and Biology Society (EMBC) (pp. 4381-4384). IEEE. doi:10.1109/EMBC44109.2020.9176675.

- M. Mamouei, M. Qassem, K. Budidha, N. Baishya, P. Vadgama, and P. A. Kyriacou, 2019, July. Comparison of a Genetic Algorithm Variable Selection and Interval Partial Least Squares for quantitative analysis of lactate in PBS*. In 2019 41st Annual International Conference of the IEEE Engineering in Medicine and Biology Society (EMBC) (pp. 3239-3242). IEEE. doi:10.1109/EMBC.2019.8856765.

- K. Budidha, M. Mamouei, N. Baishya, P. Vadgama and P. A. Kyriacou, 2019, July. In vitro quantification of lactate in Phosphate Buffer Saline (PBS) samples. In 2019 41st Annual International Conference of the IEEE Engineering in Medicine and Biology Society (EMBC) (pp. 1205-1208). IEEE. doi:10.1109/EMBC.2019.8857756.

- M. Mamouei, K. Budidha, N. Baishya, M. Qassem, P. Vadgama, and P. A. Kyriacou, The Efficacy of Support Vector Machines in Modelling Deviations from the Beer-Lambert Law for Optical Measurement of Lactate. In 2020 42nd Annual International Conference of the IEEE Engineering in Medicine and Biology Society (EMBC) (pp. 4261-4264) IEEE. doi: 10.1109/EMBC44109.2020.9175215.

Abstracts

N. Baishya, M. Mamouei, K. Budidha, M. Qassem, P. Vadgama, and P. A. Kyriacou, Towards The Development Of A Non-Invasive Optical Lactate Sensor for Early Detection of Sepsis. In Federation of Analytical Chemistry and Spectroscopy Societies, SciX (Online), October 12-15, 2020.

Acknowledgments

THANK YOU LIFE FOR ENABLING ME TO MAKE ONE MORE EFFORT.

Thank you England, specially London, a land of subatomic explorations.

This research, I believe, was possible because of a few *'Mahatmas'* in the past: Sir Isaac Newton, who identified the rainbow spectrum; Arthur Schuster, who coined the term Spectroscopy; Werner Heisenberg, who laid the foundations of light-matter interactions; Albert Einstein, Niels Bohr and Wolfgang Pauli for the Copenhagen Interpretation of quantum theory; Louis de Broglie, wave-particle duality; Max Plank, quantisation of light; and many more.

Next in line, I would like to thank my *'Guru'* Professor Panicos Kyriacou, who forced me to be myself even on days I felt like it was not worth it. Also, Dr. Triantis for the long chats and inspiring stories.

My *maa* and *deuta* who made everything possible for me to achieve this. Kosta for pushing me to do better every time I got comfortable. My *in laws* for being a constant source of support and smiles. A special shout out to Nyrvan and Kunal for showing so much strength as frontline workers in the COVID-19 pandemic. It's for people like you that I got to feel safe and write this document.

I would also like to extend my heartfelt gratitude to everyone in the Research Centre for Biomedical Engineering, for being my family in London and for those endless discussions. As to quote Heisenberg "Science rests on experiments, but science is rooted in conversations."

This is one of the many experimental research in Light-Matter interactions, ever since the first documentation of Spectroscopy by Heinrich Kayser, in 1900s. I believe, a lot has changed ever since and I am sure science will evolve more in time. So, a special thanks to all the future scientists who will bring another revolution in Science and Technology.

"Imparare non stanca mai la mente, non rende timorosi e non crea rimpianti." - LEONARDO DA VINCI

Declaration

I hereby declare that the work presented in this thesis is my own work. Any idea, result, or illustration originating from other subject's work has been acknowledged in the text by referencing to the original author. This thesis has never been published or submitted elsewhere for obtaining an academic degree or professional qualification. This dissertation is my own work and contains nothing which is the outcome of work done in collaboration with others, except as specified in the text and Acknowledgements.

I grant power of discretion to the Librarian at City, University of London to allow the thesis to be copied in whole or in part without further reference. This permission covers only single copies made for study purposes, subject to normal conditions of acknowledgement.

Nystha Baishya
September 2020

1

Introduction

1.1 Motivation

Hyperlactatemia, (or an increase in blood lactate levels, greater than 4 mM) acts as a primary haemodynamic marker for clinicians in critical care environments to assess response to therapy and guide treatment[1]. Hyperlactatemia, together with lactic acidosis (imbalance in acid-base balance), serves as a strong indicator, conditions for clinicians to identify the onset of disease states; like, haemodynamic shock, specially septic shock or, simply, sepsis[2,3,4]. Hence, measurement of these two parameters (especially, lactate) has been given profound importance and has been an on-going research interest for several

decades.

Lactate has been linked with organ dysfunction and mortality; according to the UK Sepsis Trust report in 2020, more than 245, 000 people suffer from sepsis, resulting in 48, 000 deaths, each year[5]. There was a sudden spike in these numbers due to the recent, Coronavirus Disease 2019 (COVID-19) which caused a global pandemic, affecting over 21, 000, 000 people in more than 80 countries, with more than 770, 000 deaths, worldwide (as of 17 August, 2020)[6]. The Surviving Sepsis Campaign guidelines for the management of these patients mentions that serum lactate needs to be measured and if found to be $\geq 4\ m\mathcal{M}$, it needs to be monitored until stabilised[7].

Thus, measurements of blood lactate levels are crucial in critical care environments. At present, lactate measurements are carried out using medical devices that require a blood sample to perform each measurement. This procedure is traditionally invasive, time consuming and inhibits continuous monitoring of lactate. Moreover, sample type and sample handling can also affect lactate concentrations, significantly. There is a substantial demand for a sensor technology with simple and direct measurements, rapid response, high specificity, low cost and with minimal or no sample preparation to measure lactate.

Hence, lactate concentration measurement using Absorbance/ Reflectane Spectroscopy is proposed as an alternative to the traditional methods in this thesis. This method is believed to reduce sample preparation and provide rapid response, it could also be used directly and non-invasively through human skin and hence, could provide continuous measurement of lactate. Although this technology has been explored previously, the absence of a lactate sensor using this technology can be predominantly identified as a lack of a precise understanding of the basic light-lactate molecule interaction in the optical spectrum. Hence, the research in this thesis aims in understanding the basics of the light-lactate molecular interactions in the optical spectrum. Hypothetically, a non-

invasive lactate sensor could be possible because the lactate as a molecule is sensitive to UV and infrared light in the electromagnetic spectrum. Together with the appropriate computational analysis, this property can be potentially used to measure lactate concentrations by reflecting light over the skin, which can penetrate to the vascular layers. However, absorption and light scattering makes it difficult to estimate lactate over skin but by using a broader optical spectrum and advanced multivariate analysis techniques can lead to a step forward. Moreover, spectral features are also influenced by changes in physiological conditions. Hence, an extensive study of the optical properties of lactate using broad optical spectra in different physiological conditions and media is the motivation of this study.

1.2 Aims and Objectives

The primary aims of this study is to perform a comprehensive multivariate analysis of the optical spectra of lactate in different media, with increasing complexity. These are categorized step-wise into the following different tasks with regards to the complexity of the media, study protocol and environment:

- The first set of study would be *'in-vitro* solution stoichiometry study'; spectrometry in a controlled environment using different state-of-the-art instruments with known concentrations of lactate in Isotonic Phosphate Buffer, (PBS) in deionized water, Human Serum and Whole Blood in the Ultraviolet (UV), Visible (Vis), Near Infrared (NIR) and Mid Infrared (MIR) regions of the Electromagnetic Spectrum.
- The second part will be a *'in-vivo* exercise study', where healthy volunteers will be recruited for doing supervised strenuous exercise in the laboratory and the lactate levels in blood will be measured using fingerprick tests, along with spectra from a portable spectrometer. A comparison will be done based on the optical spectra from the non-invasive portable device and blood collected during the study.

The primary aims of this study are as follows:

- Analyze the lactate *profile* across the Electromagnetic Spectrum. The optical profiling of lactate will be rigorously investigated with a focus in identifying *'signature wavelengths'* for lactate in a buffer solution of pH 7.4. These 'signature wavelengths' of lactate are devoid of O-H absorption and are indicative of lactate concentration changes, which can be quantified
- These *'signature wavelengths'* for lactate will be further analysed in different buffers of pH 7, 6.5 and 6 to understand the effects on spectral features in the UV/Vis, NIR and MIR spectral regions, due to change in pH
- Additional analysis on these *'signature wavelengths'* for lactate would be performed by varying the media from buffer to human serum and then to whole blood, in order to understand the effects on spectral features due to change in media
- Lastly, a feasibility *in-vivo* study will be carried out, where a portable spectrometer would be identified and spectra would be obtained from healthy volunteers. *'Signature wavelengths'* for lactate would again be explored on these spectra based on outputs from all the previous *in-vitro* studies.

The secondary aims of this thesis are:

- The whole NIR spectral region needs to be analysed based on sub-divisions; with and without O-H Absorption. The overtones of the water peaks, in the NIR region need special attention and should be explored on the basis of the novel approach called 'Aquaphotomics'
- A range of different bench-top spectrometers are available for the NIR spectral region (in terms of technology and size) with the advancement of technology, which needs further exploration

- The MIR spectral region needs exploration when there is a change in pH and media for lactate concentration changes.

1.3 Contribution (Novelty)

The studies mentioned above should lead to the following contributions to science:

- Enlisting the *'signature wavelengths'* of lactate in the Ultraviolet (UV), Visible (Vis), Near Infrared (NIR) and Mid Infrared (MIR) regions of the Electromagnetic Spectrum at physiological pH using state-of-the-art spectrometers.
- Exploration of the spectral feature differences while changing pH for controlled *in-vitro* studies, again, in the UV/Vis, NIR and MIR spectral regions
- Aquaphotomics principles (which will be discussed in detail in Chapter 3) will be used to study the overtones of O-H in the NIR spectral region and a comparison will be drawn for different media
- NIR instrument validation
- MIR spectral region dependence on pH and media for precise lactate concentration determination for critical care
- use of a portable spectrometer for the intention of understanding the feasibility of lactate concentration determination.

The next section outlines the structure and contents of the thesis with brief introduction to the contents of the chapters.

1.4 Thesis Structure

The thesis was structured in the following chapters:

Chapter 2, introduces lactate as a molecule; its history of discovery, mechanism of production in the human body, pathology and then substantiates hyperlactatemia as a biomarker for haemodynamic shock. It also discusses the role of lactate in acidosis in the human body towards the end.

Chapter 3, puts forward basic principles of operation of UltraViolet (UV), Visible (Vis), Near Infrared (NIR) and Mid Infrared (MIR) Spectroscopy. It expatiates vibrational spectroscopy from the very early years to recent developments; the provenance of Absorption bands in spectroscopy and introduces the instruments which are used to obtain these bands for the purpose of this thesis. The chapter concludes by introducing a few chemometrics tools used for pre-treatment and processing of the spectral data to be used for all the studies in this thesis.

Chapter 4, reviews the current state-of-the-art technology for lactate measurements, specially electrochemical, optical and electromagnetic wave sensing techniques. It also introduces a few commercially available devices used in this thesis. In the end, it discusses the work carried out to date using Absorption Spectroscopy for lactate and pH detection.

Chapter 5 and 6, discusses the methods (sample preparation, spectroscopy and spectral analysis) and results obtained from the following data-sets:

- Δ Lactate concentrations, with constant pH of the Phosphate Buffer Solution (PBS) medium
- Δ pH of the PBS medium, with constant lactate concentrations
- Δ Lactate concentrations with Δ pH of the PBS medium.

These *in-vitro* studies will be accomplished using spectrometers for UV/Vis, NIR and MIR regions of the Electromagnetic Spectrum and mathematical tools, like 2D correlation analysis, Linear Regression, Aquaphotmics and Partial Least Squares (PLS)

regression. The range of lactate concentrations which will be investigated are: 0-5 millimoles/litre (mM) at an interval of 0.25 mM, for understanding the lactate levels in the critical care and 5-20 mM, for lactate levels during strenuous exercise. The pH range will be investigated from 6-8. Based on the results and conclusions from this study the next studies will be devised and designed.

Chapter 7 and 8, will again discuss similar *in-vitro* studies for solution samples, with lactate concentration differences, using Human Serum, followed by Whole Blood as the medium. The *'signature wavelengths'* of lactate found in the chapters above, will be investigated to understand the effects of change in media, using linear regression. These data-sets will be further investigated independently and then combined with the ones obtained in the previous chapters for comparison and prediction.

Chapter 9 will illustrate the results obtained from a pilot *in-vivo* study using a portable spectrometer. Healthy volunteers will be recruited for this study and with informed consent will undertake an incremental exercise test on a cycle ergometer. Blood samples using a fingerprick method will be taken prior to non-invasive spectra collection from the thumb. Both of these acquired values will be used to build and predict lactate concentration.

Chapter 10 and 11 will finally conclude the thesis by discussing the primary results from all the *in-vitro* and *in-vivo* studies, and suggest future work.

Organic Chemistry is a part of physiology that describes the composition of living bodies, together with the chemical processes that occur in them.

Jons Jacob Berzelius, first observer of lactic acid in living tissues

2

Lactate in the Human Body

2.1 Introduction

Blood lactate is a primary biomarker for the diagnosis of diseases. Studies in the literature have investigated lactate with various patient groups, including injured Intensive Care Unit (ICU) patients[8,9,10,11], surgical ICU patients[12,13,14,15], patients with severe sepsis[16,17,18,19], and patients after cardiac surgery[20,21,22,23], etc. Lactate has also been directly linked with organ dysfunction and mortality[24,25,26,27]. Lactate is produced in the human body by an enzyme called Lactate Dehydrogenase (LDH) which

reduces pyruvate, during anaerobic glycolysis. Almost all the organs in the body are capable of producing lactate, however lactate is predominantly produced by muscles and Red Blood Cells (RBCs), whereas the liver and kidneys acts as the disposal units. The formation and excretion of lactate in the body must be such that the lactate concentration levels in blood is maintained at almost less than 2 mM and thus, only 1,500 mM/day of lactate is favourably produced in a normal adult[28]. However, hypoperfusion and hypoxia (critically ill conditions) slows down the admission of pyruvate into the Krebs cycle, which in turn gets converted into lactate instead, thus, increasing the lactate levels in the bloodstream[29]. This rise in lactate levels is known as hyperlactatemia.

The aim of this chapter is to report the history, mechanism and pathology of lactate/ lactic acid in the human body, right from its production to consumption and establish lactate as a biomarker for haemodynamic shock.

2.2 History of Lactate

The presence of lactate was first found in sour milk by a German–speaking Swedish chemist, Karl Wilhelm Scheele in the year 1780 and then, another Swedish chemist Jons Jacob Berzelius found its presence in muscle tissues of hunted stags in 1807, marking a revolution in muscle physiology[30]. The structure of Lactic Acid, CH3CH(OH)COOH, was established in 1873 by Johannes Wislicenus as shown in Figure 2.1, is an acid at physiological pH, with a pKa of 3.8[31].

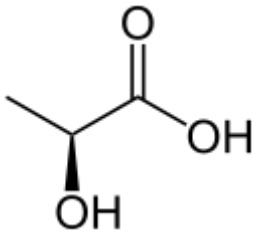

Figure 2.1: Lactic Acid (Chemical Formula).

This structure, helped identify lactate as an alpha-hydroxy acid (AHA), which is

classified as a carboxylic acid (C=O) substituted with a hydroxyl group (O-H) on the adjacent carbon. Thereafter, almost about 70 years later, a German physician-chemist Joseph Scherer indicated the presence of lactate in human blood, while investigating the blood drawn from 7 dead women due to puerperal fever (which can be identified now as septic shock)[32]. However, Carl Folwarczny, an Austrian physician, was the first to establish its presence in living beings[30] which lead Trasaburo Araki[33] and Hermann Zillessen[34], both in their independent research, to show that lactic acid can be linked to tissue hypoxia. Both concluded that lactic acid was produced when there was an irregular supply of oxygen to the muscles in mammals and birds[35]. However, in 1878, George Salomon found lactate in blood of people suffering from anaemia, congestive heart failure, pericarditis and neoplasia, which did not seem to be related to tissue hypoxia[30]. These were a few of the earliest instances reported on the presence of lactate/lactic acid. The next section describes in detail the mechanism of lactate production and consumption in the human body.

2.3 Mechanisms of Lactate in the human body

Once lactate was discovered by Berzelius in 1807, a lot of studies have been done hence, and in 1950 von Muralt identified four distinct periods in the muscle development chemistry:

- Pre-Lactic Acid Era (1808),
- Lactic Acid Era (1907[36]),
- Phosphorylation Era (1930) and
- Myosin Era (1939)[37].

The period between 1926-1932 was termed *'revolution in muscle physiology'* by A. V. Hill (1932)[38,39,40]. His idea-

"Lactic Acid was a direct energy donor for muscle contraction"

together with Meyarhof's confirmation of[41]

"glycogen was a precursor of lactate"; steered the lactic acid era.

Moreover, Adinosine Tri Phosphate (ATP) and Polymerase Chain Reaction (PCR) were also discovered by then and a lot of studies began in that direction. After the 1930s, the *'phosphorylation'* period of muscle chemistry began[42] and in 1939, the *'myosin'* (ATP dependent muscle proteins) era[37]. Also, by the early 1940, the whole 10 step Gustav **E**mben, Otto **M**eyerhof, Jakub Karol **P**arnas (EMP) or the *'glycolytic pathway'* was identified (Figure 2.2).

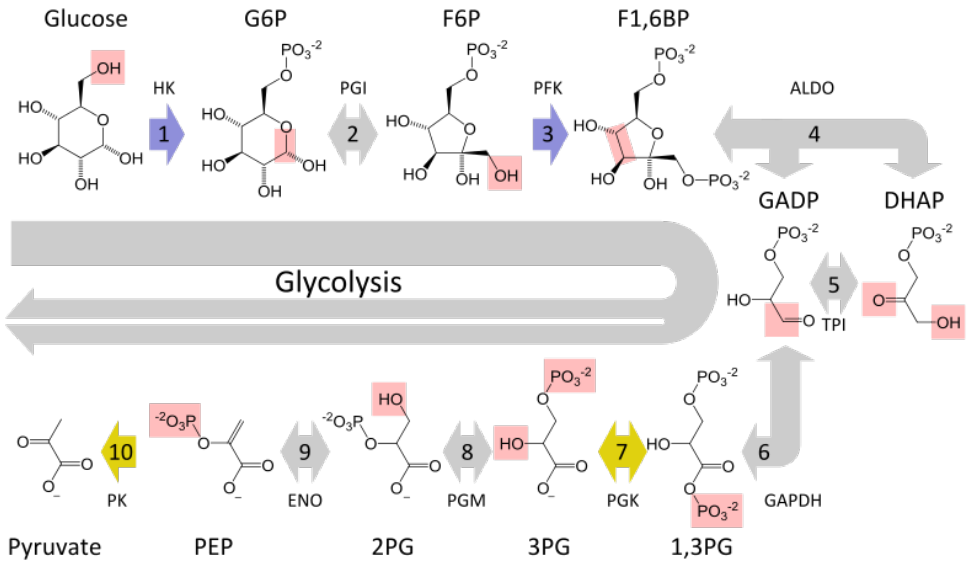

Figure 2.2: The 10 step Gustav **E**mben, Otto **M**eyerhof, Jakub Karol **P**arnas (EMP) or the *'glycolytic pathway'* which converts glucose to pyruvate. The red boxes indicate chemical modifications in the intermediate metabolites by different enzymes. Adenosine Tri Phosphate (ATP) is consumed in the first three steps (shown in blue) and produced in the next seven steps (shown in yellow). Steps 6-10 are repeated twice per glucose molecule and hence, there is a net increase (or production) of ATP in the process. HK= Hexokinase, G6P= Glucose 6-phosphate, PGI= Glucose-6-phosphate isomerase, F6P= Fructose 6-phosphate, PFK= Phosphofructokinase-1, F1,6BP= Fructose 1,6-bisphosphate, ALDO= Fructose-bisphosphate aldolase, DHAP= Dihydroxyacetone phosphate, GADP= Glyceraldehyde 3-phosphate, TPI= Triosephosphate isomerase, GAPDH= Glyceraldehyde-3-phosphate dehydrogenase 1,3PG= 1,3-Bisphosphoglycerate, PGK= Phosphoglycerate kinase, 3PG= 3-Phosphoglycerate, PGM= Phosphoglycerate mutase, 2PG= 2-Phosphoglycerate, ENO= Phosphopyruvate hydratase (enolase), PEP= Phosphoenolpyruvate, PK= Pyruvate kinase. Picture taken from[43].

All the studies done after that were mostly directed to lactic acid because of muscle hypoxia and hence, lactate was thought as a dead-end metabolite of glycolysis, until 1984 when George Brooks came up with the *'lactate shuttle hypothesis'*[44]. In this hypothesis, he mentioned that lactate is formed and consumed regularly under both aerobic and anaerobic conditions. Also, the produced lactate can be transported to different parts of the body, including the heart or skeletal muscles where there is a deficit and it can be used for oxidation as a gluconeogenic precursor or substrate.

So, during glycolysis, (shown in Figure 2.2, glycolytic pathway), which takes place in the cytosol of the cell and in the absence of oxygen, 1 mole of glucose is converted to 2 moles of pyruvate, together with 2 moles of ATP and 2 moles of reduced Nicotinamide Adenine Dinucleotide (NADH). As seen in Figure 2.3, the pyruvate then should enter the Krebs cycle (named after its discoverer, Hans Krebs) or the Tricarboxylic Acid Cycle (TCA) or Citric Acid Cycle, in ideal aerobic respiration but whenever there is a deficit of oxygen the pyruvate metabolises into lactate, with the help of LDH, as shown in Figure 2.4.

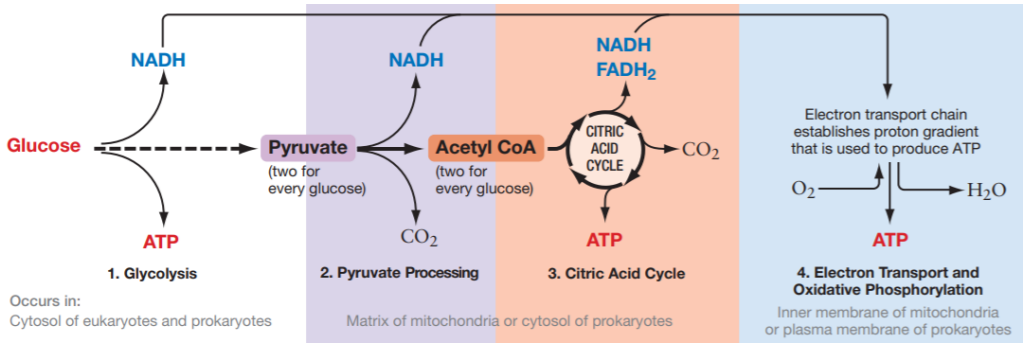

Figure 2.3: Aerobic Respiration is a metabolic pathway of converting glucose to high energy molecules (or ATP). There are four processes and they occur in the cellular level. The first three processes, i.e., 1. Glycolysis 2. Pyruvate Processing and 3. Citric Acid Cycle, produce NADH and/or Flavin Adenine Dinucleotide $FADH_2$ by oxidizing glucose. These electron carriers (NADH or $FADH_2$) are then fed into the electron transport chain for oxidative phosphorylation. Image taken from[45].

This is tissue hypoxia. Lactate dehydrogenase (LDH or LD) is an enzyme that catalyses the reaction of lactate to pyruvic acid and back, by converting NAD+ to NADH

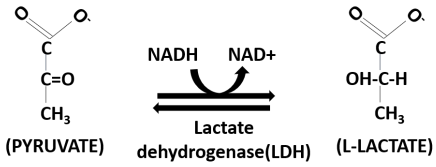

Figure 2.4: Under anaerobic conditions, instead of entering the Kerb's cycle or Citric Acid Cycle, pyruvate and NADH, which are produced during glycolysis, are reduced to lactate and NAD+. This rection is catalysed by the tetrameric enzyme Lactate dehydrogenase (LDH). Picture re-drawn from[46].

and back, and is found in almost all body tissues[47].

Pyruvate is converted to lactic acid in the liver by what is known as the Cori's or the Lactic Acid Cycle (Figure 2.5), named after it's discoverers Carl Ferdinand Cori and Gerty Cori, in the absence or in short supply of oxygen in all the tissues (gluconeogenesis).

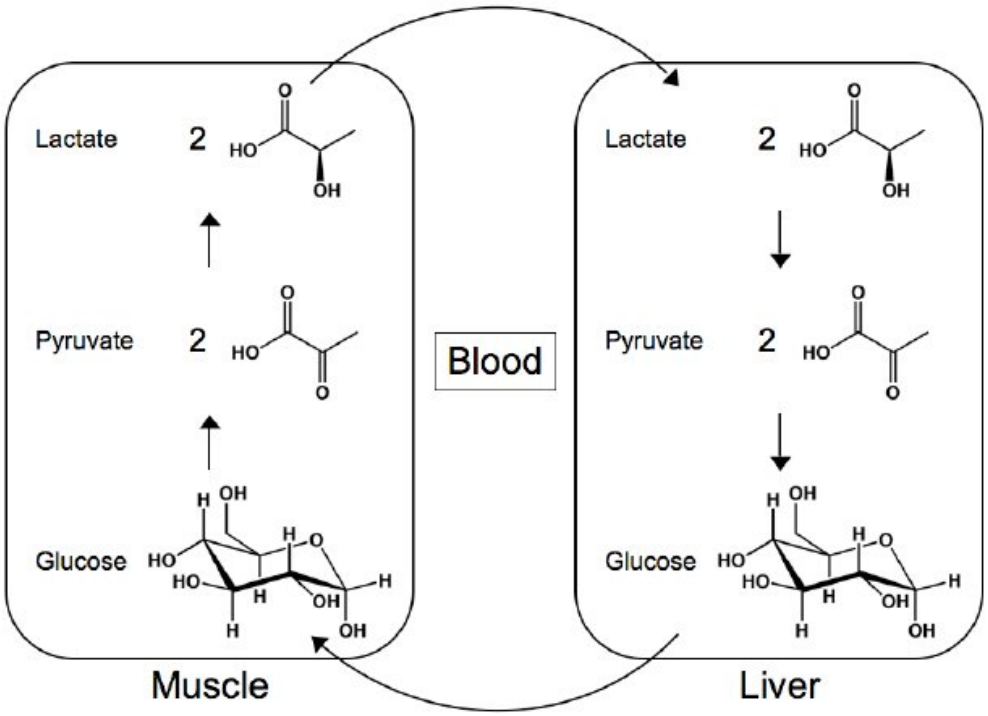

Figure 2.5: The metabolic pathway in which pyruvate is converted to lactic acid is known as the Cori's Cycle or the lactic acid cycle. During anaerobic respiration, the excess lactate which is produced in the muscles is carried to the liver. The lactate is converted back to glucose by a process called gluconeogenesis. Glucose is then carried back to the muscles for glycolysis, through bloodstream. Picture taken from[48].

The excess lactate produced in the muscle cells are transported to the liver, where

it is converted to glucose and it returns back to the muscles to be broken down again to lactate. Thus, lactate metabolism is a dynamic process. However, if the lactate production is very high, lactate concentration exceeds, and it gets accumulated. Lactate is produced in the human body, at rest, mostly by the skeletal muscle (40-50%), the brain (13%) and adipose tissue (variable). The renal medulla, Gastro-Intestinal (GI) tract, skin, red and white blood cells and platelets are also lactate producing sites[49]. In blood, the lactate production by the red blood cells, leukocytes (predominantly neutrophils) and platelets are 80, 13, and 7%, respectively[50].

The major lactate consuming tissues include the liver (20-30%), the renal cortex (20%) and the myocardium (5-15%)[49]. The excess lactate build up is usually cleared up by the kidneys with the threshold value being 6-10 $m\mathcal{M}$, but in patients with renal failure this causes immense complications because hyperlactatemia can also result from impaired lactate clearance, instead of overproduction. It is interesting to note that hepatic clearance is impaired by acidosis, hypoperfusion and hypoxia and it makes the liver a net lactate producer from a major lactate consumer site[28]. The same is also the case for brain and skeletal muscles.

Lactate is present in nature as L and D-lactate optical isomers (Figure 2.6), depending on the reaction of L or D-LDH (which is isomer specific) with pyruvate.

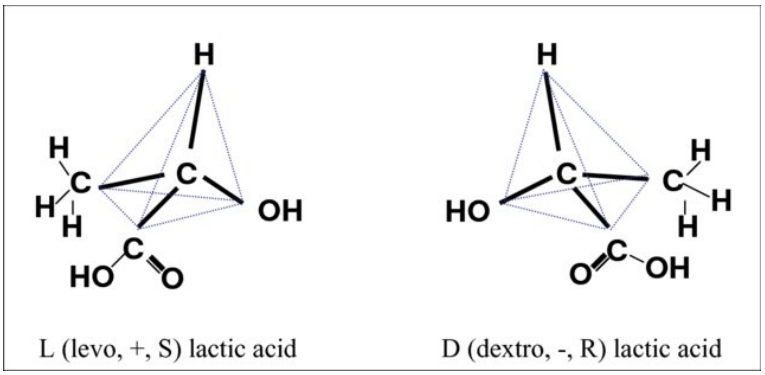

Figure 2.6: Optical isomers of Lactate (a) L-Lactate (b) D-Lactate. Figure taken from[51].

This is because lactate has one asymmetric chiral carbon and hence, two enantiomers;

L(+)lactic acid and it's optical isomer D(-)lactic acid. Out of the two, L-lactate is more commonly found in blood (100 times more than D-lactate). An interesting discovery was the methylglyoxal pathway which showed that D-lactate is metabolised by human cells, which was earlier thought of as being only produced by bacteria in the GI tract[52]. The methylglyoxal pathway converts glucose into methylglyoxal (a very toxic reactive aldehyde) and then into D-lactate which is then metabolised by the enzyme D-2-hydroxyacid-dehydrogenase into pyruvate and then the normal TriCarboxylic Acid (TCA) cycle follows. (Figure 2.7)[28]. A few studies have shown that D-lactate can be used in the study of diabetes mellitus[53], diabetes ketoacidosis[54] and intestinal ischaemia[55]. The lactic acid and lactate studies done in this report correspond to L-Lactate, unless mentioned otherwise.

The lactate produced in all the different sites are transported across cell membranes via Monocarboxylate Transporter (MCTs), has been well established by now, since its first observation by Garcia et al in 1994[56]. Out of the 14 different types of MCTs that are identified, MCT1 and MCT4 are seen in the brain, striated muscle, liver, kidneys and myocardium[57] and are responsible for transporting varieties of substrates like: lactate, pyruvate, acetate, propionate, butyrate, acetoacetate, and -hydroxybutyrate[58]. As for lactate shuttle (for example between cell to cell, intracellular, among tissues, tissue to blood, etc.) there has been lots of proposed and pending hypotheses[42,59].

2.4 Lactate in Pathology

Lactate was always thought to be produced in the human body due to hypoxia (absence of oxygen) during glycolysis, as seen in Section 2.3. However in 1996, James et al initiated the idea that there was a strong evidence that clinical hyperlactatemia is fuelled by aerobic glycolysis which activates the adrenaline- stimulated Na^+, K^+ -ATPase in the rat muscles[60,61,62]. This opened a new window for lactate metabolism in the human

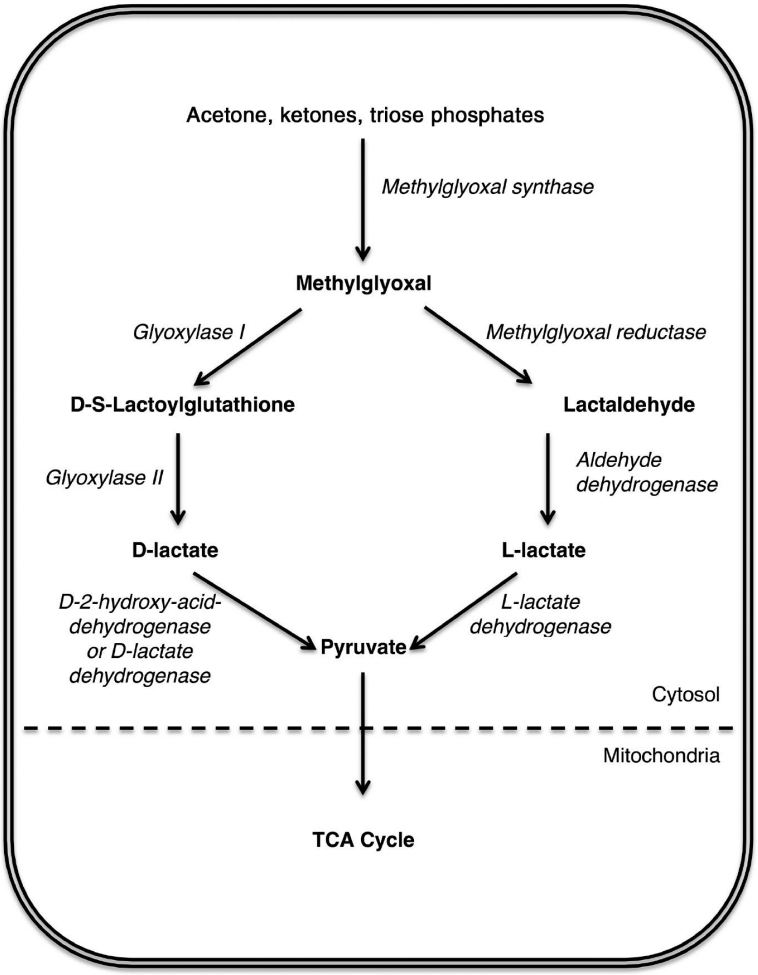

Figure 2.7: The metabolic pathway which converts glucose to methylglyoxal and D-lactate in humans is known as the Methylglyoxal cycle. It occurs adjunct to glycolysis, devoid of ATP production. Picture taken from[28].

body. Since then, the most recent study that is worth mentioning in that direction is done by Bundgaard et al in 2003, who induced endotoxins in healthy humans and it resulted in an increased level of both adrenaline and lactate with the activation of Na^+, K^+ -ATPase[63]. Luchette et al has also established the activation of Na^+, K^+ -ATPase during haemorrhage[64]. During sepsis, Na^+, K^+ -ATPase activity is increased which increases the glycolytic flux through $\beta 2$ simulation, which in turn enhances the lactate production[65].

The questions raised and answered by different groups as to the metabolism of lactate since the 18^{th} century to the late 20^{th} century,[66,67,36,68,69,70,71,72,73]; can now identified as:

- anaerobic metabolite, during anoxia
- hypoxic metabolite, during dysoxia
- aerobic metabolite, when there is an adequate presence of oxygen and glucose is used as a fuel for energy.

Hence, it has been well established that elevated levels of lactate in blood can be used as a detection tool for a lot more than just tissue hypoxia. Elevated lactate levels or Hyperlactatemia, can be an indicator or metabolic biomarker for the onset of haemodynamic shock, where the next section concentrates to establish this principle.

2.5 Hyperlactatemia as a Biomarker Marker for Haemodynamic Shock

The heart, along with the blood vessels and blood make up the circulatory system in any living being. It is responsible for delivering oxygen and nutrients to all the parts of the body and at the same time, ensure that the waste metabolites are being removed. Any obstruction in this system, whether congenital or acquired, is termed as a *'HEMODYNAMIC DISORDER'*: ischemia, infarct, thrombus, embolus, hyperaemia, atherosclerosis, edema, shock and haemorrhage, are a few examples[74]. Shock, in physiology, results from or occurs, when the circulatory system fails to supply sufficient blood to peripheral tissues in order to fulfil the basic metabolic requirements of oxygen and nutrients; or an incomplete removal of toxic intermediates from the infected ones. There have been multiple variations in the physiologic definition for the term *'Hemodynamic Shock'*, since ages, depending on the advances in medical technology and until to date no one has come to a definite conclusion but there have been a lot of interests in its detection, management and diagnosis because of its various repercussions. As to quote Frederick Heaton Millham, MD,[75] *"Perhaps we can learn from Gross[76] and Cannon[77] that it may be better to be able to recognize shock than define it"*. Shock is usually caused

by haemorrhage or any overwhelming infection in the body and in most cases, is characterized by weak, rapid pulse; low blood pressure; and cold, sweaty skin. Depending on the cause, however, some or all of these symptoms may manifest or be missing in individual cases and one particular type can lead to certain another type of shock. It leads to cellular dysfunction, cell death or impairment of organ function which might subsequently lead to death, if not detected and diagnosed at the right time.

Alfred Blalock (1899-1964) is regarded as one of the greatest contributors in this subject and in 1934, he identified five discrete physiological conditions for shock:

- Hematogenic Shock (Hypovolaemic)
- Neurogenic Shock
- Vasogenic Shock (including both anaphylactic and septic shock)
- Cardiogenic Shock, and
- Unclassified Conditions.

He soon dropped out the unclassified conditions from the list, making them four and it can be considered as one of the most significant conceptual frameworks even to this day. He was the first person to consider the different physiologies under a single theory: *"Shock results from a decrease in the ratio of the blood volume in circulation to the capacity of the vascular tree."*[78,79,80,81,82].

Hypovolaemic shock and trauma is the most studied form of Shock since the early 1900s[83,84,85,86,87]. In 1831, Laennec, introduced 'Sepsis' as a different cause of shock and was supported by Boise in 1897[88,89]. Fishberg et al came up with the concept of cardiogenic shock in 1934[90]. However, the classifications proposed by Hinshaw and Cox, in 1972[91], based on cardiovascular characteristics, were accepted by most clinicians and is still widely used even in modern days. The types are listed as follows:

- Hypovolaemic shock is the most common type of shock and is caused by insufficient blood circulation volume. Its primary causes are:
  - Haemorrhagic: trauma, gastrointestinal bleeding, retroperitoneal
  - Non haemorrhagic: excessive fluid loss from the skin due to severe burns or any external cause, high output fistulae, vomiting, etc.

  This type of shock manifests itself by a drop in ventricular preload and thus decreasing the ventricular diastolic pressures and volumes and pulse pressure. Also, a fall in mixed venous oxygen saturation (SvO_2) results; because of reduced, unchanged or increased metabolic demands in the body. It can be identified by pale, cool and clammy skin; tachycardia; tachypnea; decreased urine output and altered mental state. Several studies have shown that the loss of circulating volume from the body has significant changes in the clinical observations:
  - $\leq$ 10 % volume loss: tachycardia is the only indication
  - 20-25 % volume loss: decreased Cardiac Index (CI) with a moderate hypotension, noticeable increase in Systemic Vascular Resistance (SVR) and serum lactate levels may raise with an apparent orthostatic.
  - 40 % or $>$ volume loss: noticeable hypotension with other clinical signs of shock, CI and tissue perfusion maybe reduced to half of the normal values and lactic acidosis is usually seen[92].
- Cardiogenic shock happens when the heart fails to pump effectively. This often follows after a large myocardial infarction, in most cases, weakens the heart muscles. Other causes include dysrhythmias, cardiomyopathy/myocarditis, Congestive Heart Failure (CHF), contusio cordis or cardiac valve problems.

- Obstructive shock happens when blood flow is obstructed extrinsic to the heart. It can happen due to:
  - pulmonary embolism: a block in one of the arteries which impedes the return of the blood to the heart
  - tension pneumothorax: increased intrathoracic pressure; leading to a reduced venous return
  - cardiac tamponade: fluid in the area between the heart and the pericardium builds up; resulting in less venous flow
  - aortic stenosis: obstructs the ventricular outflow tract; causing a inhibiting circulation.

  The two types of shock mentioned above induces ventricular preload and SVR and reduces CI, like hypovolaemic shock. The SvO_2 level is subsequently reduced because of inefficient tissue perfusion. The lactic acidosis level can help predict the mortality in this type of shock[93]. According to a study done by World Health Organization in 2015 (which is done every 5 years), ischaemic heart disease and stroke are the leading causes of death; held responsible for the death of 15 million deaths, combined, which is around 54 % of the total deaths worldwide[94]. They are the most studied form of shock until this date because of their relation to myocardial infarction.

- Distributive shock happens when the absorbed oxygen has impaired utilization which leads to insufficient energy production by the cells. These can be classified further as:
  - Septic shock: occurs when an infectious agent, the mediators produced by them or the reaction of the immune system to these agents combine to generate an infection, cardiovascular instability and organ dysfunction or failure.

The awareness of this type of shock has spread to a great extent, such as Surviving Sepsis Campaign[95], since it has one of the highest rates of mortality amongst the patients in an ICU[96]. The Surviving Sepsis Campaign revisits the criteria for management of septic shock every year and the latest one was in 2018[97]

- Anaphylactic shock: caused by a severe anaphylactic reaction to an allergen, antigen, drug or a foreign protein which releases histamine resulting in extensive vasodilation, which in turn leads to hypotension and increased capillary permeability
- Neurogenic shock: it is one of the rarest forms of shock caused by an injury to the spinal cord.

Distributive shock is characterized hemodynamically by a decrease in an overall SRV: CI (initially but after fluid resuscitation there is usually an upsurge) and ventricular stroke work indices (because of hypotension). The SvO_2 level is usually very high and despite of which, there is a demand of oxygen levels in blood. Owing to which there is an ineffective tissue perfusion which leads to lactic acidosis and makes the cells unable to use Adenosine Tri Phosphate (ATP). Unlike in the other types of shock, the patients are warm, featuring a decreased diastolic blood pressure but an increase in pulse pressure.

According to a recent study, the incidences of shock are increasing for non-traumatic patients every passing day, hypovolaemia being the most common among them. Sepsis has been observed in around 2 % of patients, especially among older people and around 7-9 % of acute myocardial infarcted patients end up with cardiogenic shock[98]. Amongst the number of patients who are admitted to the ICU, almost one third are shocked, with sepsis being the most common cause here (62 %), followed by cardiogenic causes

(17 %) and hypovolaemia (16 %). Mortality among these shocked patients in the ICU are really high as well; deaths due to cardiogenic shock has been reduced from 60 % in 1995 to only 48 % in 2004 (which is still quite high)[99] and septic shock or 'septicaemia' contributes to around 30-50 %, annually[75]. According to the most recent systematic review (January 2020), which had taken into account data from 196 countries for the years 1990-2017, states that sepsis-related mortality has decreased by 52.8 % in those years. However, sepsis still contributed to 19.7 % of all the causes of deaths globally in 2017 (48.9 million reported incidents and 11 million deaths)[100].

Each of these variants of shock has their own specific way of presenting the symptoms and also specific markers to detect their effects and stages of occurrence. However, it is worth mentioning that even if there exists a specific hemodynamic-based classification, the shock states converges with one another and a certain form can give rise to one another form of shock. Another additional aspect to this is that there has been no defining *"stages of spread of shock"* till date which makes the detection very challenging as well[95]. There are various symptoms that have been identified, till date, which can be used as an indication towards that state but except for lactic acidosis, which can be seen in all the types of shock, the rest of the symptoms are seen to vary in all the different shock states. Hence, it can be concluded that the concentration of lactate increase (hyperlactatemia) in blood together with variations in pH (lactic acidosis) can be a very important biomarker in the detection and management of shock.

Hyperlactatemia is commonly seen as an important biomarker for morbidity and mortality in critically ill patients (especially sepsis)[101]. It was Broder and Weil[102], in 1964 who first suggested this, and, in their study, they reported that the survival rate of patients with excess lactate concentrations and circulatory shock was only 11 % ($>4\ mM$). After a year, Peretz et al[103] listed that with lactate levels $>4.4\ mM$ the mortality rate in patients with shock syndrome increased from 18 % to 73 %. In 1970, Weil and Afifi[104]

documented that with increasing lactate concentration from 2 to 8 mM, the estimated survival probability rate in patients with circulatory shock decreased from 90 % to 10 %. Then in 1971, Vitek and Cowley[105] mentioned that the pathology of the shock states is also a major contributor to the patient survival probability, while also confirming the previous observations. In 1991, Kruse et al[106], in their study, documented a surprising increase in mortality rate as lactate concentrations in the critically ill patients increased from as low as >2.5 mM[71]. In fact, a study carried out by Stacpoole et al lead to the understanding that blood lactate concentrations >5 mM together with acidosis (pH <7.35), caused a mortality of 80 %[44]. In another study done by Khosravani et al[107] in an ICU in Calgary, indicated that an admission lactate of 2 mM can be a substantial independent predictor of mortality. Another most important thing to consider here is that the time between inception of insufficient tissue perfusion and death is very short, less than 1 h[108] and hence a prompt and adequate hemodynamic resuscitation protocol is necessary[65]. With severe lactic acidosis and pH of under 7.0, no survival cases have been reported by far for a shocked patient[109].

Early predictions of lactic acidosis values can serve as a prognosticator for mortality in critical care as well[110]. Therefore, it is worth understanding the basic underlying mechanisms of Lactic Acidosis as well, which is explained in the following section.

2.6 Lactate and Acidosis

Lactic Acidosis is categorized into two types (Type A and B) by Cohen and Woods in 1976, depending on the presence or absence of tissue hypoxia. Type B was further divided into B1, B2 and B3 which are associated with diseases such as liver failure, drugs and toxins and innate flaws of metabolism, respectively[111].

Type A lactic acidosis is the most common amongst the two and tissue hypoxia is generally caused by systemic or local hypoperfusion, increased glycolytic flux, abridged

oxygen carrying capacity of the blood or reduced tissue oxygen delivery[111]. Type B lactic acidosis is associated with underlying diseases, drugs and toxins or congenital errors in metabolism.

However, the distinction between the two types can sometimes be indistinct during sepsis or septic shock as the patients manifests symptoms like circulatory dysfunction, which is typical of Type A, in addition to incapacitated lactate clearance and aberrant mitochondrial function like in Type B. Now it is established that sepsis-associated hyperlactatemia is a result of the upshot of pyruvate production rate and epinephrine (adrenaline) concentrations. The lactate release is basically controlled by the catecholamine stimulation of 2-adrenoceptors and not tissue hypoxia alone[112].

Lactic acidosis is a type of metabolic acidosis in blood and can be calculated with the help of two equations:

Modified Henderson-Hasselbach Equation (1918)

$$pH = 6.1 + \log \frac{[HCO_3^-]}{0.0307 \times p_{co_2}} \tag{2.1}$$

where, pH is the acidity in the blood, $[HCO_3^-]$ is the concentration of bicarbonate in the blood, 0.0307 mM/mmHg is the dissociation constant (K_{HCO_2}) which includes the solubility of CO_2 in blood, p_{co_2} is the partial pressure of carbon dioxide in the arterial blood[113,114].

Base Excess (BE) Approach (1958)

$$pH = pK + \log \frac{[HCO_3^-]}{[CO_2]} \tag{2.2}$$

Calculations are based on the modified Henderson-Hasselbalch equation and Siggaard-Anderson equations.

$$BE = 0.02786 \times p_{co_2} \times 10^{(pH-6.1)} + 13.77 \times pH - 124.58 \text{[115]} \tag{2.3}$$

Base excess beyond the reference range is indicated as follows:

- metabolic alkalosis, if too high (more than +2 mEq/L)
- metabolic acidosis, if too low (less than −2 mEq/L)[115].

These were the early means of lactic acidosis calculations and it was thought of the result of dissociation of lactic acid and the release of H^+ (Hydrogen cation) to maintain the electroneutrality of the blood lowering the pH. In 2004, Robergs put forward the idea that lactate and not lactic acid was produced by the reaction catalysed by LDH and it consumes H^+, thus disapproving the old idea that lactic acidosis was the cause of metabolic acidosis[116]. However, Stewart came up with an alternative idea of acid-base balance which could explain the role of lactic acid and was later modified by Figge and colleagues who included plasma proteins in the idea. The idea states that there are three interacting independent variables and they maintain an acid-base equilibrium; $PaCO_2$, the difference between the sum of all the Strong Base Ions (SID_a) and the weak acid and proteins (SID_e) in plasma[64]. The present day view is that lactic acidosis is associated with Serum Anion Gap (AG) or the Strong Ion Gap (SIG) which is the difference between the concentrations of primary measured cations (Sodium ($[Na^+]$) and Potassium ($[K^+]$)) and the primary measured anions (Chloride ($[Cl^-]$) and Bicarbonate ($[HCO_3^-]$)) in serum[117].The predominant strong cations in blood are $[Na^+]$, $[K^+]$, $[Ca^{2+}]$, and $[Mg^{2+}]$, and $[Cl^-]$, whereas the weak ions include: Plasma protein, mainly albumin $[Alb^-]$ and Phosphate $[HPO_4^{2-}]$.

$$SID_a = ([Na^+] + [K^+] + [Ca^{2+}] + [Mg^{2+})] - ([Cl^-] + lactate); \tag{2.4}$$

Equation 2.4 does not include the plasma proteins.

$$SID_e = 2.46 \times 10^{-8} \times pCO_2(mmHg)/10^{-pH} + (albumin(g/l)) \times (0.123 \times pH - 0.631) + (phosphate(mg/dl)) \times (0.309 \times pH - 0.469); \quad (2.5)$$

Equation 2.5 is the modified formula by Figge and colleagues, which gives the Strong Ion Difference, SID_e.

And combining the two gives the Strong Ion Gap (SIG):

$$SIG = SID_a - SID_e. \quad (2.6)$$

These are the standards that are being followed in today's medicine textbooks. However, the association of lactate and acidosis, especially in aerobic hyperlactatemia (Type B), is very complex and still debatable[118,119,120,121,122,123,124,125,126,127,128,129,130]. To understand the complex relationship and mention all the hypotheses is beyond the scope of this report and hence, the rather traditional relationship of pH is followed.

The pH in blood is usually measured in a critical care unit with the help of Blood Gas Analysers (BGA) using the equations mentioned above, depending on the manufacturer. The mechanisms responsible for acid – base balance in the human body are still incompletely understood[131]. A great variability also lies in between different analysers and is a major limitation when comparing studies regarding acid – base disorders. However, it has been standardised that in the absence of any pathological states, the physiological pH in blood for the human body should lie in the range of 7.35 to 7.45. The cellular pH is however a little lower and it should be maintained in the range of 6.0-7.4[132]. pH in critical care is usually calculated using an add-on capability of a blood-gas analyser and hence, only blood pH is measured and if the values tend towards 7.1 (which is considered as severe acidemia), it has to be regulated with urgent resuscitation. Early predictions of lactic acidosis values can serve as a prognosticator for mortality in critical care[110].

2.7 Summary

This chapter highlighted the history of lactate, mechanism of production, consumption and disposal of lactate/ lactic acid in the human body, establishing lactate as a biomarker marker for haemodynamic shock states and the relationship of lactate with pH in the human body. The following chapter explains the basics of Spectroscopy, as it will be the main technique for investigating lactate/lactic acid in this research.

Seeing is in some respect an art, which must be learnt.

William Herschel, discoverer of IR Spectroscopy

3 Spectroscopy

3.1 Introduction

Spectroscopy is the study of Light (Electromagnetic Radiation) and Matter interactions. The response of any given sample (matter) to a known stimulus of calculated wavelength (λ) and frequency (ν) of light is observed in spectroscopy. This chapter aims in providing a good understanding of the electromagnetic (EM) spectrum (Ultra Violet (UV), Visible (Vis), Near Infrared (NIR) and Mid Infrared (MIR)); their principles of operation and the different types of instruments used in the experi-

mental set-up in this thesis. The last part of the chapter discusses a few mathematical tools used for the analysis of the obtained data (spectra).

3.2 History and Principle

The principle of understanding the *light-matter interactions* is usually done by two properties of light, namely, wavelength (λ) and frequency (ν). These parameters are associated with each other by the Planck–Einstein relations:

$$E = h\nu \tag{3.1}$$

$$\nu = c/\lambda \tag{3.2}$$

where, E= Energy of the incident light/photons (J),

h = Planck's constant ($6.62607015 \times 10^{-34}$ m^2 kg / s) ,

c = speed of light in vacuum (299,792,458 m / s), in International System of Units (SI) units.

The range of wavelength and frequency of light is known as the Electromagnetic Spectrum, which is divided into various regions as shown in Figure 3.1

The visible region of the spectrum constitutes photon energies ($h\nu$) of 150000 to 300000 Joules (J) and the near ultraviolet region, extends this energy range to 590000 J (200-800 nm) on the left side of the spectrum. However, ultraviolet radiation of wavelengths $\leq$ 300 nm is challenging to deal with and hence, is scarcely used as a routine tool for structural analysis of molecules. The Near Infrared region of the electromagnetic spectrum employs ($h\nu$) of 2.54 x 10^{-19} – 7.86 x 10^{-19} J, corresponding to the wavelength region of 780 - 2526 nm (wave number of 12820 - 3959 cm^{-1}), as defined by The American Society of Testing and Materials (ASTM). It is a type of vibrational spectroscopy;

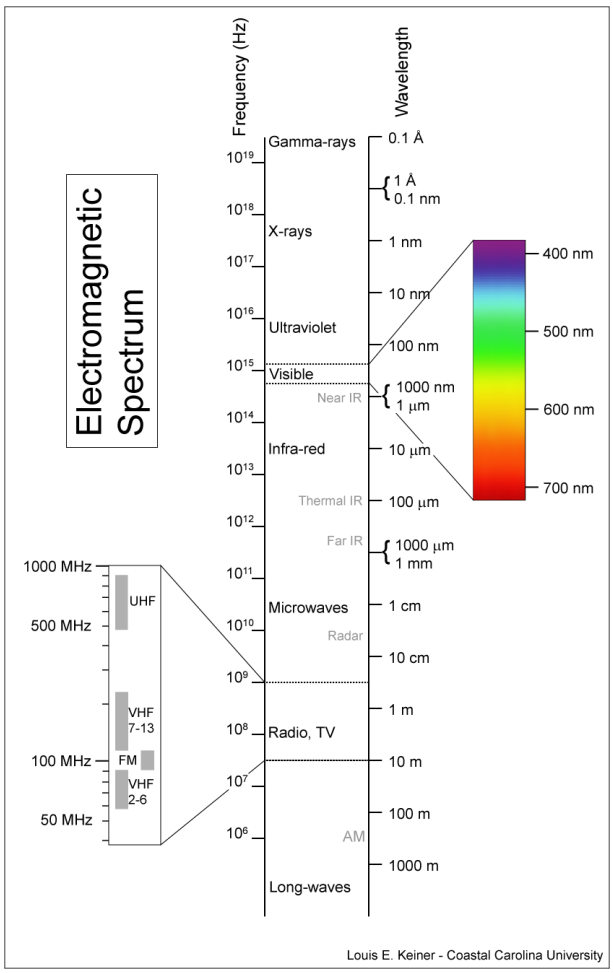

Figure 3.1: The Electromagnetic Spectrum (EM) depicting the various regions like Gamma-rays, X-rays, Ultraviolet (UV), Visible (Vis), Infrared, Microwaves, Radio, TV and Long-waves based on the frequency (Hz), ν and wavelength (length-scale), λ. The visible region is highlighted (400-700 nm). Figure taken from [133].

whose energy range is only high enough to promote electron excitation in the sample to lowest excited vibrational states. The main objective is to extricate quantitative and/or qualitative information from a sample when NIR electromagnetic waves interacts with the samples, together with the functional groups (C-H, N-H, O-H and S-H). The Mid Infrared is also a type of vibrational spectroscopy ranging from 7.94 x 10^{-20} - 7.94 x 10^{-21} J (2500 - 25000 nm or 4000 – 400 cm $^{-1}$). The mid-infrared spectrum can be approximately categorised into four regions as follows:

- X-H stretching region (4000 – 2500 cm^{-1})

- the triple-bond region (2500 – 2000 cm^{-1})
- the double-bond region (2000 – 1500 cm^{-1})
- fingerprint region (1500 – 600 cm^{-1}).

The underlying working principles of the UV/Vis and Infrared spectra are different as they deal with different wavelengths (λ) and frequencies (ν) of the EM spectrum itself. These principles are described in brief below:

3.2.1 Principle of Operation of UV/Vis Region

The light-matter interactions of Ultraviolet (UV) and Visible (Vis) radiation of the EM spectrum is affiliated to electron excitation due to Absorption, in both atoms and molecules, from lower to higher energy levels (or orbitals). Since the energy levels of matter are quantized, only light with the precise amount of energy will be absorbed which can cause transitions from one orbital (bonding or anti-bonding) to another. The allowed transitions are listed below and are as shown in Figure 3.2:

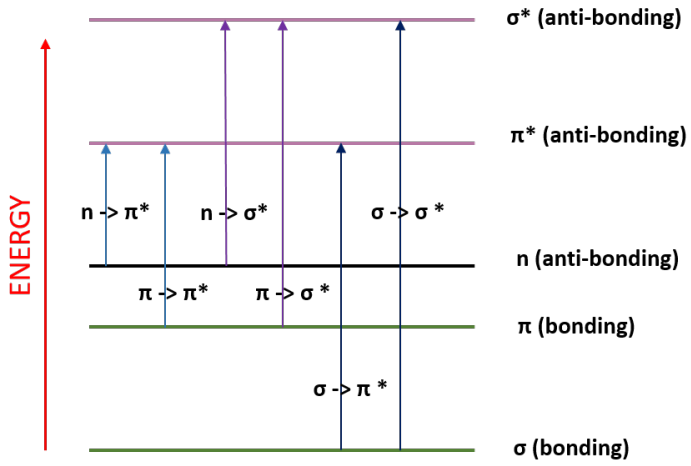

Figure 3.2: The allowed electronic transitions in energy band diagram are: n – π^* , π – π^* , n – σ^* , π – σ^* , σ – π^* , σ – σ^* (Redrawn from:[134]).

- n – π^* (n to pi star transition)

- π – π^* (pi to pi star transition)
- n – σ^* (n to pi star transition)
- π – σ^* (pi to sigma star transition)
- σ – π^* (sigma to pi star transition)
- σ – σ^* (sigma to sigma star transition)

Out of all these six transitions allowed, the lowest energy ones are achieved in the UV/Vis region; electron promotion will arise from the Highest Occupied Molecular Orbital (HOMO) to the Lowest Unoccupied Molecular Orbital (LUMO); which results in an excited state of electron. When light of a specific energy which matches a possible transition is exposed to molecules in a sample, a part the light energy will be absorbed as the electron is excited to a higher energy orbital. This part of the light which is absorbed is quantified to produce an Absorption Band because of molecular dissociation, as described in a later part of this chapter. For the infrared part of the EM, the working principles are similar to the UV/Vis region, however, this region has a bit more complex theory as the absorption band arising in this region is because of the influence of the vibrational motion of the atoms in a molecule. Hence, the study of the light-matter interactions in this region is also called *Vibrational Spectroscopy*.

3.2.2 Principle of Operation of Infrared (NIR and MIR) Region

The first part of the non-visible electromagnetic spectra was first noticed by a curious German born English scientist, Frederick William Herschel in the 1800s when he found the temperature change after the red visible part of the spectrum. He termed it 'Calorific Rays' which was later named 'Infra-red' (Greek prefix 'infra' means 'below'). The work initiated by Coblentz in 1900 gave this spectral region wide acceptance when he started

obtaining absorbance spectra of pure substances and was successful in identifying the organic functional groups[135].

There are three types of vibrational spectroscopy techniques usually available: Near Infrared (NIR), Mid Infrared (MIR) and Raman Spectroscopy. These techniques have the same aspects regarding the physical origin: *they study the periodic vibrational motions of the atomic nuclei within molecules which results in respective molecular spectra.* However, they vary in different aspects like Raman Spectroscopy deals with fundamental mode electronic scattering techniques in 2500 - 200000 nm (4000 - 50 cm^{-1}) using a monochromatic Vis/NIR laser radiation as light source. While both NIR and MIR deals with absorption techniques using polychromatic (dispersed) radiation light source. The NIR region, 800 - 2500 nm (12500 - 4000 cm $^{-1}$) interprets the overtones and combination bands of the C-H, O-H and N-H functionalities in a molecule and the MIR region, 2500 - 50000 nm (4000 - 200 cm $^{-1}$), mostly observes polar bonds like C=O[136]. It can be thus seen that the vibrational frequencies (ν) are sensitive to the structure of the compound under investigation and hence, these techniques are used profoundly in the determination of the structures in unknown samples. The next section describes the theory in more detail.

3.2.3 Theory of vibrational spectroscopy

In classical physics the atoms are considered as particles with known masses connected by a spring in a simple diatomic oscillator, as shown in Figure 3.3.

In the IR absorption process, the vibrational frequencies (ν) of these diatomic molecules are based on the harmonic oscillator approximation and the molecular parameters are correlated with the help of relationships derived from Hooke's Law and Newton's second law of motion:

$$\nu = 1/2\pi\sqrt{(f/\mu)} \tag{3.3}$$

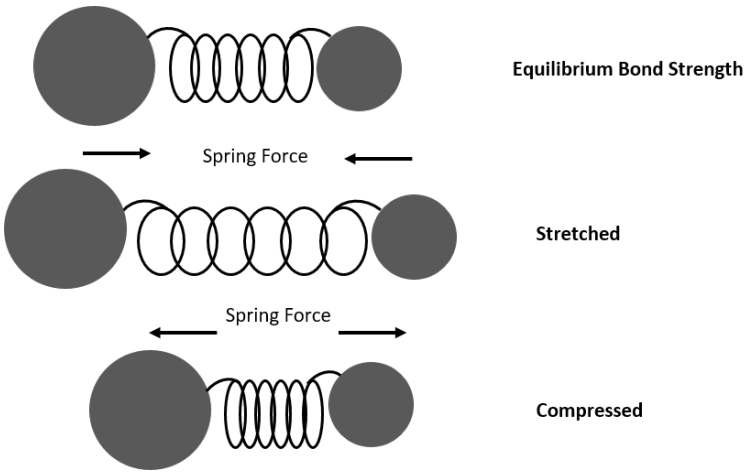

Figure 3.3: Mechanical Model of a diatomic system, where there are two masses, M and m, connected by a spring (Redrawn from:[137]).

where, f = strength of the bond between the two masses, m and M,

μ = reduced mass, which is given by:

$$\mu = mM/(m+M) \tag{3.4}$$

The total energy of the electromagnetic radiation is:

$$E = h/2\pi\sqrt{(f/\mu)} \tag{3.5}$$

The molecular dipoles which can be considered as a two-mass system (m and M) connected by a spring (which is the simplest model for diatomic molecules) owe their vibrational frequencies to the vibrations and rotations of the atoms in a molecular system. For a diatomic molecule, vibration of the bond is possible corresponding to the stretching and compression, thus has three Degree of Freedom (DOF). In polyatomic (both linear and non-linear) molecules there are 3N DOFs, where N is the number of atoms. Vibrations in a molecule changes the bond length (stretching (ν)), bond angle (bending)-which can be in-phase (δ) or out-of-phase (γ), depending on the similarity or asimilarity of the atoms in the molecule, as shown in Figure 3.4. There can be either

one of these fundamental vibrations or a combination of them in a molecule. These vibrations give rise to a dipole moment in a molecule which in turn absorbs the infrared radiation of the electromagnetic spectra; the incoming infrared radiation has the same frequency (ν) as one of the fundamental modes of vibration of the molecule. The different types of dipoles in the carbonyl group, for example, arises because of the differences in the electro-negativity of the atoms. And the discrete energy levels, E_ν can be calculated using:

$$E_\nu = (\upsilon + 1/2)h\nu \tag{3.6}$$

where, υ = vibrational quantum number.

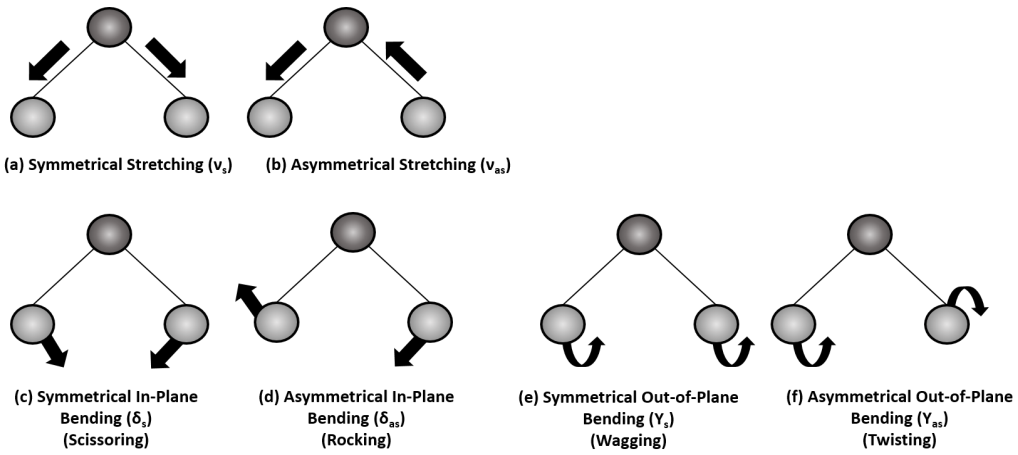

Figure 3.4: Fundamental modes of vibrations in a molecule (a) Symmetrical Stretching (ν_s), (b) Asymmetrical Stretching (ν_{as}), (c) Symmetrical In-Plane Bending (∂_s) (Scissoring), (d) Asymmetrical In-Plane Bending (∂_{as}) (Rocking), (e) Symmetrical Out-of-Plane Bending (γ_s) (Wagging) and (f) Asymmetrical Out-of-Plane Bending (γ_{as}) (Twisting) (Redrawn from:[138]).

However, in practical scenario, the model is more complex and there are a lot of factors, adding to the complications in the model. In a more accurate mechanical model for a diatomic molecule the variation in the vibrational frequency, (ν), arises because of the repulsion between the two electronic clouds when the two nuclei approaches towards or moves further away from each other. In an actual molecule, when this phenomenon

is occurring, there is a possibility that the bonds may rupture due to over displacement of the atomic nuclei, leading to dissociation of the atoms. Hence, a composite function of the Potential Energy, V is assumed to define the last effect which is possible to approximate using higher order terms of displacement, as depicted in the equation:

$$V = k_1 x^2 + k_3 x^4 + ... \tag{3.7}$$

The harmonic oscillator model, which is a two mass system (m and M, as seen in Figure 3.3), connected by a spring and considered within the spring's elastic limit, therefore, has to be replaced by an anharmonic behaviour for a diatomic molecule, as seen in Figure 3.5.

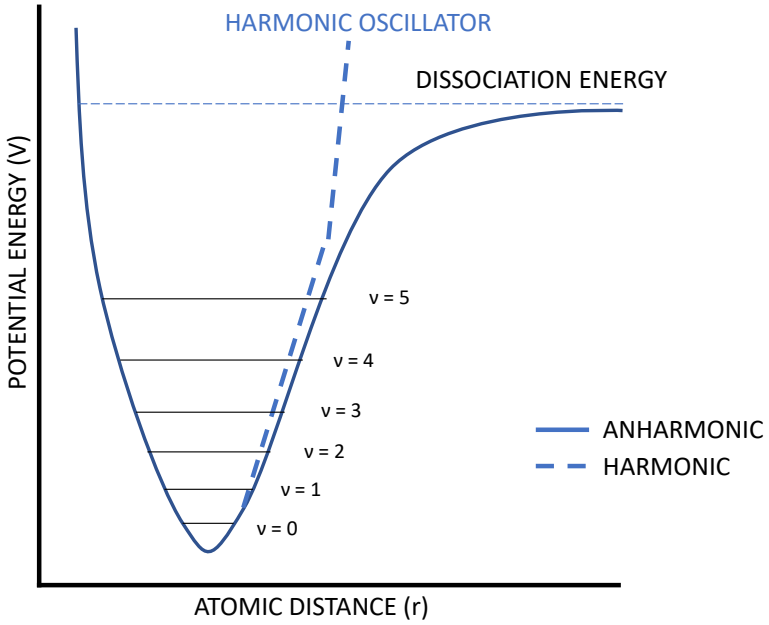

Figure 3.5: Model of the harmonic and anharmonic oscillators with vibrational energy levels (Redrawn from:[139]).

These anharmonic behaviour for a diatomic molecule can be explained with the help of another oscillator known as the Morse oscillator. The vibrational states of this oscillator can be defined with the help of Morse Function, which can approximate the potential energy, V of the molecule as:

$$V = D_e[1 - e^{-\alpha(r-r_e)}]^2 \tag{3.8}$$

where, α = is designated to a constant of a given molecule,

D_e = spectral dissociation energy,

r and r_e = distance between the atoms at any instant and the equilibrium distance between the atoms, respectively.

Hence the energy of the vibrational states, E (which is a combination of quantum mechanics and the Morse Function) can be described as follows :

$$E = h\nu(\upsilon + (1/2)) - X_m h\nu(\upsilon + (1/2))^2 \tag{3.9}$$

where, υ = the quantum number of vibrational mode,

X_m = anharmonicity constant of the vibration, and its value ranges from 0.005 – 0.05.

The anharmonic model poses some limitations on the possible energy levels of the molecules but the occurrence of transitions with $\Delta = 2$ or greater and the combination bands within vibrations still appear; these two being the most prominent ones in the NIR region but not in the MIR region of the EM. According to this model, vibrations interact with each other and are not independent, giving rise to a total of vibrational energy, E_ν, which includes crosscutting terms from various multiple vibrations within the molecule. The interactions include some non-ideal behaviours of the oscillator, as compared to a harmonic model, such as, repulsion between electronic clouds when atomic nuclei approaches one another and the behaviour of the bond forces when atom move apart from one another.

$$E_\nu = \sum h\nu_r(\upsilon_r + 1/2) + \sum\sum hx_{rs}(\upsilon_r + 1/2)(\upsilon_s + 1/2) + \cdots \tag{3.10}$$

For r $\leq$ s;

ν_r = the fundamental frequency,

υ_r = the quantum number of vibrational mode r and

x_{rs} = the anharmonicity constant for the interaction of vibrational modes r and s.

Additionally, the electrical characteristics of a molecule can also depict some anharmonicity. It can change dipole moment of a molecule which has a non-linear association with the interatomic distance, giving rise to overtones and combination bands.

Overtones are vibrational modes when an electron is excited from $\nu = 0$ to $\nu = 2$, called the first overtone, or $\nu = 0$ to $\nu = 3$, the second overtone. The fundamental transitions, $\nu = \pm 1$, occurs most commonly and the probability of overtones rapidly decreases as $\nu = \pm n$ increases. Based on the harmonic oscillator approximation, the energy of the overtone transition will be about 'n' times the fundamental vibration associated with that transition. The anharmonic oscillator calculation shows that the overtones are usually less than a multiple of the fundamental frequency. Overtones are generally not detected in larger molecules.

Combination bands occur when more than two or more fundamental vibrations are excited simultaneously. They usually occur if a fundamental vibration does not occur because of symmetry.[135].

3.3 The Origin and Intensity of an Absorption Band

From the above sections mentioned in this chapter, it can be now understood that radiation of a distinct frequency of light can provide energy to an electron that is equal to the energy between two vibrational states (ν_r) or their overtones or combinations bands (in case of NIR) to excite them to a higher vibrational energy level. The energy provided by the incident light and the difference between the energies of the vibrational states causes a distinctive response to the molecular arrangement in a sample. Hence, in

a certain given wavelength range, a few of the frequencies will be completely absorbed while a few others only partially absorbed, and the rest maybe reflected. Now, when the different intensities of absorption are plotted against wavelength forms it produces an absorption spectrum of a sample. However, straightforward it may look, there are certain limitations with respect to each part of the spectra. A few examples are listed below:

UV/Vis spectroscopy is unsuitable for:

that undergoes a photochemical reaction near the wavelength range of interest-Samples which scatters.

A radiation absorption to happen in the infrared region, the correlation between photons' energies and vibrational states is not sufficient and an interaction between the molecule and the electrical oscillating field of the light gives rise to a vibration. This depends on the dipole moment of the molecule or vibrating atoms within the molecule which is caused by the rearrangement of atoms in the molecule; is true for fundamental modes of vibration and not for combination bands. Thus, this type of vibration will be noted only in the NIR region of the spectra and not the MIR.

In the NIR part of the spectra, hydrogen atoms together with carbon, nitrogen and sulphur (C-H, N-H, O-H, and S-H), are magnified and show huge amount of anharmonicity and bond energies. This means that their overtones and combinations are most likely to manifest in that region using NIR photons. Coupling or Resonance between various vibrations of these groups add further complexity in the NIR spectrum[135].

Coupling happens when the vibrations or the energy levels of two or more atoms mixes, which results in the same number of vibrational modes but at different frequencies and hence the bands can no longer be designated to a single bond[140].

Table 3.1, provides a summary of the wavelength (in nm) and bond assignment for C-H, O-H and C=O functional groups in the NIR spectral region.

Table 3.1: Table showcasing the approximate Wavelength (nm) which can be assigned to the functional groups C-H, O-H and C=O, together with their overtone and combination bands. Table taken from[141].

Approximate Wavelength of Some Common Functional Groups	**Wavelength (nm)**	**Functional Group**	**Wavelength (nm)**
C-H second overtone	1143	O-H stretch first overtone	1908
C=O stretch fourth overtone	1160	C=O stretch second overtone	1920
C-H second overtone	1170	O-H stretch/ HOH deformation combination	1930
C-H second overtone	1195	O-H bend second overtone	1940
C-H second overtone	1215	C=O stretch second overtone	1950
C-H second overtone	1225	O-H stretch/O-H bend combination	1960
C-H combination	1360	C=O stretch second overtone	2030
C-H combination	1395	O-H combination	2070
O-H first overtone	1410	C-H combination	2090
C-H combination	1415	O-H bend/C-O stretch combination	2100
C-H combination	1417	Asymmetric (ν_{as}) C-O-O stretch third overtone	2100
O-H first overtone	1420	C-H stretch/C=O stretch combination or symmetric (ν_s) C-H deformation	2140
C-H combination	1440	Asymmetric (ν_{as}) C-H stretch/ C-H deformation combination	2170
C-H combination	1446	C-H stretch/C=O stretch combination	2200
O-H stretch first overtone	1450	O-H stretch/C-O stretch combination	2270
C=O stretch third overtone	1450	C-H stretch/ CH_2 deformation	2280
O-H stretch first overtone	1490	C-H bend second overtone	2300
O-H stretch first overtone	1540	C-H bend second overtone	2310
C-H stretch first overtone	1620	C-H stretch/ CH_2 deformation combination	2322
C-H stretch first overtone	1685	C-H stretch/ CH_2 deformation combination	2330
C-H stretch first overtone	1695	C-H stretch/ CH_2 deformation	2335
C-H stretch first overtone	1705	CH_2 bend second overtone	2352
C-H stretch first overtone	1725	C-H stretch/C-C stretch combination	2380
O-H stretch/C-O stretch second overtone combination	1820	C-H combination	2470
C=O stretch second overtone	1900		

Thus, both MIR and NIR have their own benefits and limitations. Therefore, to completely understand the whole range of spectra, it is necessary to acquire the Absorption bands of the full length of the EM spectra from UV/Vis, NIR and MIR (300-26000 nm). These Absorption bands can be obtained with the help of instruments and a few of them are discussed in the next section.

3.4 Instrumentation

This section describes in detail the various instruments, together with their principle of operations in the different parts of the EM spectra.

3.4.1 UV/Vis Spectrometer

An UV/Vis spectrometer consists of a light source, prism/diffraction grater, mirrors, sample holders and detectors. A single beam of light from a visible and/or UV light source is divaricated into its constituent wavelengths by a prism or diffraction grating. Each of these monochromatic (single wavelength) beam is then split into two equal beams of equal intensities by a mirror system. Out of which, one of the beams (sample), passes through a small transparent container (cuvette) containing the solution of the compound together with a transparent solvent. The other beam (reference), passes through an identical cuvette containing only the transparent solvent. The intensities of these light beams, I_0 (reference) and I (sample), are then measured by electronic detectors placed at the end of the instrument and a comparison is done between the two.

3.4.2 NIR Spectrometer

Infrared or Near Infrared spectroscopy is a multifaceted experimental technique which can be used to obtain spectra from samples in solution or in the solid or gaseous state. Depending on the type of sample, the different modes of NIR spectroscopy is employed:

- Transmittance
- Diffuse Reflectance
- Transflectance

For example, transparent samples are usually evaluated in transmittance mode, whereas based on the absorption and scattering properties of turbid liquids, semi-solids and solids diffuse transmittance, diffuse reflectance or transflectance, modes are used[142]. Transflectance mode is used when partially transparent samples are analyzed. These are

measured using cells with a reflecting surface (reflector). Therefore, the reflection and transmission are both taken into account which effectively doubles the sample thickness. A light source, a monochromator, a sample holder, and a detector, granting transmittance, absorption and reflectance recordings constitutes an IR spectrophotometer device as well, like the UV/Vis. They are then categorised as single beam and double beam based on their design and most of the spectrophotometers commercially available nowadays are of the latter type. A dual beam spectrophotometer has a separate holder for the reference materials that allows real-time referencing or automatic correction, which is not possible in a single beam spectrophotometer.

The first commercial UV spectrophotometer was first developed in 1941 and is as shown in Figure 3.6. It received a lot of attention and was referred to as *"probably the most important instrument ever developed towards the advancement of bioscience"* by Bruce Merrifield, Nobel laureate[143]. Since then not a lot has changed in the design of the instrument.

For the purpose of the studies conducted in this research, a range of state-of-the-art spectrophotometers/spectrometers from Perkin Elmer (*Waltham, MA, USA*) were used. These spectrometers are in the market for the last 50 years. They are as listed below:

- UV/Vis (300-1000 nm) range Lambda 1050 spectrophotometer
- NIR (800-2600 nm) range Lambda 1050 spectrophotometer and Frontier^{TM} FTIR/NIR spectrometer
- MIR (2000-500 cm^{-1} or 5000- 20000 nm) range Spectrum 2 and Frontier^{TM} FTIR/NIR spectrometer.

Lambda 1050 spectrophotometer

The Lambda 1050 spectrophotometer, as shown in Figure 3.7, has the following parts:

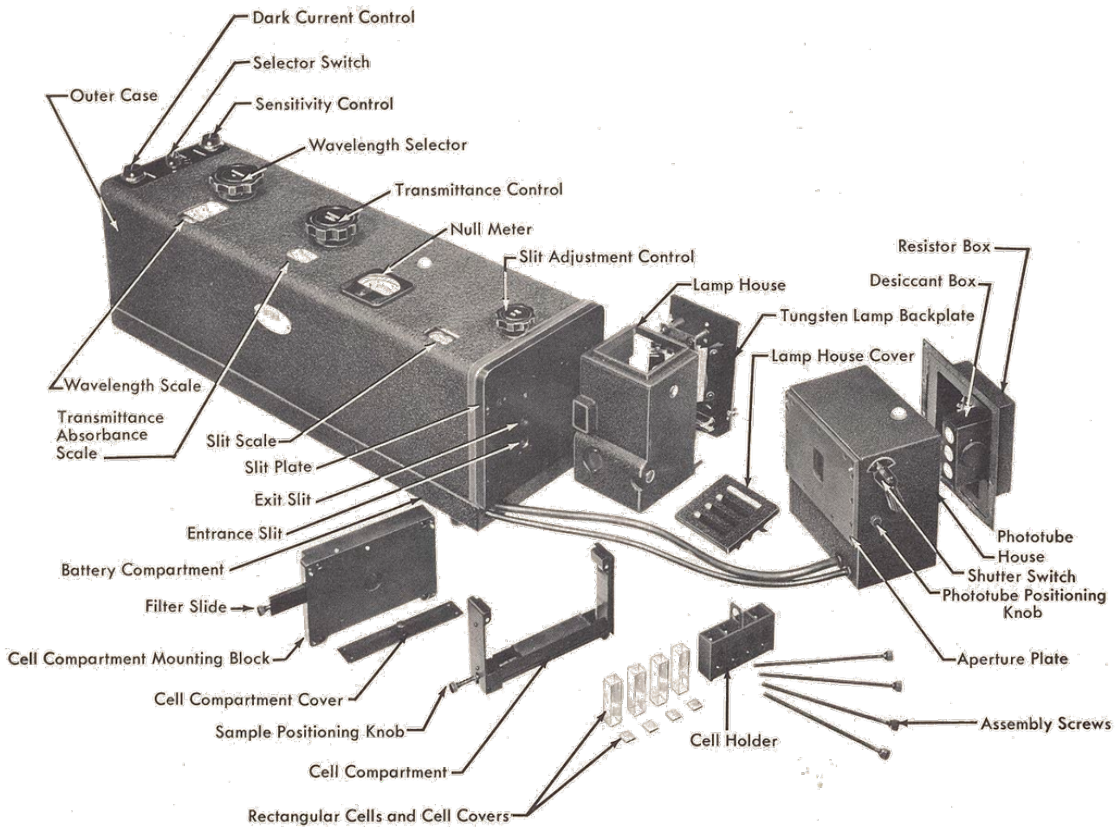

Figure 3.6: Beckman DU Spectrophotometer (Picture from the archives *Beckman Historical Collection*)[144].

Figure 3.7: The Lambda 1050 spectrophotometer, from Perkin Elmer Corp, *Waltham, MA, USA*. Picture taken from[145].

- Light source: Lambda 1050 is designed to cover a wide range of wavelengths from 175-3300 *nm* and hence, it utilizes tungsten-halogen and deuterium lamps. Deuterium lamps usually cover the UV region from 175-400 *nm* and the rest is covered by the tungsten-halogen lamp. It also exploits the use of a double-mirror system for higher sensitivity.

- Monochromator and Optical System: Double monochromators are used for wavelength selection, which usually isolates each wavelength from the large polychromatic range of wavelengths from each light source. The physical width of the slit of the monochromator determines the bandwidth of the spectra and in Lambda 1050, the bandwidth can be adjusted to ≤ 0.05 *nm* for UV/Vis. This property is mainly responsible for the resolution of the instrument. The Lambda 1050 gives 0.08 *nm* accuracy in wavelength which the *"best in class"* and thus, permits to acquire data of high resolution.

- Sample Compartment and Holder: The Lambda 1050 has two sample compartments, out of which the principle sample compartment is the biggest in all the instruments available commercially and the second sample compartment gives the flexibility for customised applications. It is very important to note that the sample holders or cuvettes which holds the sample in the compartment should be transparent in the wavelength range under consideration. For example, glass cuvettes are used in the UV/Visible region and quartz in the NIR region and the path length of the cuvettes should also be taken into consideration depending on the type of the sample. The Lambda 1050 has the flexibility in the principle sample compartment to do reflectance spectroscopy, instead of transmittance, by replacing the sample holder with fibre optic cables to do distant measurements or *in-vivo* studies. A snap-in integrating sphere can be attached to the second sample compartment which allows reflectance measurements, like diffuse and specular.

- Detectors: The various type of detectors used in a spectrophotometer are: Silicon (Photo Multiplier, PMT), Lead Sulphide (PbS) and Indium Gallium Arsenide (InGaAs). In the Lambda 1050, all the above mentioned three detectors are present in a 3-detector module to exploit each one of them for the whole spectral range. The silicon detector, PMT R6872, works in the whole UV/Vis range to 1100 *nm* and consists of multiple silicon photodiodes in the form of a single chip and can measure all the dispersed radiation of a beam concurrently. Next is a peltier-cooled PbS detector which measures the change in the electrical resistance when it is hit by a photon. It has a working range of 2500-3300 *nm* of NIR region of the spectra. Finally, there is a peltier-cooled InGaAs detector which is also the most expensive out of the three because it can combine the speed and size of the PMT detector and the wavelength range extends up to 2500 *nm*. These detectors are quite commonly used because of their sensitivity in the 1100-2500 *nm* region and a better Signal-to-Noise Ratio (SNR). The peltier cooled detectors, mentioned above, undergo thermoelectric cooling by the peltier effect and are more accurate because the process reduces thermal noise and hence increases their efficiency[145,146].

  Additionally, an 100 *mm* InGaAs integrating sphere was also used as a plug-in for the Lambda 1050, for diffuse reflectance measurements. The main purpose of using integrating sphere module over the 3 detector module was that it provides uniform detection from a sample with numerous scatterers, like whole blood.

Spectrum 2 and Frontier^{TM} FTIR/NIR spectrometer

Instruments to acquire Infrared spectra by dispersive spectrometry has been available commercially since 1940s; however, after 1960s, Fourier-transform infrared spectrometers have almost replaced the instruments measuring dispersive spectra because of three major advantages of the latter over the former. The three advantages are:

- Multiplex: An FTIR spectrophotometer has an in-built interferometer which uses a moving mirror to scan the entire infrared spectrum at one go and all the scans can be summed up to give a better accuracy of the absorbance in the spectra. This makes the FTIR much faster than its counterpart, which takes account of each wavelength (data points) in obtaining every spectrum. Moreover, repeated scans can be done in a faster way and then averaged to improve the spectrum SNR.

- Throughput: Unlike the dispersive spectrometry instrument, FTIR instruments do not limit the light from the source to reach the sample through a slit. Also, the usage of fewer mirrors limits the reflection losses of light and hence energy reaching the samples. This directly affects the SNR and it is much higher in the FTIR which makes it more sensitive for smaller peaks and as a result produces a more detailed spectrum of the same sample. This is called the Jacquinot's advantage. The SNR, which is done by signal averaging, is proportional to the square root time, is known as the Fellgett's advantage.

$$SNR \propto n^{1/2} \tag{3.11}$$

where, SNR = Signal-to-Noise Ratio,

n = Number of samples used for averaging.

- Precision: In terms of accuracy and precision, FTIR is better than its dispersive cognate because it uses a laser light source while calibrating the wavelength in the instrument. The wavelength of the laser used is of a constant value and hence the reference values of the wavelength when plotted in the absorption spectrum is constant which makes it time independent or on any other external factors, unlike

the dispersive instrument which depends on mechanical movement of diffraction gratings.

The FTIR instruments used in these study are Spectrum 2 and Frontier^{TM} FTIR/NIR from Perkin Elmer, (*Waltham, MA, USA*) with an add-on Horizontal Attenuated Total Reflection (HATR) accessory from Pike Technologies Inc, (*Madison, WI, USA*). A trough Zinc Selenide (*ZnSe*) Horizontal Attenuated Total Reflectance (HATR) accessory of 4 *mm* thickness, 80 *mm* length, 2.4 Refractive Index and 10 reflections/measurement was introduced in the systems. The HATRs are commonly used to study biological systems as it requires very small samples to provide high sensitive spectra[147].

Although both the FTIR instruments almost have the same components, the Frontier^{TM} FTIR/NIR is a more advanced version of the Spectrum 2, (Figure: 3.8).

Figure 3.8: The Frontier^{TM} FTIR/NIR spectrometer, from Perkin Elmer Corp, *(Waltham, MA, USA)*. Picture taken from[148].

.

The components of the FTIR instruments are as below:

- Light Source: Silicon Carbide based infrared lamp
- Interferometer
- Detector: Deuterated Triglycine Suflate (DTGS)
- Amplifier
- Analog-to-Digital converter
- BeamSplitter: Opt KBr (7800 - 400 cm^{-1}) for MIR and CaF_2 for NIR
- Window: KBr.

NIRQuest

Apart from the bench-top laboratory based spectrometers mentioned above, portable commercial spectrometers are available as well. The first portable commercial NIR spectrometer was introduced by Fred McClure, in 1991, which was used for measuring chlorophyll in tobacco[149,150]. NIR spectra was obtained using a Charge-Coupled Device (CCD) camera, with a silicon detector[151] and according to McClure, himself, this is the *"Age of imaging: 2000-"* for NIR technology. Ever since, there has been quite a lot of advancement in this prospective field. The recent development of 1D and 2D array solid state imaging detectors in compact integrating circuits (ICs) has revolutionized the commercial perspective of hand-held devices[152]. They allow rapid measurement, for example, the InGaAs 1D detector consisting of 512 elements, developed by Sensors Unlimited is reported to acquire as many as 30,000 spectra per second[153].

Hence, in order to carry out a feasibility study, a portable spectrometer, NIRQuest 512, from Ocean Optics (*Largo, FL, USA*), was used for reflectance *in-vivo* studies in this thesis. The NIRQuest 512, (Figure 3.9) is a portable size (182 x 110 x 47 mm) NIR spectrometer. It operates between 850 – 1700 nm with the help of an InGaAs linear array detector and fiber optic cables[154].

Figure 3.9: The NIRQuest 512 spectrometer, from Ocean Optics (*Largo, FL, USA*). Picture taken from [154].

3.5 Spectral Collection and Visualization Software

The following softwares were used for each instruments:

- UVWin Lab for LAMBDA 1050, from Perkin Elmer (*Waltham, MA, USA*)
- Spectrum 10 for Spectrum 2 and Frontier^{TM} FTIR/NIR, from Perkin Elmer (*Waltham, MA, USA*)
- OceanView 1.6.7 for NIRQuest, from Ocean Optics (*Largo, FL, USA*)

,

These softwares were used for data collection and visualisation. Once the data was collected, further analysis was done using MATLAB R2020b, MathWorks^{TM} *(Natick, MA, USA)* using a few spectral analysis techniques as discussed in the next section.

3.6 Data Analysis

The qualitative and quantitative information for correlation of all the spectra obtained by the instruments mentioned above for different lactate samples were extracted using

techniques that are described below:

3.6.1 Concentration of the Sample (Beer Lambert Law)

The instruments mentioned above provide the absorption spectrum; the values of absorption when plotted against the respective wavelength value. From this absorption profile, the concentration of the sample can be determined, which is given by the Beer-Lambert Law. The amount of light transmitted through the sample is known as Transmittance (T) and is the ratio of the light incident on the sample (I) to the light incident on the reference sample (which doesn't have the sample of interest) (I_0). As the sample of interest is not present in the reference sample, the transmittance of the reference sample is 100 %[155].

$$T = I/I_0 \tag{3.12}$$

Or

$$\%T = (I/I_0) * 100 \tag{3.13}$$

From these equations mentioned above, the Absorbance of the sample can be derived from the Beer Lambert Law which is logarithmically dependent on the transmittance as:

$$A = -log_{10}(T) \tag{3.14}$$

Or

$$A = log_{10}(I_0/I) \tag{3.15}$$

The Beer Lambert Law can be further used to determine the concentration of the sample in a solution because the absorbance is proportional to the sample concentration and the path length of the light source:

$$A = log_{10}(I_0/I) = \varepsilon lc \tag{3.16}$$

where,ε= extinction coefficient of the substance,

l = path length of the sample, and

c = molar concentration of the solution

The equation above can be rearranged to:

$$\varepsilon = A/(lc) \tag{3.17}$$

Hence, if ε is known it is possible to find the concentration of the sample from its absorbance. Usually, in IR experiments, l and ε are kept constant to quantitatively analyse c from A. Once the spectra are obtained, the next step is to understand the specific information that is usually not that evident to the naked eye. Hence a few qualitative and quantitative tools are implemented to derive necessary information from the spectra[155].

3.6.2 Pre-Treatment Techniques

A list of techniques are available for spectrum manipulation and data fetching from the available spectra, few of them are discussed below[156]:

Baseline Correction

A spectrum formed by joining the lowest absorbance points is known as a baseline spectrum. The difference between this spectrum and all the other spectrum points

which are collected are used in quantitative analysis.

Smoothing

Smoothing is used to decrease the noise in a spectrum which is generally done by lowering the resolution. This is usually carried out by the "shift and multiply" technique. In this technique, a group of adjacent points in the raw spectrum are multiplied point-by-point by a set of numbers (or coefficients) that defines the smooth shape. These products are then added up and divided by the sum of the coefficients, which becomes one point of smoothed data. The set of coefficients are then shifted to the next point in the raw spectrum and the process is repeated till the last wavelength.

Difference Spectra

This is the simplest method for spectral manipulation where one spectrum is subtracted from the other to manifest the peaks of a certain component which might be present in one and not in the other.

Derivatives

Spectral first derivative of a raw spectrum amplifies the resolution of the spectrum by removing the additive baseline shift. However, these are difficult to interpret as it produces peaks, where there were originally a maximum slope and crosses zero, where there was a peak. The second derivative is much easier to follow because it gives negative (or opposite in direction) peaks for each crest and troughs in the spectrum and hence, is more frequently used. Both the first and second derivative of the same raw spectrum could be seen in Figure 3.10.

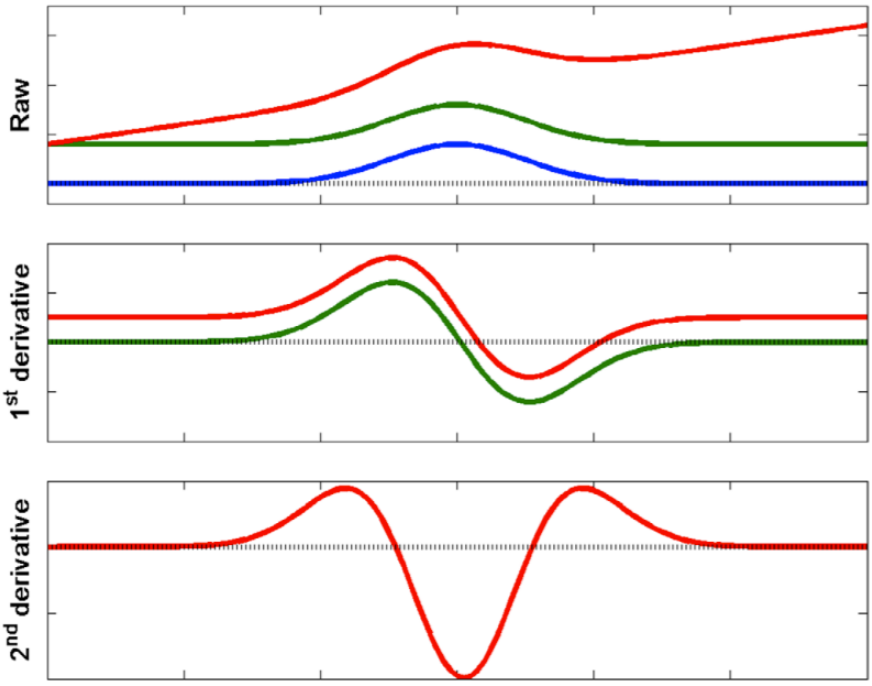

Figure 3.10: The 1^{st} and 2^{nd} derivative of the raw spectrum. Picture taken from[157].

Deconvolution

This technique helps in identifying closely spaced features in the spectrum, as a measured spectrum, F_{ms} is usually a convolution of a true spectrum, F_{ts} combined with instrumental function K(x-x').

$$F_{ms}(x) = \int_{-\infty}^{\infty} K(x - x')F_{ts}(x')dx' \tag{3.18}$$

where, x = abscissa of the spectrum (the spatial domain) (e. g., wavelength),

F_{ms} = Measured Signal,

K is the kernel,

F_{ts} = True Signal[158].

Curve-Fitting

Curve fitting of spectroscopic data is usually performed in order to reduce the data by summarizing a large set of points by an analytical function with a few adjustable parameters. These functions are mostly arbitrarily chosen, however, the adjustable parameters represent some molecular constant and the functions are algebraic representations of a physical model. These molecular constants estimated from one model can be used to derive another model which contains the same parameters.

3.6.3 Qualitative/Quantitative Techniques

There are a few qualitative or quantitative techniques for analysis of spectral data.A few of which are mentioned below:

1. Qualitative Analysis Techniques
    (a) Unsupervised Learning; e.g. Graphical Methods, Cluster Analysis by Principal Component Analysis (PCA),
    (b) Supervised Learning; e.g. Discriminant Analysis, Soft Independent Modelling of Class Analogy (SIMCA), K Nearest Neighbours Method (KNN).
2. Quantitative Analysis Techniques
    (a) Multiple Evaluation
        i. Linear Methods; e.g. Classical Least Squares Regression (CLS), Inverse Least Square Regression (ILS), Principle Component Analysis (PCR), Partial Least Square Regression (PLS),
        ii. Nonlinear Methods; e.g. Linearisation, non-linear regression, neural networks.
    (b) Univariate Methods.

3.7 Spectral Analysis

The analysis of the data reported in the following chapters of the studies were carried out with the help of a software system developed in the Research Centre for Biomedical Engineering, City, University of London. The following techniques were used after various pre-treatment (as required):

- 2D Correlation
- Aquaphonomics
- Linear Regression
- Partial Least Square (PLS).

All of these techniques are described in detail in the next section.

3.7.1 2D Correlation Analysis

2D correlation, 2DCoS, is a tool which helps in deconvolution of the spectrum and identify the comparison between different external stimuli in the sample solution. There are two parts in this spectrum (as shown in Figure 3.11), given by the equation:

$$X(\nu_1, \nu_2) = \Phi(\nu_1, \nu_2) + i\Psi(\nu_1, \nu_2) \tag{3.19}$$

where, $\Phi(\nu_1, \nu_2)$ represents the synchronous part and
$\Psi(\nu_1, \nu_2)$ represents the asynchronous part.

- Synchronous: This part delineates simultaneous or coincidental changes in the spectra. The peaks are always symmetric along the diagonal, giving information like autocorrelation (intensity of the peaks) portrays the strength and the cross

peaks (peaks off the diagonal) denotes the correlation. This part is given by the equation:

$$\Phi(\nu_1, \nu_2) = 1/(m-1) \sum_{j=1}^{m} \tilde{y}_j(\nu_1).\tilde{y}_j(\nu_2) \tag{3.20}$$

where, ν_1, ν_2 are spectral channels,

$\tilde{y}_j(\nu_i)$ is the spectral intensity at a point of physical variable t_j,

m = number of signals in the original data-set.

- Asynchronous: This part delineates progressive changes in the spectra. It's asymmetrical along the diagonal and the cross peak shows positive value when the peak from the first spectrum is more intense as compared to the next one or vice versa[159]. This part is given by the equation:

$$\Psi(\nu_1, \nu_2) = 1/(m-1) \sum_{j=1}^{m} \tilde{y}_j(\nu_1). \sum_{j=1}^{m} N_{jk}\tilde{y}_k(\nu_2) \tag{3.21}$$

where, N_{jk} corresponds to the j^{th} row and k^{th} column element of the discrete Hilbert-Noda transformation matrix given by

$$N_{jk} = \begin{cases} \{0, j = k \\ 1/\pi(k-j), otherwise. \end{cases}$$ [160]

3.7.2 Aquaphotomics

Near Infrared Absorption/Reflectance Spectroscopy (NIR) has a major disadvantage for studying biological samples as most of the contents is liquid water[162]. The dominant absorption of O-H overtone bands of water in the NIR region presents a challenge and complicates the accurate detection of other absorbers, such as lactate.

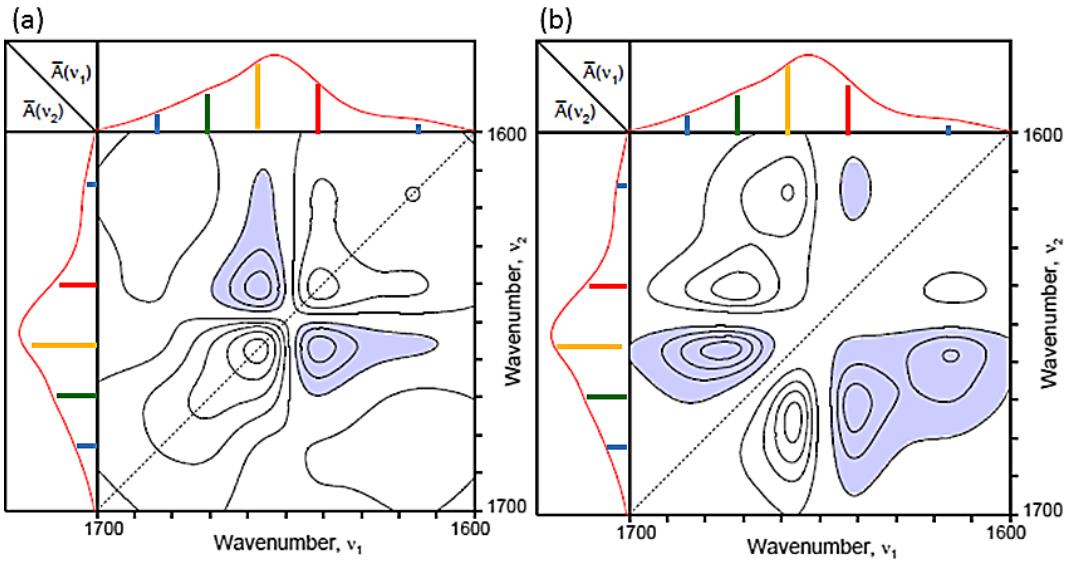

Figure 3.11: An example of (a) Synchronous and (b) Asynchronous 2D correlation spectrum. Picture taken from[161].

However, 'Aquaphotomics', which was developed in 2005 in Japan by Professor Roumiana Tsenkova, as a novel approach for estimating the solutes in an aqueous solution indirectly, by mapping the external perturbations in the water absorbance bands[163]. These maps, specially in the first overtone absorption band of O-H (1300-1600 nm), uncouples the latent information.

A few definitions (or parameters) to understand the taxonomy of this approach:

- Water Absorbance Bands (WABS): These are the raw NIR spectra of all the perturbed samples in the spectral region of 1300-1600 nm,
- Water Matrix Absorbance Coordinates (WAMACS): These are the 12 identified coordinates within the WABS, which reflects the activation due to perturbation in the system
- Water Absorbance Spectral Pattern (WAPS): The spectral patterns produced by the activated WAMACS, which are pertinent to the chosen aqueous system
- Aquagrams: They are the maps which are produced by the WAMACS[164].

Table 3.2: assignments to the 12 identified Water Matrix Absorbance Coordinates, WAMACS (C_1 to C_12) in the first Water Absorbance Bands, WAB (1300 to 1600nm) according to Aquaphotomic principles. Table taken from https://www.aquaphotomics.com/aquaphotomics-method/

WAMACS	Range (nm)	Assignment of Chemical/Molecular conformations
C_1	1336-1348	ν_{as} (H_20 asymmetric stretching vibration)
C_2	1360-1366	OH-$(H_2O)_{1,4}$ (Water solvation shell)
C_3	1370-1376	ν_s+ν_{as} (H_20 symmetric and asymmetric stretching vibration)
C_4	1380-1388	OH-$(H_2O)_{1,4}$ (Water solvation shell) O_2-$(H_2O)_4$ (Hydrated superoxide clusters) ν_s (H_20 symmetric stretching vibration)
C_5	1398-1418	Water confined in a local field of ions (trapped water) S_0 (Free Water) Water with free hydroxyl OH^- side groups
C_6	1421-1430	Water hydration band H-OH bend δ and O-H ... O
C_7	1432-1444	S_1 (Water molecules with 1 hydrogen bond)
C_8	1448-1454	OH-$(H_2O)_{4,5}$ (Water solvation shell)
C_9	1458-1468	S_2 (Water molecules with 2 hydrogen bonds) $\delta + \nu_{as}$ (Bending and asymmetrical stretching vibration)
C_{10}	1472-1482	S_3 (Water molecules with 3 hydrogen bond)
C_{11}	1482-1495	S_4 (Water molecules with 4 hydrogen bond)
C_{12}	1506-1516	ν_s (H_20 symmetric stretching vibration) δ (H_20 bending vibration) Strongly bound water

This technique has been used to understand several fundamental biological systems till date. Table 3.2 shows assignments of chemical/molecular conformations to the 12 identified WAMACS (C_1 to C_{12}) in the first WAB (1300 to 1600nm).

3.7.3 Linear Regression

A hypothesis was tested by regressing the concentration of lactate which causes statistically significant changes on the absorbance values at different wavelengths. The hypothesis was that the absorbance values at these wavelengths of interest were linear, which in turn was correlated to the concentration of lactate using the Beer-Lambert law 3.6.1. This was performed using the equation:

$$y_i = beta_0 + beta_1 * x_{wi} \tag{3.22}$$

Where,

x_{wi} is absorbance at wavelength wi,

Y_i is the concentration of lactate

$beta_0$ and $beta_1$ are the coefficients.

The p-values, which are statistical significance markers, for the hypothesis test were valued at ≤ 0.05 for a 95 % confidence interval[165]. The p-values reported in this thesis are ≤ 0.05 and all the other values are reported as 'Not Significant' for ease of differentiating.

3.7.4 Partial Least Square (PLS)

This method uses mathematical equations and establishes relationship between the input and output variables by creating predictive models[166].

PLS is a quantitative analysis method which builds models based on extracting Latent Variables (LV). These LVs correlate with known input variables, like concentrations of lactate, with the spectral features linearly describing the co-variance in a descending order[167].It is given by the equations:

$$X = TP^T + EY = UQ^T + F \tag{3.23}$$

X = nxm matrix of predictors (e.g. concentration of lactate),

Y = nxp matrix of responses (e.g. Absorbance values),

T and U are nxl matrices that are projections of X (x scores) and Y (y scores),

P and Q (mxl) and (pxl) orthogonal loading matrices,

E and F are error terms which are independent and identically distributed.

The LVs perform a dimensionality reduction of the independent variables and Prediction Error Sum of Squares (PRESS) is used to determine the optimal number of LVs to be used for each set of data. This process eliminates with the possibility of over-fitting the curve. From a fitted model, each of the predictors, x_i, i=1,2,...n, is removed and the model is refitted to the n-1 points. The predicted value $\tilde{y}_{i,-i}$ is calculated at the excluded point x_i and the PRESS statistic is given by[168]:

$$PRESS = \sum_{i=1}^{n} y - \tilde{y}_{i,-i}{}^2 \tag{3.24}$$

The PLS model used for the studies in this thesis was validated by leave-one-out cross-validation method, where one of the spectrum is kept aside for testing and the rest of the spectra in a particular set are used to develop a predictive model. The model is then used to predict the value of the test spectrum. This process is repeated N times, where N is the number of spectra in the data-set.

The accuracy or the predictive ability of the calibration model is determined by the coefficient of determination (R^2), the Root Mean Squared Error of Cross Validation (RMSECV) and Root Mean Squared Error of Prediction (RMSEP). By definition, R^2 is an indication of the percentage of the variation in Y variables (for example, the predicted concentrations of lactate) which can be explained by or attributed to all of the X variables (for example, observed/actual concentrations of lactate)[169]. While, RMSECV and RMSEP are measures of the quality of the fit in the particular model[170]. These can be determined using the following equations:

If $\bar{y}$ = mean of the observed data:

$$\bar{y} = \sum_{i=1}^{n} y_i \tag{3.25}$$

The total sum of squares (or variance of the data) is given by:

$$SS_{tot} = \sum_i (y_i - \bar{y})^2 \tag{3.26}$$

The sum of residuals, also known as residual sum of errors

$$SS_{res} = \sum_i (y_i - f_i)^2 \tag{3.27}$$

Then the Coefficient of Determination R^2 is given by

$$R^2 = 1 - SS_{res}/SS_{tot} \tag{3.28}$$

If, C_i is an observed value and ĉ is the predicted value, then the Root Mean Squared Error of Cross Validation, RMSECV value is given by:

$$RMSECV = \sqrt{(\sum_{i=1}^{i=N} (\hat{c} - c_i)^2)/N} \tag{3.29}$$

3.8 Summary

This chapter explains in detail the history, principle, theory and instrumentation of Ultraviolet (UV) and Infrared (NIR and MIR) vibrational Spectroscopy. The chapter also introduces the spectrometers which will be used in the studies described later for this thesis. Finally the chapter presents a few pre-treatment and qualitative and quantitative techniques for spectral analysis. The basics of this chapter will be used throughout the studies described in the thesis.

The philosophies of one age have become the absurdities of the next, and the foolishness of yesterday has become the wisdom of tomorrow.

William Osler, Aequanimitas 'Chauvanism in Medicine' 1914:288

4

Spectroscopy in Lactate Detection

4.1 Introduction

Lactate can act as a very important haemodynamic marker. As seen in Chapter 2 and by using the principles of Spectroscopy (Chapter 3) there is a potential for non-invasively measuring lactate levels precisely. Since the first sensing technique that has been developed for measuring lactate/lactic acid, a lot of research and development has been done towards chemical sensing of this metabolite. However, recent developments towards non-chemical lactate sensing/monitoring has gained a lot of in-

terests. This chapter aims to provide discussions at length about the current state-of-the-art technology for lactate measurements, focusing on the commercial devices that are available for lactate measurements in critical care and helps identify the gaps for the requirement of a rapid, non-invasive and continuous lactate monitoring sensor. At this stage of technological developments, non-chemical (Electromagnetic wave) sensors insinuates to address the disadvantages posed by the chemical sensing of lactate. Hence, this chapter also identifies and throws some light on the research and development of these type of sensors and concludes that Absorption Spectroscopy can be a way forward with additional research.

4.2 History

Lactate/Lactic Acid detection or monitoring has been a source of interest in the biomedical industry for many decades because lactate/lactic acid serves as an indicator for ischemia in critical care medicine, an indicator for physical training status in sports physiology, as a bio-marker for sleep and space medicine, etc. Lactate biosensors have been developed using various chemical transdution methods like colorimetric method, chemiluminescence, fluorimetric method, high performance liquid chromatography (HPLC) and magnetic resonance spectroscopy, etc[171]. However, electrochemical (amperometric and potentiometric) and optical (fluorescence and electro-chemiluminescence) sensing of lactate/lactic acid has gained considerable accentuation in the past few decades because of simplicity, integration and portability of the instrument/sensor.

It was Broader and Weil who reported the first optical sensing of lactate in whole blood in 1964. In the study, they used a Beckman DU Spectrophotometer, as seen in Figure 3.6. The study was based on the estimation of changes in the UV transmitted light through the sample using the principles of Beer-Lambert Law, (Chapter 3, Section 3.6.1)[102]. Although the UV-lactate sensing method became very popular during those

times, the major disadvantage posed by this method was that the sample had to be optically clear and hence, most of the constituents in blood, like proteins and cells, had to be precipitated or dialysed out. Hence, electrochemical-enzymatic methods attracted the attention of researchers due to the ability of the sensors to measure a wide range of concentrations directly in whole blood.

The first amperometric electrochemical sensing of L-lactate in blood using lactate dehydrogenase (LDH) enzyme was developed in 1970 by Williams et al[172]. Following the success of which the first potentiometric electrochemical enzyme electrode for lactate was developed by Shinbo et al in 1979 by coating a film of LDH-gelatin in the membrane of the sensor[173]. Both of these methods monitored the changes in the concentration ratio of the electron acceptor element (ferricyanide to ferrocyanide) due to the oxidation of lactate to pyruvate in the redox reaction:

$$\mathrm{Lactate^{-1}} + 2\,\mathrm{Fe(CN)_6^{3-}} \xrightarrow[\text{dehydrogenase}]{\text{lactate}} \text{pyruvate} + 2\,\mathrm{Fe(CN)_6^{4-}} + 2\,\mathrm{H^+} \qquad (4.2.1)$$

$$2\,\mathrm{Fe(CN)_6^{4-}} \xrightarrow{\mathrm{Pt}} 2\,\mathrm{Fe(CN)_6^{3-}} + 2\,\mathrm{e^-} \qquad (4.2.2)$$

The next section explains in detail the mechanisms of electrochemical and optical methods of lactate sensing.

4.3 Current State-of-the-Art Lactate Sensing

Most of the current state of the art lactate monitoring/ sensing devices uses chemical sensing techniques like electrochemical or optical transdution methods.

4.3.1 Electrochemical biosensors *(Few Definitions)*

According to the Technical Report (1999) of International Union of Pure and Applied Chemistry (IUPAC) on "Electrochemical Biosensors: Recommended Definitions and Classification",

"A *biosensor* is an integrated receptor-transducer device, which is capable of providing selective quantitative or semi-quantitative analytical information using a biological recognition element Fig 4.1."

"An *electrochemical biosensor* is a biosensor with an electrochemical transducer. The transducer is considered to be a Chemically Modified Electrode (CME) of electronic conducting, semiconducting or ionic conducting material and is coated with a biochemical film."

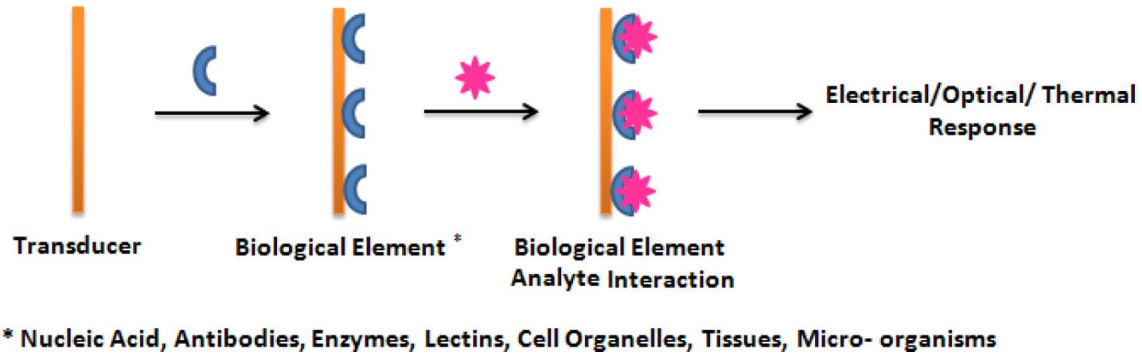

Figure 4.1: The components of a Biosensor: (a) Transducer: for signal conversion/quantification, (b) Biological Element and (c) Biological Element Analyte Interaction: for selectivity and sensitivity towards a specific analyte, and finally (d) Electrical/Optical/Thermal Response. Picture taken from[171].

"*Amperometry* is based on the measurement of the current resulting from the electrochemical oxidation or reduction of an electroactive species. It is usually performed by maintaining a constant potential at a Pt-, Au- or C-based working electrode or an array of electrodes with respect to a reference electrode, which may also serve as the auxiliary electrode, if currents are low (10^{-9} to 10^{6} A). The resulting current is directly correlated to the bulk concentration of the electroactive species or its production or consumption rate within the adjacent biocatalytic layer. As biocatalytic reaction rates

are often chosen to be first-order dependent on the bulk analyte concentration, such steady-state currents are usually proportional to the bulk analyte concentration."

"*Potentiometric* measurements involve the determination of the potential difference between either an indicator and a reference electrode or two reference electrodes separated by a permi-selective membrane, when there is no significant current flowing between them. The transducer may be an Ion-Selective Electrode (ISE), which is an electrochemical sensor based on thin films or selective membranes as recognition elements[174]."

Amperometric lactate sensors

As stated in the IUPAC definition of an amperometric electrochemical biosensor, a current is generated from a redox reaction of an electro-reactive reagent. The electro-reactive reagent is consumed by an enzyme to generate an electro active species which is monitored and correlated with the concentration of lactate. The two main enzymes used in a lactate assay are Lactate Oxidase (LOD) and LDH in the redox reactions mentioned below[175]:

$$\mathrm{L{-}Lactate} + \mathrm{O_2} \xrightarrow[\text{oxidase}]{\text{L-lactate}} \text{pyruvate} + \mathrm{H_2O_2} \tag{4.3.1}$$

$$\mathrm{H_2O_2} \longrightarrow \mathrm{O_2} + 2\,\mathrm{H^+} + 2\,\mathrm{e{-}} \tag{4.3.2}$$

and

$$\text{L}-\text{Lactate} + \text{NAD}^{+} \xrightarrow[\text{dehydrogense}]{\text{L-lactate}} \text{pyruvate} + \text{NADH} \tag{4.3.3}$$

As seen in the above reactions, when LDH is used as an enzyme for lactate detection, an additional mediator/co-factor ($ferricyanide, NAD^{+}, etc.$) is required. The mediator helps interchange of the electrons to and from the electrode and the enzyme in the system. However, it is difficult to integrate the mediators in the biosensor and hence, LOD based biosensors are preferred[175]. For LOD enzyme sensors, hydrogen peroxide (H_2O_2) is detected which is oxidised to produce a current proportional to the concentration of lactate. This process usually requires a high over-potential and hence causes interference by readily oxidizable species and requires additional electrode protection by a membrane[175].

In an extensive review done by Nikolaus and Strehlitz in 2007, on amperometric lactate biosensors, they have categorised the sensors (from 1974 to 2007) based on the construction of the sensors into the following: (a) enzyme, (b) mediator/co-factor, (c) electrode (working) material, (d) electrode set-up, (e) potential; pH and temperature (f) Sensitivity; geometric area of working electrode (g) Lower detection limit; linear range; response time (h) Operational stability; storage stability (i) Interference; protection against interference and (j) application[176]. Out of the 196 studies, taken into consideration, 50.5 % of the amperometric lactate sensors have been reported to have stated their measurements in buffers only and 14.8 % relate to medical applications. Again, amongst the ones which are related to medical applications, 24.1 % are LDH and 75.9 % are LOD enzyme based lactate biosensors, with mostly Ag/AgCl as reference electrodes and Platinum or Carbon-based electrodes as working electrodes, in a 2 or 3 electrode system. In the end, they suggested that with preponderant research in this field, the availability of commercial amperometric lactate sensors are going to increase.

In another review by Rathee et al. in 2016, the reported amperometric lactate biosensors (from 2007-2016) were again categorised in a similar manner and 26 % were related to medical applications[171]. The listed were categorised based on membrane, non-conducting polymer matrices, conducting polymer, sol-gel, hydro-gel, screen printed and nano-particle based L-lactate biosensors. They concluded the discussion with the hope that nanoparticle based amperometric lactate sensors might pave a way for semi-invasive or non-invasive commercial devices.

The most recent screen printed single use electrochemical amperometric L-lactate sensor was reported by Theuer et al in March 2020. They believe that the proposed novel design could be used for mass production of these type of sensors for POC measurements[177].

The major drawback of amperometric lactate sensors lies on the fact that the enzymes tend to get unstable over time and there is always a need for mediators/co-factors[178].

Potentiometric lactate sensors

In a potentiometric electrochemical biosensor, an ion-selective membrane is attached to the transducer for selective screening of the ionic species. The primary advantages of a potentiometric lactate biosensor over an amperometric lactate biosensor are: membranes are more flexible and mechanically durable for a wide range of pH, they are highly selective with a greater response amplification[171].

Ever since the first potentiometric lactate biosensor, various miniaturized lactate selective membranes have been developed in the last decade for mass production[175]. The latest portable, non-invasive potentiometric lactate biosensor has been reported in 2017 by Onor et al, for determination of lactate in sweat[178]. They used screen printed carbon electrode in a three electrode system (Ag/AgCl as pseudoreference electrode and Carbon as working and counter electrodes).

These type of sensors are usually bulky and heavily dependent on temperature.

4.3.2 Optical biosensors

An optical biosensor senses the number of photons involved in a product depletion/reactant formation on a sensing surface which emanates due to enzymatic reaction of a biocatalytic process[179]. Most of the optical lactate sensors employ fluorometric or (electro)chemiluminescense principles as trasdution strategies.

Fluorometric lactate biosensors

Fluorescence based biosensors are based on either the intensity of an emitted light source or the lifetime of fluorescence after a period of excitation by a light source of known wavelength. The concentration of the desired analyte is related to the fluorescence intensity by the well-known Parker equation[179]:

$$L = 2.31 I_0 \phi \varepsilon [C] l k \tag{4.3.4}$$

where,L= Fluorescence Intensity,

I_0= intensity of the excitation light,

ϕ = luminescence quantum yield,

ε = molar absorbance of the analyte at an excitation wavelength,

[C] = concentration of the desired analyte,

l= path length of light through the solution, and

k= an instrumental constant

Hence, from the above equation, it can be seen that the fluorescence intensity is directly proportional to the desired analyte concentration. Most fluorometric lactate biosensors exploits the property of the coenzyme of lactate dehydrogenase, NADH, which absorbs 340-360 nm wavelength of light and fluorescences at about 450-460 nm. As seen in Equation 4.3.1, equimolar concentrations of NADH and lactate are formed during the

chemical process and hence the molar absorptivity of NADH could indirectly predict the concentration of lactate[180].

Again in 1988, a novel fluorometric optical sensor for the detection of generation or consumption of NADH using a fibre-optic probe tip was developed by Wangsa and Arnold[181]. This method paved the way for the development of numerous NADH based sensors for reasons like: (a) absence of electrical connections and electrical interferences, unlike electrochemical sensors; (b) does not need a 'reference signal', unlike potentiometric sensors; (c) these sensors can be adopted for *in-vivo* applications and can be miniaturized; and (d) they can also be used for remote monitoring. However, a few disadvantages of fibre optic sensors can be listed as follows: (a) unless they are operate in a dark environment, ambient light may cause interferences in the signal; (b) the stability of these sensors depends on the reagent photobleaching or washout; and (c) pH dependence of these sensors makes them have a smaller dynamic range[182].

The other type of fluorometric lactate sensor is based on luminescence/fluorescence quenching, the relationship between intensity or lifetime when a quencher is present or absent can be given by the Stern and Volmer equation[179]:

$$I_0/I = 1 + K_{SV}[Q] = \tau_0/\tau \tag{4.3.5}$$

where, I_0 and I = luminescence intensities in the absence and presence of quencher Q, respectively,

K_{SV} = the Stern-Volmer constant,

[Q] = quencher concentration, and

τ_0 and τ= luminescence lifetimes in the absence and presence of quencher Q, respectively.

These type of sensors are mostly independent of pH in the physiological range but the detection limit of lactate is lower than most of the commercial devices available.

(Electro)chemiluminescence lactate biosensors

In an (electro)chemiluminescence sensor, the number of photons are calculated and analysed which are generated due to an exothermic electrochemical reaction. The electrochemical oxidation reaction is mainly due to the presence of oxygen or hydrogen peroxide, H_2O_2. The intensity of the photons produced in the reaction corresponds to the concentration of either one or all of the reagents involved in the reaction.

$$\mathrm{R + B} \xrightarrow{\text{catalyst}} \mathrm{P^*} \longrightarrow \mathrm{P + h\nu} \tag{4.3.6}$$

In the reaction above, R and B represent the reagents, P^* and P are the intermediate products and products produced in the reaction, respectively and hν represents the energy released during the exothermic reaction[183].

These type of biosensors have been used for noninvasive and disposable lactate biosensor development owing to their ease of instrument set-up, considerably low detection limits and a wide operation range. The latest development of an (electro)chemiluminescence lactate biosensor was done by Yao et al, in 2017, where they fabricated a cloth based sensor for detection in saliva[184]. However, these lactate biosensors are not reagent selective and are highly environment (pH and temperature) dependent.

There exists a wide range of lactate analysers which are available commercially and are mainly based on one of the transdution strategies discussed above. A few of those devices are discussed in the following section.

4.4 Current Commercial Devices

Arterial Blood Gas (ABG) analysis (blood sampling of arterial blood) and sometimes by venepuncture (blood sampling of venous blood) are common ways of collecting blood for

lactate detection. ABG analysis is more pronounced in critical care and blood is most commonly collected from the radial artery (more often) in the wrist, the brachial artery in the arm; or less often, the femoral artery in the groin. Blood is usually collected into heparinized syringes and can also be taken from an arterial catheter if it has already been placed in one of these arteries. The ABG analysis gives us several results but blood lactate and pH levels together are indicators of the condition of metabolic pathways.

The traditional laboratory devices adopts enzymatic amperometry as a transdution strategy, as discussed in the section 4.3.1. Two of the commercial devices used in our studies which were used to cross-validate the concentration of lactate solutions made by solution stoichiometry, adopts the same approach.

The concentrations of lactate in buffer solutions were verified using the bench-top LM5 lactate analyser from Analox Instruments Limited, (*Stourbridge, UK*), Figure 4.2. For the *in vitro* studies for human serum and whole blood, the Blood-Gas Analyser (BGA), ABL 825 from Radiometer UK Limited (*Crawley, UK*), Figure 4.3 was used. This is the gold standard in lactate measurement, as used in critical care. Finally, a hand held analyser Lactate Pro 2 from Arkay Inc, (*Flat Rock, MI, USA*) was used for the *in vivo* study for rapid measurements and low blood sample volume.

Figure 4.2: The LM5 lactate analyser from Analox Instruments Limited, (*Stourbridge, UK*). Picture taken from [185].

Figure 4.3: The Blood-Gas Analyser (BGA), ABL 825 from Radiometer UK Limited (*Crawley, UK*). Picture taken from[186].

All of these devices are Point-of-Care (POC) devices which measure the amount of hydrogen peroxide with a membrane containing an enzyme, as seen in equations 4.3.1 and 4.3.1. The oxidation of hydrogen peroxide, produced during the reaction of L-lactate and the enzyme, generates an electrical signal which is equivalent to the concentration of L-lactate levels in the sample. This method is used in all POC devices and takes a few minutes to deliver the results. The most common ones used in a hospital laboratory are: : Nova Stat Prime, Nova Biomedical, (*Waltham, MA, USA*[188,189]; RAPIDLab 1200 Systems, Siemens Healthcare Limited, (*Erlangen, Germany*); and ABL 8xx, Radiometer, (*Copenhagen, Denmark*)[190].

Apart from these devices, there are a few hand-held devices available commercially

Figure 4.4: Lactate Pro 2 hand held lactate analyser from Arkay Inc, (*Flat Rock, MI, USA*). Picture taken from[187].

for lactate sensing. In a comparative study done in 2015 by Bonaventura et al, six of these were tested for their reliability and accuracy; Lactate Pro and Lactate Pro 2, Arkay Global Business (*Kyoto, Japan*), Lactate Scout+ EKF Diagnostics (*Cardiff, UK*), StatStrip Xpress Meter, Nova Biomedical, (*Waltham, MA, USA)*, the Edge, Woodley Equipment Company Ltd, (*Lancashire, UK*) and i-Stat, Abbott, (*Chicago, IL, USA*) against ABL90, Radiometer, (*Copenhagen, Denmark*). They came to a conclusion that not a single hand held analyser was accurate, however, StatStrip Xpress Meter and the Edge had low biases for concentrations of lactate between 0-10 mM and hence could be potentially used for clinical purposes[101].

As can be seen above, all of the commercial devices available in the market for clinical applications require blood sampling for measurements. There are some factors to consider which can potentially affect the concentration of lactate in blood samples, some of which are listed below:

Blood Collection Technique: Special training is required for arterial blood collection or cauterisation considering patient safety and comfort. In critical care, when sampling patients with an intravenous catheter, contamination with intravenous fluids should be avoided, which can potentially affect the plasma lactate concentrations. Also, patients

who are struggling, trembling or having a vascular occlusion can give a false elevated lactate concentration reading[191,192].

Sampling Sites: Lactate concentrations can be measured in whole blood (refers to the mean concentration of intra erythrocytic and plasma lactate fractions following red blood cell lysis), plasma or serum. Usually in clinical practices, whole blood (without lysing) is used and hence, only report the plasma lactate concentrations; to make the process faster[49].

Sample Types: Blood collected from the arteries as mentioned before, is considered the gold standard for lactate concentrations in clinical measurements. Venous samples have been also compared and studied by groups across many years and now can be concluded that the samples from central vein or pulmonary artery with concentrations of normal or marginally increased ($< 2.0\ mM$) lactate levels, can be clinically accepted[192]. However, capillary samples, which are used in most all hand held POC devices show much higher concentrations compared to artery samples (from –0.11 mM to 1.32 mM) which varies between different studies[49].

Sample Handling: Once the samples are collected, the concentrations of lactate also depends on the time of measurement because the cells in blood utilize the glucose that is available to produce lactate; eventually increasing the concentration[49]. The concentration levels of whole blood collected in heparinized tubes increases by 0.2–0.5 mM (1.8–4.5 mg/dL) per 30 minutes at room temperature[193,194]; which can be reduced to 0.2 mM (1.8 mg/dL) after 120 minutes if stored in an ice bath. Hence, the measurements are advised to be done within 15 minutes of blood collection in dry, lyophilized lithium heparin or sodium fluoride (which is an inhibitor of in-vitro glycolysis) coated, commercially available tubes.

It can therefore be concluded that at present, lactate measurements are carried out using medical devices that require a blood sample to perform each measurement. These

procedures are invasive, time consuming and inhibit continuous monitoring of lactate. There is also a potential for bias because of the sample itself. There is a significant demand for a sensor technology with simple, direct, continuous measurements, rapid response, high specificity, low cost and minimal or no sample preparation for lactate concentration measurements, specially in critical care. Most of these demands can be answered by lactate sensing through non-invasive means, specially Absorption Spectroscopy, which could be directly used to measure lactate from the skin as light has the capacity to probe inside tissues and fetch information from blood, beneath it. This will also enable continuous monitoring of lactate.

4.5 Non-Invasive Lactate Biosensors

As could be seen in the previous section, the limitations of the current commercial devices available are mostly due to the fact that they are invasive and hence, a lot of research has been directed towards non-invasive lactate sensing/monitoring. While tears[195], saliva[196,197], sweat[198,199,200], skin[201], exhaled breath[202] and interstitial fluids[203,204] have been reported as appropriate sampling sites, the transdution strategies used are based on chemical sensing, as discussed above.

Non-chemical sensors based on understanding the properties and behaviour of lactate in different bands of the Electromagnetic (EM) Spectrum, mostly, Near Infrared (NIR) and Microwave frequencies and Magnetic Resonance Spectroscopy[205,206,207,208,209] have also been studied extensively, for non-invasive detection of lactate. In fact, the first commercial non-invasive, wearable sensor technology is based on NIRS light emitting diode (LED) detection of lactate. Absorption Spectroscopy has also been studied by different groups around the world to understand the *fingerprinting* of lactate molecule in different media; such as buffered solutions, plasma and human blood with a few successful attempts. Although these non-chemical sensors are aimed for investigation of lactate for

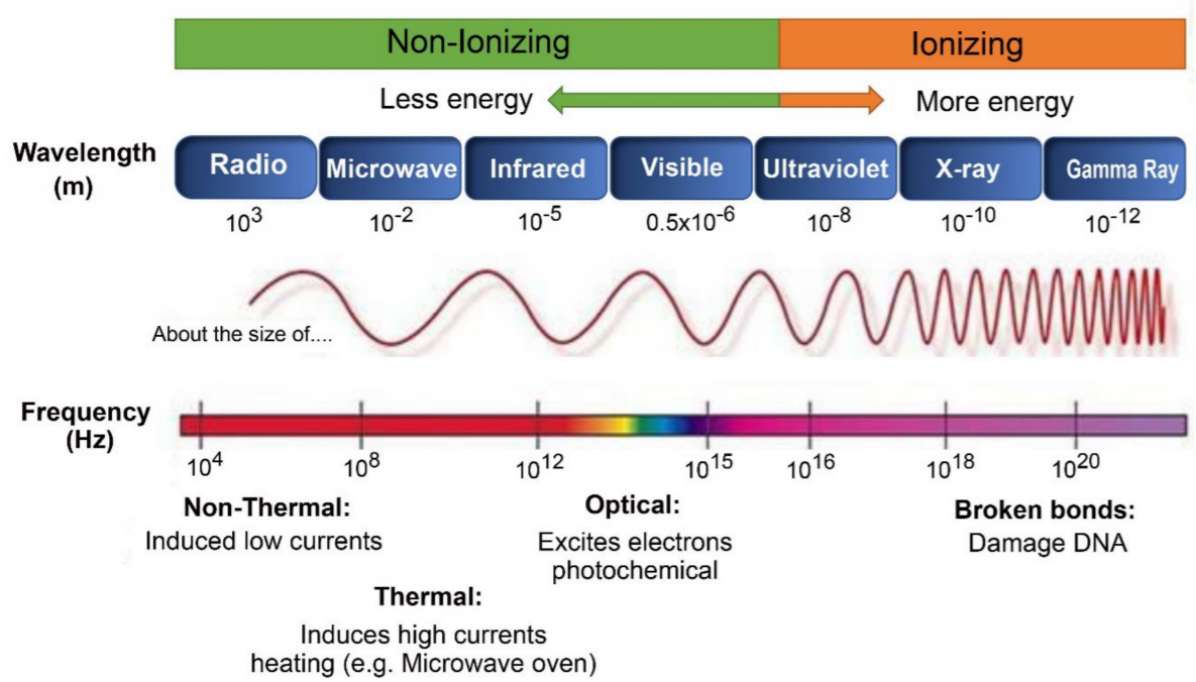

Figure 4.5: The Electromagnetic Spectrum (schematic representation) from the Radio (Wavelength: $10^3 m$, Frequency: 10^4 Hz) to the Gamma Rays (Wavelength: $10^{-12} m$, Frequency: 10^20 Hz). The Microwave, Infrared and Visible are Non-Ionizing waves, whereas, the Ultraviolet has more energy and can Ionize a molecule. Picture taken from[210].

clinical applications, right now most of these sensors are tested for understanding the variations of lactate concentrations for exercise physiology.

The next section discusses the transdution strategies based on the EM wave lactate sensing.

4.5.1 Electromagnetic wave biosensors

The Electromagnetic Spectrum (Figure 4.5), has been divided and studied by exploiting the different properties of light-matter interactions in the different bands. Properties like permittivity or reflected/transmitted light which are unique to a specific biomolecule are identified and measured.

According to the *The Authoritative Dictionary of IEEE Standards Terms*, a few definitions[211]:

Conductivity (σ): The ratio of the conduction-current density in a medium to the electric field strength. The SI unit of conductivity is the Siemen per meter (S/m).

Electric field strength (E_f): At a given point, the magnitude (modulus) of the vector limit of the quotient of the force that a small stationary charge at that point will experience to the charge as the charge approaches zero in a macroscopic sense. The SI unit of electric field strength is the Volt per meter (V/m).

Permittivity (ε_r): The ratio of the electric flux density in a medium to the electric field strength at a point. The permittivity of biological tissues is frequency dependent and may be a complex quantity. The SI unit of permittivity is the Farad per meter (F/m).

Wavelength (λ): Of a monochromatic wave, the distance between two points of corresponding phase of two consecutive cycles in the direction of propagation. The wavelength (λ) of an electromagnetic wave is related to the frequency (ν) and velocity (v) by the expression $v = \nu \times \lambda$. In free space the velocity of an electromagnetic wave is equal to the speed of light, i.e., approximately $3x10^8$ m/s. The SI unit of wavelength is the meter (m).

Microwave lactate biosensors

Microwave lactate biosensors are based on the detection and measurement of the changes in permittivity, (ε) and relaxation frequency shifts, which varies with changes in concentration of lactate, depending on the applied alternating EM field[212].

The permittivity of a dielectric is given by:

$$\varepsilon^* = \varepsilon^{'} - j\varepsilon^{''} \tag{4.5.1}$$

where, ε^* = permittivity,

$\varepsilon^{'}$ = real permittivity, and

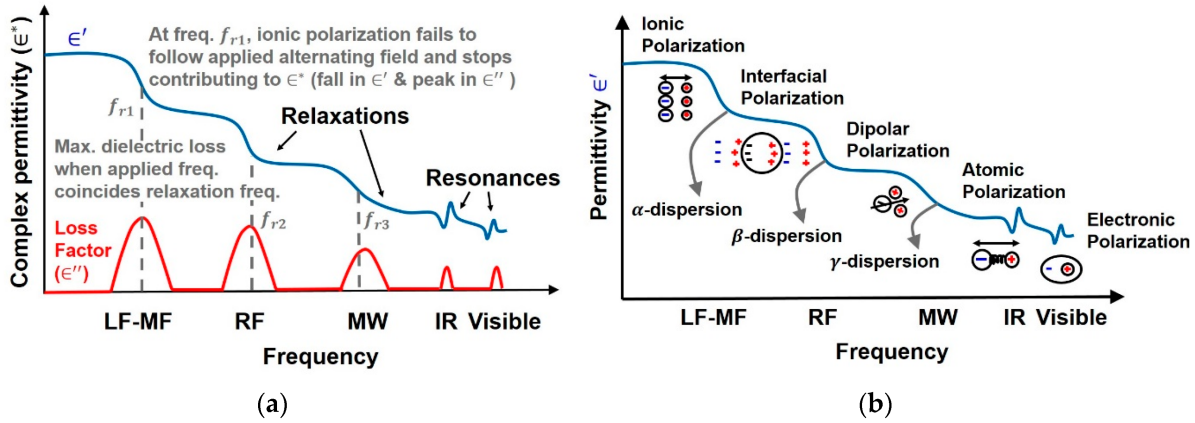

Figure 4.6: The picture depicts the behavior of a medium in the following parts of the Electromagnetic Spectrum: LF-MF: Low and Medium Frequency, RF: Radio Frequency, MW: Microwave, IR: Infrared and Visible, when an increasing frequency alternating field is applied. (a) The behaviour when the medium is a dielectric. Relaxations are noted in the Radio Frequency and Microwave frequencies, whereas, resonances in the Infrared and Visible frequencies. These relaxation frequency shifts occur due to change in permittivity of a material. (b) Polarization and relaxation shifts are also seen in these frequency ranges as Ionic, followed by interfacial, dipolar, atomic and electronic. Picture taken from[212].

ε'' = loss factor which arises because of conduction and dipolar, electronic, atomic, inter-facial and ionic polarization, Figure 4.6[212]

Lactate being a polar molecule the dipolar polarisation caused in the molecular structure makes it to rotate after a time lag, when an alternating EM field is applied. Dispersions (change in permittivity as a function of frequency) occur because of this lag time and dielectric relaxations occur in the microwave band, as seen in Figure 4.6, as there is not enough time for the molecule to go back to it's original state.

The first microwave EM lactate sensor for detection of lactic acid in cerebrospinal fluid in-vitro was developed in 2011 by Goh et al, in Liverpool, UK[213,214]. The same group in 2017 reported another *in-vivo* study for non-invasive real-time monitoring of lactate profile on exercising human participants[215]. Although the results seem promising, more research has to be conducted for sensor data validation, miniaturizing the sensor, testing the practicability of the sensor for critical care, etc.

Near Infrared Spectroscopy (NIRS) lactate biosensors

Near Infrared Spectroscopy (NIRS) biosensors are a type of optical sensors, as described in Section 4.3.2. While most of the chemical lactate biosensors described in the above section are based on the UV region of the EM, the NIRS lactate biosensors take advantage of the fact that NIR (700-1000 nm) light is able to penetrate through biological tissues. This property of NIRS biosensors facilitates non-invasive, continuous monitoring of lactate and addresses the previous concerns of enabling to take measurements on only optically clear samples.

The NIRS sensors are based on measurements of light attenuation due to variation in tissue oximeters (oxyhemoglobin [HbO_2] , deoxyhemoglobin [HbR], cytochrome c oxidase [CytOx], myoglobin), chromophores of set concentrations (melanin, water, collagen, lipids) or light scattering. The attenuation of light is calculated by the modified Beer-Lambert Law given by the Delpy et al. equation:

$$Attenuation = -log(I/I_0) = \varepsilon cd(DPF) + G \tag{4.5.2}$$

where, I and I_0= intensities of incident and emergent light, respectively,

ε = extinction coefficient of the absorbing chromophore of interest,

c = concentration of the chromophore of interest,

DPF = Differential Path Length factor, and

G= unknown factor, which changes with the tissue geometry taken into consideration[216].

Ever since Jobsis adopted NIRS technology to monitor cerebral tissue oxygenation of cats in 1977[218], a lot of research has been dedicated towards the development of technology and instrumentation to understand the cerebral tissue oximeters, as seen in Figure 4.7[217]. It has also been shown that NIRS systems can be employed to understand

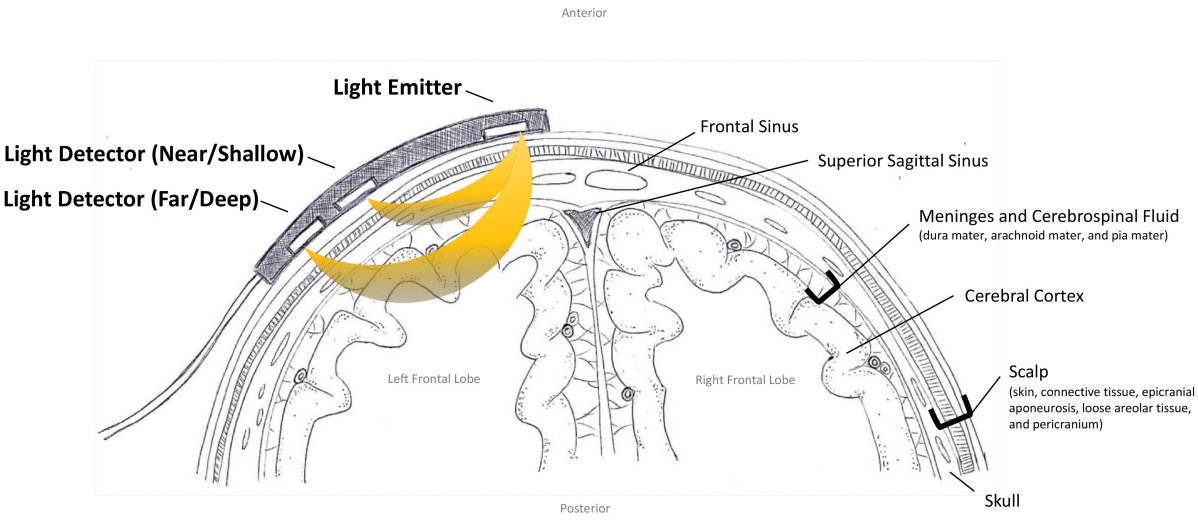

Figure 4.7: Cross-section of the cerebral tissue with a NIR light emitter and detector in Reflectance mode. Light travels a banana shaped path from the emitter, inside the tissue layers, back to the detector. Picture taken from[217].

and monitor muscle tissue oxygenation, as well, which inspects the absorption of NIR light by oxyhemoglobin ($[HbO_2]$) and deoxyhemoglobin ([HbR]). The total hemoglobin concentration ([HbT]) is given by,

$$[HbT] = [HbO_2] + [HbR] \tag{4.5.3}$$

This finds application in sports physiology to monitor oxygenation of peripheral muscles during incremental/ strenuous exercise for athletic training. Athletic training demands the need to measure precise muscle oxygen saturation (SmO_2) , concentration of lactate (or the lactate threshold (LT)) and maximum oxygen consumption ($V_{O_{2max}}$)[219]. Inter-relationships between these parameters have been studied over the years through volunteer studies during incremental exercise (a few of which are mentioned below);

$V_{O_{2max}}$ can be calculated by rate of conversion of $[HbO_2]$ to [HbR] devoid of any occlusion[220,221], SmO_2 is the measurement of changes in $[HbO_2]$ and [HbT], when a venous occlusion is applied[222], Grassi et al came to a conclusion that muscle deoxygenation Δ $[[HbO_2] - \text{HbR}]$ is correlated with the initiation of lactate accumulation and they ap-

pear at 60-65 % of the V_{O_2} peak[223]. Wang et al studied different parameters like [HbO_2], [HbR] and tissue oxygenation index (TOI) to estimate LT and also demonstrated that [HbR] can be used to indicate LT[224].

Right now there are a few low cost, wireless, wearable, real-time NIRS monitors commercially available for athletic training, out of which Portamon, from Artinis Medical System *(Einsteinweg, Netherlands)* and Moxy Monitor, from Fortiori Design *(Hutchinson, MN, USA)* measures [HbO_2], [HbR] and [HbT] in muscles, while BSX Insight, from BSX Athletics *(*Austin, TX, USA) and Humon Beta, from Dynometrics, Inc. *(Cambridge, MA, USA)* gives lactate values as well. When tested against conventional benchtop lactate measurement devices both of these devices were found to estimate acceptable ranges for lactate threshold[219,225].

The NIRS lactate sensors research has accomplished great heights in exercise physiology in the past few decades; however, they still have to be validated for clinical applications apart from the obstacles in the technology itself[226].

Absorption Spectroscopy lactate biosensors

The absorption spectroscopy lactate sensors are also a type of EM sensors and have the principles as described in detail in Chapter 3. Until date, the determination of lactate has been done by different research groups in different media using different wavelength ranges in the EM region. Few of these reported texts are discussed below:

Absorption spectroscopy in the UV and Vis range has been reported by Kossowski et al in 2017 and they found that the wavelengths 623, 646, 722, 728, 733, 777, 839, 939, 996, 1015 and 1024 *nm* could be attributed to the absorption peaks of glucose and 747, 823, 923 and 1047 *nm* for lactic acid[227]. The study was done *in-vivo* with six LEDs as light source and a silicon PIN diode as a detector. Although there are other reports on the understanding of the lactate molecule in the Ultraviolet (UV) and Visible (Vis) regions of the EM, most of these studies are done for determination of lactate

concentrations in food-processing industry for beverages, meat, etc.[228].

Burger et al used NIR Raman Spectroscopy to identify different biological analytes in an aqueous medium in 1996[229]. While Chung et al, in the same year used NIR (2000 - 2500 nm) to identify lactate in a pool of different analytes in aqueous medium[230]. McShane et al reported their study in 1998 for the range 2000 - 2500 nm, identification of glucose, lactate, and ammonia separately, in a cell culture medium and lactate was predicted with an error of 8 %[231]. All these studies used multivariate analysis, like Partial Least Squares (PLS), to identify lactate and in 1998, McShane et al, assessed these multivariate models and came to a conclusion that these methods need further development for better segregation of similar chemically structured analytes in the NIR region[232].

Yano et al in 2002, used NIR absorption spectroscopy in the wavelength range from 400 - 2500 nm in peritoneal dialysis solutions (pH 5.2-5.5) to identify lactate and glucose from the same spectrum. They assigned the wavelengths 1268 nm and 1688 nm for lactate determination and reported that with multivariate analysis, lactate could be predicted with $R^2 = 0.997$[233].

In 2000 and 2008, Riley et al considered the range from 2083.33 - 2380.95 nm in the NIR region and was successful in isolating lactate from 5 (initially) to 19 (later) different analytes, respectively in an aqueous medium and animal cell culture medium using FTIR spectroscopy[234,235,236].

Another study, in the year 2000, was done by Lafrance et al in the NIR region (890 - 2500 nm) and for prediction of lactate concentration in human plasma the wavelength chosen was 2050 - 2400 nm , using a Fourier transform near-infrared (FT-NIR) spectrometer. They reported that lactate could be predicted with an $R^2 = 0.995$ and a standard error of 0.51 mM, as compared to an electromagnetic enzymatic commercial device[237]. They found that the lactate peaks were centered around 2166, 2254 and 2292 nm. The

same group in 2003, reported another similar study in the same range of the NIR spectrum but in whole human blood. In this study, as reported, lactate could be predicted with an $R^2 = 0.978$ and a standard error of 0.65 $m\mathcal{M}$[238]. Finally in 2004, they performed an *in-vivo* study by diffuse reflectance spectroscopy (1500 - 1750 nm) in the fingernail of healthy subjects during an incremental exercise cycle study. From this study they concluded that NIR absorption spectroscopy can be an efficacious tool for assessing any physiological parameters in vivo, while predicting lactate with an $R^2 = 0.97$ and a standard error of 0.76 $m\mathcal{M}$[239]. They also managed to assign three wavelengths 1675, 1690 and 1730 nm, to the lactate molecule in the range 1500-1750 nm.

The Mid-Infrared (MIR) range, together with Raman Spectroscopy, from 3600 to 100 cm^{-1} (2777.78- 100000 nm) was studied by Cassanas et al, in 1991, where they assigned the fundamental modes of vibrations for three different compounds (lactic acid, lactate ion and methyl lactate). They came to a conclusion that both lactic acid and the lactate ion co-exists in a solution because of inter-molecular Hydrogen bonds. Hydrogen bonds between the 'pseudo free' hydroxyl groups of the two compounds occur as the oxygen atom acts as a proton acceptor.

Table 4.1 shows the wavenumber (cm^{-1}) and assignment of functional groups for lactate ion and lactic acid in the IR region[240].

Another study was done by Petibois et al, 4000–500 cm^{-1} (2500 - 20000 nm), using an FTIR spectrometer to identify 20 different bio-molecules, including lactate and glucose in human plasma. They suggested that lactate concentrations could be determined with clinical accuracy in wavelength range 1300–900 cm^{-1} (7692.31 - 11111.11 nm) and lactate manifests a weak absorption peak at 1399 cm^{-1} (7147.96 nm)[241]. They had previously also reported that lactate concentrations could be determined with an $R^2 = 0.96$, at wavelength 1127 cm^{-1} (8873.11 nm), another absorption peak of lactate[242].

As could be seen from the previous discussions, Absorption Spectroscopy Lactate

Table 4.1: Wavenumber (cm^{-1}) MIR Band Assignment for Lactic Acid and Lactate Ion in aqueous solutions. Subscripts: AL = alcohol; b = Intermolecular hydrogen bond c = Solvated OH. The fundamental modes of vibration for IR bands are as shown in Figure 3.4 Table taken from[240].

Lactate Complex		**Lactate Ion**	
Wavenumber (cm^{-1})	Functional Group	Wavenumber (cm^{-1})	Functional Group
1725	ν C=O	1585	$\nu_{as}\ CO_2^-$
1475	$\gamma_{as}\ CH_3$	1470	$\gamma_{as}\ CH_3$
1455	$\gamma_{as}\ CH_3$	1455	$\gamma_{as}\ CH_3$
1420	γ_{ac} O-H + ν_{ac} CO	1420	$\nu_s\ CO_2^-$
1380	$\gamma_s\ CH_3$, $\gamma_s\ O-H^b$	1390	$\gamma_{al}\ O-H^b$
1335	γ C-H	1370	$\gamma_s\ CH_3$
1285	$\gamma_{AL}\ O-H^c$	1320	γ C-H
1240	ν_{ac} CO + γ_{ac} O-H	1280	γ C-H
1130	$\delta_{as}\ CH_3$, $\nu_{al}\ CO^b$	1270	$\gamma_{AL}\ O-H^c$
1090	$\nu_{al}\ CO^c$	1125	$\delta_{as}\ CH_3$
1050	ν C-CH_3	1090	$\nu_{AL}\ CO^c$
930	$\delta_{as}\ CH_3$	1045	ν C-CH_3
		930	$\delta_{as}\ CH_3$
		860	ν C-CO_2^-

Biosensors have been studied extensively for *fingerprinting* and predicting lactate concentrations in different media. This technology has shown promising results for non-invasive lactate monitoring and concentration determination. However, this technology poses limitations, such as the overtones and combination bands of water and other organic functional groups in the NIR region, penetration depth of the UV, Vis and MIR regions, etc. Hence, most of the studies which are reported have excluded the water absorption bands in the IR region. Research in this particular technology is required to fulfil the lack of a comprehensive contribution to knowledge for interpreting the interaction of various regions of the EM spectrum (UV, Vis, NIR and MIR) with the lactate molecule in different physiological conditions and media.

Absorption Spectroscopy pH biosensors

Similar to lactate, estimation of pH through Absorption Spectroscopy was also attempted previously. It was Soller et al, in 1996, who first established the feasibility for such a biosensor[243]. They measured tissue pH on five New Zealand white rabbits in the wavelength range 700 and 1100 nm, in NIR Reflectance Mode. Multivariate modelling based prediction models showed a Coefficient of Determination (R^2) of 0.98 and a prediction error (RMSECV) of 0.016 +/- 0.002 pH units. This was followed by a study in 1999, by Alam et al, in which they considered the wavelength range 1500-1785 nm to understand the pH changes in whole blood. They suggested that the changes could be seen in the spectra due to the structural change of hemoglobin-histidine interactions[244]. And finally, Rosen et al in 2002, did their study using reflectance near-infrared spectroscopy on human whole blood cells in the region 600-2200 nm. They concluded that the wavelength range 650-1050 nm could be used to predict pH in clinical ranges with very high accuracy[245].

To the best of knowledge, the only study reported towards understanding of pH dependent lactic acid solutions was by Ube et al in 2017. In this study, the region between

900 – 2000 cm^{-1} was considered and pH of the lactic acid solutions were varied from 2.66 – 1.59. Furthermore, Density Functional Theory (DFT) calculations were used to assign 12 absorption peaks for lactate and lactic acid. These peaks seem to align with the previous study done by Cassanas et al (mentioned previously). They also came to a conclusion that when pH is increased, the absorption of lactate ion seemed to increase compared to lactic acid, which is a consequence of de-protonation of the acid to ion[246].

4.6 Summary

This chapter identifies the technological advances in lactate concentration determination ever since the first attempt for an optical lactate sensor in 1964. Chemical lactate biosensors, both electrochemical and optical, were discussed, with the introduction of a few commercially available devices. This chapter also presents a few non-chemical electromagnetic wave lactate biosensor technologies, like: Microwave lactate biosensors, Near Infrared Spectroscopy (NIRS) lactate biosensors and Absorption Spectroscopy lactate biosensor, and finally identifies the need for more advanced research towards a lactate biosensor based on Absorption Spectroscopy.

We might as well attempt to introduce a new planet into the solar system or annihilate one already in existence, as to create or destroy a particle of hydrogen.

John Dalton, A New System of Chemical Philosophy (first documentation of 'the atom')

5

In-vitro Spectrometric Analysis of Lactate in Buffer Solution

5.1 Introduction

*O*ptical 'Fingerprinting' of lactate in buffer solution samples using Absorption Spectroscopy needs to be thoroughly investigated. A comprehensive understanding of the UV/Vis/ NIR/ MIR spectral regions for lactate is essential for *'profiling'* the molecule. *'Profiling'* here denotes locating *'signature wavelengths'* for

lactate in the electromagnetic spectrum. These 'signature wavelengths' of lactate are the ones where the Absorbance values vary linearly with the concentration changes of lactate or are found to be associated with lactate in literature. It has been already identified in the previous chapter that an in-depth research is essential in this direction. Hence, the aim of this chapter is to understand the behaviour of lactate in a buffer solution of pH 7.4 in the UV/Vis/NIR/MIR spectral region using state-of-the-art spectrometers and data analysis techniques described in the previous chapters. This chapter also aims to validate the results which were previously seen in literature as *'signature wavelengths'* for the lactate molecule.

For this purpose, lactate solution samples of varying concentration were prepared and spectroscopy was performed on all the samples. This was followed by spectral pre-treatments and analysis. The results together with a brief summary are presented at the end of the chapter.

5.2 Sample Preparation

In order to investigate the concentration changes of lactate using Absorption Spectroscopy, the first step was to prepare laboratory based quality controlled solutions. The solutions and methods are discussed below:

5.2.1 Phosphate Buffer Solution (PBS)

A stock solution of isotonic Phosphate Buffer Solution of pH 7.4 $\pm$ 0.02 at 24° C was prepared using isotonic PBS salts in dry form (analytical grade) and de-ionized water from Deionized Water Company (*Brandon, UK*). Isotonic buffer solution (1 M, X1) with appropriate amounts of salts like: disodium hydrogen phosphate (N_2HPO_4), sodium chloride (NaCl), potassium chloride (KCl) and potassium dihydrogen phosphate (KH_2PO_4), was used to maintain physiological pH and osmolarity as the human body.

5.2.2 Lactate Stock Solution

A 600 mM lactate stock solution was prepared using Na-L-Lactate and Phosphate Buffer Solution (as mentioned above) using solution stoichiometry. The powders of analytical grade were obtained from Thermo Fisher Scientific (*Waltham, MA, USA*).

These two stock solutions were used for all in-vitro experiments throughout the thesis, unless mentioned otherwise.

5.2.3 Lactate Solutions in PBS

The lactate stock solution was diluted in 37 different vials, 30 mL each, of varying lactate concentrations; 0-5 mM with an iteration of 0.25 mM in between each sample and then from 5-20 mM with an iteration of 1.0 mM. The first set of lactate concentrations (0-5 mM) were prepared in an effort to understand the lactate concentration levels matching patients in shock states (or critical care) (Chapter 2, Section 2.5). While, the later set (5-20 mM) reflected the localized lactate level concentrations in muscle during strenuous physical activity (Chapter 2, Section 2.3). A LM5 Lactate Analyzer from Analox Instrument Limited, (*Stourbridge, UK*), (Section 4.4, Figure 4.2) was used to test the concentration of each sample before collection of the spectra. The reported range from the manufacturers for a linear dependency for lactate is 0-10 mM. The pH and temperatures of all the solutions were measured using Orion Star A211 Advanced pH Benchtop Meter Kit, from Thermo Fisher Scientific, *(Waltham, MA, USA*), just before spectroscopic measurements.

These solutions were used in all the studies henceforth, throughout the thesis.

5.3 Spectroscopy (UV/Vis, NIR and MIR)

A total Reflectance spectrum of Na-lactate powder from $250 - 2500$ nm was taken using the LAMBDA 100 mm PMT/InGaAs Integrating Sphere detector from Perkin Elmer

Corp (*Waltham, MA, USA*). The Na-L-Lactate powder was introduced in the Lambda 1050 spectrophotometer using a 100 *mm* powder cell sample holder, in the reflectance small spot kit. A similar standard white cell from the same manufacturer was used for reference measurements. The resulting spectrum, as seen in Figure 5.1, was used as a reference for a pure lactate sample for the UV/Vis and NIR spectral regions.

The solution samples of varying concentrations of lactate were kept at room temperature and Absorbance spectra of individual samples were taken separately in the UV/Vis, NIR and MIR spectral regions, as discussed in the next sections.

UV/Vis and NIR Spectroscopy

The Lambda 1050 dual beam spectrophotometer, (Chapter 3, Section 3.4.2, Figure 3.7), was used to collect three spectra from each sample in the region from 300-1000 *nm* (UV/Vis) and 800-2600 *nm* (NIR) with step increments of 1 *nm*. The spectrum of each sample was then obtained by averaging the three obtained spectra and used for further analysis. The samples were chosen at random from the set of 37 to prevent bias. The light sources used were a deuterium lamp from 300-319 *nm* and then changed to halogen tungsten lamp for the rest of the wavelength range. The detectors settings are as shown in Table 5.1. These were used in order to prevent oversaturation of all the detectors. In addition, the reference beam was set at 1% attenuation, for the purpose of noise reduction at high absorbance values.

Table 5.1: Detector Settings for UV/Vis and NIR Spectroscopy.

Detectors	Wavelength Range (*nm*)	Slit Size	Gain	Response Time (s)
PMT	300-860	Fixed (2 *nm*)	Auto	0.2
InGaAs	800-1800	Servo Mode	5	0.2
PbS	1800-2600	Servo Mode	1	0.2

Baseline correction of 100% Transmittance/ 0% Absorption for both the UV/Vis and

NIR spectral regions in the spectrophotometer was also added to reduce "background noise" or peaks arising from the ambient environment. The samples were placed in the sample holder of the spectrophotometer in macro glass cuvettes for 300-1000 nm (UV) wavelength, of 10 mm path length (Hellma (*GmbH & Co., Germany*)). Quartz cuvettes (Hellma (*GmbH & Co., Germany*)) of 1mm path length were used for 800-2600 nm (NIR). Two of each cuvette of the same specifications were placed in each slot; one in the sample slot, with the solution sample in it and the other, empty, in the reference slot.

MIR Spectroscopy

The Spectrum 2, (Chapter 3, Section 3.4.2), with HATR accessory was used to collect the MIR (FTIR) spectra. The wavenumber chosen was from 2000-500 cm^{-1} (5000 - 20000 nm), with a data interval of 1 cm^{-1}. The range from 4000-2000 cm^{-1} (2500-5000 nm) were not considered here because of the water peaks (3277 cm^{-1} and 3490 cm^{-1}) in the region to avoid false correlations. The spectral resolution was kept at 4 cm^{-1} as there was a fixed internal J-stop (Jacquinot-stop) of 8.94 mm, inbuilt in the instrument. The J-stop is used to manipulate the divergence of the beam arising from the source in the spectrometer and it changes with the spectral resolution. An average of 50 scans per sample with a scan speed of 0.2 cm s^{-1} were taken, as part of spectra acquisition in the study. With large multiplexing, the Signal-to-Noise Ratio (SNR) increases (Equation 3.11), which increases the sensitivity of the instrument. A 70 μL sample was laid out directly on the ZnSe crystal, at room temperature covering the whole crystal. A background scan with the empty crystal was taken every 20 min.

A total of 259 spectra (111 for UV/Vis, 111 for NIR and 37 for MIR) were collected, visualised and analysed.

5.4 Data Analysis (UV/Vis, NIR and MIR)

Spectra collection and visualization was done using the software, as mentioned in Chapter 3 Section 3.5, for each instrument. However, pre-treatment and analysis on all the spectra was done using MATLAB R2020b, MathWorks^{TM} *(Natick, MA, USA)* as described in detail in the following sections.

5.4.1 Pre-Treatment of spectral data

Pre-processing of all the three sets of spectra was performed separately to understand the distinct spectral features in the three different wavelength ranges discretely. As mentioned in Chapter 3, Section 3.6, the raw spectra had to be pre-treated before analysis. The following methods were used as part of pre-treatment:

- Spectral Difference: The spectrum of the first sample (0.25 mM concentration of lactate) was subtracted from all the 36 spectra across the three sets
- Extended Multiplicative Scatter Correction (EMSC) with quadratic polynomial baseline correction to reduce multiplicative effects was used for UV/Vis and MIR data-sets[247]. Multiplicative effects of spectra arise due to light scattering variations or optical path length variations. They vary from sample to sample and EMSC improves the path length estimation be utilising the knowledge of the analytes present in the spectra and their interference effects. While, Linear Robust Multiplicative Scatter Correction (MSC) was used for the NIR data-set for the same purpose[248].
- Savitzky-Golay (SG) filter was used for smoothing the spectra and intensifying the absorption peaks. Table 5.2 shows the values of the Polynomial Order, Derivative and Window Length of the SG filter for the three sets[249]. These values were

decided as a trade-off between noise suppression and feature enhancement in the plots through visual inspection.

Table 5.2: Parameters for Savitzky-Golay (SG) Filter.

Data-Set	Polynomial Order	Derivative	Window Length
UV/Vis	2	1	5
NIR	2	1	101
MIR (FTIR)	2	1	101

5.4.2 Spectral Analysis

The pre-treated spectra were then analysed using the following methods, as mentioned in Chapter 3, Section 3.7:

- 2D correlation (Section 3.7.1) synchronous plot gave an understanding of the systematic variations in spectral intensities (both absorbance and wavelength) for different wavelength ranges. These variations, along the diagonal in the plots, could be seen as a result of the induced changes in the spectra caused by the changes in the concentration of lactate. These plots together with the pure solid lactate powder spectrum were used to navigate through the wavelength ranges through the different data-sets to understand the marked presence of lactate in the EM Spectrum.

- Linear Regression (Section 3.7.3) was done individually on the Absorption peaks in each region. These results were used not only to help identify the lactate wavelengths of interest in the whole EM region but also to validate all the results found in existing literature.

- Aquagram (Section 3.7.2) was constructed for the wavelength range of 1200-1600 nm in NIR spectral region. The wavelengths taken into account were: 1342 nm, 1364 nm, 1374 nm, 1384 nm, 1412 nm, 1426 nm, 1440 nm, 1452 nm, 1460 nm, 1476 nm, 1488 nm and 1512 nm. Only high concentration of lactate (5-20 mM) were used to construct these Aquagrams in order to reduce noise and for other comparative studies which will be seen in the later part of the thesis.

- Partial Least Square (PLS) (Section 3.7.4) leave-one-out cross-validation method was used for each data-set independently. In this process, thirty-six spectra were used to build predictive models for concentrations of lactate. This model is then used to predict one of spectrum which was kept aside initially. The process was then repeated 36 times for each set to predict each spectra while training the rest.

  The number of LVs to be used were determined by the PRESS for every set. The Coefficient of Determination (R^2), together with the Root Mean Squared Error of Cross Validation (RMSECV), were used to understand the prediction accuracy of the calibration models for each set of spectra, where the predicted concentrations of lactate are compared against the ones obtained from the commercial lactate analysers.

5.5 Results

Figure 5.1 shows the total Reflectance spectrum of Na-lactate powder from 250-2500 nm. The three sets of raw Absorption spectra of the UV/Vis, NIR and MIR (FTIR) are as shown in Figure 5.2 (a-c). Figure 5.3 (a-c) shows the pre-treated spectra of the UV/Vis, NIR and MIR spectral regions. In order to identify the regions of interest for lactate, 2D synchronous contour plots were constructed for the three wavelength ranges, as seen in Figure 5.4 (a-c).

Figure 5.2 (b) shows high-frequency noise peaks in the region from 1900-1960 nm and

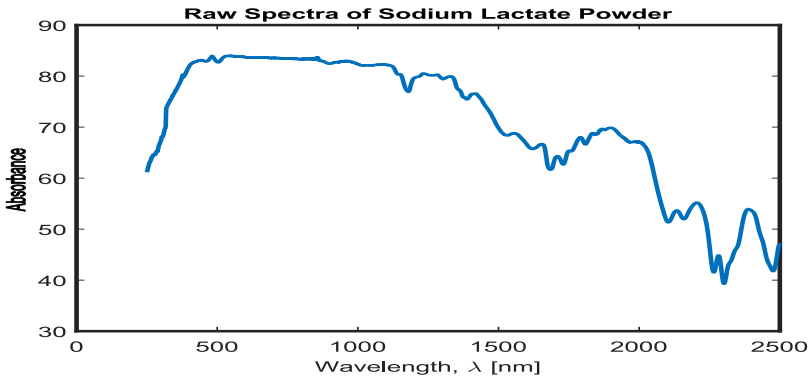

Figure 5.1: Raw spectrum of Sodium L-Lactate Powder through Reflectance Spectroscopy in 250-2500 *nm*.

2350-2600 *nm*. This is due to detector saturation resulting from the high absorption of O-H functional group in those regions. Hence, these regions were removed manually from the spectra to reduce unwanted correlations in further analysis of these spectra. Therefore, in Figure 5.3 (b), flat connecting lines are observed in the region 1900-1960 *nm* and the spectral range in the NIR set culminates at 2350 *nm*.

In order to understand the complete spectral regions of the EM, which reflects lactate concentration changes, the results were classified into the following:

- Spectral regions without O-H Absorption interference
- Spectral regions of O-H Absorption
- Entire spectral regions for predictive models.

5.5.1 Spectral regions without O-H Absorption interference

The O-H absorption is quite prominent in the NIR spectral region of EM due to the overtones and combination bands, as seen in Chapter 3 Section 3.2.3, while the UV/Vis and MIR spectral regions are not affected by the O-H absorbance as much. In the NIR spectral region, there exists parts of regions which are not affected by the O-H

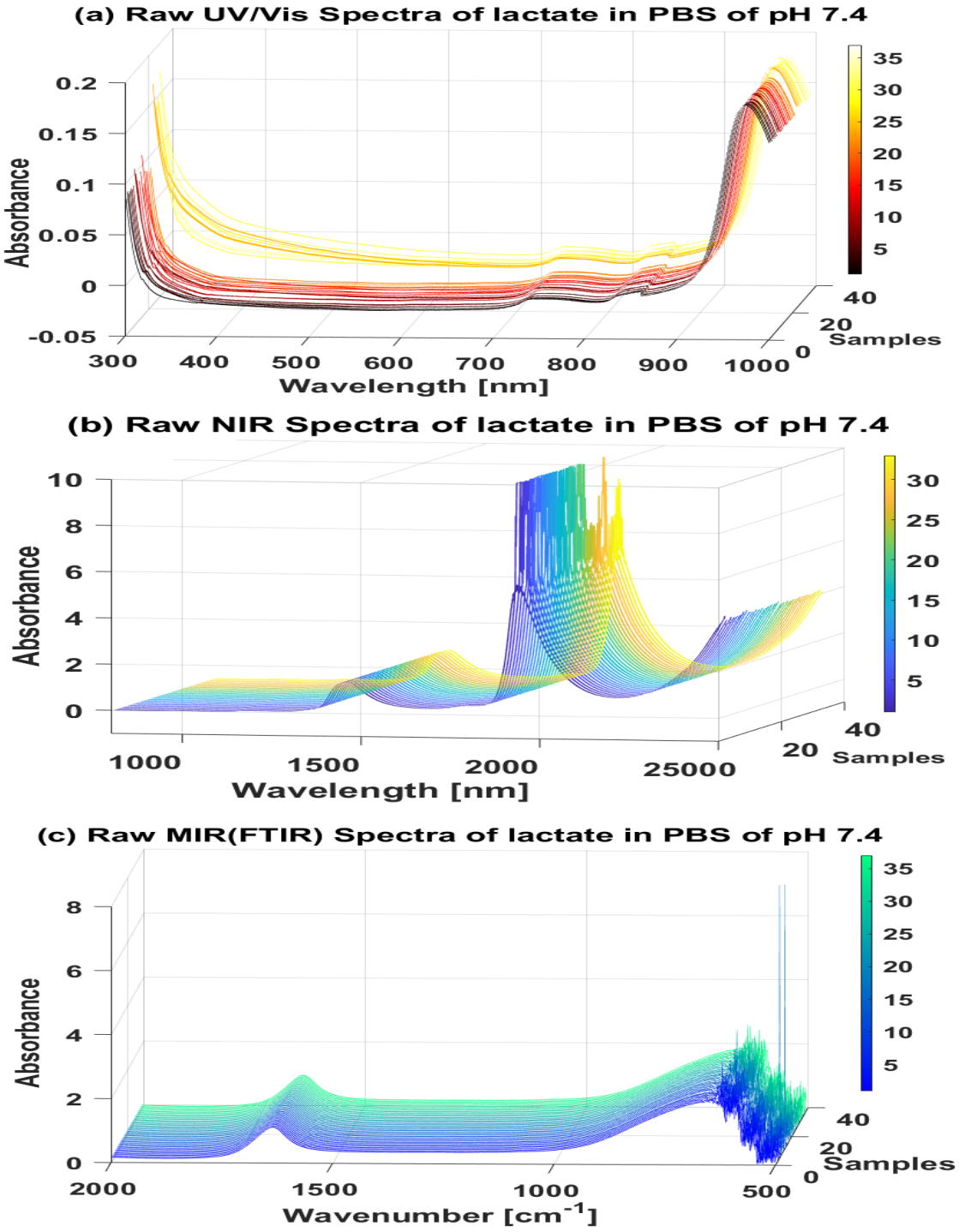

Figure 5.2: Raw spectra of thirty-seven Sodium (Na)-L-Lactate solutions of varying concentration ranging between 0–20 mM in Phosphate Buffer Saline (PBS) samples. (a) UV/Vis (300-1000 nm) raw spectra of 37 samples of Na-L-Lactate (0-20 mM) in PBS; (b) NIR (800-2600 nm) raw spectra of 37 samples of Na-L-Lactate (0-20 mM) in PBS; (c) MIR (2000-500 cm^{-1}) raw spectra of 37 samples of Na-L-Lactate (0-20 mM) in PBS.

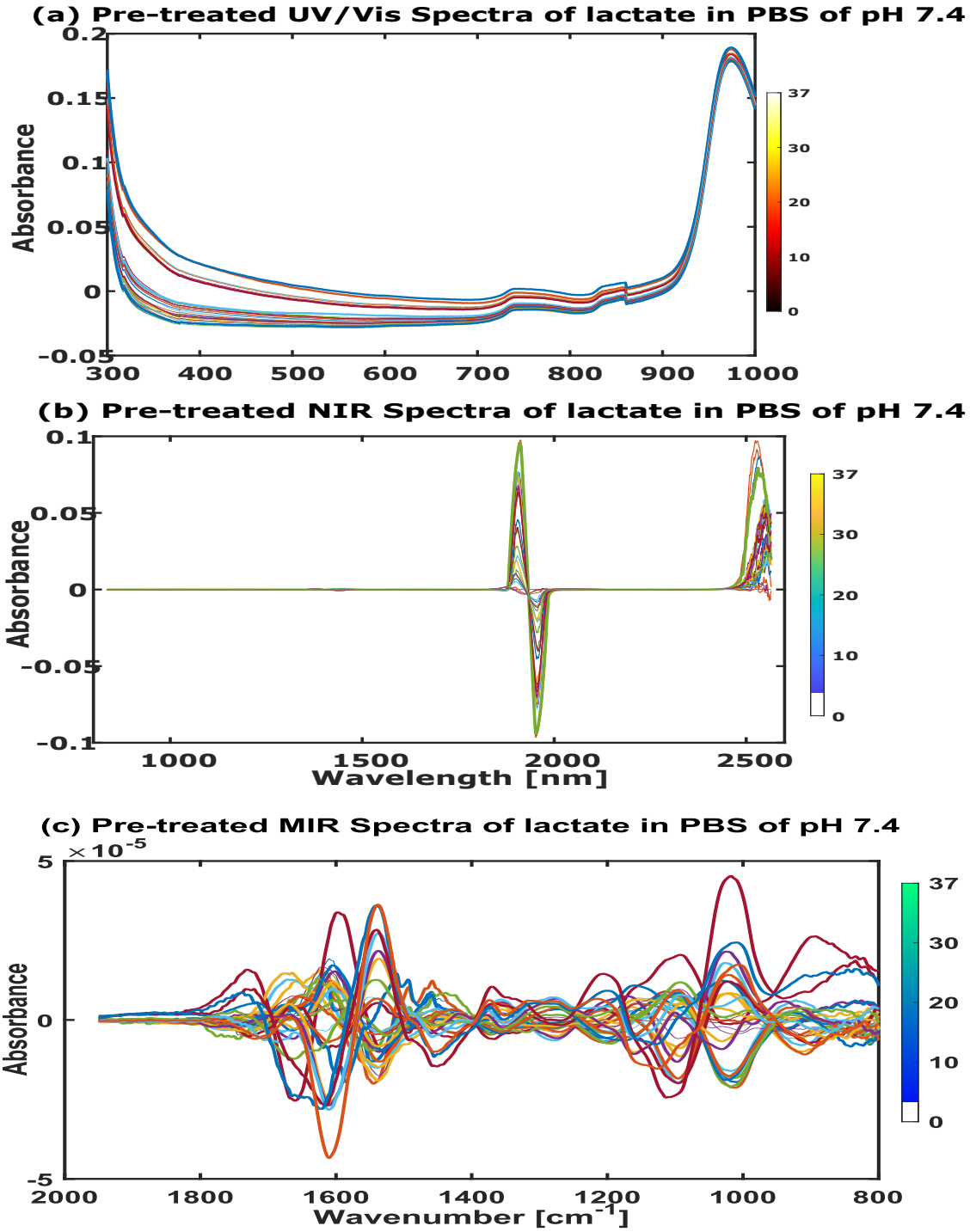

Figure 5.3: Pre-treated spectra of the UV/Vis, NIR and MIR (FTIR) of all the samples after pre-processing; subtraction of base sample (0.25 $m\mathcal{M}$ of lactate concentration), Extended Mean Signal Correction (EMSC) and Savitzk-Golay (SG) derivation. (a) 36 pre treated spectra in the UV/Vis spectral region; (b) 36 pre treated spectra in the NIR spectral region; (c) 36 pre treated spectra in the MIR region.

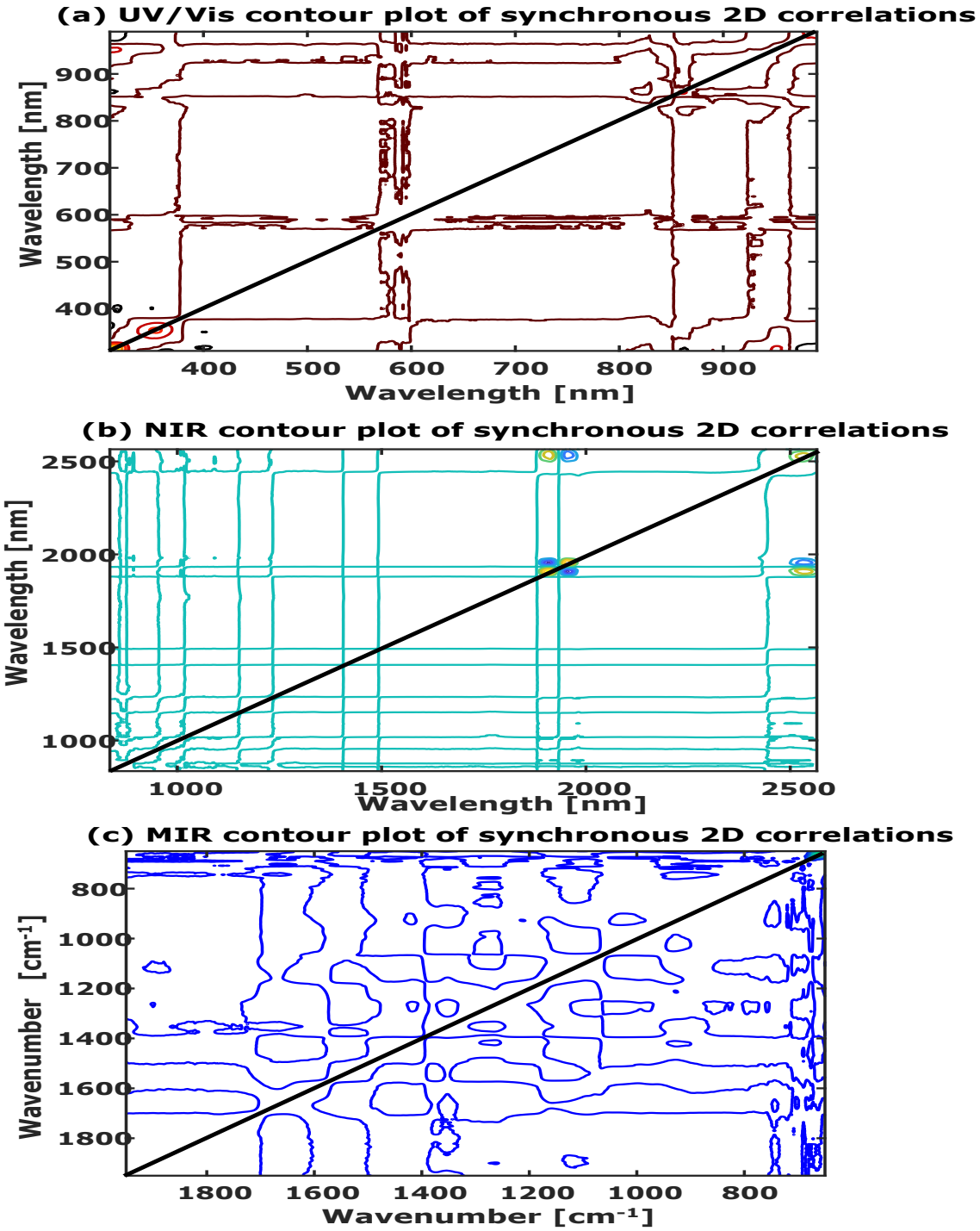

Figure 5.4: Two-dimensional synchronous correlation plot depicting the correlation changes in the 36 spectra in the UV/Vis, NIR and MIR (FTIR) Spectra. (a) 2D synchronous correlation plot in the UV/Vis spectral region; (b) 2D synchronous correlation plot in the NIR spectral region; (c) 2D synchronous correlation plot in the MIR spectral region.

absorption, too. These regions of the EM spectrum which are not affected by the O-H absorption are being analysed in this section.

UV/Vis spectral region

The UV region (Figure 2(a)) demonstrated one distinguishable peak at 320 nm, which could also be seen in the pure solid lactate powder spectrum in Figure 5.1. As can be seen from Figure 5.2 (a) and 5.3 (a), there were not any visible changes in the region 400-700 nm (visible spectral range), as the lactate aqueous solutions are colorless. In Figure 5.4 (a), the spectral regions of interest highlighted were from 800-900 nm, which were part of the NIR spectral region.

NIR spectral region

Scanning through the solid powder spectrum, the consequent peaks that were featured in the region from 800-840 nm, were at wavelengths 820 nm, 830 nm and 850 nm, in the NIR spectral region. This region could also be seen as highlighted in the 2D correlation synchronous contour plots (Figure 5.4 (a)).

For the NIR spectral region, minute highlights could be seen in the regions between 1050-1220 nm, 1660-1780 nm and 2200-2400 nm (Figure 5.4 (b)). The wavelengths that were identified in these highlighted regions from the solid lactate spectrum 5.1, were 1142 nm, 1233 nm, 1710 nm, 1750 nm, 2205 nm, 2319 nm and 2341 nm. These highlights were too minute to be visibly seen in the spectra and hence, another six spectra of very high lactate concentrations (100 mM, 200 mM, 300 mM, 400 mM, 500 mM and 600 mM) were obtained using the same process as discussed above. The purpose of these spectra were solely to visually inspect the highlighted NIR spectral regions in Figure 5.4. The highlighted regions are as shown in Figure 5.5.

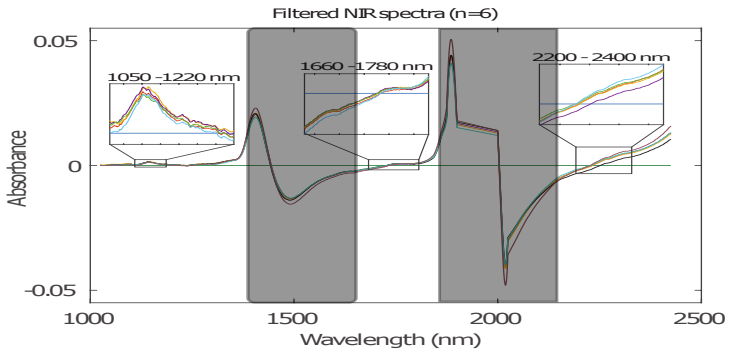

Figure 5.5: The regions of interest in the NIR spectral region pertinent to high lactate concentration changes are 1050-1220 nm, 1660-1780 nm and 2200-2400 nm. The grey areas 1450-1600 nm and 1960-2250 nm are influenced by OH bonds. Figure taken from [250].

Table 5.3: Significant Wavelengths for Lactate Detection obtained from the L-Lactate powder spectrum and 2D synchronous correlation plot.

UV/Vis (nm)	NIR (nm)	MIR (cm^{-1})
320	1142	1747
	1233	1783
	1710	1399
	1750	1039
	2205	1021
	2319	
	2341	

MIR spectral region

The MIR 2D synchronous contour plots (Figure 5.4 (c)) showed minute correlations throughout the spectral range, with some highlights in the 1150-1000 cm^{-1} and 1740-1800 cm^{-1}.

The wavelengths which were identified in all the three wavelength spectral ranges are as shown in Table 5.3. Linear Regression on the NIR wavelengths was performed and the p-values are as shown in Table 5.4.

Apart from the wavelengths mentioned above, a few wavelengths were also found in

Table 5.4: p-values of the linear regression done on the NIR wavelengths of Table 5.3.

Wavelength (nm)	p-values
1142	1.45E-05
1233	1.39E-05
1710	0.027
1750	1.19E-05
2205	5.41E-07
2319	0.0016
2341	0.032

the literature.

In order to validate all the wavelengths and wavenumbers, linear regression was performed individually on all of them. The wavelengths/wavenumbers and the p-values are given in Tables 5.5 and 5.6. It is to be noted that only the wavenumbers with p-values ≤ 0.05 were reported for these sets of spectra. Thus the wavelengths: 823 nm, 923 nm, 1142 nm, 1233 nm, 1710 nm, 1730 nm, 1750 nm, 2205 nm, 2292 nm, 2319 nm and 2341 nm in the NIR region and wavenumbers: 1747 cm^{-1}, 1783 cm^{-1}, 1127 cm^{-1}, 1039 cm^{-1} and 1021 cm^{-1} in the MIR region were significant, with p-values ≤ 0.05. These wavenumbers could be attributed as the *'signature wavelengths'* of lactate molecule at pH 7.4. A few of these wavenumbers could be seen in Figure 5.6, when the Absorbance of very high concentrations of lactate (100-600 mM) were plotted.

5.5.2 Spectral regions of O-H Absorption

In Figure 5.4 (a), the region that was highlighted is the O-H Absorption peak at 970 nm, which lies in the NIR spectral region. Also, O-H Absorption bands were found in 1450 nm, 1960 nm, and 2500 nm and peaks exhibiting O-H functional group exists in the wavelengths 1490 nm, 1540 nm, 1820 nm, 2070 nm and 2100 nm Table 3.1 in Chapter 3.

Except for 1490 nm and 1820 nm, with p-values of 0.04, no other wavelength had

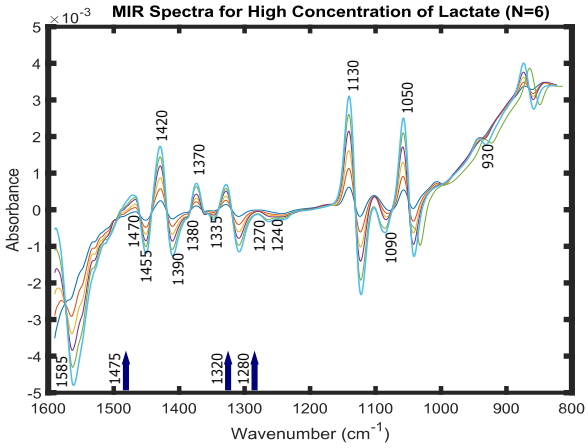

Figure 5.6: Wavenumbers of interest in the MIR spectral region 800-1600 cm^{-1}, pertinent to high lactate concentration changes. The set of six spectra (after pre-processing) of very high concentration of lactate in PBS (100 (dark green), 200 (orange), 300 (yellow), 400 (red), 500 (light green) and 600 mM (blue)) obtained in the MIR(FTIR) range. The wavenumbers 860 cm^{-1}, 930 cm^{-1}, 1050 cm^{-1}, 1090 cm^{-1}, 1130 cm^{-1}, 1240 cm^{-1}, 1270 cm^{-1}, 1280 cm^{-1}, 1320 cm^{-1}, 1335 cm^{-1}, 1370 cm^{-1}, 1380 cm^{-1}, 1390 cm^{-1}, 1420 cm^{-1}, 1470 cm^{-1}, 1475 cm^{-1} and 1585 cm^{-1} could be visibly seen in the spectra. Figure taken from [251].

Table 5.5: Significant Wavelengths for Lactate Detection with p-values ≤ 0.05

Wavelengths	p-values	Region
823 nm	0.0022	NIR
923 nm	2.01E-06	NIR
1730 nm	0.036	NIR
2292 nm	0.0030	NIR
1747 cm^{-1}	1.86E-07	MIR
1783 cm^{-1}	1.69E-07	MIR
1127 cm^{-1}	5.25E-06	MIR
1039 cm^{-1}	1.46E-05	MIR
1021 cm^{-1}	4.25E-05	MIR

Table 5.6: Significant Wavelengths for Lactate containing complex and Lactate ion in the MIR region, from Table 4.1.

Lactic Acid		**Lactate Ion**	
Wavenumber (cm^{-1})	p-values	Wavenumber (cm^{-1})	p-values
1725	4.47E-07	1585	0.0051
1475	2.28E-07	1470	2.07E-06
1455	0.0141	1390	2.40E-08
1420	1.69E-06	1370	0.000905
1380	0.000429	1320	0.00613
1240	0.00312	1280	0.00195
1130	4.45E-10	1270	7.51E-05
1090	0.000347	1125	2.65E-07
1050	1.08E-05	1045	3.09E-05
930	0.00019	860	2.46E-05

p-values ≤ 0.05.

An Aquagram was also constructed for the wavelength range 1200-1600 nm as shown in Figure 5.7.

5.5.3 Entire spectral regions for predictive models

The entire spectral ranges for the three sets of data were used to construct PLS calibration models, individually. PRESS was then used to create the simplest model with least number of LVs. Hence, from Figure 5.8, the number of LVs used for UV/Vis set was 2, NIR set was 8 and MIR (FTIR) set was 18.

Finally, Figure 5.9, depicts observed (known) concentration of lactate and predicted concentrations by the predictive PLS models built using leave-one-out cross-validation analysis. The coefficients of determination (R^2) of each set, as shown in the figure; UV/Vis set 0.59, NIR set 0.98 and MIR (FTIR) set was 0.96. The root mean squared error of cross validation (RMSECV) for UV/Vis set 4.27 mM, NIR set 0.89 mM and MIR (FTIR) set was 1.16 mM.

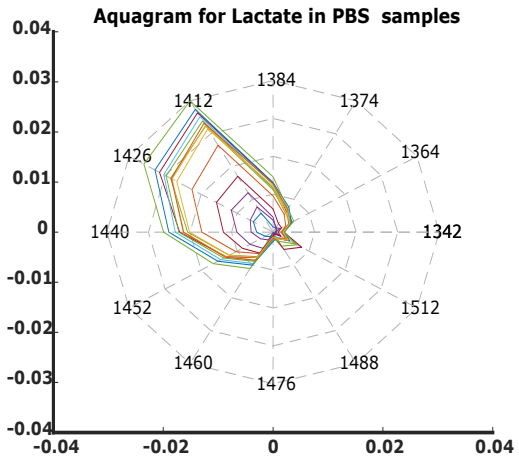

Figure 5.7: Aquagrams for lactate in PBS samples in Water Absorbance Bands (WAB): 1300-1600 nm, showing Water Absorbance Spectral Pattern (WAPS) in the Water matrix co-ordinates (WAMACS) of varying concentrations of lactate in PBS samples. The WAMACS: 1342, 1364, 1374, 1384, 1412, 1426, 1440, 1452, 1460, 1476, 1488 and 1512 depicts molecular conformations which arises due to water-NIR light-lactate molecule interactions.

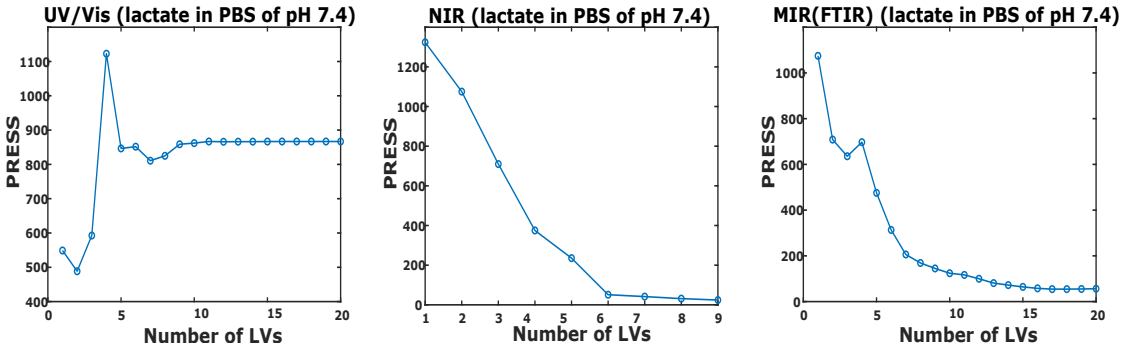

Figure 5.8: Prediction Error Sum of Squares (PRESS) versus number of latent variables (LV). (a) The number of LVs in the UV/Vis spectral region used was 2; (b) The number of LVs in the NIR spectral region used was 8; (c) The number of LVs in the MIR spectral region used was 18.

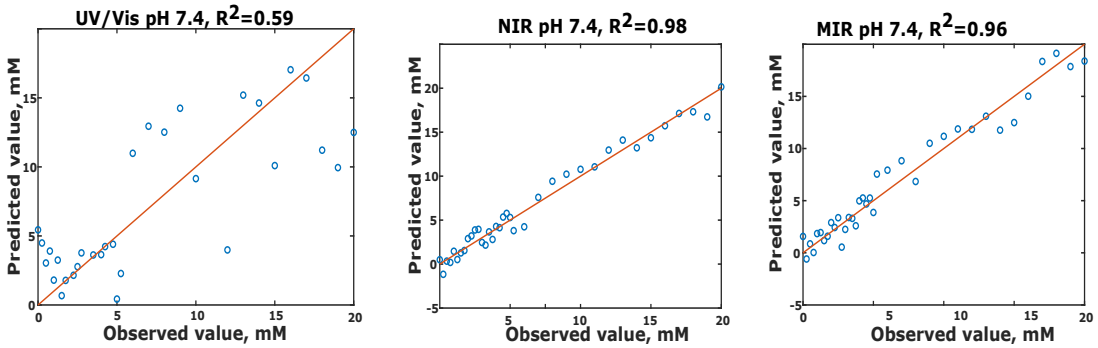

Figure 5.9: Observed (known) lactate concentration versus the Predicted concentrations of thirty-seven PBS samples of lactate prepared using solution stoichiometry. The correlation coefficient (R^2) and the root mean squared error of cross validation (RMSECV) for each set are also shown. (a) The Coefficient of Determination (R^2) and the root mean squared error of cross validation (RMSECV) for UV/Vis set is 0.59 and 4.27 mM respectively; (b) The Coefficient of Determination (R^2) and the root mean squared error of cross validation (RMSECV) for NIR set is 0.98 and 0.89 mM respectively; (c) The Coefficient of Determination (R^2) and the root mean squared error of cross validation (RMSECV) for MIR (FTIR) set is 0.96 and 1.16 mM respectively.

5.6 Summary

This chapter aims to provide comprehensive insights of the lactate-electromagnetic region (UV/ Vis/ NIR/ MIR) intermolecular interactions at a constant pH of 7.4 in Phosphate Buffer Solution. For this purpose, each region of the EM spectrum were analysed independently.

The results show that there was one wavelength (320 nm) in the UV region which could be of interest for lactate concentration prediction. The predictive Partial Least-Squares (PLS) regression analysis and leave-one-out cross-validation for the UV/Vis spectral data showed a Coefficients of Determination (R^2) of 0.59 and the Root Mean Squared Error of Cross Validation (RMSECV) was 0.39 mM, between the predicted and prepared samples.

Following the visible spectral region, where there were no wavelengths of interest, in the NIR spectral region (800-2600 nm), according to the experimental data, there were eleven wavelengths of interest (823 nm, 923 nm, 1142 nm, 1233 nm, 1710 nm, 1730 nm, 1750 nm, 2205 nm, 2292 nm, 2319 nm and 2341 nm). These wavelengths

lie in the spectral regions where there is no O-H Absorption interference. Finally, the PLS regression analysis and leave-one-out cross-validation models for NIR spectral data showed a Coefficients of Determination (R^2) of 0.98 and the Root Mean Squared Error of Cross Validation (RMSECV) was 0.89 $m\mathcal{M}$, between the predicted and prepared samples.

Lastly, the MIR spectral region (2000-500 cm^{-1}) showed three wavenumbers 1783 cm^{-1}, 1747 cm^{-1} and 1725 cm^{-1} in the range 2000-1500 cm^{-1}. This is followed by a list of wavenumbers in the spectral range 1500-600 cm^{-1} which correlate linearly with the concentration changes of lactic acid and lactate ion. These wavelengths are in agreement with those found in the literature and serve as signatures for the molecule for pH of 7.4. Finally, the PLS regression analysis and leave-one-out cross-validation for MIR spectral data showed a Coefficients of Determination (R^2) of 0.96 and the Root Mean Squared Error of Cross Validation (RMSECV) was 1.16 $m\mathcal{M}$, between the predicted and prepared samples.

This chapter helps identify the *'signature wavelengths'* of the lactate molecule in the whole Electromagnetic Spectrum for solutions with pH 7.4. The next chapter discusses in detail the additional effects of pH on each part of EM spectrum.

...despite the clear biochemical evidence against a lactic acid cause of metabolic acidosis, there remains strong inertia in science for continuing to use the simple lactic acid explanation for acidosis.

Baker, McCormick and Roberts (2010)

6

In-vitro Spectrometric Analysis of Lactate in Buffer Solution of changing pH

6.1 Introduction

Spectral features can be affected by change in pH of the same medium. This chapter aims in identifying the effects of pH on lactate buffer solutions for each part of the EM spectrum. As seen in the last chapter, *'signature wavelengths'* of lactate were identified in parts of the EM spectrum which has no O-H absorption interference

and PLS regression models were built using entire sets to predict and cross-validate the concentration changes of lactate. This chapter intends to investigate the effects of pH on similar spectra sets.

Hence, similar analysis were performed on solution sample sets of varying pH (6-8) and constant lactate concentration (2 mM). Also, on spectra sets with constant pH (7, 6.5 and 6), with varying lactate concentrations (0.25 - 20 mM).

Lactate concentration changes in different solution samples of varying pH were also calculated using theoretical equations. The results from these calculations are also presented and compared with the spectral changes.

Finally, each set of pH was investigated independently in all three spectral region and then together in the NIR and MIR spectral region to understand the spectral feature changes for each set.

6.2 Sample Preparation

Two sets of samples were prepared in order to understand the effects of pH with respect to spectral feature behaviour, mostly in the NIR spectral region of the EM spectrum. The first set had twenty samples, where lactate concentrations were maintained at 2 mM and pH was varied from 6-8, at 0.1 intervals. As seen in Chapter 2 Section 2.6, the physiological range of pH lies between 7.35 - 7.45, hence this range was selected for the investigation.

The second set of samples, had (3x37) one hundred and eleven samples, where thirty seven different lactate concentrations were prepared for each of three sets of varying pH (6, 6.5 and 7) buffers, indicating physiological and cellular pH[132]. Detailed description of the sample preparation methods are as follows:

6.2.1 Lactate Concentration Constant, Δ pH

For this set of twenty samples, a 1L stock solution of isotonic Phosphate Buffer Solution (PBS) was prepared, as mentioned in Chapter 5, Section 5.2.1. pH of this stock solution was changed (6-8, at 0.1 intervals) by adding Hydrochloric Acid (HCl) or Sodium Hydroxide (NaOH) of appropriate quantities. These values were measured using the Orion Star A211 Advanced pH Benchtop Meter Kit, from Thermo Fisher Scientific, *(Waltham, MA, USA)*.

The stock solution of 600 mM of lactate, as mentioned in Chapter 5, Section 5.2.2, was then diluted to make solutions of varying pH with constant lactate concentration. Hence, 20 solutions of 30 mL each were made by mixing aliquots of the stock solution of lactate and buffers of changing pH to maintain a 2 mM lactate concentration for all the solution samples. The lactate concentration was verified using LM5 Lactate Analyzer from Analox Instrument Limited, (*Stourbridge, UK*).

6.2.2 Δ Lactate Concentration, pH constant

For this set of solutions, buffers of 1L each were prepared of pH values: 7, 6.5 and 6, by adding drops of HCl into the stock solution of pH 7.4 (Chapter 5, Section 5.2.1). Thereby, thirty seven samples of varying lactate concentration solutions for each pH buffer set were prepared by mixing aliquots of buffer and lactate stock solution (Chapter 5, Section 5.2.2).

The concentrations of the lactate solutions were maintained similar to the process described in Chapter 5.

The first set will be referred to as Set 6.2.1 and the second as Set 6.2.2, throughout the Chapter and the thesis (where ever mentioned).

6.3 Lactate Concentration Measurements (Theoretical)

Lactate concentration of each solution was measured just before experiments and they were maintained at 2 mM. However, the concentrations would slightly change in each solution because of the ionization of lactate from $C_3H_6O_3$ to $C_3H_5O_3^-$. The changes would happen in each sample depending on the acidity of the solution, when lactate was introduced. These change in values could be calculated using theoretical equations as discussed below.

As seen in Chapter 2, Section 2.6, pH for physiological measurements are calculated using the modified Henderson-Hasselbach equation 2.1. The same equation could be used in analytical chemistry measurements, as:

$$pH = pK_a + \log \frac{[A^-]}{[HA]} \tag{6.3.1}$$

where, pK_a = -logK_a, K_a is the dissociation constant of an acid; pK_a of lactic acid is 3.8,

[HA] and $[A^-]$ = concentration of the salt and it's conjugate base, respectively[252,253].

6.3.1 Lactate Concentration for Set 6.2.1

The calculated lactate concentrations in the sample solutions vs pH changes are as shown in Figure 6.1.

From Figure 6.1, a decreasing trend of a second degree polynomial order in the concentrations of lactate is seen, as the pH increased from 6-8.

6.3.2 Lactate Concentration for Set 6.2.2

For this set of solutions, the theoretical calculations were based on the following principle:

The pH of each buffer set were kept constant at 7.4, 7, 6.5 and 6. Now, when the

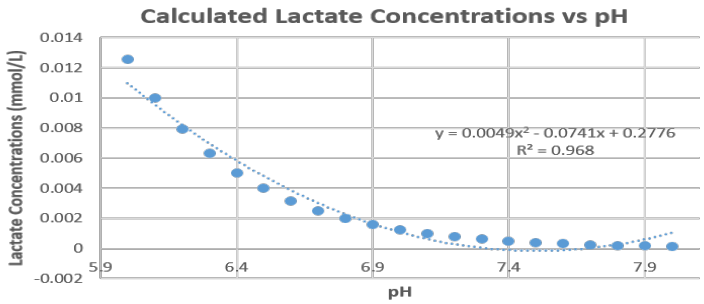

Figure 6.1: Theoretically calculated concentrations of lactate vs pH (6-8) using the Henderson- Hasselbach equation. The fit of the curve follows the equation of y = $0.0049x^2$ - 0.0741x + 0.2776, with R^2=0.968. Figure taken from[254].

concentration of lactate was increased (from 0-20 mM), the concentration of lactate anion ($CH_3CH(OH)COO^-$) increased in each sample solution[246]. This increase in the lactate anion, increased the degree of ionisation, based on the equation mentioned above.

The subtle changes in the concentrations of lactate were so minute that they were beyond the detection limits of any commercial lactate analyser.

6.4 Spectroscopy (UV/Vis, NIR and MIR)

Once the solutions were prepared, spectroscopy was performed on each of the sample solutions.

6.4.1 NIR Spectroscopy for Set 6.2.1

The first set of solutions were investigated only in the NIR spectral region (800-2500 nm) to visualise the effects of the O-H overtone and combination bands. Hence, sixty NIR spectra were obtained from this set of samples. The methods were maintained consistent as described in Chapter 5, Section 5.3.

6.4.2 UV/Vis, NIR and MIR) Spectroscopy for Set 6.2.2

For these sets of solution, spectroscopy of the UV/Vis, NIR and MIR were performed separately on all the solution samples. The methods and parameters for each instrument in all the regions were maintained as mentioned in Chapter 5, Section 5.3.

Hence, a total of 111 spectra were obtained for each region of the EM spectrum. These (111x3) spectra were then analysed as discussed in the next section.

6.5 Data Analysis (UV/Vis, NIR and MIR)

The spectra for both the sets were pre-treated and analysed independently using the techniques as discussed below:

6.5.1 Pre-Treatment of spectral data

Spectral pre-treatment of Set 6.2.1

The following techniques were used as pre-treatment:

- Spectral Difference: the spectra of pH 6 and pH 8 (the lowest value and highest value) were subtracted from pH set 6.1-7 and pH set 7-7.9, respectively
- Extended Multiplicative Scattering Correction (EMSC) with quadratic polynomial baseline correction was performed to reduce sample multiplicative effects and enhance spectral features[248]
- Savitzky-Golay filter (Polynomial Order=2, Derivative=1, Window Length=71) was used for smoothing of the spectra and intensifying the absorption peaks[249].

Spectral pre-treatment of Set 6.2.2

The pre-treatment techniques were kept consistent across all three sets, as mentioned in Chapter 5, Section 5.4.1.

However, values for the parameters (polynomial order, derivative and window length) of the Savitzky-Golay filter were varied for each set. As mentioned in Chapter 5, Section 5.4.1, these parameters were chosen as a trade-off between noise suppression and feature enhancement. These values are mentioned in Tables: 6.1, 6.2 and 6.3.

Table 6.1: Parameters for Savitzky-Golay (SG) Filter for UV/Vis data-sets of pH 7, pH 6.5 and pH 6

UV/Vis data-set	Polynomial Order	Derivative	Window Length
pH 7	2	1	5
pH 6.5	2	1	21
pH 6	2	1	5

Table 6.2: Parameters for Savitzky-Golay (SG) Filter for NIR data-set of pH 7, pH 6.5 and pH 6

NIR Data-Set	Polynomial Order	Derivative	Window Length
pH 7	2	1	101
pH 6.5	2	1	101
pH 6	2	1	101

Table 6.3: Parameters for Savitzky-Golay (SG) Filter for MIR data-sets of pH 7, pH 6.5 and pH 6

MIR Data-Set	Polynomial Order	Derivative	Window Length
pH 7	2	2	7
pH 6.5	1	1	101
pH 6	2	1	601

6.5.2 Spectral Analysis

After pre-treatment, for Set 6.2.1, Absorbance values at each wavelength of interest in the NIR spectral region, as seen in Chapter 5 was plotted. This was done in order to understand the behaviour of the Absorbance peaks with change in pH for a constant lactate concentration.

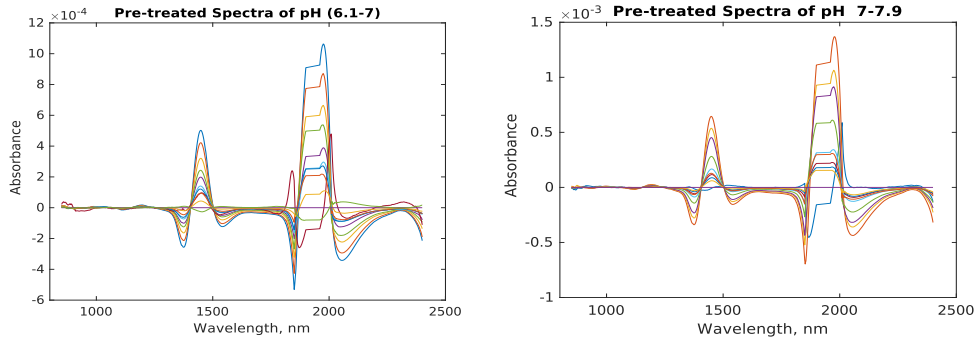

Figure 6.2: Pre-treated Spectra, Extended Multiplicative Scatter Correction (EMSC) and Savitzky-Golay filtering of pH 6-8. (a) Pre-treated Spectra of pH 6.1-7 (b) Pre-treated Spectra of pH 7-7.9. Figure taken from [254].

As for set 6.2.2, a rigorous analysis was done on all the three sets separately. The techniques which were applied are the same as mentioned in Chapter 5, Section 3.7.

6.6 Results

The raw Absorption spectra, pre-treated spectra and 2D synchronous contour plots looked exactly the same as the Figures 5.2, 5.3 and 5.4, in the previous Chapter. The changes were so minute that it could not be perceived visibly.

However, in the Set 6.2.1, through visual inspection, a distinction could be made in spectra from pH 6-7 and pH 7-8, as seen in Figure 6.2. While the spectra of pH 7 appeared to be different in both the data-sets.

The results of both the sets were again separated to three spectral regions like in Chapter 5 for a complete understanding of the data. They are as follows:

6.6.1 Spectral regions without O-H Absorption interference

The regions of the EM spectrum which are not affected by the overtone and combination bands of O-H absorbance were analysed in the following section. They include the UV/Vis spectral region, parts of the NIR spectral region (1050-1300 nm, 1660-1780 nm and 2200-2400 nm) and the MIR spectral region.

Results of Set 6.2.1

The NIR spectral region was divided into three sections, as mentioned above, and the Absorbance values of the wavelengths mentioned in Table 5.3 (Chapter 5) were plotted, as shown in Figure 6.3.

The Absorbance values of the wavelengths behaved in the following way:

- 1142 *nm* did not follow any trend with respect to the changes in pH
- 1233 *nm* showed a decreasing negative trend, with R^2=0.80
- 1710 *nm* and 1750*nm* also displayed a continuous steep decline in a second degree polynomial order in the absorbance values with increase in pH, with R^2 of 0.91 and 0.90, respectively
- 2205 *nm*, 2319 *nm* and 2341 *nm*, followed a second degree polynomial order curve with R^2 values of 0.96, 0.94 and 0.90, respectively, with the changes in pH from 6-7. It was followed by a dip and then again from pH 7.1-8, the wavelengths followed another second degree polynomial curve with R^2 values of 0.97, 0.96 and 0.95, respectively.

Results of Set 6.2.2

The wavelengths pertinent to lactate for these three data-sets in each region were chosen from Table 5.3 (Chapter 5) and the wavelengths found in literature, as seen in Chapter 4, Section 4.5.1. Linear Regression was performed on all the wavelengths and Table 6.4 shows the p-values. While, Tables: 6.5, 6.6, 6.7 and 6.8, displays the p-values of the UV/Vis, NIR and MIR wavelengths found in literature. Tables 6.9 and 6.10, shows the p-values for the linear regression done on the wavenumbers of lactic acid and lactate, respectively found in Table 4.1.

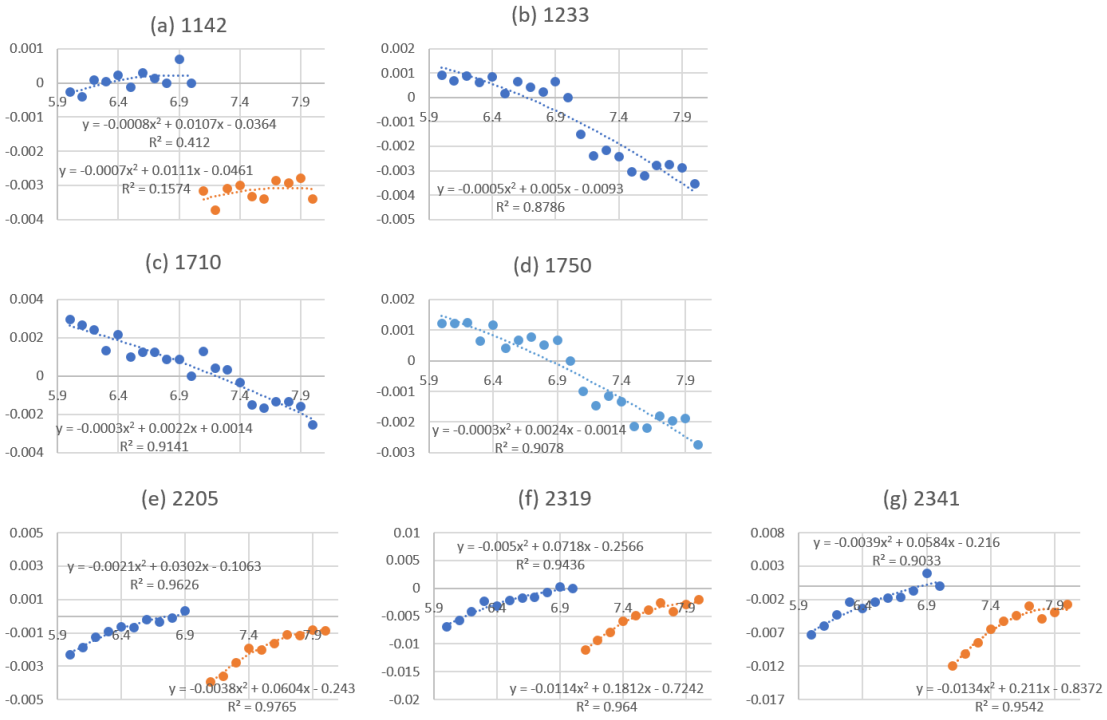

Figure 6.3: Absorbance vs pH of wavelengths: (a) 1142nm (b) 1233nm (c) 1710nm (d) 1750nm (e) 2205nm (f) 2319nm (g) 2341nm. Figure taken from[254].

Table 6.4: p-values of the linear regression done on the NIR wavelengths of Table 5.3.

NIR	Wavelengths (nm)							
Data Sets	1142	1233	1280	1330	1882	2205	2319	2341
7	5.63E-08	0.008	0.0072	1.92E-08	2.11E-05	6.52E-05	0.0081	0.0020
6.5	0.0030	4.66E-04	Not Significant	3.79E-06	0.017	0.044	Not Significant	Not Significant
6	Not Significant	Not Significant	Not Significant	Not Significant	Not Significant	Not Significant	Not Significant	Not Significant

Table 6.5: p-values of the Linear Regression done on the wavelengths (nm) on UV/Vis data-sets of pH 7, pH 6.5 and pH 6.

UV/Vis	Wavelengths (nm)	
Data-Set	320	747
pH 7	Not Significant	4.02E-07
pH 6.5	Not Significant	Not Significant
pH 6	Not Significant	0.0085

Table 6.6: p-values of the Linear Regression done on the wavelengths (nm) on NIR data-sets (800-1050nm) of pH 7, pH 6.5 and pH 6.

NIR	Wavelengths (nm)			
Data-Set	820	823	923	1047
pH 7	9.09E-04	0.0542	5.54E-07	5.34E-05
pH 6.5	Not Significant	Not Significant	Not Significant	8.86E-10
pH 6	0.012	Not Significant	0.044	0.044

6.6.2 Spectral regions of O-H Absorption

This section investigates the wavelengths which reflects O-H absorption in the NIR spectral region (as mentioned in Table 3.1) in Chapter 3.

Table 6.7: p-values of the Linear Regression done on the wavelengths (nm) on NIR data-sets (1600-2500nm) of pH 7, pH 6.5 and pH 6.

NIR	Wavelengths (nm)					
Data-Set	1675	1690	1730	2166	2254	2292
pH 7	1.73E-04	1.1E-04	4.9E-04	2.98E-04	9.51E-07	9.34E-08
pH 6.5	3.17E-03	5.55E-04	4.68E-04	2.99E-02	1.22E-05	5.99E-08
pH 6	Not Significant	Not Significant	Not Significant	Not Significant	Not Significant	Not Significant

Table 6.8: p-values of the Linear Regression done on the wavenumber (cm^{-1}) on MIR data-sets for Lactate Ion of pH 7, pH 6.5 and pH 6.

MIR	Wavenumber (cm^{-1})					
Data-Set	1127	1399	1747	1783	1039	1021
pH 7	5.87E-09	3.21E-04	1.45E-05	0.0951	0.0034	0.0037
pH 6.5	5.54E-08	Not Significant	0.019	0.047	2.15E-06	5.64E-07
pH 6	0.028	1.06E-07	1.56E-07	4.34E-08	Not Significant	Not Significant

Table 6.9: p-values of the Linear Regression done on the wavenumbers (cm^{-1}) for Lactate Complex on MIR data-sets of pH 7, pH 6.5 and pH 6.

MIR	Wavenumbers (cm^{-1})										
Data-Sets	1725	1475	1455	1420	1380	1335	1285	1240	1130	1090	1050
pH 7	1.97e-07	3.36E-04	0.0026	0.0025	0.0026	0.0015	2.03E-04	0.0051	0.0014	0.0019	0.0118
pH 6.5	3.98e-08	0.0022	2.99E-04	8.74E-08	6.39E-06	1.72E-06	5.7E-06	0.019	4.6E-08	5.13E-06	8.84E-08
pH 6	4.09e-08	0.0337	2.17E-06	4.35e-07	8.20E-04	0.030	4.16E-11	1.43E-15	6.53E-04	4.0939e-08	4.0939e-08

Table 6.10: p-values of the Linear Regression done on the wavenumbers (cm^{-1}) for Lactate ion on MIR data-sets of pH 7, pH 6.5 and pH 6.

MIR	Wavenumbers (cm^{-1})								
Data-Sets	1585	1470	1390	1370	1280	1270	1125	1045	860
pH 7	1.32E-04	0.0020	0.0069	0.0060	0.034	0.0072	3.8031e-11	0.0076	0.0094
pH 6.5	0.0041	0.0039	2.29E-05	6.14E-07	6.96E-05	0.0017	3.05E-08	1.92E-07	8.71E-05
pH 6	8.91E-05	5.9E-04	6.66e-08	2.17e-07	8.43E-11	0.00042	0.028	4.09e-08	4.09e-08

Table 6.11: p-values of the peaks corresponding to the O-H Absorption bonds in Near Infrared Region for Set 6.2.1.

Wavelength corresponding to O-H functional group (nm)	Functional Groups	p-values
970	O-H stretch	1.84E-06
1450	O-H stretch first overtone	3.99E-09
1490	O-H stretch first overtone	0.023
1540	O-H stretch first overtone	0.00291
1820	O-H stretch	0.00758
2070	O-H combination	0.019
2100	O-H bend	0.0086

Results of Set 6.2.1

Tables 6.11 shows the wavelengths with p-values (≤ 0.05) for the set of 20 spectra of varying pH and constant lactate concentration.

Results of Set 6.2.2

For these sets of spectra, except for 1540 *nm* and 1820 *nm* for pH data-set of 7 and 1820 *nm* for pH data-set of 6.5, no other wavelength showed p-values of ≤ 0.05.

6.6.3 Entire spectral regions for predictive models

Finally, the entire spectral ranges for all the nine sets were used to construct PLS calibration models, individually (like the previous chapter). PRESS vs LVs for the nine sets are shown in Figures 6.4, 6.5 and 6.6. The number of LVs used for the UV/Vis prediction models for pH 7, 6.5 and 6 were 3, 3 and 4, respectively. The number of LVs used for the NIR prediction models for pH 7, 6.5 and 6 were 8, 8 and 8, respectively. The number of LVs used for the MIR prediction models for pH 7, 6.5 and 6 were 3, 12 and 16, respectively.

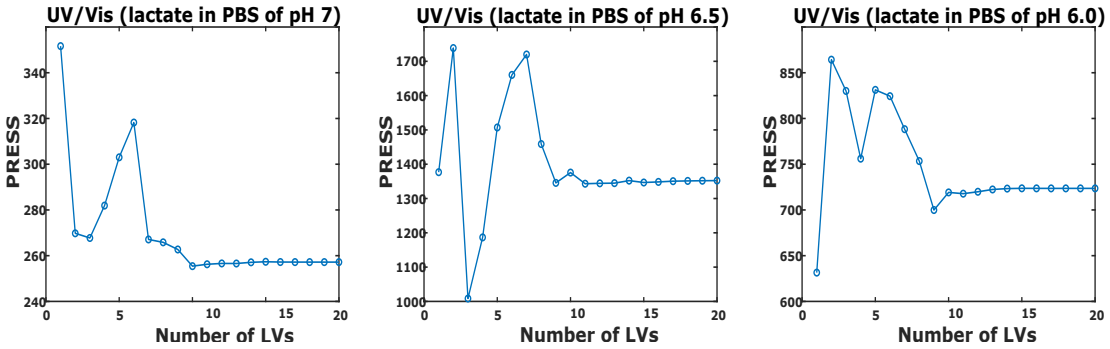

Figure 6.4: Prediction Error Sum of Squares (PRESS) versus number of latent variables (LV). (a) The number of LVs in the UV/Vis spectral region for pH 7 used was 3; (b) The number of LVs in the UV/Vis spectral region for pH 6.5 used was 3; (c) The number of LVs in the UV/Vis spectral region for pH 6 used was 4.

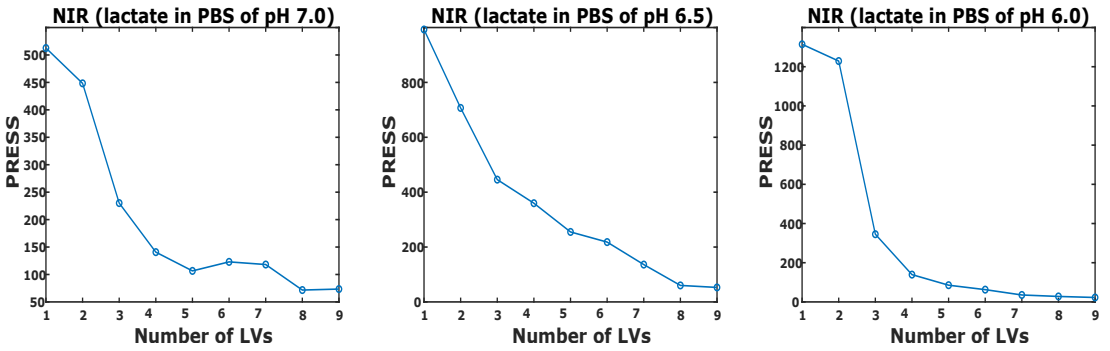

Figure 6.5: Prediction Error Sum of Squares (PRESS) versus number of latent variables (LV). (a) The number of LVs in the NIR spectral region for pH 7 used was 8; (b) The number of LVs in the NIR spectral region for pH 6.5 used was 8; (c) The number of LVs in the NIR spectral region for pH 6 used was 8.

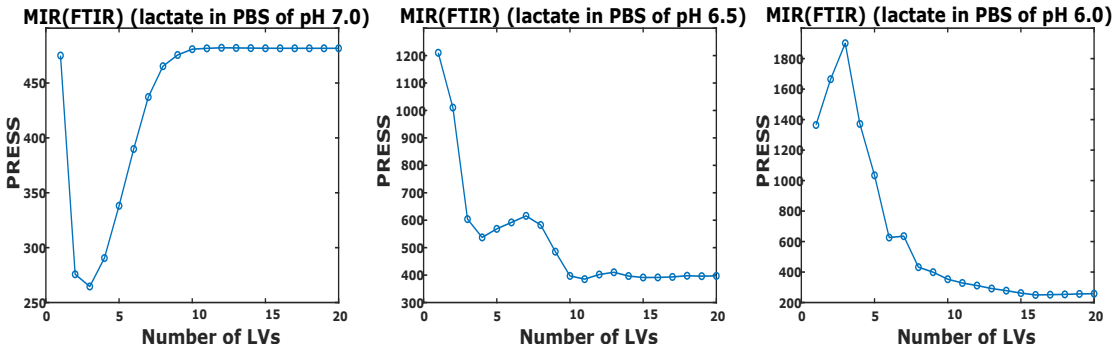

Figure 6.6: Prediction Error Sum of Squares (PRESS) versus number of latent variables (LV). (a) The number of LVs in the MIR spectral region for pH 7 used was 3; (b) The number of LVs in the MIR spectral region for pH 6.5 used was 12; (c) The number of LVs in the MIR spectral region for pH 6 used was 16.

Table 6.12: Coefficient of Determination (R^2) and Root Mean Squared Error Prediction (RMSECV) between the predicted and prepared samples for the MIR data-sets in the *'fingerprint region'* 600-1500 cm^{-1}.

MIR Data-Set	No. of LVs used	R^2	RMSECV (mM)
7.4	12	0.98	1.16
7	13	0.97	1.34
6.5	2	0.97	1.48
6	20	0.92	1.94

Lastly, Figures 6.7, 6.8 and 6.9 depicts observed (known) concentrations of lactate vs predicted concentrations by the nine predictive PLS models built using leave-one-out cross-validation analysis. The coefficients of determination R^2 of each of the nine sets are displayed in the figure;

- for the UV/Vis sets of pH 7, 6.5 and 6 the R^2 values were: 0.79, 0.32 and 0.62, respectively
- for the NIR sets of pH 7, 6.5 and 6 the R^2 values were: 0.91, 0.95 and 0.98, respectively
- for the MIR sets of pH 7, 6.5 and 6 the R^2 values were: 0.67, 0.69 and 0.80, respectively.

The root mean squared error of cross validation (RMSECV) for

- UV/Vis sets of pH 7, 6.5 and 6 were: 2.73 mM, 6.27 mM and 4.17 mM, respectively
- NIR sets of pH 7, 6.5 and 6 were: 0.63 mM, 0.44 mM and 0.42 mM, respectively
- MIR sets of pH 7, 6.5 and 6 were: 4.21 mM, 5.13 mM and 6.52 mM, respectively

However, for the MIR region, when PLS regression models are built using only the *'fingerprint region'*, 1500-600 cm^{-1}, the PRESS, R^2 and RMSECV values are as shown in Table 6.12.

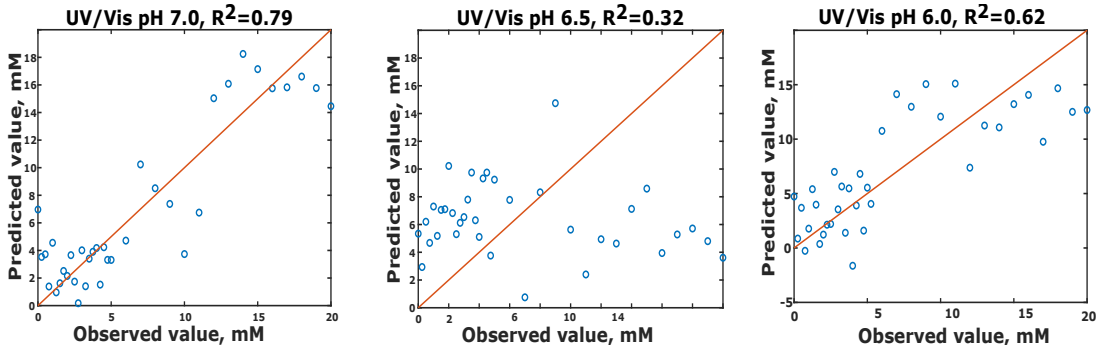

Figure 6.7: Observed (known) lactate concentration versus the Predicted concentrations of thirty-seven PBS samples of lactate prepared using solution stoichiometry. The correlation coefficient (R^2) and the root mean squared error of cross validation (RMSECV) for each set are also shown. (a) The Coefficient of Determination (R^2) and the root mean squared error of cross validation (RMSECV) for UV/Vis pH 7 set is 0.79 and 2.73 mM, respectively; (b) The Coefficient of Determination (R^2) and the root mean squared error of cross validation (RMSECV) for UV/Vis pH 6.5 set is 0.32 and 6.27 mM, respectively; (c) The Coefficient of Determination (R^2) and the root mean squared error of cross validation (RMSECV) for UV/Vis pH 6 set is 0.62 and 4.17 mM, respectively.

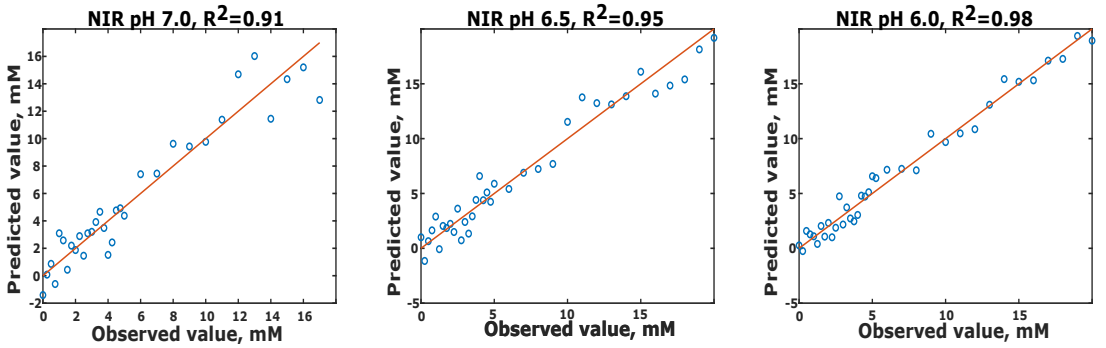

Figure 6.8: Observed (known) lactate concentration versus the Predicted concentrations of thirty-seven PBS samples of lactate prepared using solution stoichiometry. The correlation coefficient (R^2) and the root mean squared error of cross validation (RMSECV) for each set are also shown. (a) The Coefficient of Determination (R^2) and the root mean squared error of cross validation (RMSECV) for NIR pH 7 set is 0.91 and 0.63 mM, respectively; (b) The Coefficient of Determination (R^2) and the root mean squared error of cross validation (RMSECV) for NIR pH 6.5 set is 0.95 and 0.44 mM, respectively; (c) The Coefficient of Determination (R^2) and the root mean squared error of cross validation (RMSECV) for NIR pH 6 set is 0.98 and 0.42 mM, respectively.

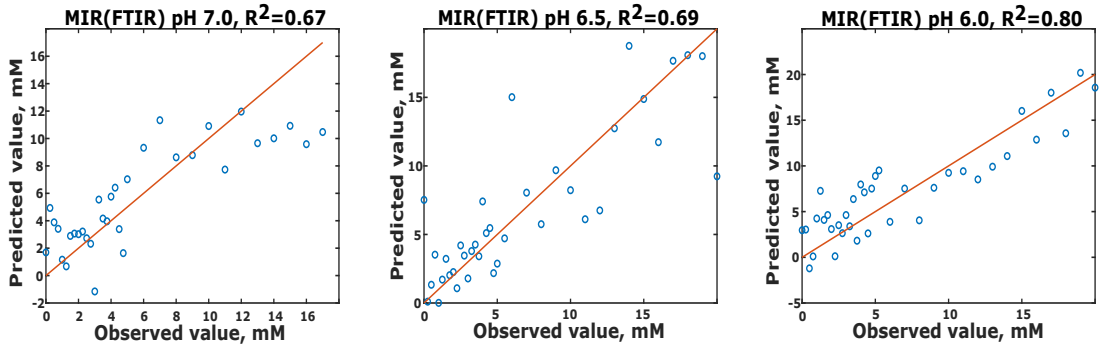

Figure 6.9: Observed (known) lactate concentration versus the Predicted concentrations of thirty-seven PBS samples of lactate prepared using solution stoichiometry. The correlation coefficient (R^2) and the root mean squared error of cross validation (RMSECV) for each set are also shown. (a) The Coefficient of Determination (R^2) and the root mean squared error of cross validation (RMSECV) for MIR pH 7 set is 0.67 and 4.21 mM, respectively; (b) The Coefficient of Determination (R^2) and the root mean squared error of cross validation (RMSECV) for MIR pH 6.5 set is 0.69 and 5.13 mM, respectively; (c) The Coefficient of Determination (R^2) and the root mean squared error of cross validation (RMSECV) for MIR pH 6 set is 0.80 and 6.52 mM, respectively.

Table 6.13: Linear Regression results of the pH NIR data-sets used to build predictive models.

Data-Sets Used for Training	Data-Set Predicted	No of LVs used	R^2	RMSEP (mM)
7.4, 7 and 6.5	6	9	-3.26	8.51
7.4, 7 and 6	6.5	9	-2.19	1.85
7.4, 6.5 and 6	7	9	-2.74	1.81
7, 6.5 and 6	7.4	9	-1.33	1.98

Moreover, to investigate further the inter-dependence of lactate concentration and pH, the effects of which would be reflected on the spectra, PLS models were built using three data-sets, while attempting to predict the concentration of the remaining data-set for the NIR and MIR region. Table 6.13 and 6.14 shows the PRESS, R^2 and Root Mean Squared Error of Prediction (RMSEP) values for these predictive models for the NIR and MIR (1500-600 cm^{-1}) data-sets, respectively.

6.7 Summary

The effects of pH on spectral features of solution samples with varied lactate concentrations were studied in this chapter. Two sets of solution samples were prepared: one,

Table 6.14: Linear Regression results of all the MIR data-sets of pH 7.4, 7, 6.5 and 6 used to build predictive models.

Data-Sets Used for Training	Data-Set Predicted	No of LVs used	R^2	RMSEP (mM)
7.4, 7 and 6.5	6	15	0.99	1.13
7.4, 7 and 6	6.5	15	0.97	1.13
7.4, 6.5 and 6	7	15	0.98	1.13
7, 6.5 and 6	7.4	15	0.97	1.13

where the lactate concentration was kept constant with varying pH from 6-8 and the other, in which there were 37 different lactate concentrations for 3 different data-sets of constant pH (7, 6.5 and 6). The spectra of both the sets were studied separately to understand the effects of pH in both scenarios.

The results for both the sets were separated on the basis of spectral regions with and void of O-H absorption, like the previous chapter. The first part were the spectral regions without O-H interference;

For the first set of spectra, the Absorbance values of the wavelengths 1233 nm, 1710 nm, 1750 nm, 2205 nm, 2319 nm and 2341 nm followed second degree polynomial order curves similar to theoretical calculations. While, for the second set, the wavelengths 747 nm, 1047 nm and 1127 cm^{-1} showed linear correlations across all three pH. pH 7 seemed to follow the trends for *'signature wavelengths'* of lactate, which were found for pH 7.4 in the previous chapter. However, the other data-sets did not correlate well with the previous wavelengths. It could be very clearly seen that the *'signature wavelengths'* of lactate are affected by the changes in pH.

The second part of the spectral regions under analysis were the regions of O-H absorption. The first set of spectra showed good correlation with all the wavelengths pertinent to O-H absorption whereas, where the second set showed almost no correlation.

The third part of spectral analysis was done, where the whole spectra for each set, independently, were considered to build PLS regression models using LVs from PRESS results. The cross-validation of the predictive models for each data-set was done using

the leave-one-out model. In the UV region, the data-set of pH 7 showed good predictions: R^2 of 0.79 and RMSECV was 2.73 mM, between predicted and prepared samples. In the NIR, all three sets showed very high R^2 and relatively low RMSECV values. However, different pH data-sets had different *'signature wavelengths'* in the whole of the Electromagnetic Spectrum and this could be further verified using predictive models which were built using three data-sets, while attempting the predict the remaining.

Finally in the MIR region, the data-set pH 6 showed the best R^2 of 0.80 and the RMSECV was 6.52 mM, between predicted and prepared samples. However, when the *fingerprint region* (1500-600 cm^{-1}) was used to predict lactate concentrations for each data-set independently, the results were consistent with $R^2 \geq 0.90$ and relatively low RMSECV. Moreover, the R^2 values were also ≥ 0.97 when one data-set was predicted using the other three in the same region. Hence, it could be concluded that pH does not have an affect on the spectral features in the *'fingerprint region'* of the EM spectrum.

The next chapter aims in understanding similar in-vitro experimental spectra for lactate concentration changes in human serum.

Trying to determine the structure of a protein by UV spectroscopy was like trying to determine the structure of a piano by listening to the sound it made while being dropped down a flight of stairs.

Francis Crick, Nobel Prize in Physiology or Medicine for DNA Helix structure, 1962

7

In-vitro Spectrometric Analysis of Lactate in Human Serum

7.1 Introduction

Spectral features can be affected by a change in medium. Studies from the previous chapters, have shown that the *'Absorption profile'* of lactate is largely influenced by pH in the same medium. In this chapter, the effects on the spectral features when the PBS buffer medium is replaced by human serum, at physiological pH, is investigated.

Human Serum is a part of whole blood consisting of water, electrolytes and proteins like albumin and globulins. The addition of proteins in the solution samples of changing lactate concentration was expected to alter spectral features because of the effects of mild scattering *.

Spectra were collected from solution samples of changing lactate concentration in the NIR and *'fingerprint region'* of the MIR spectral regions. These were then pre-treated and analysed. In addition, this chapter introduces spectra collected from a state-of-the-art Fourier Transformed Near Infrared (FTNIR) spectrometer, as opposed to a dual beam dispersive spectrophotometer (as seen in previous chapters). Hence, a comparison was drawn based on the characteristic spectral feature changes while predicting lactate concentrations in the NIR region. The next sections describe the methods and results elaborately.

7.2 Sample Preparation

Human Serum Mixed Pool, Sterile Filtered, "Off the Clot" was commercially purchased from TCS Biosciences Ltd (*Buckingham, UK*). "Off the Clot" human serum was chosen because these products are devoid of any artificially added anticoagulants and are hence, ideal for laboratory based research. Upon arrival, the products were taken out from the dry ice box and kept at room temperature. Lactate concentration and pH were measured as soon as the temperature reached 25 °C using the Blood-Gas Analyser (BGA), ABL 825, from Radiometer UK Limited (*Crawley, UK*), (as seen in Chapter 4, Figure 4.3). The initial values for the lactate concentration and pH were 7.7 mM and 7.3, respectively. In order to broaden the range of lactate concentrations in the physiological range, for developing a robust mathematical model, this was divided into 41 vials of 19 mL each. These samples were stored in the refrigerator at 4° C.

*The study was approved by the Senate Research Ethics Committee (SREC), City, University of London, (Ethics Application is included in Appendix A), because of the involvement of biological fluids.

The next step was to prepare solution samples of known lactate concentration using solution stoichiometry, like the previous chapters. Lactate Stock Solution, (Chapter 5, Section 5.2.2) was diluted to forty one different concentrations of lactate in separate vials of 30 mL each using Phosphate Buffer Solution (Chapter 5, Section 5.2.1). The concentrations of lactate in the vials ranged from 0 to 10 mM, at intervals of 0.5 mM. All the samples were again kept at room temperature and pH of each sample was maintained at 7.4.

Thereafter, each of 1 mL of the prepared lactate and PBS samples were introduced in the vials containing 19 mL of serum to obtain 41 samples of varying lactate concentrations of 20 mL each. Lactate concentrations and pH of the prepared samples were re-measured using the BGA, ABL 825. The range of lactate concentrations varied from 7.7 to 15 mM and pH from 7.1 to 7.4. The prepared samples were once again refrigerated at 4° C and measurements for lactate and pH were repeated again just before introducing the samples in the spectrometer. Since the spectra collection lasted for only a week, both values were consistent.

7.3 Spectroscopy (Dual Beam Dispersive NIR, FTNIR and MIR)

The samples were taken out of the refrigerator and kept in a cool dry place until the temperature rose to room temperature. These were remeasured for lactate and pH like mentioned before and then introduced in the spectrometers for spectra collection. The following spectrometers were used for spectra collection in the defined wavelength ranges:

- NIR: Lambda 1050, (800-2600 nm)
- FTNIR: Frontier (900-3000 nm)
- FTIR: Frontier (2500-500 cm^{-1})

Each of the spectral collection methods are described in detail below:

7.3.1 Dual Beam Dispersive NIR Spectroscopy

Similar to the previous chapters, the Lambda 1050 dual beam spectrophotometer, (Chapter 3, Section 3.4.2, Figure 3.7), was again used to collect three spectra from each sample, at random, with step increments of 2 *nm*. These were then averaged to obtain the final spectrum and hence, forty one spectra were obtained from the total 123 spectra.

The light source used was a halogen-tungsten lamp and the detectors settings were kept similar to Chapter 5, Table 5.1. Again, the reference beam and baseline correction were set at 1% attenuation and 100% Transmittance/ 0% Absorption, respectively to reduce background noise. The same quartz cuvettes (Hellma (*GmbH & Co., Germany*)) of 1 *mm* path length were used in similar manner.

7.3.2 FTNIR and FTIR Spectroscopy

The *Frontier*^{TM} FTIR/NIR Spectrometer, (Chapter 3, Section 3.4.2 Figure 3.8), with a HATR accessory was used to collect the FTNIR and FTIR spectra.

Spectra were collected at data intervals of 0.2 cm^{-1} and 0.1 cm^{-1} for FTNIR and FTIR, respectively. The spectral resolution was maintained at 0.1 cm^{-1} for both the data-sets and the variable J-stop (Jacquinot-stop) was kept at default (3.16 *mm* at 4000 cm^{-1}). Similar to the previous chapter, an average of 50 scans per sample with a scan speed of 0.2 cm s^{-1} were taken, as part of spectra acquisition in the study. Again, like the previous chapters, a sample size of 70 μL was laid out directly on the ZnSe crystal, covering the whole crystal. A background scan with the empty crystal was taken every 20 min in the study.

Spectra collection and visualisation was carried out using the software, mentioned in Chapter 3, Section 3.5.

7.4 Data Analysis (Dual Beam Dispersive NIR, FTNIR and MIR)

Pre-treatment and analysis on all the data-sets was realized in MATLAB R2020b, MathWorks^{TM} *(Natick, MA, USA)*, much like the previous chapters and are described in detail in the following sections.

7.4.1 Pre-Treatment and spectral analysis

Pre-treatment and spectral analysis techniques were implemented in succession on each of the spectral data-sets, like as mentioned in Chapter 5, Section 5.4.1 and 5.4.2:

- Spectral Difference: The spectrum of the first sample (7.7 mM concentration of lactate) was subtracted from the rest of the spectra.
- Linear Robust Multiplicative Scatter Correction (MSC) was used for the dual beam dispersive NIR and FTNIR data-sets. While, Extended Multiplicative Scatter Correction (EMSC) with quadratic polynomial baseline correction was used for MIR data set.
- Savitzky-Golay (SG) filter parameters (Polynomial Order, Derivative and Window Length) for the three data-sets are mentioned in Table 7.1.

Table 7.1: Parameters for Savitzky-Golay (SG) Filter.

Data-Set	Polynomial Order	Derivative	Window Length
Dual Beam Dispersive NIR	2	1	151
FTNIR	2	1	7
MIR (FTIR)	2	1	151

The spectral analysis techniques those were executed were:

- 2D correlation

- Linear Regression was performed on selected wavelengths which were significant (with p-values ≤ 0.05) for pH data-set 7.4 and 7, only, as seen from the Chapters 5 and 6
- Aquagrams
- Partial Least Square (PLS).

7.5 Results

Likewise, as mentioned in the previous chapter, the raw Absorption spectra, pre-treated spectra and 2D synchronous contour plots looked exactly the same as the Figures 5.2 (b and c), 5.3 (b and c) and 5.4 (b and c), in Chapter 5, respectively. The changes in the spectra due to the change of medium were infinitesimal as water constitutes a large part of Human Serum and dominates the Absorption spectral features.

Again, for simplicity of understanding, the spectral regions were separated into three regions and the results are as follows:

7.5.1 Spectral regions without O-H Absorption interference

The data-sets dual beam dispersive NIR and FTIR were used for linear regression to maintain consistency with the previous results for comparison.

The *'signature wavelengths'* of lactate in the NIR region which were relevant in the previous chapters for pH data-sets 7.4 and 7 (as found in literature) were:

923 *nm*, 1047 *nm*, 1675 *nm*, 1690 *nm*, 1730 *nm*, 2166 *nm*, 2254 *nm*, 2292 *nm*, as found in literature;

and the wavelengths 1142 *nm*, 1233 *nm*, 1280 *nm*, 1330 *nm*, 1710 *nm*, 1750 *nm*, 1882 *nm*, 2205 *nm*, 2319 *nm* and 2341 *nm* were found from the solid lactate spectra and 2D Correlation from Table 5.3. These wavelengths were also significant with p-values (≤ 0.05) for data-sets with pH 7.4 and 7, as seen in Table 5.4 and Table 6.4, respectively.

Table 7.2: p-values for significant lactate wavelengths for dual beam dispersive NIR human serum data-set.

Wavelength (nm)	1675	1690	1710	2292	2319
p-values	0.014	0.00069	0.00019	5.32E-05	0.00049

Table 7.3: p-values for significant lactate ion wavenumbers for MIR human serum data-set.

Wavenumber (cm^{-1})	1585	1470	1390	1320
p-values	6.40E-09	0.00223	0.00662	3.91E-06

Table 7.2 indicates the significant lactate wavelengths with p-values (≤ 0.05) for the dual beam dispersive NIR human serum data-set.

Table 7.3 and 7.4 indicates the significant wavelengths for lactate ion and lactic acid, respectively with p-values (≤ 0.05) for the MIR human serum data-set.

7.5.2 Spectral regions with O-H Absorption interference

The wavelength 1450 nm, indicated p-value ≤ 0.05 amidst all the O-H absorption bands or bond as mentioned in Table 3.1, Chapter 3.

An aquagram was also constructed as seen in Figure 7.1 for the dual beam dispersive NIR data-set.

7.5.3 Entire spectral regions for predictive models

Subsequently, PLS calibration models were constructed for the three data-sets separately, using reduced/selected wavelength ranges as follows:

- dual beam dispersive NIR: 800-1900 nm and 1960-2400 nm

Table 7.4: p-values for significant lactate complex wavenumbers for MIR human serum data-set.

Wavenumber (cm^{-1})	1725	1475	1380	1335	1130	1050
p-values	4.6649e-15	0.00337	0.00013	0.0531	1.67E-11	1.66E-06

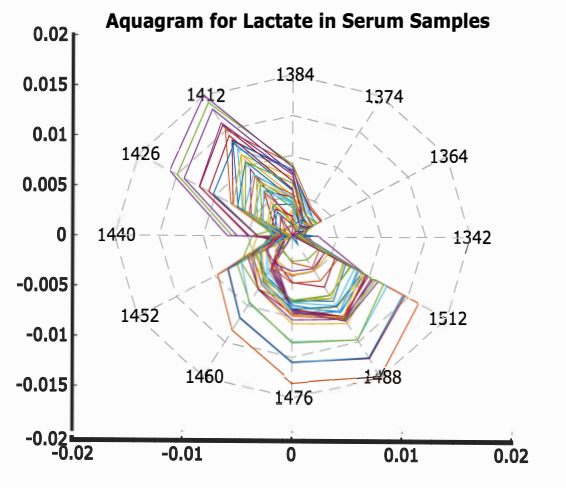

Figure 7.1: Aquagram for lactate in Serum samples in Water Absorbance Bands (WAB): 1300-1600nm, showing Water Absorbance Spectral Pattern (WAPS) in the Water matrix co-ordinates (WAMACS) of varying concentrations of lactate in human serum samples. The WAMACS: 1342, 1364, 1374, 1384, 1412, 1426, 1440, 1452, 1460, 1476, 1488 and 1512 depicts molecular conformations which arises due to water-NIR light-lactate molecule interactions.

- FTNIR: 900-2340 nm
- FTIR: 800-1600 cm^{-1}.

The wavelengths were reduced in the NIR spectral ranges to avoid unwanted interference due to noise region of overtone and combination bands of C=O and O-H functional groups (Chapter 3, Table 3.1). PRESS was again used to create the simplest model with least number of LVs. Hence, from Figure 7.2, the number of LVs used for dual beam dispersive NIR set was 9, FTNIR set was 3 and MIR (FTIR) set was 18.

Finally, Figure 7.3, plots observed (known) concentration of lactate and predicted concentrations by the predictive PLS models build using leave-one-out cross-validation analysis. The Coefficients of Determination (R^2) for each set, as shown in the figure; dual beam dispersive NIR set was 0.77, FTNIR set was 0.90 and MIR (FTIR) set was 0.94. The Root Mean Squared Error of Cross Validation (RMSECV) for dual beam dispersive NIR set 1.11 $m\mathcal{M}$, FTNIR set 1.75 $m\mathcal{M}$ and MIR (FTIR) set was 1.31 $m\mathcal{M}$.

Furthermore, PLS models were also built in order to investigate the inter-dependence

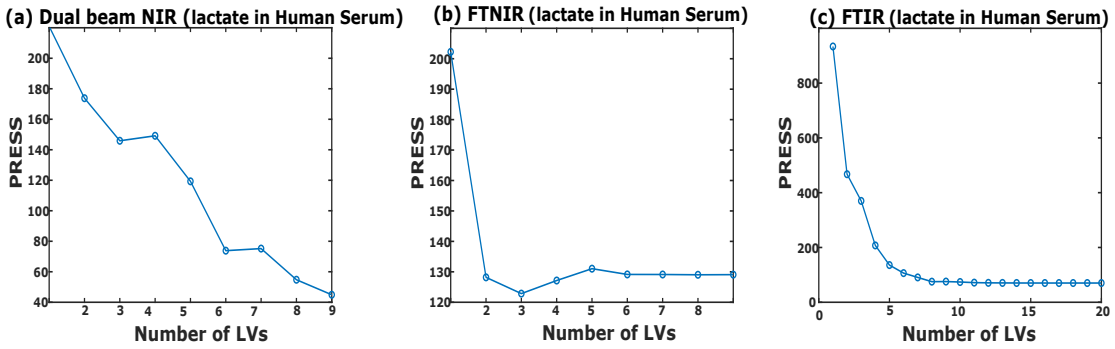

Figure 7.2: Prediction Error Sum of Squares (PRESS) versus number of latent variables (LV) for of 41 samples of Lactate solutions in Human Serum for dual beam dispersive NIR data-set, FTNIR data-set and MIR (FTIR) data-set. (a) The number of LVs for the dual beam dispersive NIR data-set used was 9; (b) The number of LVs for the FTNIR data-set used was 3; (c) The number of LVs for the MIR data-set used was 18.

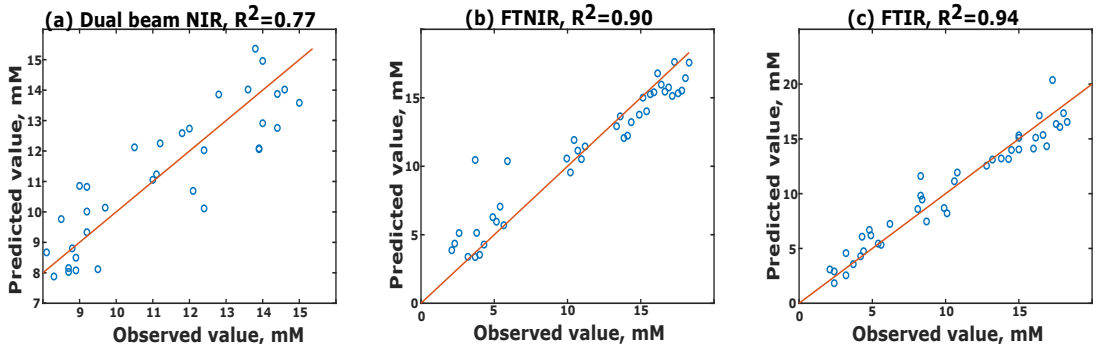

Figure 7.3: Observed (known) lactate concentration versus the Predicted concentrations of forty-one samples of lactate in Human Serum. The correlation coefficient (R^2) and the Root Mean Squared Error of Cross Validation (RMSECV) for each set are also shown. (a) The Coefficient of Determination (R^2) and the Root Mean Squared Error of Cross Validation (RMSECV) for dual beam dispersive NIR data-set are 0.77 and 1.11 mM respectively; (b) The Coefficient of Determination (R^2) and the Root Mean Squared Error of Cross Validation (RMSECV) for FTNIR set are 0.90 and 1.75 mM respectively; (c) The Coefficient of Determination (R^2) and the Root Mean Squared Error of Cross Validation (RMSECV) for MIR (FTIR) set are 0.94 and 1.31 mM respectively.

Table 7.5: Linear Regression results of the MIR data-sets of lactate in PBS of pH 7.4, 7, 6.5, 6 and human serum used to build predictive models.

Data-Sets Used for Training	Data-Set Predicted	No. of LVs used	(R^2)	RMSEP (mM)
pH 7.4, 7, 6.5 and 6	Human Serum	13	0.97	1.98
pH 7, 6.5, 6 and Human Serum	pH 7.4	13	0.97	1.98
pH 7.4, 6.5, 6 and Human Serum	pH 7	13	0.98	1.98
pH 7.4, 7, 6 and Human Serum	pH 6.5	13	0.97	1.98
pH 7.4, 7, 6.5 and Human Serum	pH 6	13	0.99	1.98

of lactate concentrations, change in pH and media in the *'fingerprint region'* of the MIR region. Table 7.5 shows the PRESS, (R^2) and RMSEP values for these predictive models for the MIR (1500-600 cm^{-1}) using data-sets of lactate in PBS of pH 7.4, 7, 6.5, 6.0 (from the previous chapters) and human serum. Like previously, models were built using four data-sets, while setting aside one of them. These models were then used to predict the remaining data-set which was set aside in the beginning.

7.6 Summary

In this chapter, the changes in spectra due to substitution of the medium was investigated. Solution samples were prepared of varying lactate concentrations in human serum (bought commercially) and spectra was obtained in the NIR and the *fingerprint region* of the MIR spectral regions. For the NIR spectral region, two state-of-the-art spectrometers (LAMBDA 1050 and Frontier^{TM} FTIR/NIR) were used to compare the instrument capabilities for predicting lactate concentrations. The LAMBDA 1050 being a dual beam dispersive spectrophotometer while, the Frontier^{TM} records the Fourier Transformed NIR signals.

Pre-treatment and spectral analysis of the obtained spectra was performed using similar techniques as described in the previous chapters. In the spectral regions which lie external to the influence of O-H absorption, linear regression was performed on wavelengths which were found significant in the previous chapters for pH 7.4 and 7. The

wavelengths 1675 nm, 1690 nm, 1710 nm, 2292 nm and 2319 nm were found to be significant (p-values ≤ 0.05) in the NIR spectral region. In the MIR spectral region, wavenumbers 1585 cm^{-1}, 1470 cm^{-1}, 1390 cm^{-1} and 1320 cm^{-1} were linearly correlated to the concentration changes of lactate ion and 1725 cm^{-1}, 1475 cm^{-1}, 1380 cm^{-1}, 1335 cm^{-1}, 1130 cm^{-1} and 1050 cm^{-1} for lactic acid. There was one wavelength at 1450 nm, which was found to be linearly correlated in the spectral regions of O-H absorbance interference.

Finally, the whole spectral range was used to obtain PLS regression models using leave-one-out cross-validation, for the three data-sets; dual beam dispersive NIR, FTNIR and the FTIR using LVs 9, 3 and 18, respectively. The Coefficients of Determination (R^2) for the dual beam dispersive NIR, FTNIR and FTIR was 0.77, 0.90 and 0.94, respectively. While, the Root Mean Squared Error of Cross Validation (RMSECV) for dual beam dispersive NIR, FTNIR and the FTIR sets was 1.11 mM, 1.75 mM and 1.31 mM, respectively, between the predicted and prepared samples.

Furthermore, the effects of the change in medium on the spectra, with respect to the variations in lactate concentration changes in the MIR region was also inspected. For this purpose, five PLS regression models were built using the pH data-sets from the previous chapters and the human serum data-set, as seen in this chapter. Cross-validation results provided very high values of R^2 and an acceptable RMSEP value. This shows that a change in medium does not have an effect in the *'fingerprint region'* of the MIR spectral region of the EM spectrum.

Water seems unaware of the rules of chemistry or laws of physics.

Bill Bryson, The Bounding Main, A Short History of Nearly Everything, 2003.

8

In-vitro Spectrometric Analysis of Lactate in Whole Blood

8.1 Introduction

Whole Blood is a biological fluid medium with multifarious complex elements and scatterers. As seen in the previous chapter, the Absorption spectra of lactate is influenced by a change in the medium. Adding to the complexity of the medium, in this chapter, the effects of lactate concentration changes in whole blood,

as a medium, are investigated. Whole blood consists of components like red blood cells (erythrocytes), white blood cells (leukocytes), platelets (thrombocytes) and blood plasma (containing water, electrolytes, plasma proteins, etc) at various concentrations and each factor contributes to absorption features in the spectra because of scattering. This chapter aims in understanding these changes in the spectral features in the NIR and MIR spectral region with lactate concentration changes.

The methods were kept consistent like the previous chapter to facilitate comparison studies. * The following sections expatiates the methods and results.

8.2 Sample Preparation

Samples for this study were prepared using the same procedure, as described in Chapter 7, Section 7.2. Whole sheep blood in Alsever's † was purchased from TCS Biosciences Ltd (*Buckingham, UK*). Sheep blood was chosen for this study because the normal and temporal variation of lactate was found to be very similar to human lactate concentrations in whole blood[255].

Initial measurements using the ABL 825 from Radiometer UK Limited (*Crawley, UK*), (Chapter 4, Figure 4.3) at 25 °C, displayed lactate concentration of 4.2 mM (average) at a pH of 7.3.

On addition of 1 mL of lactate in PBS solution of known concentration to 19 mL of whole blood, the yielded range of lactate concentrations was from 4.5 to 13.8 mM at pH of 7.1 to 7.3. Spectra for these 41 samples of lactate in whole blood samples were then collected in the different regions as described in the next section.

*This study was also approved by the Senate Research Ethics Committee (SREC), City, University of London, (The document is as seen in the previous chapter and is included in Appendix A).

†Alsever's Solution is an isotonic solution with NaCl, Citric Acid and D-Glucose, which is typically used for preservation and anti-coagulation of whole blood (almost 10 weeks at 2-8 °C).

8.3 Spectroscopy (Dual Beam Dispersive NIR, FTNIR and MIR)

NIR Specta for the samples were collected again using two different instruments (Lambda 1050 (Chapter 3, Section 3.4.2, Figure 3.7) and Frontier^{TM} FTIR/NIR (Chapter 3, Section 3.4.2 Figure 3.8)). The Frontier^{TM} FTIR/NIR was also used to collect spectra of the MIR region like the previous chapter.

However, unlike all the previous chapters, a 100 *mm* PMT/InGaAs integrating sphere detector was used instead of the three detector module for dual beam spectra acquisition in the LAMBDA 1050. The detector was set at 0 deg transmission mode at a wavelength range of 870-2600 *nm* at 2 *nm* data interval. The reason behind this substitution was to explore the capabilities of the integrating sphere detector for a homogenised scattering of the light. Light transmitted through the whole blood sample is bound to scatter in multiple directions due to the numerous scatterers present in the sample. Hence, in order to preserve the power of the light, so that more light which is present inside the sphere is irradiated on the detector, after multiple diffuse reflections on the walls of the integrating sphere. This change in the detector might provide superior results for this data-set, compared to the previous chapters. Also, for the NIR wavelength ranges, the absorption profile of whole blood is mainly influenced by the O-H bonds of water, as seen in all the previous chapters[256]. Hence, to impede oversaturation of the InGaAs detector, the settings in the detector were maintained as follows: Gain = 0, Response Time = 0.2 s and Slit Size = 2*nm*. The attenuation of the reference beam was kept at 1 %, and the same quartz cuvettes from (Hellma (*GmbH & Co., Germany*)) of 1*mm* path length were used for sample introduction in the spectrophotometer. A Spectralon Diffuse Reflectance Standard from Lapsphere *(North Sutton, NH, USA)*, was placed at the aperture of the sphere for both baseline corrections and sample spectra collections.

Similar to the previous chapter, FTNIR and FTIR spectra were collected using the Frontier^{TM} FTIR/NIR for wavelength ranges of 900-4000 *nm* at 0.8 *nm* intervals and

2500-500 cm^{-1} at 2 cm^{-1}, respectively and spectral resolution of 2 cm^{-1}, for both, the variable J-stop (Jacquinot-stop) was kept at 3.16 mm at 4000 cm^{-1}.

Again, a total of 123 (41 for each set) spectra were collocated into three separate data-sets for processing and analysis.

8.4 Data Analysis (Dual Beam Dispersive NIR, FTNIR and MIR)

After spectra collection, the next step was pre-treatment and like the previous chapters, the following techniques were implemented on each of the data-sets separately, in succession:

- Spectral Difference: The spectrum of the first sample (4.2 mM concentration of lactate) was abated from the rest of the spectra.
- Linear Robust Multiplicative Scatter Correction (MSC) was used for the dual beam dispersive NIR and FTNIR data-sets. While, Extended Multiplicative Scatter Correction (EMSC) with quadratic polynomial baseline correction was used for MIR data set.
- Savitzky-Golay (SG) filter parameters (Polynomial Order, Derivative and Window Length) for the three data-sets are mentioned in Table 8.1.

Table 8.1: Parameters for Savitzky-Golay (SG) Filter.

Data-Set	Polynomial Order	Derivative	Window Length
Dual Beam Dispersive NIR	2	1	7
FTNIR	2	1	31
MIR (FTIR)	2	1	55

Finally, similar to the previous chapter, spectral analysis techniques those were performed were:

- 2D correlation
- Linear Regression was performed on selected wavelengths as seen in the previous chapter
- Aquagrams
- Partial Least Square (PLS).

8.5 Results

As mentioned previously, in the NIR spectral region, the O-H overtones and combination bands of the water region overshadows all the crucial lactate peaks to be visually detected. Hence, the spectra again looked like the raw Absorption spectra, pre-treated spectra and 2D synchronous contour plots as the Figures 5.2 (b and c), 5.3 (b and c) and 5.4 (b and c), in Chapter 5, respectively. In order to draw out the relevant lactate peaks in all the three data-sets, each of them were divided into three regions, as follows:

8.5.1 Spectral regions without O-H Absorption interference

Linear regression was performed on all the wavelengths which were identified in the previous chapter, as seen in Section 7.5.1.

Table 8.2 indicates the significant lactate wavelengths [‡] with p-values (≤ 0.05) for the dual beam dispersive NIR whole blood data-set. The wavelengths 1046 nm, 1142 nm, 1232 nm, 1280 nm, 1330 nm, 1690 nm, 1710 nm, 1750 nm, 2166 nm, 2320 nm and 2341 nm were significant with p-values ≤ 0.05.

Table 8.3 and 8.4 indicates the significant wavelengths for lactate ion and lactic acid, respectively with p-values (≤ 0.05) for the MIR whole blood data-set.

[‡]The wavelength (or step) increments were $2nm$ for this data-sets. Hence, the wavelengths nearest to the original values were considered.

Table 8.2: p-values for significant lactate wavelengths for dual beam dispersive NIR whole blood data-set.

Wavelength (nm)	1046	1142	1232	1280	1330	1690	1710	1750	2166	2320	2342
p-values	8.90E-04	8.47E-10	2.55E-06	0.033	0.016	2.60E-04	0.0013	0.0092	0.028	4.60E-04	0.029

Table 8.3: p-values for significant lactate ion wavenumbers for MIR whole blood data-set.

Wavenumber (cm^{-1})	1585	1390	1320	1280	1270	1125	1045	860
p-values	6.14E-12	0.029	0.0017	0.016	0.052	6.14E-12	6.14E-12	0.013

8.5.2 Spectral regions with O-H Absorption interference

The p-values for the wavelengths 1450 *nm*, 1820 *nm* and 2100 *nm* were 0.0115, 0.0153 and 0.0344, respectively.

Figure 8.1 shows an Aquagram constructed for the dual beam dispersive NIR data-set.

8.5.3 Entire spectral regions for predictive models

PLS predictive models were constructed using the three data-sets for this chapter, as well. The LVs used to create the simplest models for each data-set are as shown in Figure 8.2. The number of LVs used for the dual beam dispersive NIR data-set was 9, number of LVs used for the FTNIR data-set was 6. Figure 8.2 (c) doesnot show show a clear saddle point like the previous figures, hence, the lowest of those points are considered and the number of LVs used for FTIR data-set was 11.

After building the PLS models, cross-validation by leave-one-out was realised on individual data-sets. The results are as shown in Figure 8.3. The coefficients of determination (R^2) of each set, as shown in the figure; dual beam dispersive NIR set 0.75, FTNIR set 0.85 and MIR (FTIR) set was 0.93. The Root Mean Squared Error of Cross

Table 8.4: p-values for significant lactate complex wavenumbers for MIR whole blood data-set.

Wavenumber (cm^{-1})	1725	1475	1455	1420	1335	1285	1130	1090	930
p-values	6.14E-12	6.14E-12	6.14E-12	1.4E-04	6.14E-12	6.14E-12	0.0116	5.5E-04	0.0361

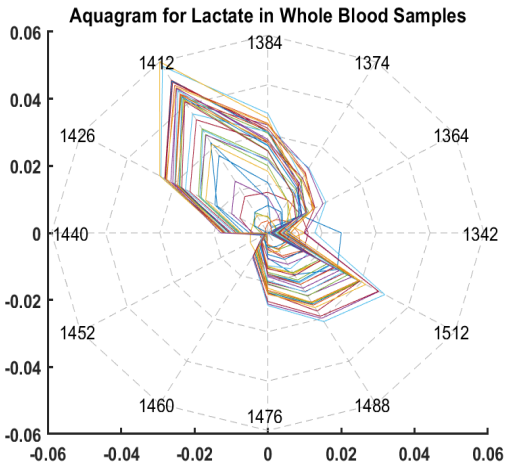

Figure 8.1: Aquagram for lactate in Whole Blood samples in Water Absorbance Bands (WAB): 1300-1600nm, showing Water Absorbance Spectral Pattern (WAPS) in the Water matrix co-ordinates (WAMACS) of varying concentrations of lactate in whole blood samples. The WAMACS: 1342, 1364, 1374, 1384, 1412, 1426, 1440, 1452, 1460, 1476, 1488 and 1512 depicts molecular conformations which arises due to water-NIR light-lactate molecule interactions.

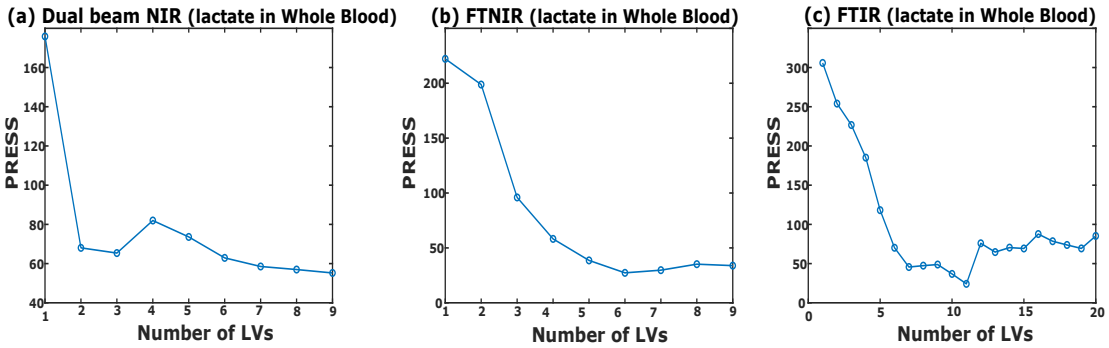

Figure 8.2: Prediction Error Sum of Squares (PRESS) versus number of latent variables (LV) for 41 samples of Lactate solutions in whole blood for dual beam dispersive NIR data-set, FTNIR data-set and MIR (FTIR) data-set. (a) The number of LVs for the dual beam dispersive NIR data-set used was 9; (b) The number of LVs for the FTNIR data-set used was 6; (c) The number of LVs for the MIR data-set used was 11.

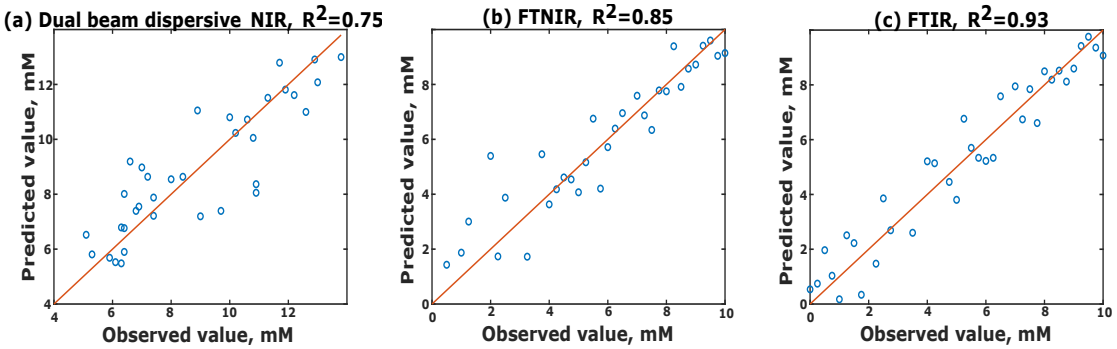

Figure 8.3: Observed (known) lactate concentration versus the Predicted concentrations of forty-one samples of lactate in whole blood. The correlation coefficient (R^2) and the Root Mean Squared Error of Cross Validation (RMSECV) for each set are also shown. (a) The Coefficient of Determination (R^2) and the Root Mean Squared Error of Cross Validation (RMSECV) for dual beam dispersive NIR data-set are 0.75 and 1.23 mM respectively; (b) The Coefficient of Determination (R^2) and the Root Mean Squared Error of Cross Validation (RMSECV) for FTNIR set are 0.85 and 1.02 mM respectively; (c) The Coefficient of Determination (R^2) and the Root Mean Squared Error of Cross Validation (RMSECV) for MIR (FTIR) set are 0.93 and 0.78 mM respectively.

Table 8.5: Linear Regression results of the MIR data-sets of lactate in PBS of pH 7.4, 7, 6.5, 6, human serum and whole blood used to build predictive models.

Data-Sets Used for Training	Data-Set Predicted	No. of LVs used	(R^2)	RMSEP (mM)
pH 7.4, 7, 6.5, 6 and Human Serum	Whole Blood	18	0.94	2.41
pH 7, 6.5, 6, Human Serum and Whole Blood	pH 7.4	18	0.93	2.41
pH 7.4, 6.5, 6, Human Serum and Whole Blood	pH 7	18	0.93	2.41
pH 7.4, 7, 6, Human Serum and Whole Blood	pH 6.5	18	0.92	2.41
pH 7.4, 7, 6.5, Human Serum and Whole Blood	pH 6	18	0.94	2.41
pH 7.4, 7, 6.5, 6 and Whole Blood	Human Serum	18	0.93	2.41

Validation (RMSECV) for dual beam dispersive NIR set 1.23 mM, FTNIR set 1.02 mM and MIR (FTIR) set was 0.78 mM.

Additionally, PLS regression models were also built using pH data-sets, human serum data-set (from previous chapters) and whole blood data-set. Table 8.5 shows the no of LVs from PRESS, R^2 and RMSEP values for these predictive models for the MIR (1500-600 cm^{-1}) spectral region. This analysis was performed to increase complexity on the previously built models and experimentalize further the effects of changing media on the Absorption spectra in the *'fingerprint region'* of the MIR spectral region.

8.6 Summary

This chapter explores further the effects of changing medium on the Absorption spectrum of lactate in the NIR and *'fingerprint region'* of the MIR spectral regions. Solution samples of varying lactate concentrations in whole blood were prepared and spectra were again collected using two different instruments and compiled in three data-sets; Dual Beam Dispersive NIR, FTNIR and FTIR.

Subsequently, pre-treatment and analysis were carried out using techniques which could be seen in the previous chapters. Again in the spectral regions without O-H absorption interference, the wavelengths 1046 nm, 1142 nm, 1232 nm, 1280 nm, 1330 nm, 1690 nm, 1710 nm, 1750 nm, 2166 nm, 2320 nm and 2342 nm were linearly correlated (p-values ≤ 0.05) with the concentration changes of lactate. Similarly, for the MIR region, wavenumbers 1585 cm^{-1}, 1390 cm^{-1}, 1320 cm^{-1}, 1280 cm^{-1}, 1270 cm^{-1}, 1125 cm^{-1}, 1045 cm^{-1} and 860 cm^{-1} were linearly correlated with the lactate ion, while the wavenumbers 1725 cm^{-1}, 1475 cm^{-1}, 1455 cm^{-1}, 1420 cm^{-1}, 1335 cm^{-1}, 1285 cm^{-1}, 1130 cm^{-1}, 1090 cm^{-1} and 930 cm^{-1} were linearly correlated with lactic acid. The wavelengths 1450 nm, 1820 nm and 2100 nm also showed linear correlations with lactate concentration changes in the spectral regions with O-H Absorption interference.

Also, PLS regression models were built with LVs 9, 6 and 11 for Dual beam dispersive NIR, FTNIR and FTNIR data-sets, respectively. The The Coefficients of Determination (R^2) and Root Mean Squared Error of Cross Validation (RMSECV) for the three data-sets were 0.75, 0.85 and 0.93 and 1.23 mM, 1.02 mM and 0.78 mM, respectively.

Moreover, the effects of pH and medium were studied by additionally including the whole blood data-set in building PLS regression models. The R^2 values were quite high for all the models, while the RMSEP values were moderately high too, considering the number of spectra used to build the models.

I discovered when I went all out, when I put 100 percent of my energy into some intense, impossible task-when my heart was jack-hammering, when lactic acid was sizzling through my muscles-that's when I felt good, normal, balanced.

Daniel Coyle, author of Lance Armstrong's war

9

In-vivo Spectrometric Analysis of Lactate in Healthy Volunteers

9.1 Introduction

Lactate can also be determined *in-vivo* using Absorbance/Reflectance Spectroscopy. A small pilot study was performed to understand the spectral feature changes while performing spectroscopy by non-invasive means, in healthy human volunteers. NIR reflectance spectra through the skin were collected and lactate concentrations

were measured intermittently on exercising (cycling) volunteers.

The motivation of this study was to understand the correlation between lactate concentration changes and the obtained NIR spectra, using a portable spectrometer. This chapter commences by introducing the measurement systems, investigation set-ups and protocols. The methods for collecting the diffuse reflectance spectra using a portable spectrometer are described, followed by the pre-treatment of the spectra and analysis. The subsequent sections expound these methods and results in detail.

9.2 Measurements set-up and protocols

The measurement systems, volunteer protocols and investigation set-up used for this study are discussed in the next sections.

9.2.1 Measurement system

The NIRQuest from Ocean Optics (*Largo, FL, USA*), as mentioned in Chapter 3, Section 3.4.2, was used to collect spectra from healthy volunteers. Reflectance spectra was obtained using fibre optic cables, NANOQ-PROBE-600-VIS-NIR, also from Ocean Optics (*Largo, FL, USA*). These measurements were taken intermittently while the volunteer was engaged in an incremental exercise test. The incremental exercise test was conducted using a cycle ergometer, indoor Pro/Trainer from Wattbike *(Nottingham, UK)*, which is a standard exercise bike. Lactate concentrations, during those intermittent intervals were also measured using a hand held analyser Lactate Pro 2 from Arkay Inc, (*Flat Rock, MI, USA*), as mentioned in Chapter 2, Figure 4.4. This device was chosen for this study as it was reported to be more stable, with higher accuracy and reliability, compared to the other hand held analysers for lactate concentration changes concerning training/exercise levels[101,257,258].

9.2.2 Volunteers and investigation set-up

Eight (8) healthy volunteers with mean age ± SD of 28 ± 6.7 (4 males and 4 females) were recruited for the investigation. Ethical approval was attained from the Senate Research Ethics Committee (SREC) at City, University London. The recruitment drive, inclusion, exclusion criteria, etc. could be found in the Ethics Application in Appendix B.

Once the volunteers were recruited, they were asked to have a meal at least 3 hours prior to the exercise protocol and fast, thereafter. Upon arrival, they were asked to sign a written consent, after a thorough review of the participant information sheet and health questionnaire together with the researcher. They were then allowed to enter a temperature-controlled room which had the measurement systems. An initial reading of lactate concentration was taken using the Lactate Pro 2 by the fingerprick method. NIR diffuse reflectance spectra was also collected using the NIRQuest portable spectrometer. The measurements were taken by placing the upper part of the right thumb of each volunteer on the reflectance probe holder, in which the fibre optic probe was securely held. This set-up minimised any movements from the volunteer while obtaining the spectra. The volunteer was then made to seat on the cycle for the incremental cycle exercise study. The set up is as shown in Figure 9.1.

9.2.3 Investigation protocol

The incremental exercise study commenced with cycling for 1 minute at a constant cadence of 60 rpm on an unloaded bike. This was followed by a rest period of 1 minute and then subsequent increase in air resistance was made by 2 units after every two minute cycling-rest sequence, at constant cadence of 60 rpm. The 1 minute load-rest cycle was chosen because lactate levels in healthy human volunteers would be restored to the initial value if kept rested for a longer time during the initial measurements.

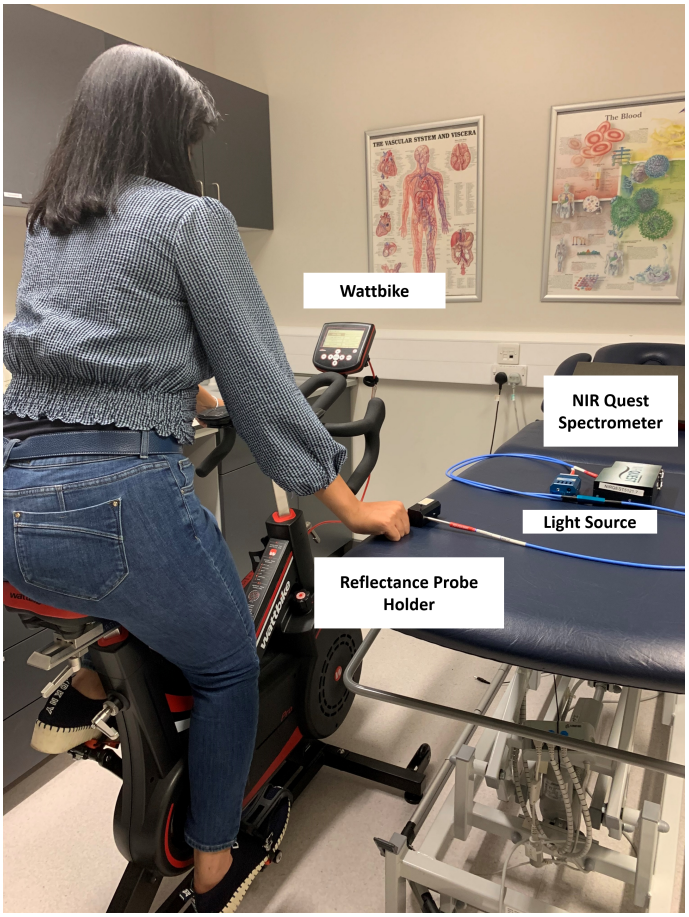

Figure 9.1: Set-up of the in-vivo experiments where a volunteer was recruited for an incremental exercise bike study and NIR spectra was collected from the thumb using a portable NIR spectrometer, NIR Quest, a light source and a reflectance probe holder.

While, the magnetic resistance on the Wattbike was kept constant at 6 units. This increase in the resistance was being carried out until volitional exhaustion or reaching approximately 90 % predicted maximal heart rate (derived using the equation max heart rate = 220 – age in years). Lactate concentration was measured using the Lactate Pro 2 during each rest cycle, followed by spectra collection using the NIRQuest spectrometer from the same thumb. These measurements were continued every minute for further three minutes even after the end of the exercise.

9.3 Reflectance Spectroscopy (NIR)

In-vivo diffuse reflectance spectra from 900 to 1300 nm wavelength range was collected using the NIRQuest portable spectrometer from Ocean Optics (*Largo, FL, USA*). The spectrometer was equipped with a Hamamatsu G9204-512, InGaAs linear array detector, as mentioned in Chapter 3, Section 3.4.2. The detector had 512 pixels with sizes of 25 μm x 500 μm. A Tungsten-Halogen light source, LS-1-LL, also from Ocean Optics (*Largo, FL, USA*) was attached to the spectrometer and was operated at a slit width of 25 μm, which provides an optical resolution of $\sim$ 3.1 nm.

The integration time was kept as automatic and reference spectrum of the light source were taken using the Spectralon Diffuse Reflectance Standard from Lapsphere *(North Sutton, NH, USA)*, as seen in the previous chapter. The dark or the background spectrum was taken by switching off the light source and covering the fibre optic cable by a black sheet. A total of 10 spectra were collected for every measurement and averaged. Each of these spectra were coallated and analysed as discussed in the following sections.

9.4 Spectral Analysis (NIR)

The concentrations of lactate varied from 1.6-19 mM and a total of 59 diffused reflectance spectra were collected. However, by visual inspection, only 29 spectra from four (4)

volunteers were used for analysis from the whole set due to noise. The noise was identified as either due to human/operator error, shaking of the instrument due to heavy volunteer breathing or instability in the instrument placement itself. These spectra were pre-treated by the implementation of the following techniques subsequently:

- Spectral Difference: The spectrum of the first spectrum (1.6 mM concentration of lactate) was subtracted from the rest of the spectra.
- Linear Robust Multiplicative Scatter Correction (MSC) was used for this set of spectra.
- Savitzky-Golay (SG) filter parameters (Polynomial Order= 2, Derivative= 1 and Window Length= 31) were applied.

The resulting spectra set was analysed using the following:

- 2D correlation
- Linear Regression was performed on selected wavelengths as seen in the previous chapters
- Aquagrams
- Principal component analysis (PCA)
- Partial Least Square (PLS).

The results obtained from these analysis techniques are presented in the next section.

9.5 Results

The raw NIR reflectance spectra (900-1650 nm) from the upper part of the right thumb are as shown in Figure 9.2. The synchronous 2D correlated contour plot is as shown in

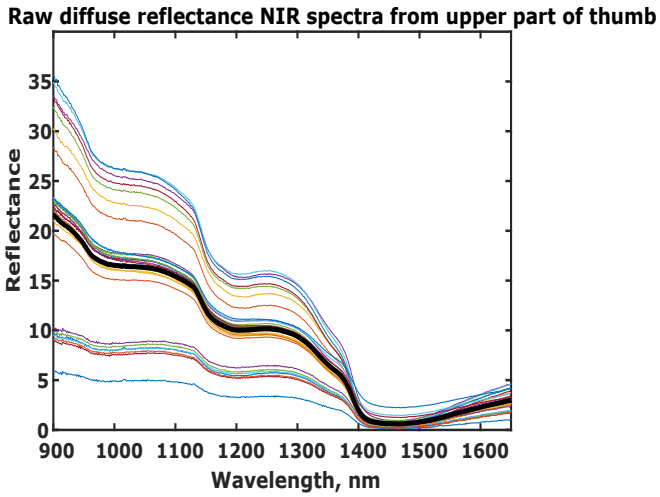

Figure 9.2: Raw diffuse reflectance NIR spectra (900-1650nm) from upper part of thumb obtained by NIRQuest portable spectrometer from Ocean Optics (*Largo, FL, USA*).

Table 9.1: p-values for significant lactate wavelengths for *in-vivo* diffuse reflectance NIR spectra.

Wavelengths (nm)	923	1047	1142	1233	1280	1330
p-values	7.18E-05	2.47E-04	2.08E-05	8.08E-08	5.80E-05	1.20E-05

Figure 9.3. As seen in the figure, a few regions were highlighted along the diagonal and the wavelengths that are of interest in those regions were: 923 nm, 1047 nm, 1142 nm, 1233 nm, 1280 nm and 1330 nm. Table 9.1 presents the p-values of these wavelengths. These wavelengths were from the spectral regions without O-H absorbance. In the spectral regions of O-H absorbance, wavelengths 970 nm, 1450 nm, 1490 nm and 1540 nm also showed linear correlations. An Aquagram was also constructed, as shown in Figure 9.4.

Finally, a PLS predictive model was constructed using LVs from PRESS results as shown in Figure 9.5. The number of LVs used to build the model was 4, however it could be seen there was a chance of over-fitting due to a smaller number of spectra in this data-set. Cross-validation was carried out by leave-one-out and the results are as shown in Figure 9.6. The Coefficient of Determination (R^2) was 0.95 and the Root Mean

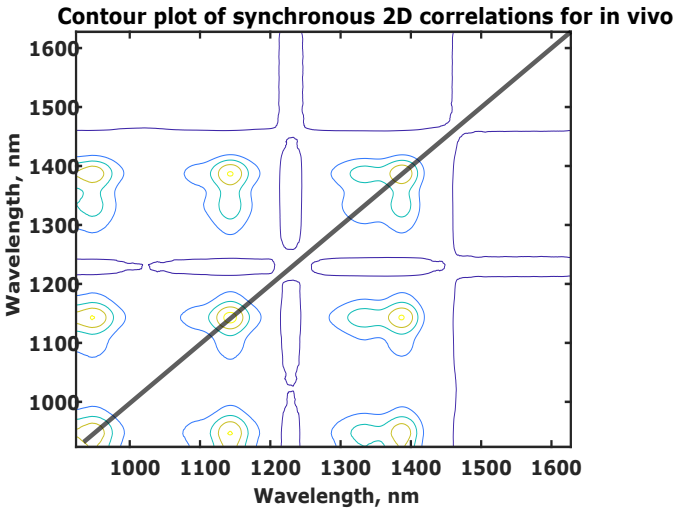

Figure 9.3: Synchronous 2D correlations contour plot for *in-vivo* NIR reflectance spectra obtained from upper part of thumb obtained by NIRQuest portable spectrometer from Ocean Optics (*Largo, FL, USA*).

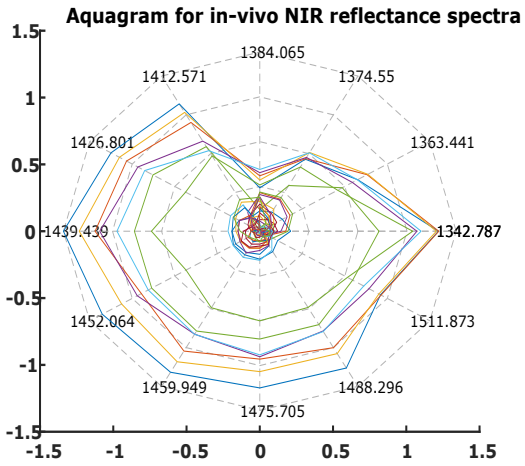

Figure 9.4: Aquagram for *in-vivo* NIR reflectance spectra from upper part of thumb obtained by NIRQuest portable spectrometer from Ocean Optics (*Largo, FL, USA*). Water Absorbance Bands (WAB): 1300-1600nm, showing Water Absorbance Spectral Pattern (WAPS) in the Water matrix co-ordinates (WAMACS) of varying concentrations of lactate *in-vivo*. The WAMACS: 1342.787, 1364.441, 1374.55, 1384.065, 1412.571, 1426.801, 1439.430, 1452.064, 1459.705, 1475.705, 1488.296 and 1512.873 depicts molecular conformations which arises due to water-NIR light-lactate molecule interactions.

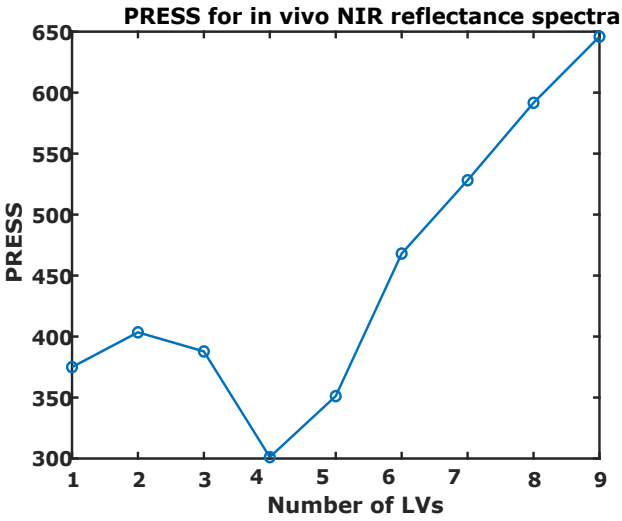

Figure 9.5: Prediction Error Sum of Squares (PRESS) versus number of latent variables (LV) for *in-vivo* NIR reflectance spectra. The number of LVs used was 4.

Squared Error of Cross Validation (RMSECV) was 3.22 mM.

9.6 Summary

This chapter studies the feasibility of exploiting reflectance spectra obtained by a portable NIR spectrometer for non-invasive lactate concentration measurement through human skin. Diffuse reflectance spectra were obtained from healthy human volunteers intermittently, while they were engaged in an incremental intensity cycling test. Lactate concentrations were also measured using a 'fingerprick test', prior to spectra collection and these values were correlated.

The wavelengths 923 nm, 1047 nm, 1142 nm, 1233 nm, 1280 nm and 1330 nm showed linear correlation, with the concentration changes of lactate (with p-values ≤ 0.05). However, the wavelengths 970 nm, 1450 nm, 1490 nm and 1540 nm, (O-H absorbance wavelengths) showed linear correlations, as well. This demonstrated the fact that these spectra contain extensive information and are not lactate sensitive. Hence, in order to understand the effects of lactate on the spectral features, PLS regression model was

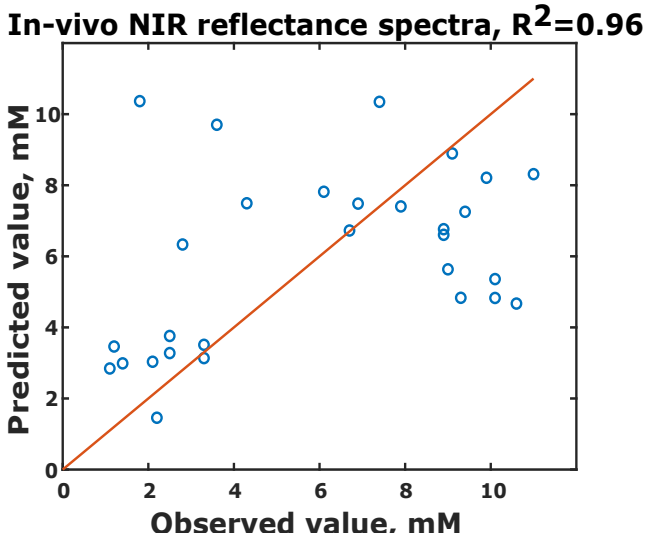

Figure 9.6: Observed (known) lactate concentration versus the Predicted concentrations for *in-vivo* NIR reflectance spectra. The correlation coefficient (R^2) and the Root Mean Squared Error of Cross Validation (RMSECV) are 0.96 and 3.22 mM, respectively.

build using 4 LVs. Cross-validation using leave-one-out showed the Coefficient of Determination (R^2) and the Root Mean Squared Error of Cross Validation (RMSECV) value to be 0.95 and 3.22 mM, respectively.

The next chapter puts together the results of all the chapters in the thesis and critically discusses them at length.

Epicurus.... supposes not only all mixt bodies, but all others to be produced by the various and casual occursions of atoms, moving themselves to and fro by an internal principle in the immense or rather infinite vacuum.

Robert Boyle, The Sceptical Chymist or Chymico-Physical Doubts and Paradoxes, 1661.

10 Discussion

10.1 Introduction

Lactate can be detected in different media through Absorption Spectroscopy. This chapter intends to rationalise the results obtained in all the studies, which are described in previous chapters.

The results for Chapters 5 and 6 are discussed collectively. This was followed by the discussions from Chapters 7 and 8 together. Finally the results of Chapter 9 are discussed towards the end.

10.2 Discussion for Chapters 5 and 6

The Chapters, 5 and 6, present the results of the solution samples in Phosphate Buffer Solution. Chapter 5 exhibits the results of solution samples of varying concentration of lactate in PBS at a constant pH of 7.4. While Chapter 6 presents the results of solution sample sets with varying pH and lactate concentrations. The spectral regions under investigation were divided into UV/Vis, NIR and MIR spectral regions for understanding the conspicuous features in each region. Studies related to Absorption Spectroscopy for lactate[237,238] and pH[243,244,245] has been reported previously, however, most of the studies had considered only reduced spectral ranges for their studies. Hence, according to the best of knowledge of the author, for the first time, a consolidated study of lactate in the three spectral regions could be seen in this thesis. Moreover, further subdivisions of the results into three spectral regions, for each region (UV/Vis, NIR and MIR) could also be seen for the first time. The sub-divisions were made depending on the interference of O-H Absorption bands or bonds and entire sets for predictive modelling.

The data was obtained with the help of state-of-the-art instruments for each spectral region, which has been described in detail, in previous chapters. Prior to data collection, solution samples for all the different sets of varying pH were prepared using solution stoichiometry. The concentration of lactate and pH in all the solutions were verified using commercially available state-of-the-art devices. This was followed by calculating the actual (or theoretical) concentrations of lactate in every solution sample. These minor differences in lactate concentration is believed to occur due to ionization/ de-protonation of lactic acid to lactate ($CH3CH(OH)COO^{-}$), as reported by Ube et al[246]. This in turn cause minor changes in the spectral features, which could be correlated to the concentration difference of the molecule. These changes (for every wavelength), were then recognised as linear or not significant based on the p-values obtained through linear regression. Moreover, in a particular set in the NIR region, the Absorbance values

(A) were investigated, which could be interrelated to the concentration of the sample (C) using the Beer-Lambert Law (as seen in Chapter 3, Section 3.6.1):

$$A \propto C \tag{10.2.1}$$

The Absorbance values of each wavelength reflected the actual concentration of lactate. These changes in the concentrations of lactate were imperceptible for the commercial lactate analysers to distinguish.

Also, every data-set was analysed independently and collectively, using multi-variate method called Partial Least Square (PLS) regression analysis to understand the spectra feature changes and the linear dependence of concentrations of lactate on these features. Prediction models were built using the least number of Latent Variables (LV) for dimentionality reduction, which were determined using Prediction Error Sum of Squares (PRESS). The validation of these predictive models which were built for each data-set was carried out using the leave-one-out cross-validation method. The accuracy was then determined using the Coefficient of Determination (R^2) and the Root Mean Squared Error of Cross Validation (RMSECV) or Root Mean Squared Error of Prediction (RMSEP) for each model. The models with higher (R^2) and lower RMSECV/RMSEP values were desired.

The subsequent sections discuss these concepts in detail for every spectral wavelength ranges.

10.2.1 UV/Vis Spectral Region

The Absorption spectra of this region of the EM spectrum, as shown in Chapter 3 Section 3.2.1, arises due to electron excitation from lower (HOMO) to higher (LUMO) orbitals. The segment of the lactate molecule, from Figure 2.1, which might be allowed this type of transition would be the carboxyl group (COOH). There are evidences that the C=O

Table 10.1: Coefficient of Determination (R^2) and Root Mean Squared Error of Cross Validation (RMSECV) between the predicted and prepared samples for the UV/Vis data sets.

UV/Vis Data-set	Coefficient of Determination (R^2)	Root Mean Squared Error of Cross Validation (RMSECV) mM
7.4	0.59	4.27
7	0.79	2.73
6.5	0.32	6.27
6	0.62	4.17

group shows one distinct Absorption peak in the UV spectral region[259,260,261]. Hence, the peak at 320 nm, which could be seen in Figures 5.2 (a), and 5.1 might reflect the COOH group of the lactate molecule. However, from Table 6.5, it could be seen that this wavelength does not correlate linearly (p-values $\nleq 0.05$) with the concentration changes of lactate.

The lactate solution samples were colorless and hence, it was evident that there would be no Absoprtion peaks in the visible spectral region. This spectral region also does not have any visible O-H Absorption bands like the NIR spectral range.

PLS regression models were built for all four UV/Vis data-sets using LVs 2, 3, 3 and 4 for pH data-sets 7.4, 7, 6.5 and 6, respectively. These LVs were obtained from PRESS results as shown in Figures 5.8 (a) and 6.4. The R^2 and RMSECV values for all four data-sets are as shown in Table 10.1. From this table, it is evident that pH data-set 7 is moderately good, with acceptable values of R^2 (high) and RMSECV (low), compared to the set of the data-sets in this spectral region.

10.2.2 NIR Spectral Region

The Absorption spectra of a NIR spectral region would reflect the vibrations or rotations of the atoms in a molecule, as seen in detail in Chapter 3, Section 3.2.3. Furthermore, anharmonic overtones and combination bands were also expected to be seen in this spectral region, due to changes in dipole moments, arising because of non-linear inter-atomic distances within molecules. The overtones of the primary functional groups

O-H, C-H and C=O, arises in this spectral region (as mentioned in Table 3.1). The effects of these functional groups were expected to be quite evident in this study for the NIR spectral range, as lactate is a small organic molecule, which contains all the above mentioned groups. Moreover, spectra was collected of solution samples which would depict very high O-H absorbance in the NIR region. Therefore, the NIR region was divided into two spectral regions, as below:

- regions without the influence of O-H absorbance, and
- regions of O-H absorbance.

Spectral Regions without the influence of O-H absorbance

The first set of peaks in this region, as seen in Chapter 5, were between 820-840 *nm* wavelength range, which were observed while scanning through the solid powder spectrum at wavelengths 820 *nm*, 823 *nm* and 830 *nm*. This region, could also be seen as highlighted in the 2D correlation synchronous contour plots (Figure 4(a)). The wavelength 823 *nm* was also attributed to lactate by Kossowski et al[227]. Spectral data-sets with pH 7.4 and 7 showed linear correlation with the wavelength 820 *nm* with p-values ≤ 0.05 (Tables: 5.5 and 6.6), while pH data-sets 6.5 and 6 showed no correlation.

Following this, the 2D correlation plot (Figure 4(a)) showed some highlights in the wavelength range 920-1000 *nm*. In this region, lies a lactate peak at 923 *nm*[227]. Linear Regression at 923 *nm* showed good correlation for data-sets of pH 7.4, 7 and 6 (Tables: 5.5 and 6.6). These wavelengths were ascribed to lactate by Kossowski et al[227], from an *in-vivo* study with human volunteers (Chapter 4, Section 4.5.1). Although the pH was not reported, it could be expected to be around 7.35 -7.45 (Chapter 2 Section 2.6) for a healthy volunteer. Hence, for the pH data-sets 7.4 and 7, at the wavelengths 823 *nm* and 923 *nm*, lactate concentrations could be seen as linearly correlated and not for the other data-sets.

The next range of wavelengths under investigation was 1000-1300 nm, which could be mostly attributed to the C-H second overtone (Table 3.1). From this range on-wards in the NIR regions, two types of analysis were executed to understand the lactate molecule fingerprints:

- different lactate concentration (0-20 $m\mathcal{M}$) in different pH data-sets (7.4, 7, 6.5 and 6)
- different pH (6-8) with constant lactate concentration (2 $m\mathcal{M}$).

The effects of pH in this region (1000-1300 nm), were studied on two wavelengths, 1142 nm and 1233 nm (according to Table 5.3). As seen in Figure 6.3, the Absorbance values for wavelength 1142 nm did not show the expected decreasing trend of a second degree polynomial, with increase in pH[254]. However, the Absorbance values for wavelength 1233 nm behaved according to theoretical calculations (Figure 6.1) with increasing pH. 1142 nm, on the other hand, showed linear correlations for pH data-sets 7.4, 7 and 6.5, while 1233 nm showed linear correlations for pH data-sets 7 and 6.5, only. Two more wavelengths 1280 nm and 1330 nm, from Table 5.3, showed linear correlation for pH data-set 7 only (Table 6.4).

Also, in this wavelength range, the wavelengths, 1268 nm, 1688 nm[233] and 1047 nm[227] were found to be associated with lactate. Linear regression on 1268 nm and 1688 nm, did not show correlation in any of the four data-sets of pH. However, wavelength 1047 nm, showed good correlations for pH data-set of 7, 6.5 and 6 (Table: 6.6). The reason for this might be that the studies reported by Yano et al were for lactate measurements in peritoneal dialysis solutions, which usually has an acidic pH of 5.2 –5.5, hence, the peaks were non linear in data-sets of higher pH. As mentioned above, the wavelength 1047 nm was expected to be linearly correlated with pH of 7, as the study involved human volunteers[227].

The third region of NIR, under investigation, was 1600-1900 nm, which could be assigned to the C-H stretch (ν) first overtone (Table 3.1). Again, the Absorbance values of two wavelengths, 1710 nm and 1750 nm, showed similar continuous steep decline of second degree polynomial order (Figure 6.3 and 6.1) for the data-set 6.2.1[254]. Both these wavelengths showed no correlations for linear regression across any of the pH data-sets, except 7.4. Another wavelength 1882 nm (Table 5.3), showed good linear correlations for pH data-sets 7 and 6.5.

This region attracted immense interest when Lafrance et al did their study in human serum and whole blood, while looking for lactate through NIR Absorption/Reflectance spectroscopy[237,238]. Through the results of the studies, it was suggested the wavelengths 1675 nm, 1690 nm and 1730 nm reflects lactate concentration changes. While, wavelengths 1675 nm and 1690 nm showed correlations for pH data-sets 7 and 6.5 only, wavelength 1730 nm, showed good correlations for the pH data-sets 7, 6.5, including 7.4. The studies for these wavelengths were conducted in solutions of high concentrations of lactate in various media and pH ranging from 7.44 -7.66 in whole blood, while buffered solutions of pH 7.2 were added to the serum samples to increase the quantity of samples. Hence, not all the wavelengths were expected to be linear for all four data-sets.

The final wavelength range of interest in the NIR region was 2200-2400 nm, which mostly manifests the combinations of C-H or $C-H_2$ functional group (stretch, deformation, bend second overtone, etc), as seen in Table 3.1. For the set 6.2.1, the Absorbance values of wavelengths 2205 nm, 2319 nm and 2314 nm showed deviations from the expected theoretical trends, as opposed to the previous two wavelength ranges in the NIR region. The Absorbance values of these wavelengths, showed two separate second degree polynomial order curves, with a dip at pH 7, most importantly, in the upward direction (as seen in Figure 6.3 and 6.1). The difference in trend in these wavelengths, could be explained as a possible consequence of the polarization of the L(+) lactate stereoiso-

form in this NIR spectral region. This possibility arises from the fact that lactate has a chiral carbon which makes the molecule optically active (as seen in Chapter 2, Section 2.2)[254]. All three wavelengths showed good linear correlation for the pH data-sets 7.4 and 7. The wavelength 2205 *nm*, 2319 *nm* and 2341 *nm* reflects vibrations related to C-H stretch/ C=O stretch combination, C-H bend second overtone and C-H stretch/ C-H deformation, respectively.

Spectral Regions of O-H absorbance

Most of the sample solution content is liquid water, hence O-H bands and peaks were expected to be quite evident in the NIR region. These peaks were substantial and hence, overshadows the crucial lactate peaks of interest for discernible changes in the spectra. The water absorbance bands could be seen at 970 *nm*, 1450 *nm*, 1950 *nm* and 2500 *nm*. The spectra of UV/Vis (Figure 5.2 (a)) shows a significant peak at 970 *nm*, owing to the absorption peak of water ($a\nu_s + b\nu_{as}$, a+b=3, where, a and b are integers, ≥ 0)[262,263]. NIR (Figure 5.2 (b)) also shows three substantial water overtone bands at around 1450 *nm* ($a\nu_s + b\nu_{as}$, a+b=2), 1950 *nm* ($a\nu_s + \delta_s + b\nu_{as}$, a+b=1), and 2500 *nm* (ν_{as} where, a and b are integers ≥ 0)[260,264].

As seen in Chapter 3, Figure 3.4, ν_s is Symmetrical Stretching, ν_{as} is Asymmetrical Stretching and δ_s is the Symmetrical In-Plane Bending, are all fundamental modes of vibrations in a molecule. Also, minor O-H Absorbance peaks could be seen in wavelengths 1490 *nm*, 1540 *nm*, 1820 *nm*, 2070 *nm* and 2100 *nm*, as seen in Table 3.1.

Now, linear regression on these wavelengths were performed and from Table 6.11, it could be noted that all the p-values were significant (≤ 0.05). This shows that in this spectral region, the absorbance values reflects minute changes in pH for Set 6.2.1, linearly[254]. However, for data-sets where the pH is constant, only a few wavelengths are observed to behave linearly at certain pH; 1490 *nm* and 1820 *nm* for pH data-set of 7.4, 1540 *nm* and 1820 *nm* for pH data-set of 7 and 1820 *nm* for pH data-set of 6.5.

The features in this region could hence, act as distinguishing elements for understanding lactic acidosis and hyperlactatemia (Chapter 2, Sections 2.5 and 2.6).

Entire spectral regions for predictive models

Finally, PLS regression models were built for all four NIR data-sets using LVs 8, 8, 8 and 8 for pH data-sets 7.4, 7, 6.5 and 6, respectively. These LVs were obtained from PRESS results as shown in Figures 5.8 (b) and 6.5. The R^2 and RMSECV values for all four data-sets are as shown in Table 10.2. From this table it is seen that the R^2 values are very high, which is desirable. However, the RMSECV values seem to be relatively low which shows that these data-sets could be used for predicting clinical concentrations of lactate. These results are in accordance with the ones found in literature. Most of the studies for lactate determination in this region, as could be seen in Chapter 4, was done by Lafrance et al[237,238,239]. The R^2 values for their predictive models were very high and so were the RMSECV values, quite similar to the values seen in this thesis.

Furthermore, in order to understand the pH effects on the spectra, PLS regression models were built using 3 different data-sets, while trying to predict the one which was left out. Table 6.13, in Chapter 6, shows the results of the linear models based on the predictions. From this table it was evident that lactate concentration predictions are infeasible using data-sets of different pH. This concludes that Absorption Spectroscopy in the NIR spectral region is highly pH dependent and pH values of the sample has to be estimated prior to measuring lactate concentrations.

10.2.3 MIR Spectral Region

The last spectral region under investigation was the MIR spectral region (4000 - 600 cm^{-1}). This spectral region could be categorised into the following four regions which manifests different vibrations based on the types of functional group, as seen in Chapter 3, Section

Table 10.2: Coefficient of Determination (R^2) and Root Mean Squared Error of Cross Validation (RMSECV) between the predicted and prepared samples for the NIR data sets.

NIR Data-set	Coefficient of Determination (R^2)	Root Mean Squared Error of Cross Validation (RMSECV) mM
7.4	0.98	0.89
7	0.91	0.63
6.5	0.95	0.44
6	0.98	0.42

3.2. In this study, the MIR spectral range taken into consideration was from 2000-500 cm^{-1}, this region can be subdivided into the following regions as discussed below.

Double-bond MIR Spectral Region

Lactate molecule is an alpha-hydroxy acid (AHA), with a carboxylic acid group (C=O), as seen in Figure 2.1, in Chapter 2. Hence, this region of the MIR spectral region was expected to show some highlights in the 2D correlation (Figure 5.4 (c)). Hence, as seen from Table 5.5, two wavenumbers 1783 cm^{-1} and 1747 cm^{-1} showed good correlations with the concentration changes of lactate for pH 7.4. Also, as seen from Table, 6.8, both the wavenumbers were significant for all the other three pH as well, and hence, it could be deduced that lactate concentration could be linearly predicted in these two wavelengths.

Again, from Table 4.1, two wavenumbers 1725 cm^{-1} and 1585 cm^{-1} were also found which manifests double bonds of lactate. Both of these wavenumbers were significant for pH of 7.4, 6.5 and 6 (Tables 5.6 and 6.10). This shows that for this region, pH does not have an effect of lactate concentration changes and are linearly correlated.

Fingerprint MIR Spectral Region

The *fingerprint* region of the MIR (1500 – 600 cm^{-1}), holds information specific to every molecule. The wavenumbers in this region were expected to be consistently linear across all four pH data-sets as these wavenumbers serve as signatures for each molecule.

Hence, the presence of lactate in the form of lactate ion or lactic complex could be predicted in this spectral region. Although Cassanas et al mentioned the presence of lactic acid in the solution and assigned specific peaks to the acid, at the pH values for this study, the amount of unionized lactic acid would be present in negligible amounts. However, the presence of the cation Na^+, was present in the solutions, and additional lactate ion interaction could have led to the independent peaks assignable to lactate complexes as seen in all the studies present in this thesis. Carboxylate ion association with divalent cations is well understood, but assumed not to occur with monovalent cations. Remarkably, there is previous spectroscopic evidence of $-COO-..Na+$ bonding interaction in aqueous solution which has yet to be recognized in biological samples which might explain the peaks in this thesis[265,251].

The first part of this spectral region (2000 – 1500 cm^{-1}), could be assigned to the ν_{al} CO^{ϵ} and ν C-CH_3 stretching vibrations associated to free O-H and CH_3 functional groups[240]. The peak 1127 cm^{-1} was reported by Petibois et al,[241] and from the Figure 5.4 (c), wavenumbers 1039 cm^{-1} and 1021 cm^{-1} were found to be highlighted. The wavenumber 1127 cm^{-1}, was significant for all four pH data-sets (Table 5.5 and 6.8). While the wavenumbers 1039 cm^{-1} and 1021 cm^{-1} were significant for pH data-sets 7.4, 7 and 6.5. It could be understood that for pH data-set 6, not all wavelengths there exists signatures of lactate ion and lactic acid. The most likely explanation for this might be due to less intermolecular hydrogen bonds between hydroxyl groups of the buffer and lactate because of lower H^+ concentration.

For the rest of the range (1500 – 600 cm^{-1}), as seen in Tables 5.6, 6.9 and 6.10 in the region, 1500-1100 cm^{-1}, both lactic ion and lactic acid are found to follow specific signatures, which seem to be linear across all four pH data-sets.

Lastly, PLS regression models were built for all four MIR data-sets using LVs 18, 3, 12 and 16 for pH data-sets 7.4, 7, 6.5 and 6, respectively. These LVs were obtained from

Table 10.3: Coefficient of Determination (R^2) and Root Mean Squared Error of Cross Validation (RMSECV) between the predicted and prepared samples for the MIR data sets.

MIR Data-set	Coefficient of Determination (R^2)	Root Mean Squared Error of Cross Validation (RMSECV) mM
7.4	0.96	1.16
7	0.67	4.21
6.5	0.69	5.13
6	0.80	6.52

PRESS results as shown in Figures 5.8 (c) and 6.6. The R^2 and RMSECV values for all four data-sets are as shown in Table 10.3. From this table, it was evident that the data-set pH 7.4 gives the best predictive model compared to the data-sets of UV/Vis and NIR of pH 7.4. The data-sets pH 6, 6.5 and 7 are moderately good. However, as seen in Table 6.12, when the PLS regression models were used using only the *Fingerprint spectral region*, the R^2 and RMSECV values were significantly high and moderately low, respectively for all the pH data-sets. Hence, it could be inferred that the *'fingerprint region'* serves as a preferred region for lactate concentration determination. Moreover, as seen in Table 6.14, when three of the MIR pH sets were used for training, while predicting the remaining set, unlike NIR, the R^2 values were quite high for all the sets, with a moderately low RMSEP values. This also proves that in the MIR *'Fingerprint'* spectral region, 1500-600 cm^{-1}, pH has no effect and lactate can be predicted with more than 90 % accuracy using any of the pH data-sets. As stated above, lactate could be estimated with clinical accuracy in this wavelength range[241,251].

Thus, it could be seen that although the UV/Vis spectral region, showed good predictions for pH 7, there were hardly any major regions of interest. Hence, this region was not investigated from herein. The NIR spectral region showed interesting results based on O-H absorption overtone and combination bands, which could be seen only in this spectral region. The effects of pH were quite evident in these O-H Absorption spectral windows, which could also be used to distinguish pH changes and lactate concentration changes in the same medium. PLS regression for the NIR spectral regions

showed promising results with high R^2 and low RMSECV values, when considered independently. The MIR spectral region also showed some encouraging results, specially in the *'fingerprint region'*, where the effects of pH were not visible. Concentrations of lactate could also be predicted with accuracy appropriate for clinical care settings. Hence, for the next studies in this thesis, only the NIR and MIR *'fingerprint'* spectral regions were considered for investigations.

The next section describes in detail the results of Chapters 7 and 8.

10.3 Discussions for Chapters 7 and 8

Chapter 7 outlines the results of solution samples for varying concentrations of lactate in human serum, while Chapter 8 lays out the results in whole blood. The ability to predict lactate concentrations in PBS in the NIR and MIR spectral regions using Absorption Spectroscopy has been successfully demonstrated in the previous section, albeit, only when the pH is known. Therefore, lactate concentrations and pH for all the samples were measured just before experiments. The values for lactate and pH were 7.7 to 15 mM and 7.1 to 7.4 for human serum samples and 4.5 to 13.8 mM and 7.1 to 7.3 for whole blood samples. Hence, the wavelengths that were examined in this spectral region were the ones which were significant (with p-values ≤ 0.05) or depicting linear variations of lactate concentration changes for the data-sets 7.4 and 7 in the previous two chapters.

Analogous to the previous chapters, samples were prepared using solution stoichiometry and spectra was compiled using state-of-the-art spectrometers in the NIR and MIR spectral regions. In addition to the dual beam dispersive spectrophotometer, LAMBDA 1050 from Perkin Elmer Corp. spectra in the NIR spectral region was also collected using the Frontier^{TM} FTIR/NIR spectrometer, also from Perkin Elmer Corp. The reason behind this was to compare and validate the two instruments/technologies for lactate concentration prediction in the NIR spectral region. The dual beam dispersive spec-

trophotometer has advantages over the FTNIR, in terms of sensitivity (preferable Signal to Noise Ratio), stability (not requiring operator intervention for background/ambient environment spectral effect subtraction), accuracy and spectral resolution[266]. However, the FTNIR instrument was initially invented to address the short-comings of the dual beam dispersive spectrophotometer. The advantages offered by the latter are: speed (all the wavenumbers are computed concurrently), enhanced electronics (with lesser moving parts), superior spectral resolution and impervious to temperature and vibrational variations[267,268], apart from the three major ones, as discussed in Chapter 3, Section 3.4.2. Hence, spectra from both the instruments were acquired simultaneously, using the same sample and environmental conditions for lactate concentration predictions using PLS leave-on-out cross validation analysis and were compared.

The next sections discusses the three spectral data-sets for both the chapters, in two spectral regions (NIR and MIR), in detail.

10.3.1 NIR Spectral Region

Spectra from the human serum and whole blood data-sets were collected in the NIR region from 800-2600 *nm* using the dual beam dispersive NIR spectrophtotometer and from 900-3000 *nm* using the FTNIR spectrometer. These regions were again subdivided into three sections, as seen below.

Spectral Regions without the influence of O-H absorbance

As seen in Table 7.2, the peaks at the wavelengths those were significant (or depicted linearity) for human serum samples were: 1675 *nm*, 1690 *nm*, 1710 *nm*, 2292 *nm* and 2319 *nm*. From these results, it could be presumed that a change in media had an effect on the spectral features. However, as shown in Table 8.2 the wavelengths which were significant for whole blood samples were: 1046 *nm*, 1142 *nm*, 1232 *nm*, 1280 *nm*, 1330 *nm*, 1690 *nm*, 1710 *nm*, 1750 *nm*, 2166 *nm*, 2320 *nm* and 2341 *nm*. Hence, only

the wavelengths, 1710nm and 2319nm remained unaffected by the change in medium, amongst all the others; medium here refers to buffer solutions, human serum and whole blood.

While, the whole blood samples showed linear correlations for eleven wavelengths, out of eighteen, which were previously found to be significant, the human serum samples showed only five significant wavelengths. The reason might be the detector change for the whole blood data-set. For the whole blood samples, an InGaAs integrating sphere detector from Perkin Elmer Corp. was used, rather than the 3-detector module used for the human serum samples. This change was made because, as initially thought, the signal-to-noise ratio of the three detector module would not be high enough for the whole blood samples. As whole blood is a heterogeneous mixture and each distinct component contributes to separate scattering properties to the transmitted light, through the samples. Whereas, the human serum samples were less heterogeneous, with fewer scatterers and the sensitivity of the three detector module would produce a high enough signal-to-noise ratio. However, it might be possible that the noise levels in the human serum data-set was still high and a change in the detector could have yielded better results.

A higher sensitivity, with a better signal-to-noise ratio is achievable in the integrating sphere detector, because of the multiple diffuse or scattering reflections which occur inside the white inner surface. These reflections reduce the spatial effects of the scatterers in a sample, while increasing the radiant flux. Hence, a conclusion could not be drawn with utmost certainty if there were significant spectral feature changes with change in media from human serum to whole blood samples. Nevertheless, there exists significant spectral feature changes when the media was changed from buffer to human serum samples (as both of the data-sets used the three detector module during spectra collection).

Spectral Regions of O-H absorbance

As seen in all the data-sets presented in this thesis, the O-H absorption bestrides all the other peaks in the NIR spectral region. Although individual wavelengths were linear (or significant) for one particular data-set (Set 6.2.1), for the rest of the data-sets there were only a few significant ones. Likewise, linear regression was performed on all the wavelengths for these two data-sets as well. Wavelengths, like 1450 nm for the human serum data-set and 1450 nm, 1820 nm and 2100 nm for the whole blood data-set showed linear correlations for lactate concentration changes. These wavelengths were not consistent for linear changes as seen previously for O-H absorbance in PBS samples, except for 1820 nm, which was seen in pH data-set of 7.4 and 7, as well. Hence, this spectral region was further inspected, according to the principles of Aquaphotomics, as seen in Chapter 3, Section 3.7.2.

Aquagrams depicting activated Water Absorbance Spectral Pattern (WAPS) were constructed using 12 Water Matrix Absorbance Coordinates (WAMACS) in the first Water Absorbance Bands (WABS) (1300-1600 nm). Figures 5.7, 7.1 and 8.1 represent Aquagrams for lactate concentration changes in PBS, human serum and whole blood, respectively. These Aquagrams, depicting concentration changes of lactate in different media, could be seen for the first time, according to the best of knowledge of the author. As seen in the first Aquagram (Figure 5.7, Chapter 5),the WAMACs that were activated are: 1412 nm (C_5), 1426 nm (C_6) and 1440 nm (C_7). From Table 3.2, (Chapter 3, Section 3.7.2), chemical/molecular conformations that could be assigned to these WAMACs are the following : C_5: water with free hydroxyl OH^- side groups, C_6: H-OH bend (δ), C_7: water molecules with 1 H bond.

As the WAMACs in only the shorter wavelength ranges were activated for this aqueous system (PBS), it indicates the existence of a few lactate-water molecular clusters and more free OH^- side groups. These free hydroxyl side groups form weaker hydrogen

bond clusters in between themselves. They are therefore, affected by the concentration of any other solutes/analytes that are present in the aqueous system[269]. Hence, a PLS model was constructed using this aqueous system in the wavelength range 1300-1600 nm with 7 LVs (found from PRESS). The Coefficient of Determination (R^2) and the Root mean squared error of cross validation (RMSECV) were found to be 0.77 and 2.43 mM, respectively.

Now, in the second and third aquagrams (Figure 7.1, Chapter 7 and Figure 8.1, Chapter 8), apart from the shorter wavelengths 1412 nm and 1426 nm the longer wavelengths 1476 nm, 1488 nm and 1512 nm were activated as well. These wavelengths could be assigned the following WAMACS and chemical/molecular coformations: C_{10}: water molecules with 2 H bonds, C_{11}: water molecules with 3 H bonds, C_{12}: strongly bound water. These bound water conformations might be seen as a result of the water-lactate molecular interactions and ionic lactate complex clusters found in these two aqueous systems. As both these aqueous systems are more polar than the buffer aqueous system, there exists more ionic components, like calcium, which could bond with lactate. Evidences of lactate/lactic acid affecting calcium complexes (ionized, protein-bound, and complex-bound) in blood and serum in previous studies had also mentioned about a direct affect in the acid-base balance, causing lactic acidosis[270,271,272]. Patients with lactic acidosis have been generally seen to have reduced amounts of plasma ionised calcium or hypocalcemia[273]. Hypocalcemia had also been linked to patients in critical care[274,275] and sepsis[276,277,278]. However, for the whole blood aqueous system, most of the calcium ions might have been removed by the citrate present in the Alsever's solution, which was used as an anti-coagulant. The bonded structures of lactate in this aqueous solution might have been due to the lactate ions bound to proteins[279] or deoxy and oxy haemoglobin[280].

Moreover, PLS models built for these two aqueous systems with 5 and 2 LVs, showed

Coefficient of Determination (R^2) and Root mean squared error of cross validation (RMSECV) of 0.27 and 1.99 mM for human serum and 0.51 and 1.28 mM for whole blood, respectively. Thus, validating the presence of bound water in these aqueous systems as the (R^2) values were significantly low. Hence, a direct comparison is possible for lactate found in free or bound states in different media. Specially for *in-vivo* studies, where water is found in free states in blood-stream while, in bound states in soft tissues in the subcutaneous levels[281]. This could be used as an indirect method to understand NIR light penetration for *in-vivo* studies.

Finally, in the next section, the results of the predictive models which were built using the entire spectral regions are discussed.

Entire spectral regions for predictive models

The Coefficient of Determination (R^2) and Root Mean Squared Error of Cross Validation (RMSECV) between the predicted and prepared samples for the Human Serum and Whole Blood data-sets are shown in Tables 10.4 and 10.5. These were obtained by building PLS models using leave-one-out cross-validation method. From both the tables, it is evident that FTNIR is a better instrument for detection/prediction of lactate concentrations, accurately. The possible advantages of the FTNIR over the dual beam dispersive NIR instrument has been discussed previously. Hence, for the same reasons, the FTNIR instrument is believed to provide better results as compared to its counterpart.

The next section inspects the MIR region for the same two data-sets.

10.3.2 MIR Spectral Region

As seen from the previous results for PBS, in the *fingerprint region* of the MIR, lactate concentrations could be predicted with clinical accuracy. Hence, this section explores the capability of the same region in the human serum and whole blood data-sets.

Table 10.4: Coefficient of Determination (R^2) and Root Mean Squared Error of Cross Validation (RMSECV) between the predicted and prepared samples for the Human Serum data-sets.

Data-Sets	Coefficients of Determination (R^2)	Root Mean Squared Error of Cross Validation (RMSECV) mM
Dual Beam dispersive NIR	0.77	1.11
FTNIR	0.90	1.75

Table 10.5: Coefficient of Determination (R^2) and Root Mean Squared Error of Cross Validation (RMSECV) between the predicted and prepared samples for the Whole Blood data-sets.

Data-Sets	Coefficients of Determination (R^2)	Root Mean Squared Error of Cross Validation (RMSECV) mM
Dual Beam dispersive NIR	0.75	1.23
FTNIR	0.85	1.02

Fingerprint MIR Spectral Region

Tables 7.3 and 7.4 exhibits the wavenumbers that are linearly correlated to the lactate ion and lactic acid, respectively for the human serum data-set. These wavenumbers demonstrate the presence of both lactate and lactic acid in the solutions. However, not all the wavenumbers, as seen in Chapter 4 Table 4.1, which signify signatures of both chemical moieties are seen to be linear. The rationale behind this might be lower Signal-to-Noise ratio in this set of spectra. As seen in Chapter 7 Section 7.3.2, the spectra was obtained in a data interval of 0.1 cm^{-1}, with a spectral resolution of 0.1 cm^{-1}. The lower spectral resolution is believed to have lowered the signal-to-noise ratio in the spectra[282]. Studies previously has also reported that the higher spectral resolution provides better signal-to-noise ratio, which enhances sensitivity of the instrument[283].

Hence, in Chapter 8, the spectral resolution was increased to 2 cm^{-1} for the whole blood samples while collecting the FTIR spectra. As a result of which, all the wavenumbers except for 1470 cm^{-1} and 1370 cm^{-1} for lactate ion and 1380 cm^{-1}, 1240 cm^{-1} and

1050 cm^{-1} for lactic acid, were linearly correlated, as seen in Tables 8.3 and 8.4. Interestingly, these results did not have any affect when the whole *'fingerprint region'* MIR spectral region was considered for PLS prediction analysis. This proves the presence of both lactate ion and lactic acid in the whole blood data-set.

As seen from Figure 7.3 in Chapter 7, the Coefficient of Determination (R^2) and the Root Mean Squared Error of Cross Validation (RMSECV) for MIR (FTIR) set in human serum was 0.94 and 1.31 mM, respectively. Similarly, from Figure 8.3 in Chapter 8, the Coefficient of Determination (R^2) and the Root Mean Squared Error of Cross Validation (RMSECV) for MIR (FTIR) set for whole blood was 0.93 and 0.78 mM, respectively. Hence, it could be observed again that the Coefficient of Determination (R^2) values were high and Root Mean Squared Error of Cross Validation (RMSECV) values were moderately low for both the data-sets. Therefore, it could be concluded that this region can be used for lactate concentration prediction in human serum and whole blood with clinical accuracy.

Moreover, the effects of pH together with the change in media was also reviewed. This was done by building PLS regression models using four data-sets, while predicting the remaining data-set (data-sets of varying pH in PBS and human serum). From Chapter 7, Table 7.5, it could be seen that the results were impervious of the changing conditions. This process was again repeated in the next chapter, where PLS regression models were made using five data-sets, while predicting the remaining data-set ((of varying pH in PBS, human serum and whole blood)). From Chapter 8, Table 8.5, it could be again seen that the results were consistent. Hence, it could be further established that the *fingerprint region* of the MIR spectral region is the most preferred spectral region for detection (or prediction) of lactate concentrations in-vitro[251]. In this spectral region, variations in lactate concentration could be predicted with more than 90 % accuracy for each data-set independently and also while combining multiple data-sets with changes

in pH or medium.

Hitherto, all the investigations for lactate concentration changes in different pH and media were performed in-vitro. The studies were performed using laboratory based bench top devices. However, one of the main motivations behind this study is to explore the possibility of a bed-side portable instrument for rapid estimation of lactate in critical care using Transmittance/Reflectance spectroscopy. Hence, a feasibility study was conducted to measure lactate non-invasively, using a portable NIR spectrometer.

The next chapter discusses the results obtained from a pilot *in-vivo* study, conducted at the Research Centre of Biomedical Engineering Lab, City, University of London.

10.4 Discussions for Chapter 9

An *in-vivo* feasibility study was conducted to examine the spectral pattern changes, in order to detect lactate/lactic acid by Absorption/Reflectance Spectroscopy. As seen from the discussion above, the *'fingerprint region'* of MIR is the most preferred spectral region for lactate concentration detection. However, it is well known that the penetration depth of MIR light is much less than the NIR in human tissue. In fact, a study on the human nail had shown that ATR-FTIR lacks sensitivity, while diffuse refelectance could fetch information from deep within the finger[284]. Another study had shown that the detectors available for NIR spectral region are relatively more sensitive and brighter than the MIR detectors[152]. Moreover, it has also been established that an "optical window" exists between 600-1300 *nm* for larger depths of penetrations for chromophore detection[285].

Also, another and most important factor considered here was identifying a portable spectrometer. Firstly, to serve the purpose for bedside continuous monitoring of lactate in critical care and secondly, to achieve the accuracy needed for the same. Hence, the NIRQuest portable NIR spectrometer was appealing because it had a state-of-the-art

system with high sensitivity in 900-1700 *nm* region.

Utilizing this spectrometer, in Chapter 9, a small feasibility study was therefore conducted, with an attempt to detect lactate, non-invasively, through the skins of healthy volunteers. The study was designed to induce an increase in lactate concentrations *in-vivo*, when the volunteers were engaged in a high-intensity incremental cycling-rest test cycles, in a controlled environment. Spectra was collected in the range of 900-1700 *nm*, with subsequent finger-prick blood sampling, during the rest periods from 8 volunteers. A total of 29 spectra were taken for analysis where the lactate concentrations varied from 1.6-19 *mM*. The pH was assumed to be 7.4, as the spectra were collected from healthy volunteers.

According to the best of knowledge of the author, raw *in-vivo* spectra, as seen in Chapter 9, Figure 9.2, from the human thumb, using NIRQuest 512 spectrometer, could be seen for the first time in this thesis. From Table 9.1 in Chapter 9, it could be seen that the wavelengths pertinent to lactate showed linear correlations (p-values ≤ 0.05) with the concentration changes of lactate. However, all the wavelengths representing O-H absorption were seen to be linear as well. This shows that these spectra were not selective to lactate.

This could be also confirmed by the Aquagram, which was constructed using the *in-vivo* spectra, as shown in Figure 9.4. The WAMACs, C1, C5-C11 were seen to be activated. From Chapter 3, Table 3.2, it could be seen that these WAMACs indicate the presence of assymmetric stretching (C1), free water (C5), water hydration band (C6), water molecules with 1, 2, 3 and 4 hydrogen bonds (C7, C9, C10 and C11, respectively) and water solvation shell (C8). As seen in the previous discussions, the presence of free water could potentially mean that the spectra were obtained from the blood stream and not bound water in the subcutaneous tissue levels. Also, the effect the lesser -H bond clusters could also reflect the concentration changes of lactate. Hence, a PLS model was

constructed using this aqueous system in the wavelength range 1300-1600 nm with 9 LVs (found from PRESS). The Coefficient of Determination (R^2) and the Root mean squared error of cross validation (RMSECV) were found to be 0.98 and 3.37 mM. This further proves that a linear model could be used to accurately predict lactate concentration changes.

Hence, at the end, PLS regression models were constructed using the whole wavelength range. From Figure 9.6, it could be seen that the Coefficient of Determination (R^2) and the Root Mean Squared Error of Cross Validation (RMSECV) were 0.95 and 3.22 mM. This preliminary investigation manifests the feasibility of a portable NIR spectrometer for lactate concentration determination *in-vivo*. However, the regression model might need further validation with a larger sample sets to achieve accuracy and precision needed for critical care applications.

The next chapter concludes the thesis by highlighting the main findings and contributions.

"Quantum physics tells us that no matter how thorough our observation of the present, the (unobserved) past, like the future, is indefinite and exists only as a spectrum of possibilities.

Stephen Hawking, The Grand Design

11

Conclusion and Future Scope of Work

11.1 Introduction

Lactate concentration changes can be measured in-vitro and in-vivo through Absorption/Reflectance Spectroscopy. This chapter aims to conclude this thesis by encapsulating the fundamental results and associating them to the introductory aims and objectives as set out in Chapter 1. Towards the end, conclusive remarks on possible improvements for methodologies used in this thesis have been suggested together with some future scope of work.

11.2 Major Conclusions and Contributions

The primary motivation of this thesis was to reconnoiter the possibility of Absorption/Reflectance Spectroscopy for lactate detection, both *in-vitro* and *in-vivo*. In pursuit of this objective, solution samples of varying lactate concentrations were prepared in disparate media; Phosphate Buffer Solution, Human Serum and Whole Blood. UV/Vis, NIR and MIR spectra of all the prepared solution samples were acquired and analysed. Spectra from healthy human volunteers were also obtained non-invasively, from the thumb, while they were engaged in an incremental exercise test, in order to artificially elevate the lactate levels in blood.

As a first step, spectra for solution samples of varying lactate concentrations in PBS (pH 7.4) were obtained, from UV/Vis, NIR and MIR regions of the Electromagnetic Spectrum, and analysed. These spectral regions were further sub-divided into regions with and without O-H interference for the NIR spectral region.

Results revealed that the UV/Vis spectral region had only one particular *'signature wavelength'* of lactate; 320 nm. However, in the NIR and MIR spectral regions, there existed wavelengths and wavenumbers, which exhibited linear correlations with the concentration changes of lactate. The wavelengths in the NIR spectral region were: 823 nm, 923 nm, 1142 nm, 1233 nm, 1710 nm,1730 nm, 1750 nm, 2205 nm, 2292 nm, 2319 nm and 2341 nm. In the MIR spectral region, wavenumbers 1783 cm^{-1}, 1747 cm^{-1} and 1725 cm^{-1} showed linear correlations with the concentration changes of lactate, followed by the *'fingerprint region'* which constituted the list of known wavelengths for lactate and lactic acid.

These wavelengths and wavenumbers obtained were further analysed by performing linear regression using the spectra obtained from another three data-sets of varying pH (7.0, 6.5 and 6). The wavelength in the UV spectral region, did not correlate linearly. Not all wavelengths or wavenumbers in the NIR and MIR spectral regions showed consistent

linear correlations with the concentration changes of lactate for the different data-sets. Nevertheless, variations in lactate concentration could be predicted with more than 90 % accuracy for each pH data-sets in the NIR and the *'fingerprint region'* of the MIR, independently, but when combining multiple pH data sets into the model, predictions results were non-linear for the NIR data-sets. Hence, it could be deduced that pH definitely has an effect on the spectral features. In order to predict the concentrations of lactate, pH values should be already known in the NIR region.

Hence, for the first time, according to the best of the knowledge of the author, *in-vitro* spectral analysis and results for combined effects of lactate (hyperlactatemia) and pH (lactic acidosis) could be seen for three spectral regions (UV/Vis, NIR and MIR). Moreover, the effects of variations in pH with the same concentration of lactate in the NIR spectral region was also be seen for the first time. These results reveal that spectral regions of O-H absorption could serve as a marker for pH (or lactic acidosis) determination alone.

It could not be surmised for certain that a change in media from human serum to whole blood has an effect on the spectral features, because the methods for spectral collection were partially different. The limitations of this study, which was performed by changing the detector in the spectrometer, has been previously acknowledged in the Discussion chapter. However, it could be concluded with utmost certainty that a change in media changes the spectral features in the NIR spectral region. Moreover, the overtones of water in this region could be used to distinguish lactate concentration changes in different media using the *'water mirror approach'* of Aquaphotomics. The aquagrams which were created based on lactate concentration changes in different media, also, could be seen in this thesis for the very first time, according to the best of knowledge.

However, the *'fingerprint region'* of the MIR region showed no effects of either the change in pH or media and these data-sets could be used to predict each and every

data-set, linearly and with more than 90 % accuracy. This, again, according to the best of the knowledge of the author, could be seen in this thesis for the first time for lactate concentration predictions.

Furthermore, in the NIR region, for the human serum and whole blood data-sets, spectra were collected from two different instruments to obtain a set containing dual beam dispersive NIR spectra and FTNIR spectra. It could also be inferred with certainty that the FTNIR spectra provided better accuracy for lactate concentration prediction than the former. Although similar comparisons for spectra collected from the above mentioned instruments had been reported previously, according to the best of the knowledge of the author, such comparisons has not been reported for lactate, and could be seen for the first time in this thesis.

Finally, a pilot *in-vivo* study was conducted to test the feasibility of a portable NIR spectrometer for lactate concentration determination non-invasively. Diffuse reflectance spectra were obtained from the portable spectrometer, which showed linear correlation to the *'significant wavelengths'* of lactate. However, these spectra lacked sensitivity towards lactate. Nonetheless, the results from this preliminary investigation showed encouraging prediction results with more than 90 % predictive ability. Hence, an improved *in-vivo* volunteer study, with a larger number of volunteers and physiological measurements is proposed, in order to build a more robust computational model. This will hopefully help to increase sensitivity towards lactate with better prediction capabilities of concentrations of lactate.

The results from all the studies indicate that Absorbance/Reflectance Spectroscopy in the NIR region could be used for non-invasive, rapid and direct lactate measurements, when the pH is known. However, the MIR(FTIR) region could be used for precise lactate measurements in critical care.

11.3 Future Scope of Work

As seen from the above studies the FT-NIR instrument seemed to be a better choice than its NIR counterpart. Hence, a comparative study could focus on the portable NIR and FT-NIR spectrometers. As recently, single-chip Michelson interferometer, MEMS-based FT-NIR spectrometer was announced by Si-Ware Systems (Cairo, Egypt) known as Neo-Spectra. OceanOptics also has a similar product, known as NANOQuest-2.5. These products might reveal better sensitivity towards lactate.

Moreover, as more demand for hand-held devices are turning towards smart phone spectroscopy and portable hyperspectral imaging, lactate detection using these technologies should also be explored.

In conclusion, the results exhibited in this thesis proclaims that Absorption/Reflectance Spectroscopy could be a novel potential tool for non-invasive lactate monitoring in critical care and beyond.

References

[1] C. B. Kjelland and D. Djogovic, "The role of serum lactate in the acute care setting." *Journal of intensive care medicine*, vol. 25, pp. 286–300, Sep. 2010. [Online]. Available: https://doi.org/10.1177/0885066610371191.

[2] S. Lee, Y. Hong, D. Park, S. Choi, S. Moon, J. Park, J. Kim, and K. Baek, "Lactic acidosis not hyperlactatemia as a predictor of inhospital mortality in septic emergency patients." *Emergency Medicine Journal*, vol. 25, no. 10, pp. 659–665, Oct. 2008. [Online]. Available: http://dx.doi.org/10.1136/emj.2007.055558.

[3] A. Montagnani and R. Nardi, "Lactic acidosis, hyperlactatemia and sepsis." *Italian Journal of Medicine*, vol. 10, pp. 282–288, Dec. 2016. [Online]. Available: https://doi.org/10.4081/itjm.2016.793.

[4] B. Wernly, N. Heramvand, M. Masyuk, R. Rezar, R. R. Bruno, M. Kelm, D. Niederseer, M. Lichtenauer, U. C. Hoppe, J. Bakker, and C. Jung, "Acidosis predicts mortality independently from hyperlactatemia in patients with sepsis." *European Journal of Internal Medicine*, vol. 76, pp. 76–81, Mar. 2020. [Online]. Available: https://doi.org/10.1016/j.ejim.2020.02.027.

[5] D. Lepkowska, "Sepsis: The importance of knowing the signs and symptoms." *British Journal of Child Health*, vol. 1, no. 1, pp. 34–35, Mar. 2020. [Online]. Available: https://doi.org/10.12968/chhe.2020.1.1.34.

[6] European Centre for Disease Prevention and Control (accessed on 17-August-2020). [Online]. Available: https://www.ecdc.europa.eu/en/geographical-distribution-2019-ncov-cases.

[7] W. Alhazzani, M. H. Møller, Y. M. Arabi, M. Loeb, M. N. Gong, E. Fan, S. Oczkowski, M. M. Levy, L. Derde, A. Dzierba, B. Du, M. Aboodi, H. Wunsch, M. Cecconi, Y. Koh, D. S. Chertow, K. Maitland, F. Alshamsi, E. Belley-Cote, M. Greco, M. Laundy, J. S. Morgan, J. Kesecioglu, A. McGeer, L. Mermel, M. J. Mammen, P. E. Alexander, A. Arrington, J. E. Centofanti, G. Citerio, B. Baw, Z. A. Memish, N. Hammond, F. G. Hayden, L. Evans, and A. Rhodes, "Surviving Sepsis Campaign: guidelines on the management of critically ill adults with Coronavirus Disease 2019 (COVID-19)." *Intensive Care Medicine*, vol. 46, no. 5, pp. 854–887, May 2020. [Online]. Available: https://doi.org/10.1007/s00134-020-06022-5.

[8] A. Lozano, F. Franchi, R. J. Seastres, M. Oddo, O. Lheureux, R. Badenes, S. Scolletta, J.-L. Vincent, J. Creteur, and F. S. Taccone, "Glucose and lactate concentrations in cerebrospinal fluid after traumatic brain injury," *Journal of Neurosurgical Anesthesiology*, vol. 32, pp. 162–169, Apr. 2020. [Online]. Available: https://doi.org/10.1097/ana.0000000000000582.

[9] Y.-C. Hsu and C.-W. Hsu, "Septic acute kidney injury patients in emergency department: The risk factors and its correlation to serum lactate," *The American Journal of Emergency Medicine*, vol. 37, no. 2, pp. 204–208, Feb. 2019. [Online]. Available: https://doi.org/10.1016/j.ajem.2018.05.012.

[10] Y. qiang Fu, K. Bai, and C. jun Liu, "The impact of admission serum lactate on children with moderate to severe traumatic brain injury," *Plos One*, vol. 14, no. 9, p. e0222591, Sep. 2019. [Online]. Available: https://doi.org/10.1371/journal.pone.0222591.

[11] T. K. Oh, C. Im, and I.-A. Song, "Lactate level and unplanned readmission to the surgical intensive care unit: a retrospective cohort study." *Annals of palliative medicine*, Sep. 2020. [Online]. Available: https://doi.org/10.21037/apm-20-291.

[12] K. Stahl, M. Busch, S. K. Maschke, A. Schneider, M. P. Manns, J. Fuge, O. Wiesner, B. C. Meyer, M. M. Hoeper, J. B. Hinrichs, and S. David, "A retrospective analysis of nonocclusive mesenteric ischemia in medical and surgical icu patients: Clinical data on demography, clinical signs, and survival." *Journal of intensive care medicine*, p. 885066619837911, Mar. 2019. [Online]. Available: https://doi.org/10.1177/0885066619837911.

[13] X. Chen, J. Bi, J. Zhang, Z. Du, Y. Ren, S. Wei, F. Ren, Z. Wu, Y. Lv, and R. Wu, "The impact of serum glucose on the predictive value of serum lactate for hospital mortality in critically ill surgical patients." *Disease markers*, vol. 2019, p. 1578502, 2019. [Online]. Available: https://doi.org/10.1155/2019/1578502.

[14] T. K. Oh, I.-A. Song, and Y.-T. Jeon, "Peri-operative serum lactate level and postoperative 90-day mortality in a surgical icu: A retrospective association study," *European Journal of Anaesthesiology (EJA)*, vol. 37, no. 1, pp. 31–37, Jan. 2020. [Online]. Available: https://doi.org/10.1097/EJA.0000000000001117.

[15] H. P. Gupta, P. R. Khichar, R. Porwal, A. Singh, A. K. Sharma, M. Beniwal, and S. Singh, "The duration of intra-abdominal hypertension and increased serum lactate level are important prognostic markers in critically ill surgical patient's outcome: A prospective, observational study." *Nigerian journal of surgery : official publication of the Nigerian Surgical Research Society*, vol. 25, pp. 1–8, 2019. [Online]. Available: https://doi.org/10.4103/njs.NJS_7_18.

[16] A. L. Webb, N. Kramer, J. Rosario, L. Dub, D. Lebowitz, K. Amico, L. Leon, T. G. Stead, A. Vera, and L. Ganti, "Delta lactate (three-hour lactate minus

initial lactate) prediction of in-hospital death in sepsis patients." *Cureus*, vol. 12, p. e7863, Apr. 2020. [Online]. Available: https://doi.org/10.7759/cureus.7863.

[17] X.-F. Ding, Z.-Y. Yang, Z.-T. Xu, L.-F. Li, B. Yuan, L.-N. Guo, L.-X. Wang, X. Zhu, and T.-W. Sun, "Early goal-directed and lactate-guided therapy in adult patients with severe sepsis and septic shock: a meta-analysis of randomized controlled trials." *Journal of translational medicine*, vol. 16, p. 331, Nov. 2018. [Online]. Available: https://doi.org/10.1186/s12967-018-1700-7.

[18] Y. Lu, H. Zhang, F. Teng, W.-J. Xia, G.-X. Sun, and A.-Q. Wen, "Early goal-directed therapy in severe sepsis and septic shock: A meta-analysis and trial sequential analysis of randomized controlled trials." *Journal of intensive care medicine*, vol. 33, pp. 296–309, May 2018. [Online]. Available: https://doi.org/10.1177/0885066616671710.

[19] E. Bolvardi, J. Malmir, H. Reihani, A. M. Hashemian, M. Bahramian, P. Khademhosseini, and K. Ahmadi, "The role of lactate clearance as a predictor of orgen dysfunction and mortality in patients with severe sepsis." *Materia socio-medica*, vol. 28, pp. 57–60, Feb. 2016. [Online]. Available: https://doi.org/10.5455/msm.2016.28.57-60

[20] J. C. Lopez-Delgado, F. Esteve, C. Javierre, H. Torrado, D. Rodriguez-Castro, M. L. Carrio, E. Farrero, K. Skaltsa, R. Mañez, and J. L. Ventura, "Evaluation of serial arterial lactate levels as a predictor of hospital and long-term mortality in patients after cardiac surgery." *Journal of cardiothoracic and vascular anesthesia*, vol. 29, pp. 1441–1453, Dec. 2015. [Online]. Available: https://doi.org/10.1053/j.jvca.2015.04.024.

[21] M. C. Haanschoten, H. G. Kreeftenberg, R. Arthur Bouwman, A. H. M. van Straten, W. F. Buhre, and M. A. Soliman Hamad, "Use of postoperative peak arterial lactate level to predict outcome after cardiac surgery." *Journal of cardiothoracic and vascular anesthesia*, vol. 31, pp. 45–53, Feb. 2017. [Online]. Available: https://doi.org/10.1053/j.jvca.2016.04.017.

[22] L. W. Andersen, "Lactate elevation during and after major cardiac surgery in adults: A review of etiology, prognostic value, and management." *Anesthesia and analgesia*, vol. 125, pp. 743–752, Sep. 2017. [Online]. Available: https://doi.org/10.1213/ANE.0000000000001928.

[23] P. Govender, W. Tosh, C. Burt, and F. Falter, "Evaluation of increase in intraoperative lactate level as a predictor of outcome in adults after cardiac surgery." *Journal of cardiothoracic and vascular anesthesia*, vol. 34, pp. 877–884, Apr. 2020. [Online]. Available: https://doi.org/10.1053/j.jvca.2019.10.039

[24] S. Trzeciak, R. P. Dellinger, M. E. Chansky, R. C. Arnold, C. Schorr, B. Milcarek, S. M. Hollenberg, and J. E. Parrillo, "Serum lactate as a predictor of mortality in

patients with infection." *Intensive care medicine*, vol. 33, pp. 970–977, Jun. 2007. [Online]. Available: https://doi.org/10.1007/s00134-007-0563-9.

[25] J. P. Green, T. Berger, N. Garg, and N. I. Shapiro, "Serum lactate is a better predictor of short-term mortality when stratified by c-reactive protein in adult emergency department patients hospitalized for a suspected infection." *Annals of emergency medicine*, vol. 57, pp. 291–295, Mar. 2011. [Online]. Available: https://doi.org/10.1016/j.annemergmed.2010.10.016.

[26] M. E. Mikkelsen, A. N. Miltiades, D. F. Gaieski, M. Goyal, B. D. Fuchs, C. V. Shah, S. L. Bellamy, and J. D. Christie, "Serum lactate is associated with mortality in severe sepsis independent of organ failure and shock." *Critical care medicine*, vol. 37, pp. 1670–1677, May 2009. [Online]. Available: https://doi.org/10.1097/CCM.0b013e31819fcf68.

[27] D. A. del Portal, F. Shofer, M. E. Mikkelsen, P. J. Dorsey, D. F. Gaieski, M. Goyal, M. Synnestvedt, M. G. Weiner, and J. M. Pines, "Emergency department lactate is associated with mortality in older adults admitted with and without infections." *Academic emergency medicine : official journal of the Society for Academic Emergency Medicine*, vol. 17, pp. 260–268, Mar. 2010. [Online]. Available: https://doi.org/10.1111/j.1553-2712.2010.00681.x.

[28] J. Seheult, G. Fitzpatrick, and G. Boran, "Lactic acidosis: an update." *Clinical chemistry and laboratory medicine*, vol. 55, pp. 322–333, Mar. 2017. [Online]. Available: https://doi.org/10.1515/cclm-2016-0438.

[29] J.-L. Vincent, D. O Cortés, and A. Acheampong, "Current haemodynamic management of septic shock." *Presse medicale (Paris, France : 1983)*, vol. 45, pp. e99–e103, Apr. 2016. [Online]. Available: https://doi.org/10.1016/j.lpm.2016.03.005.

[30] E. J. O. Kompanje, T. Jansen, B. V der Hoven, and J. Bakker, "The first demonstration of lactic acid in human blood in shock by johann joseph scherer (1814–1869) in january 1843." *Intensive care medicine*, vol. 33, no. 11, pp. 1967–1971, 2007. [Online]. Available: https://doi.org/10.1007/s00134-007-0788-7.

[31] C. F. Cori, "The role of lactic acid in the development of biochemistry." in *Reflections on Biochemistry*. Elsevier, 1976, pp. 17–26. [Online]. Available: https://doi.org/10.1016/C2013-0-02804-6.

[32] C. Vernon and J. L. LeTourneau, "Lactic acidosis: recognition, kinetics, and associated prognosis." *Critical care clinics*, vol. 26, no. 2, pp. 255–283, Apr. 2010. [Online]. Available: https://doi.org/10.1016/j.ccc.2009.12.007.

[33] T. Araki, "Ueber die bildung von milchsäure und glycose im organismus bei sauerstoffmangel. dritte mittheilung." *Zeitschrift für physiologische Chemie*,

vol. 16, no. 6, pp. 453–459, Nov. 1892. [Online]. Available: https://doi.org/10.1515/bchm1.1892.16.6.453.

[34] O. N. Okorie and P. Dellinger, "Lactate: biomarker and potential therapeutic target." *Critical care clinics*, vol. 27, no. 2, pp. 299–326, Apr. 2011. [Online]. Available: 10.1016/j.ccc.2010.12.013.

[35] M. M. Levy, Ed., *Biomarkers in the Critically Ill Patient.* Elsevier Health Sciences, Apr. 2011. [Online]. Available: https://doi.org/10.1016/j.ccc.2010.12.013.

[36] W. M. Fletcher, "Lactic acid in amphibian muscle." *The Journal of physiology*, vol. 35, pp. 247–309, Mar. 1907. [Online]. Available: https://doi.org/10.1113/jphysiol.1907.sp001194.

[37] A. Von Muralt, "The development of muscle-chemistry, a lesson in neurophysiology." *Biochimica et biophysica acta*, vol. 4, pp. 126–129, Apr. 1950. [Online]. Available: https://doi.org/10.1016/0006-3002(50)90015-1.

[38] A. V. Hill, "The diffusion of oxygen and lactic acid through tissues." *Proceedings of the Royal Society of London. Series B, Containing Papers of a Biological Character*, vol. 104, no. 728, pp. 39–96, Dec. 1928. [Online]. Available: https://doi.org/10.1098/rspb.1928.0064.

[39] A. Hill and H. Lupton, "Muscular exercise, lactic acid, and the supply and utilization of oxygen." *QJM: An International Journal of Medicine*, no. 62, pp. 135–171, Jan. 1923. [Online]. Available: https://doi.org/10.1093/qjmed/os-16.62.135.

[40] A. V. Hill, *First and last experiments in muscle mechanics.* Cambridge University Press, Sep. 1970, vol. 169. [Online]. Available: https://doi.org/10.1126/science.169.3950.1068-a.

[41] O. Meyerhof, "Die energieumwandlungen im muskel. i. über die beziehungen der milchsaure zur warmebildung and arbeitsleistung des muskels in der anaerobiose." *Pflugers Arch Ges Physiol Mensch Tiere*, vol. 182, pp. 232–283, 1920.

[42] L. B. Gladden, "Lactate metabolism: a new paradigm for the third millennium." *The Journal of Physiology*, vol. 558, no. 1, pp. 5–30, Jun. 2004. [Online]. Available: https://doi.org/10.1113/jphysiol.2003.058701.

[43] T. Shafee, "File:Glycolysis metabolic pathway 3 annotated.svg (accessed on 06-december-2019)," Apr. 2015. [Online]. Available: https://en.wikipedia.org/wiki/File:Glycolysis_metabolic_pathway_3_annotated.svg#filehistory.

[44] G. A. Brooks and L. B. Gladden, "chapter 8 - The metabolic systems: Anaerobic metabolism (glycolytic and phosphagen)." in *Exercise Physiology*, C. M. Tipton, Ed. Oxford: American Psychological Association, Jan. 2003, pp. 322–360. [Online]. Available: https://doi.org/10.1016/B978-019512527-6.50009-X.

[45] "Cellular respiration and fermentation (accessed on 04-may-2020)," Tech. Rep. [Online]. Available: https://www.pearson.com/content/dam/one-dot-com/one-dot-com/us/en/higher-ed/en/products-services/freeman-bio-6e-info/pdf/freeman-6e-ch9-cell-respiration.pdf.

[46] C. J. Valvona, H. L. Fillmore, P. B. Nunn, and G. J. Pilkington, "The regulation and function of lactate dehydrogenase a: therapeutic potential in brain tumor." *Brain pathology*, vol. 26, no. 1, pp. 3–17, Aug. 2016. [Online]. Available: https://doi.org/10.1111/bpa.12299.

[47] J. M. Berg, J. L. Tymoczko, and L. Stryer, "The Citric Acid Cycle," *Biochemistry. 5th edition (accessed on 06-December-2019)*, 2002. [Online]. Available: https://www.ncbi.nlm.nih.gov/books/NBK21163/.

[48] D. G. Barrett and M. N. Yousaf, "Design and applications of biodegradable polyester tissue scaffolds based on endogenous monomers found in human metabolism." *Molecules*, vol. 14, no. 10, pp. 4022–4050, Oct. 2009. [Online]. Available: https://doi.org/10.3390/molecules14104022.

[49] P. G. Rosenstein, B. S. Tennent-Brown, and D. Hughes, "Clinical use of plasma lactate concentration. part 1: Physiology, pathophysiology, and measurement." *Journal of veterinary emergency and critical care (San Antonio, Tex. : 2001)*, vol. 28, pp. 85–105, Mar. 2018. [Online]. Available: https://doi.org/10.1111/vec.12708.

[50] P. G. Haji-Michael, L. Ladrière, A. Sener, J. L. Vincent, and W. J. Malaisse, "Leukocyte glycolysis and lactate output in animal sepsis and ex vivo human blood." *Metabolism: clinical and experimental*, vol. 48, pp. 779–785, Jun. 1999. [Online]. Available: https://doi.org/10.1016/s0026-0495(99)90179-8.

[51] S. Abeysekara, "D-lactic acid metabolism and control of acidosis." Ph.D. dissertation, University of Saskatchewan, University of Saskatchewan Saskatoon Saskatchewan, Mar. 2009.

[52] J. Uribarri, M. S. Oh, and H. J. Carroll, "D-lactic acidosis. a review of clinical presentation, biochemical features, and pathophysiologic mechanisms." *Medicine*, vol. 77, pp. 73–82, Mar. 1998. [Online]. Available: https://doi.org/10.1097/00005792-199803000-00001.

[53] N. Rabbani and P. J. Thornalley, "The critical role of methylglyoxal and glyoxalase 1 in diabetic nephropathy." *Diabetes*, vol. 63, pp. 50–52, Jan. 2014. [Online]. Available: https://doi.org/10.2337/db13-1606.

[54] J. Lu, G. A. Zello, E. Randell, K. Adeli, J. Krahn, and Q. H. Meng, "Closing the anion gap: contribution of d-lactate to diabetic ketoacidosis." *Clinica chimica acta; international journal of clinical chemistry*, vol. 412, pp. 286–291, Jan. 2011. [Online]. Available: https://doi.org/10.1016/j.cca.2010.10.020.

[55] N. J. Evennett, M. S. Petrov, A. Mittal, and J. A. Windsor, "Systematic review and pooled estimates for the diagnostic accuracy of serological markers for intestinal ischemia." *World journal of surgery*, vol. 33, pp. 1374–1383, Jul. 2009. [Online]. Available: https://doi.org/10.1007/s00268-009-0074-7.

[56] C. K. Garcia, J. L. Goldstein, R. K. Pathak, R. G. Anderson, and M. S. Brown, "Molecular characterization of a membrane transporter for lactate, pyruvate, and other monocarboxylates: implications for the Cori cycle." *Cell*, vol. 76, no. 5, pp. 865–873, Mar. 1994. [Online]. Available: https://doi.org/10.1016/0092-8674(94)90361-1.

[57] J. Bakker, M. W. Nijsten, and T. C. Jansen, "Clinical use of lactate monitoring in critically ill patients." *Annals of intensive care*, vol. 3, p. 12, May 2013. [Online]. Available: https://doi.org/10.1186/2110-5820-3-12.

[58] A. P. Halestrap and M. C. Wilson, "The monocarboxylate transporter family–role and regulation." *IUBMB life*, vol. 64, pp. 109–119, Feb. 2012. [Online]. Available: https://doi.org/10.1002/iub.572.

[59] G. A. Brooks, "The science and translation of lactate shuttle theory." *Cell metabolism*, vol. 27, pp. 757–785, Apr. 2018. [Online]. Available: https://doi.org/10.1016/j.cmet.2018.03.008

[60] J. H. James, C. H. Fang, S. J. Schrantz, P. O. Hasselgren, R. J. Paul, and J. E. Fischer, "Linkage of aerobic glycolysis to sodium-potassium transport in rat skeletal muscle. implications for increased muscle lactate production in sepsis." *The Journal of clinical investigation*, vol. 98, pp. 2388–2397, Nov. 1996. [Online]. Available: https://doi.org/10.1172/JCI119052.

[61] J. H. James, F. A. Luchette, F. D. McCarter, and J. E. Fischer, "Lactate is an unreliable indicator of tissue hypoxia in injury or sepsis." *Lancet (London, England)*, vol. 354, pp. 505–508, Aug. 1999. [Online]. Available: https://doi.org/10.1016/S0140-6736(98)91132-1.

[62] J. H. James, K. R. Wagner, J. K. King, R. E. Leffler, R. K. Upputuri, A. Balasubramaniam, L. A. Friend, D. A. Shelly, R. J. Paul, and J. E. Fischer, "Stimulation of both aerobic glycolysis and na(+)-k(+)-atpase activity in skeletal muscle by epinephrine or amylin." *The American journal of physiology*, vol. 277, pp. E176–E186, Jul. 1999. [Online]. Available: https://doi.org/10.1152/ajpendo.1999.277.1.E176.

[63] H. Bundgaard, K. Kjeldsen, K. Suarez Krabbe, G. van Hall, L. Simonsen, J. Qvist, C. M. Hansen, K. Moller, L. Fonsmark, P. Lav Madsen, and B. Klarlund Pedersen, "Endotoxemia stimulates skeletal muscle na+-k+-atpase and raises blood lactate under aerobic conditions in humans." *American journal of physiology. Heart and circulatory physiology*, vol. 284, pp. H1028–H1034, Mar. 2003. [Online]. Available: https://doi.org/10.1152/ajpheart.00639.2002.

[64] F. A. Luchette, W. A. Jenkins, L. A. Friend, C. Su, J. E. Fischer, and J. H. James, "Hypoxia is not the sole cause of lactate production during shock." *The Journal of Trauma*, vol. 52, no. 3, pp. 415–419, Mar. 2002. [Online]. Available: https://doi.org/10.1097/00005373-200203000-00001.

[65] B. Suetrong and K. R. Walley, "Lactic Acidosis in Sepsis: It's Not All Anaerobic: Implications for Diagnosis and Management." *Chest*, vol. 149, no. 1, pp. 252–261, Jan. 2016. [Online]. Available: https://doi.org/10.1378/chest.15-1703.

[66] A. L. Greenbaum, "The history of cell respiration and cytochrome, by david keilin, cambridge university press." *Medical History*, vol. 10, no. 4, p. 419–420, 1966. [Online]. Available: https://doi.org/10.1017/S0025727300011637.

[67] J. Karlsson, "Lactate and phosphagen concentrations in working muscle of man with special reference to oxygen deficit at the onset of work." *Acta physiologica Scandinavica. Supplementum*, vol. 358, pp. 1–72, Dec. 1971.

[68] R. J. Connett, T. E. Gayeski, and C. R. Honig, "Lactate efflux is unrelated to intracellular PO2 in a working red muscle in situ." *Journal of Applied Physiology*, vol. 61, no. 2, pp. 402–408, Aug. 1986. [Online]. Available: https://doi.org/10.1152/jappl.1986.61.2.402.

[69] R. J. Connett, C. R. Honig, T. E. Gayeski, and G. A. Brooks, "Defining hypoxia: a systems view of vo2, glycolysis, energetics, and intracellular po2." *Journal of applied physiology*, vol. 68, pp. 833–842, Mar. 1990. [Online]. Available: https://doi.org/10.1152/jappl.1990.68.3.833.

[70] K. Wasserman, "The anaerobic threshold measurement to evaluate exercise performance." *The American Review of Respiratory Disease*, vol. 129, no. 2 Pt 2, pp. S35–40, Feb. 1984. [Online]. Available: https://doi.org/10.1164/arrd.1984.129.2P2.S35.

[71] B. A. Mizock and J. L. Falk, "Lactic acidosis in critical illness." *Critical care medicine*, vol. 20, pp. 80–93, Jan. 1992. [Online]. Available: https://doi.org/10.1097/00003246-199201000-00020.

[72] L. B. Gladden, *Lactate Transport and Exchange During Exercise.* American Cancer Society, 2011, pp. 614–648. [Online]. Available: https://doi.org/10.1002/cphy.cp120114.

[73] ——, *Lactate Metabolism during Exercise.*, 3rd ed., J. R. Poortmans, Ed. Basel: Karger, 2003. [Online]. Available: https://doi.org/10.1159/000074368.

[74] "Cardiovascular disease - Hemodynamic disorders (accessed on 07-december-2019)." [Online]. Available: https://www.britannica.com/science/cardiovascular-disease.

[75] F. H. Millham, "A brief history of shock." *Surgery*, vol. 148, no. 5, pp. 1026–1037, Nov. 2010. [Online]. Available: https://doi.org/10.1016/j.surg.2010.02.014.

[76] S. Gross, "A manual of military surgery (accessed on 07-december-2019)," 1861. [Online]. Available: https://jdc.jefferson.edu/milsurgusa/.

[77] W. B. Cannon, "The course of events in secondary wound shock." *Journal of the American Medical Association*, vol. 73, no. 3, pp. 174–181, Jul. 1919. [Online]. Available: https://doi.org/10.1001/jama.1919.02610290016008.

[78] A. Blalock, "Mechanism and treatment of experimental shock: I shock following hemorrhage." *Archives of Surgery*, vol. 15, no. 5, pp. 762–798, Nov. 1927. [Online]. Available: https://doi.org/10.1001/archsurg.1927.01130230098008.

[79] ——, "Experimental shock: The cause of the low blood pressure by muscle injury." *Archives of Surgery*, vol. 20, no. 6, pp. 959–996, Jun. 1930. [Online]. Available: https://doi.org/10.1001/archsurg.1930.01150120077005.

[80] A. Blalock and H. B. Bradburn, "Trauma to central nrevous system: it's effects on cardiac output and blood pressure, an experimental study." *Archives of Surgery*, vol. 19, no. 4, pp. 725–734, Oct. 1929. [Online]. Available: https://doi.org/10.1001/archsurg.1929.01150040161006.

[81] A. Blalock, "Shock and Hemorrhage." *Bulletin of the New York Academy of Medicine*, vol. 12, no. 11, pp. 610–622, Nov. 1936. [Online]. Available: https://www.ncbi.nlm.nih.gov/pubmed/19312004.

[82] H. A. Salzmann, "Principles of surgical care, shock and other problems: By Alfred Blalock, M.D., Professor of Surgery, Vanderbilt University School of Medicine, Nashville, Tenn. St. Louis." *American Journal of Orthodontics and Dentofacial Orthopedics*, vol. 27, no. 2, p. 114, Feb. 1941. [Online]. Available: https://doi.org/10.1016/S0096-6347(41)90352-6.

[83] C. J. Wiggers, "The Pathologic Physiology of the Circulation during Hemorrhage." *Archives of Internal Medicine*, vol. XIV, no. 1, pp. 33–47, Jul. 1914. [Online]. Available: https://doi.org/10.1001/archinte.1914.00070130040003.

[84] ——, "The failure of transfusions in irreversible hemorrhagic shock." *American Journal of Physiology-Legacy Content*, vol. 144, no. 1, pp. 91–101, Jun. 1945. [Online]. Available: https://www.physiology.org/doi/abs/10.1152/ajplegacy.1945.144.1.91.

[85] G. T. Shires, J. N. Cunningham, C. R. Backer, S. F. Reeder, H. Illner, I. Y. Wagner, and J. Maher, "Alterations in cellular membrane function during hemorrhagic shock in primates." *Annals of surgery*, vol. 176, no. 3, pp. 288–295, Sep. 1972. [Online]. Available: https://doi.org/10.1097/00000658-197209000-00004.

[86] C. R. Baxter and T. Shires, "Physiological response to crystalloid resuscitation of severe burns." *Annals of the New York Academy of Sciences*, vol. 150, pp. 874–894, Aug. 1968. [Online]. Available: https://doi.org/10.1111/j.1749-6632.1968.tb14738.x.

[87] C. R. Baxter, "Fluid volume and electrolyte changes of the early postburn period." *Clinics in Plastic Surgery*, vol. 1, no. 4, pp. 693–703, Oct. 1974. [Online]. Available: https://doi.org/10.1016/S0094-1298(20)30126-7.

[88] R.-T.-H. Laennec and A.-L.-J. Bayle, *Traité de l'auscultation médiate et des maladies des poumons et du cœur (Nouv. éd.) / par R.-T.-H. Laënnec... ; publ. par les soins du Dr C.-J.-B. Comet ; augm. d'une Notice historique sur Laënnec réd. par M. Bayle (accessed on 07-December-2020).*, 1828. [Online]. Available: https://gallica.bnf.fr/ark:/12148/bpt6k829237.

[89] D. Funk, J. Parrillo, and A. Kumar, "Sepsis and septic shock: A history." *Critical care clinics*, vol. 25, pp. 83–101, viii, Jan. 2009. [Online]. Available: https://doi.org/10.1016/j.ccc.2008.12.003.

[90] A. M. Fishberg, W. M. Hitzig, and F. H. King, "Circulatory Dynamics in Myocardial Infarction." *Archives of Internal Medicine*, vol. 54, no. 6, pp. 997–1019, Dec. 1934. [Online]. Available: https://doi.org/10.1001/archinte.1934.00160180171012.

[91] M. B. Visscher, "Introduction: An Overview of the Shock Problem." in *The Fundamental Mechanisms of Shock: Proceedings of a Symposium Held in Oklahoma City, Oklahoma, October 1–2, 1971*, ser. Advances in Experimental Medicine and Biology, L. B. Hinshaw and B. G. Cox, Eds. Boston, MA: Springer US, Oct. 1972, pp. 3–7. [Online]. Available: https://doi.org/10.1007/978-1-4615-9014-9_1.

[92] A. Kumar and J. E. Parrillo, "Chapter 22 - Shock: Classification, Pathophysiology, and Approach to Management." in *Critical Care Medicine (Third Edition)*, J. E. Parrillo and R. P. Dellinger, Eds. Philadelphia: Mosby, Jan. 2008, pp. 379–422. [Online]. Available: https://doi.org/10.1016/B978-032304841-5.50024-8.

[93] A. A. Afifi, P. C. Chang, V. Y. Liu, P. L. da Luz, M. H. Weil, and H. Shubin, "Prognostic indexes in acute myocardial infarction complicated by shock." *The American journal of cardiology*, vol. 33, pp. 826–832, Jun. 1974. [Online]. Available: https://doi.org/10.1016/0002-9149(74)90628-6.

[94] "The top 10 causes of death. (accessed on 07-december-2019)." [Online]. Available: https://www.who.int/news-room/fact-sheets/detail/the-top-10-causes-of-death.

[95] A. Rhodes, L. E. Evans, W. Alhazzani, M. M. Levy, M. Antonelli, R. Ferrer, A. Kumar, J. E. Sevransky, C. L. Sprung, M. E. Nunnally, B. Rochwerg, G. D. Rubenfeld, D. C. Angus, D. Annane, R. J. Beale, G. J. Bellinghan, G. R. Bernard, J.-D. Chiche, C. Coopersmith, D. P. De Backer, C. J. French, S. Fujishima, H. Gerlach, J. L. Hidalgo, S. M. Hollenberg, A. E. Jones, D. R.

Karnad, R. M. Kleinpell, Y. Koh, T. C. Lisboa, F. R. Machado, J. J. Marini, J. C. Marshall, J. E. Mazuski, L. A. McIntyre, A. S. McLean, S. Mehta, R. P. Moreno, J. Myburgh, P. Navalesi, O. Nishida, T. M. Osborn, A. Perner, C. M. Plunkett, M. Ranieri, C. A. Schorr, M. A. Seckel, C. W. Seymour, L. Shieh, K. A. Shukri, S. Q. Simpson, M. Singer, B. T. Thompson, S. R. Townsend, T. Van der Poll, J.-L. Vincent, W. J. Wiersinga, J. L. Zimmerman, and R. P. Dellinger, "Surviving sepsis campaign: International guidelines for management of sepsis and septic shock: 2016." *Intensive care medicine*, vol. 43, pp. 304–377, Mar. 2017. [Online]. Available: https://doi.org/10.1007/s00134-017-4683-6.

[96] C. Fleischmann, A. Scherag, N. K. J. Adhikari, C. S. Hartog, T. Tsaganos, P. Schlattmann, D. C. Angus, K. Reinhart, and I. F. of Acute Care Trialists, "Assessment of global incidence and mortality of hospital-treated sepsis. current estimates and limitations." *American journal of respiratory and critical care medicine*, vol. 193, pp. 259–272, Feb. 2016. [Online]. Available: https://doi.org/10.1164/rccm.201504-0781OC.

[97] M. M. Levy, L. E. Evans, and A. Rhodes, "The Surviving Sepsis Campaign Bundle: 2018 update." *Intensive Care Medicine*, vol. 44, no. 6, pp. 925–928, Jun. 2018. [Online]. Available: https://doi.org/10.1007/s00134-018-5085-0.

[98] J.-L. Vincent, C. Ince, and J. Bakker, "Clinical review: Circulatory shock–an update: a tribute to Professor Max Harry Weil." *Critical Care (London, England)*, vol. 16, no. 6, p. 239, Nov. 2012. [Online]. Available: https://doi.org/10.1186/cc11510.

[99] A. Babaev, "Trends in management and outcomes of patients with acute myocardial infarction complicated by cardiogenic shock." *JAMA*, vol. 49, p. 120, Jul. 2007. [Online]. Available: https://doi.org/10.1016/j.annemergmed.2006.11.023.

[100] K. E. Rudd, S. C. Johnson, K. M. Agesa, K. A. Shackelford, D. Tsoi, D. R. Kievlan, D. V. Colombara, K. S. Ikuta, N. Kissoon, S. Finfer *et al.*, "Global, regional, and national sepsis incidence and mortality, 1990–2017: analysis for the global burden of disease study." *The Lancet*, vol. 395, no. 10219, pp. 200–211, Jan. 2020. [Online]. Available: https://doi.org/10.1016/S0140-6736(19)32989-7.

[101] J. M. Bonaventura, K. Sharpe, E. Knight, K. L. Fuller, R. K. Tanner, and C. J. Gore, "Reliability and accuracy of six hand-held blood lactate analysers." *Journal of sports science & medicine*, vol. 14, pp. 203–214, Mar. 2015. [Online]. Available: https://www.ncbi.nlm.nih.gov/pmc/articles/PMC4306774/.

[102] G. Broder and M. H. Weil, "Excess lactate: An index of reversibility of shock in human patients." *Science*, vol. 143, pp. 1457–1459, Jan. 1964. [Online]. Available: https://doi.org/10.1126/science.143.3613.1457.

[103] D. I. Peretz, H. M. Scott, J. Duff, J. B. Dossetor, L. D. MacLean, and M. McGregor, "The significance of lacticacidemia in the shock syndrome." *Annals*

of the New York Academy of Sciences, vol. 119, no. 3, pp. 1133–1141, Jul. 1965. [Online]. Available: https://doi.org/10.1111/j.1749-6632.1965.tb47467.x.

[104] M. H. Weil and A. A. Afifi, "Experimental and clinical studies on lactate and pyruvate as indicators of the severity of acute circulatory failure (shock)." *Circulation*, vol. 41, pp. 989–1001, Jun. 1970. [Online]. Available: https://doi.org/10.1161/01.cir.41.6.989.

[105] V. Vitek and R. A. Cowley, "Blood lactate in the prognosis of various forms of shock." *Annals of surgery*, vol. 173, pp. 308–313, Feb. 1971. [Online]. Available: https://doi.org/10.1097/00000658-197102000-00021.

[106] J. A. Kruse and R. W. Carlson, "Use of vasoactive drugs to support oxygen transport in sepsis." *Critical care medicine*, vol. 19, pp. 144–146, Feb. 1991. [Online]. Available: https://doi.org/10.1097/00003246-199102000-00005.

[107] H. Khosravani, R. Shahpori, H. T. Stelfox, A. W. Kirkpatrick, and K. B. Laupland, "Occurrence and adverse effect on outcome of hyperlactatemia in the critically ill." *Critical care (London, England)*, vol. 13, p. R90, Jun. 2009. [Online]. Available: https://doi.org/10.1186/cc7918.

[108] J. J. Ronco, J. C. Fenwick, M. G. Tweeddale, B. R. Wiggs, P. T. Phang, D. J. Cooper, K. F. Cunningham, J. A. Russell, and K. R. Walley, "Identification of the critical oxygen delivery for anaerobic metabolism in critically ill septic and nonseptic humans." *JAMA*, vol. 270, pp. 1724–1730, Oct. 1993. [Online]. Available: https://doi.org/10.1001/jama.271.15.1158.

[109] C. D. Foucher and R. E. Tubben, "Lactic Acidosis (accessed on 07-december-2019)," in *StatPearls*. Treasure Island (FL): StatPearls Publishing, 2019. [Online]. Available: http://www.ncbi.nlm.nih.gov/books/NBK470202/.

[110] S. Samanta, R. K. Singh, A. K. Baronia, P. Mishra, B. Poddar, A. Azim, and M. Gurjar, "Early ph change predicts intensive care unit mortality." *Indian journal of critical care medicine : peer-reviewed, official publication of Indian Society of Critical Care Medicine*, vol. 22, pp. 697–705, Oct. 2018. [Online]. Available: https://doi.org/10.4103/ijccm.IJCCM_129_18.

[111] R. D. Cohen and H. F. Woods, *Clinical and biochemical aspects of lactic acidosis : by Robert D. Cohen, H. Frank Woods.* Oxford, Nov. 1976. [Online]. Available: https://doi.org/10.1016/0014-5793(76)80789-2.

[112] B. Levy, O. Desebbe, C. Montemont, and S. Gibot, "Increased aerobic glycolysis through beta2 stimulation is a common mechanism involved in lactate formation during shock states." *Shock (Augusta, Ga.)*, vol. 30, pp. 417–421, Oct. 2008. [Online]. Available: https://doi.org/10.1097/SHK.0b013e318167378f.

[113] "Chapter 5: Historical Review." *Acta Medica Scandinavica*, vol. 165, no. S348, pp. 28–35, 1959. [Online]. Available: https://onlinelibrary.wiley.com/doi/abs/10.1111/j.0954-6820.1959.tb02285.x.

[114] K. Hasselbalch, "The calculation of the hydrogen content in blood from free and combined carbonic acid, and the oxygen compound of the blood as the function of the hydrogen content." *Biochem Z*, vol. 78, pp. 112–144, 1917.

[115] K. Berend, "Diagnostic use of base excess in acid-base disorders." *The New England journal of medicine*, vol. 379, p. 496, Aug. 2018. [Online]. Available: https://doi.org/10.1056/NEJMc1806372.

[116] R. A. Robergs, F. Ghiasvand, and D. Parker, "Biochemistry of exercise-induced metabolic acidosis." *American journal of physiology. Regulatory, integrative and comparative physiology*, vol. 287, pp. R502–R516, Sep. 2004. [Online]. Available: https://doi.org/10.1152/ajpregu.00114.2004.

[117] D. A. Story, "Stewart Acid-Base: A Simplified Bedside Approach." *Anesthesia & Analgesia*, vol. 123, no. 2, pp. 511–515, Aug. 2016. [Online]. Available: https://doi.org/10.1213/ANE.0000000000001261.

[118] R. A. Robergs, "Counterpoint: Muscle lactate and h+ production do not have a 1:1 association in skeletal muscle." *Journal of applied physiology*, vol. 110, pp. 1489–91; discussion 1498, May 2011. [Online]. Available: https://doi.org/10.1152/japplphysiol.01506.2010a.

[119] E. S. Prakash, "Good bye "lactic acid"; hello lactate and acid." *Journal of applied physiology*, vol. 105, p. 363, Jul. 2008. [Online]. Available: https://doi.org/10.1152/japplphysiol.zdg-8016-pcpcomm.2008.

[120] M. I. Lindinger, J. M. Kowalchuk, and G. J. F. Heigenhauser, "Applying physicochemical principles to skeletal muscle acid-base status." *American journal of physiology. Regulatory, integrative and comparative physiology*, vol. 289, pp. R904–910, Sep. 2005. [Online]. Available: https://doi.org/10.1152/ajpregu.00225.2005.

[121] A. T. Maciel and M. Park, "Unmeasured anions account for most of the metabolic acidosis in patients with hyperlactatemia." *Clinics (Sao Paulo, Brazil)*, vol. 62, pp. 55–62, Feb. 2007. [Online]. Available: https://doi.org/10.1590/s1807-59322007000100009.

[122] K. Hopper and S. C. Haskins, "A case-based review of a simplified quantitative approach to acid-base analysis." *Journal of Veterinary Emergency and Critical Care*, vol. 18, no. 5, pp. 467–476, 2008. [Online]. Available: https://doi.org/10.1111/j.1476-4431.2008.00344.x.

[123] K. C. Vinnakota, J. Rusk, L. Palmer, E. Shankland, and M. J. Kushmerick, "Common phenotype of resting mouse extensor digitorum longus and soleus muscles: equal atpase and glycolytic flux during transient anoxia." *The Journal of physiology*, vol. 588, pp. 1961–1983, Jun. 2010. [Online]. Available: https://doi.org/10.1113/jphysiol.2009.185934.

[124] D. J. Marcinek, M. J. Kushmerick, and K. E. Conley, "Lactic acidosis in vivo: testing the link between lactate generation and h+ accumulation in ischemic mouse muscle." *Journal of applied physiology*, vol. 108, pp. 1479–1486, Jun. 2010. [Online]. Available: https://doi.org/10.1152/japplphysiol.01189.2009.

[125] D. Böning, C. Klarholz, B. Himmelsbach, M. Hütler, and N. Maassen, "Causes of differences in exercise-induced changes of base excess and blood lactate." *European journal of applied physiology*, vol. 99, pp. 163–171, Jan. 2007. [Online]. Available: https://doi.org/10.1007/s00421-006-0328-0.

[126] J. M. Kowalchuk, G. J. Heigenhauser, M. I. Lindinger, J. R. Sutton, and N. L. Jones, "Factors influencing hydrogen ion concentration in muscle after intense exercise," *Journal of Applied Physiology.*, vol. 65, no. 5, pp. 2080–2089, Nov. 1988. [Online]. Available: https://doi.org/10.1152/jappl.1988.65.5.2080.

[127] T. C. Jansen, J. van Bommel, and J. Bakker, "Blood lactate monitoring in critically ill patients: a systematic health technology assessment." *Critical care medicine*, vol. 37, pp. 2827–2839, Oct. 2009. [Online]. Available: https://doi.org/10.1097/CCM.0b013e3181a98899.

[128] G. Gutierrez and M. E. Wulf, "Lactic acidosis in sepsis: a commentary." *Intensive care medicine*, vol. 22, pp. 6–16, Jan. 1996. [Online]. Available: https://doi.org/10.1007/bf01728325.

[129] J. Handy, "The origin and interpretation of hyperlactataemia during low oxygen delivery states." *Critical care (London, England)*, vol. 11, p. 104, Jan. 2007. [Online]. Available: https://doi.org/10.1186/cc5137.

[130] J. B. Jeppesen, C. Mortensen, F. Bendtsen, and S. Møller, "Lactate metabolism in chronic liver disease." *Scandinavian journal of clinical and laboratory investigation*, vol. 73, pp. 293–299, Mar. 2013. [Online]. Available: https://doi.org/10.3109/00365513.2013.773591.

[131] K. Berend, "Acid–base pathophysiology after 130 years: confusing, irrational and controversial." *Journal of Nephrology*, vol. 26, pp. 254–265, Sep. 2012. [Online]. Available: https://doi.org/10.5301/jn.5000191.

[132] R. A. Robergs, C. R. McNulty, G. M. Minett, J. Holland, and G. Trajano, "Lactate, not lactic acid, is produced by cellular cytosolic energy catabolism." *Physiology*, vol. 33, pp. 10–12, Dec. 2018. [Online]. Available: https://doi.org/10.1152/physiol.00033.2017.

[133] "Electromagnetic Spectrum – (accessed on 09-december-2020)." [Online]. Available: https://ips.org.uk/encyclopedia/electromagnetic-spectrum/.

[134] "What is light? (accessed on 18-august-2020)." Sep. 2019. [Online]. Available: https://www.ssi.shimadzu.com/products/uv-vis-spectrophotometers/faqs/light-and-theory.html#how-does-absorption-spectroscopy-work.

[135] C. Pasquini, "Near infrared spectroscopy: fundamentals, practical aspects and analytical applications." *Journal of the Brazilian chemical society*, vol. 14, no. 2, pp. 198–219, Mar. 2003. [Online]. Available: https://doi.org/10.1590/S0103-50532003000200006.

[136] H. W. Siesler, Y. Ozaki, S. Kawata, and H. M. Heise, *Principles of Near-Spectroscopy.* John Wiley & Sons, Nov. 2002. [Online]. Available: https://doi.org/10.1002/cem.762.

[137] "IR Spectrum (accessed on 10-december-2019)." [Online]. Available: http://www.wag.caltech.edu/home/jang/genchem/infrared.htm.

[138] W.-F. Su, "Characterization of Polymer." in *Principles of Polymer Design and Synthesis*, ser. Lecture Notes in Chemistry, W.-F. Su, Ed. Berlin, Heidelberg: Springer, 2013, pp. 89–110. [Online]. Available: https://doi.org/10.1007/978-3-642-38730-2_5.

[139] C. Huck, *Infrared Spectroscopic Technologies for the Quality Control of Herbal Medicines.* Elsevier, 2015. [Online]. Available: https://doi.org/10.1016/b978-0-12-800874-4.00022-2.

[140] M. Diem, *Molecular Vibrational Motion.* John Wiley & Sons, Jun. 2015. [Online]. Available: https://doi.org/10.1002/9781118824924.

[141] A. B. Eldin, *Near Infra Red Spectroscopy, Wide Spectra of Quality Control.*, I. Akyar, Ed. IntechOpen, Nov. 2011. [Online]. Available: https://doi.org/10.5772/1142.

[142] G. Reich, "Near-infrared spectroscopy and imaging: basic principles and pharmaceutical applications." *Advanced drug delivery reviews*, vol. 57, no. 8, pp. 1109–1143, Jun. 2005. [Online]. Available: https://doi.org/10.1016/j.addr.2005.01.020.

[143] R. D. Simoni, R. L. Hill, M. Vaughan, and H. Tabor, "A Classic Instrument: The Beckman DU Spectrophotometer and Its Inventor, Arnold O. Beckman (accessed on 19-november-2019)," *Journal of Biological Chemistry*, vol. 278, no. 49, pp. e1–e1, May 2003. [Online]. Available: http://www.jbc.org/content/278/49/e1.

[144] A. W. Scholl, "The Beckman Model DU Spectrophotometer and Accessories Instruction Manual (accessed on 18-november-2019)," 1954. [Online]. Available: https://digital.sciencehistory.org/works/r207tp471.

[145] "LAMBDA 1050+ UV/Vis/NIR Spectrophotometer-L6020056|PerkinElmer (accessed on 19-november-2019)." [Online]. Available: https://www.perkinelmer.com/product/lambda-1050-2d-system-l6020056

[146] "Technical Specifications for the LAMBDA 1050 UV/Vis/NIR and LAMBDA 950 UV/Vis/NIR Spectrophotometers (accessed on 19-november-2020)." [Online]. Available: https://www.perkinelmer.com/lab-solutions/resources/docs/BRO_LAMBDA8509501050.pdf.

[147] C. Vigano, J.-M. Ruysschaert, and E. Goormaghtigh, "Sensor applications of attenuated total reflection infrared spectroscopy." *Talanta*, vol. 65, no. 5, pp. 1132–1142, Mar. 2005. [Online]. Available: https://doi.org/10.1016/j.talanta.2004.07.052.

[148] "FRONTIER MIR/FIR |PerkinElmer (accessed on 04-may-2020)." library Catalog: www.perkinelmer.com. [Online]. Available: https://www.perkinelmer.com/product/frontier-mir-fir-sp10-std-l1280044.

[149] W. F. McClure, D. Moody, D. L. Stanfield, and O. Kinoshita, "Hand-held nir spectrometry. part ii: An economical no-moving parts spectrometer for measuring chlorophyll and moisture." *Applied Spectroscopy*, vol. 56, no. 6, pp. 720–724, Jan. 2002. [Online]. Available: https://doi.org/10.1366/000370202760077432.

[150] S. Saranwong and S. Kawano, "Commercial portable nir instruments in japan." *IR News*, vol. 16, no. 7, pp. 27–30, Nov. 2005. [Online]. Available: https://doi.org/10.1255/nirn.859.

[151] W. F. McClure, "204 years of near infrared technology: 1800–2003." *Journal of Near Infrared Spectroscopy*, vol. 11, no. 6, pp. 487–518, dec 2003. [Online]. Available: https://doi.org/10.1255/jnirs.399.

[152] R. A. Crocombe, "Portable spectroscopy." *Applied Spectroscopy*, vol. 72, pp. 1701–1751, Dec. 2018. [Online]. Available: https://doi.org/10.1177/0003702818809719.

[153] M. J. Cohen, M. H. Ettenberg, M. J. Lange, and G. H. Olsen, "Commercial and industrial applications of indium gallium arsenide near-infrared focal plane arrays." in *Part of the SPIE Conference on Infrared Technology and Applications XXV*, Jul. 1999. [Online]. Available: https://doi.org/10.1117/12.354547.

[154] A. Lisk, "NIRQuest Installation and Operation Manual (accessed on 05-may-2020)," Ocean Optics, Tech. Rep., 2010. [Online]. Available: https://www.oceaninsight.com/products/spectrometers/near-infrared/nirquest-series/.

[155] B. Staurt, "Infrared spectroscopy: fundamentals and applications." *John Wiley and Sons, Ltd.*, vol. 10, Jun. 2004. [Online]. Available: https://doi.org/10.1002/0470011149.

[156] C. L. M. Morais, K. M. G. Lima, M. Singh, and F. L. Martin, "Tutorial: multivariate classification for vibrational spectroscopy in biological samples," *Nature Protocols*, vol. 15, pp. 2143–2162, Jun. 2020. [Online]. Available: https://doi.org/10.1038/s41596-020-0322-8

[157] Å. Rinnan, F. Van Den Berg, and S. B. Engelsen, "Review of the most common pre-processing techniques for near-infrared spectra," *TrAC Trends in Analytical Chemistry*, vol. 28, no. 10, pp. 1201–1222, 2009.

[158] J. Dubrovkin, "Critical analysis of spectral deconvolution methods," *International Journal of Emerging Technologies in Computational and Applied Sciences*, vol. 1, p. 10, 2014.

[159] T. Pazderka and V. Kopeckỳ Jr, "2d correlation spectroscopy and its application in vibrational spectroscopy using matlab (accessed on 19-november-2019)." *Technical Computing Prague*, 2008. [Online]. Available: http://dsp.vscht.cz/konference_matlab/MATLAB08/prispevky/081_pazderka.pdf.

[160] I. Noda, "Generalized two-dimensional correlation spectroscopy," pp. 367–381, 2009.

[161] ——, "Techniques of two-dimensional (2d) correlation spectroscopy useful in life science research," *Biomedical Spectroscopy and Imaging*, vol. 4, pp. 109–127, 2015.

[162] A. Ghita, T. Hubbard, P. Matousek, and N. Stone, "Noninvasive detection of differential water content inside biological samples using deep raman spectroscopy." *Analytical Chemistry*, vol. 92, no. 14, pp. 9449–9453, Jun. 2020. [Online]. Available: https://doi.org/10.1021/acs.analchem.0c01842.

[163] R. Tsenkova, "Aquaphotomics: Dynamic spectroscopy of aqueous and biological systems describes peculiarities of water." *Journal of Near Infrared Spectroscopy*, vol. 17, pp. 303–313, Jan. 2009. [Online]. Available: https://doi.org/10.1255/jnirs.869.

[164] R. Tsenkova, Z. Kovacs, and Y. Kubota, *Aquaphotomics: Near Infrared Spectroscopy and Water States in Biological Systems.*, E. Disalvo, Ed. Springer, 2015, vol. 71. [Online]. Available: https://doi.org/10.1007/978-3-319-19060-0_8.

[165] "Interpret Linear Regression Results - MATLAB & Simulink (accessed on 16-march-2020)." [Online]. Available: https://www.mathworks.com/help/stats/understanding-linear-regression-outputs.html.

[166] H. Abdi and L. J. Williams, "Partial least squares methods: Partial least squares correlation and partial least square regression." *Methods in Molecular Biology*, pp. 549–579, Dec. 2012. [Online]. Available: https://doi.org/10.1007/978-1-62703-059-5_23.

[167] H. Abdi, "Partial least squares regression and projection on latent structure regression (pls regression)." *Wiley Interdisciplinary Reviews: Computational Statistics*, vol. 2, pp. 97–106, Jan. 2010. [Online]. Available: https://doi.org/10.1002/wics.51.

[168] D. M. Allen, "Mean square error of prediction as a criterion for selecting variables," vol. 13, pp. 469–475, 1971.

[169] A. F. Siegel, *Part IV: Regression and Time Series.*, 7th ed. Academic Press, 2017. [Online]. Available: https://doi.org/10.1016/b978-0-12-804250-2.00012-2.

[170] M. Mamouei, M. Qassem, K. Budidha, N. Baishya, P. Vadgama, and P. A. Kyriacou, "Comparison of a genetic algorithm variable selection and interval partial least squares for quantitative analysis of lactate in pbs." in *41st Annual International Conference of the IEEE Engineering in Medicine and Biology Society (EMBC)*, Oct. 2019. [Online]. Available: https://doi.org/10.1109/embc.2019.8856765.

[171] K. Rathee, V. Dhull, R. Dhull, and S. Singh, "Biosensors based on electrochemical lactate detection: A comprehensive review." *Biochemistry and Biophysics Reports*, vol. 5, pp. 35–54, Mar. 2016. [Online]. Available: https://doi.org/10.1016/j.bbrep.2015.11.010.

[172] D. L. Williams, A. R. Doig, and A. Korosi, "Electrochemical-enzymatic analysis of blood glucose and lactate." *Analytical Chemistry*, vol. 42, pp. 118–121, Jan. 1970. [Online]. Available: https://doi.org/10.1021/ac60283a032.

[173] T. Shinbo, M. Sugiura, and N. Kamo, "Potentiometric enzyme electrode for lactate." *Analytical Chemistry*, vol. 51, pp. 100–104, Jan. 1979. [Online]. Available: https://doi.org/10.1021/ac50037a032.

[174] D. R. Thevenot, K. Tóth, R. A. Durst, and G. S. Wilson, "Electrochemical biosensors: Recommended definitions and classification." *Biosensors and Bioelectronics*, vol. 71, pp. 2333–2348, Jan. 1999. [Online]. Available: https://doi.org/10.1351/pac199971122333.

[175] L. Rassaei, W. Olthuis, S. Tsujimura, E. J. R. Sudhölter, and A. van den Berg, "Lactate biosensors: current status and outlook." *Analytical and Bioanalytical Chemistry*, vol. 406, pp. 123–137, Sep. 2014. [Online]. Available: https://doi.org/10.1007/s00216-013-7307-1.

[176] N. Nikolaus and B. Strehlitz, "Amperometric lactate biosensors and their application in (sports) medicine, for life quality and wellbeing." *Microchimica Acta*, vol. 160, pp. 15–55, Sept. 2008. [Online]. Available: https://doi.org/10.1007/s00604-007-0834-8.

[177] L. Theuer, J. Randek, S. Junne, P. Neubauer, C.-F. Mandenius, and V. Beni, "Single-use printed biosensor for l-lactate and its application in bioprocess monitoring." *Processes*, vol. 8, p. 321, Mar. 2020. [Online]. Available: https://doi.org/10.3390/pr8030321.

[178] M. Onor, S. Gufoni, T. Lomonaco, S. Ghimenti, P. Salvo, F. Sorrentino, and E. Bramanti, "Potentiometric sensor for non invasive lactate determination in human sweat." *Analytica Chimica Acta*, vol. 989, pp. 80–87, Oct. 2017. [Online]. Available: https://doi.org/10.1016/j.aca.2017.07.050.

[179] M. M. F. Choi, "Progress in enzyme-based biosensors using optical transducers." *Microchimica Acta*, vol. 148, pp. 107–132, Dec. 2004. [Online]. Available: https://doi.org/10.1007/s00604-004-0273-8.

[180] R. B. McComb, L. W. Bond, R. W. Burnett, R. C. Keech, and G. N. Bowers, "Determination of the molar absorptivity of nadh." *Clinical chemistry*, vol. 22, pp. 141–150, Feb. 1976. [Online]. Available: http://citeseerx.ist.psu.edu/viewdoc/download?doi=10.1.1.496.1139&rep=rep1&type=pdf.

[181] J. Wangsa and M. A. Arnold, "Fiber-optic biosensors based on the fluorometric detection of reduced nicotinamide adenine dinucleotide." *Analytical Chemistry*, vol. 60, pp. 1080–1082, May 1988. [Online]. Available: https://doi.org/10.1021/ac00161a027.

[182] C. Cámara, M. C. Moreno, and G. Orellana, *Chemical Sensing with Fiberoptic Devices.*, W. L. Wise D.L., Ed. Humana Press, Totowa, NJ, 1991. [Online]. Available: https://doi.org/10.1007/978-1-4612-0483-1_2.

[183] T. H. Fereja, A. Hymete, and T. Gunasekaran, "A recent review on chemiluminescence reaction, principle and application on pharmaceutical analysis." *ISRN Spectroscopy*, vol. 2013, pp. 1–12, Nov. 2013. [Online]. Available: https://doi.org/10.1155/2013/230858.

[184] Y. Yao, H. Li, D. Wang, C. Liu, and C. Zhang, "An electrochemiluminescence cloth-based biosensor with smartphone-based imaging for detection of lactate in saliva." *Analyst*, vol. 142, no. 19, pp. 3715–3724, Aug. 2017. [Online]. Available: https://doi.org/10.1039/C7AN01008G.

[185] "LM5 Lactate Analyser - Analox (accessed on 04-may-2020)." [Online]. Available: https://www.analox.com/analysers/lm5/.

[186] "ABL800 FLEX blood gas analyzer - Radiometer (accessed on 04-may-2020)." [Online]. Available: https://www.radiometeramerica.com/en-us/products/blood-gas-testing/abl800-flex-blood-gas-analyzer.

[187] "Lactate Pro 2 (accessed on 22-may-2020)," library Catalog: www.habdirect.co.uk. [Online]. Available: https://www.habdirect.co.uk/product/lactate-pro-2/.

[188] W. Brinkert, J. H. Rommes, and J. Bakker, "Lactate measurements in critically ill patients with a hand-held analyser." *Intensive care medicine*, vol. 25, pp. 966–969, Sep. 1999. [Online]. Available: https://doi.org/10.1007/s001340050990.

[189] J. Aduen, W. K. Bernstein, T. Khastgir, J. Miller, R. Kerzner, A. Bhatiani, J. Lustgarten, A. S. Bassin, L. Davison, and B. Chernow, "The use and clinical importance of a substrate-specific electrode for rapid determination of blood lactate concentrations." *JAMA*, vol. 272, pp. 1678–1685, Dec. 1994. [Online]. Available: https://doi.org/10.1001/jama.1994.03520210062033.

[190] T. L. Shirey, "Poc lactate: A marker for diagnosis, prognosis, and guiding therapy in the critically ill." *Point of Care: The Journal of Near-Patient Testing Technology*, vol. 6, pp. 192–200, Sep. 2007. [Online]. Available: https://doi.org/10.1097/poc.0b013e3181271545.

[191] E. M. Sillos, J. L. Shenep, G. A. Burghen, C. H. Pui, F. G. Behm, and J. T. Sandlund, "Lactic acidosis: a metabolic complication of hematologic malignancies: case report and review of the literature." *Cancer*, vol. 92, pp. 2237–2246, Nov. 2001. [Online]. Available: https://doi.org/10.1002/1097-0142(20011101)92:9<2237::AID-CNCR1569>3.0.CO;2-9.

[192] C. Chrusch, C. Bands, D. Bose, X. Li, H. Jacobs, K. Duke, E. Bautista, G. Eschun, R. B. Light, and S. N. Mink, "Impaired hepatic extraction and increased splanchnic production contribute to lactic acidosis in canine sepsis." *American journal of respiratory and critical care medicine*, vol. 161, pp. 517–526, Feb. 2000. [Online]. Available: https://doi.org/10.1164/ajrccm.161.2.9902403.

[193] J. Toffaletti, M. E. Hammes, R. Gray, B. Lineberry, and B. Abrams, "Lactate measured in diluted and undiluted whole blood and plasma: comparison of methods and effect of hematocrit." *Clinical chemistry*, vol. 38, pp. 2430–2434, Dec. 1992. [Online]. Available: https://doi.org/10.1093/clinchem/38.12.2430.

[194] R. Astles, C. P. Williams, and F. Sedor, "Stability of plasma lactate in vitro in the presence of antiglycolytic agents." *Clinical chemistry*, vol. 40, pp. 1327–1330, Jul. 1994. [Online]. Available: https://doi.org/10.1093/clinchem/40.7.1327.

[195] N. Thomas, I. Lähdesmäki, and B. A. Parviz, "A contact lens with an integrated lactate sensor." *Sensors and Actuators B: Chemical*, vol. 162, no. 1, pp. 128–134, Feb. 2012. [Online]. Available: https://doi.org/10.1016/j.snb.2011.12.049.

[196] C. Schabmueller, D. Loppow, G. Piechotta, B. Schütze, J. Albers, and R. Hintsche, "Micromachined sensor for lactate monitoring in saliva." *Biosensors and Bioelectronics*, vol. 21, no. 9, pp. 1770–1776, Nov. 2006. [Online]. Available: https://doi.org/10.1016/j.bios.2005.09.015.

[197] É. Tékus, M. Kaj, E. Szabó, N. Szénási, I. Kerepesi, M. Figler, R. Gábriel, and M. Wilhelm, "Comparison of blood and saliva lactate level after maximum

intensity exercise." *Acta Biologica Hungarica*, vol. 63, no. Supplement 1, pp. 89–98, Feb. 2012. [Online]. Available: https://doi.org/10.1556/ABiol.63.2012.Suppl.1.9.

[198] Y. Lei, W. Zhao, Y. Zhang, Q. Jiang, J.-H. He, A. J. Baeumner, O. S. Wolfbeis, Z. L. Wang, K. N. Salama, and H. N. Alshareef, "A mxene-based wearable biosensor system for high-performance in vitro perspiration analysis." *Small (Weinheim an der Bergstrasse, Germany)*, vol. 15, May 2019. [Online]. Available: https://doi.org/10.1002/smll.201901190.

[199] K. Nagamine, T. Mano, A. Nomura, Y. Ichimura, R. Izawa, H. Furusawa, H. Matsui, D. Kumaki, and S. Tokito, "Noninvasive sweat-lactate biosensor emplsoying a hydrogel-based touch pad." *Scientific reports*, vol. 9, Jul. 2019. [Online]. Available: https://doi.org/10.1038/s41598-019-46611-z.

[200] Q. Zhang, D. Jiang, C. Xu, Y. Ge, X. Liu, Q. Wei, L. Huang, X. Ren, C. Wang, and Y. Wang, "Wearable electrochemical biosensor based on molecularly imprinted ag nanowires for noninvasive monitoring lactate in human sweat." *Sensors and Actuators B: Chemical*, vol. 320, p. 128325, Oct. 2020. [Online]. Available: https://doi.org/10.1016/j.snb.2020.128325.

[201] B. K. Ashley, M. S. Brown, Y. Park, S. Kuan, and A. Koh, "Skin-inspired, open mesh electrochemical sensors for lactate and oxygen monitoring." *Biosensors & bioelectronics*, vol. 132, pp. 343–351, May 2019. [Online]. Available: https://doi.org/10.1016/j.bios.2019.02.041.

[202] E. M. Marek, J. Volke, I. Hawener, P. Platen, K. Mückenhoff, and W. Marek, "Measurements of lactate in exhaled breath condensate at rest and after maximal exercise in young and healthy subjects." *Journal of Breath Research*, vol. 4, no. 1, Jan. 2010. [Online]. Available: https://doi.org/10.1088/1752-7155/4/1/017105.

[203] B. Enderle, I. Moser, C. Kannan, K. O. Schwab, and G. Urban, "Interstitial glucose and lactate levels are inversely correlated with the body mass index: Need for in vivo calibration of glucose sensor results with blood values in obese patients." *Journal of diabetes science and technology*, vol. 12, pp. 341–348, Mar. 2018. [Online]. Available: https://doi.org/10.1177/1932296817730377.

[204] P. Bollella, S. Sharma, A. E. G. Cass, and R. Antiochia, "Microneedle-based biosensor for minimally-invasive lactate detection." *Biosensors & bioelectronics*, vol. 123, pp. 152–159, Jan. 2019. [Online]. Available: https://doi.org/10.1016/j.bios.2018.08.010.

[205] H. P. Hetherington, J. R. Hamm, J. W. Pan, D. L. Rothman, and R. G. Shulman, "A fully localized 1h homonuclear editing sequence to observe lactate in human skeletal muscle after exercise." *Journal of Magnetic Resonance*, vol. 82, pp. 86–96, Mar. 1989. [Online]. Available: https://doi.org/10.1016/0022-2364(89)90167-4.

[206] J. Ren, A. D. Sherry, and C. R. Malloy, "Noninvasive monitoring of lactate dynamics in human forearm muscle after exhaustive exercise by1h-magnetic resonance spectroscopy at 7 tesla." *Magnetic Resonance in Medicine*, vol. 70, pp. 610–619, Nov. 2013. [Online]. Available: https://doi.org/10.1002/mrm.24526.

[207] B. Schaller, R. Mekle, L. Xin, N. Kunz, and R. Gruetter, "Net increase of lactate and glutamate concentration in activated human visual cortex detected with magnetic resonance spectroscopy at 7 tesla." *Journal of Neuroscience Research*, vol. 91, pp. 1076–1083, Feb. 2013. [Online]. Available: https://doi.org/10.1002/jnr.23194.

[208] D. Sappey-Marinier, G. Calabrese, G. Fein, J. W. Hugg, C. Biggins, and M. W. Weiner, "Effect of photic stimulation on human visual cortex lactate and phosphates using 1h and 31p magnetic resonance spectroscopy." *Journal of Cerebral Blood Flow and Metabolism*, vol. 5, pp. 130–131, Apr. 1993. [Online]. Available: https://doi.org/10.1038/jcbfm.1992.82.

[209] M. Meyerspeer, G. J. Kemp, V. Mlynárik, M. Krššák, J. Szendroedi, P. Nowotny, M. Roden, and E. Moser, "Direct noninvasive quantification of lactate and high energy phosphates simultaneously in exercising human skeletal muscle by localized magnetic resonance spectroscopy." *Magnetic Resonance in Medicine*, vol. 57, pp. 654–660, Mar. 2007. [Online]. Available: https://doi.org/10.1002/mrm.21188.

[210] J.-L. Damez and S. Clerjon, "Quantifying and predicting meat and meat products quality attributes using electromagnetic waves: An overview." *Meat Science*, vol. 95, pp. 879–896, Dec. 2013. [Online]. Available: https://doi.org/10.1016/j.meatsci.2013.04.037.

[211] A. W. Guy, "Safety level with respect to human exposure to radiofrequency electromagnetic fields (300 khz-100 ghz)," *1980 IEEE MTT-S International Microwave symposium Digest*, pp. 335–336, 1980. [Online]. Available: https://doi.org/10.1109/mwsym.1980.1124279.

[212] P. Mehrotra, B. Chatterjee, and S. Sen, "Em-wave biosensors: A review of rf, microwave, mm-wave and optical sensing." *Sensors (Basel, Switzerland)*, vol. 19, Feb. 2019. [Online]. Available: https://doi.org/10.3390/s19051013.

[213] S. B. Wortis and F. Marsh, "Lactic acid content of the blood and of the cerebrospinal fluid." *Archives of Neurology Psychiatry*, vol. 35, no. 4, pp. 717–722, Apr. 1936. [Online]. Available: https://doi.org/10.1001/archneurpsyc.1936.02260040025002.

[214] J. H. Goh, A. Mason, A. I. Al-Shamma'a, M. Field, M. Shackcloth, and P. Browning, "Non invasive microwave sensor for the detection of lactic acid in cerebrospinal fluid (csf)." *Journal of Physics: Conference Series*, vol. 307, 2011. [Online]. Available: https://doi.org/10.1088/1742-6596/307/1/012017.

[215] A. Mason, J. Louis, J. Greene, O. Korostynska, L. E. Cordova-Lopez, B. Abdullah, R. Connell, and J. Hopkins, "Non-invasive measurement of blood lactate in humans using microwave sensors." *IEEE Transactions on Biomedical Engineering*, vol. 65, no. 3, pp. 698–705, Mar. 2017. [Online]. Available: https://doi.org/10.1109/ukrcon.2017.8100481.

[216] D. T. Delpy and M. Cope, "Quantification in tissue near-infrared spectroscopy." *Philosophical Transactions of the Royal Society B: Biological Sciences*, vol. 352, pp. 649–659, Jun. 1997. [Online]. Available: https://doi.org/10.1098/rstb.1997.0046.

[217] K. L. Zaleski and B. D. Kussman, "Near-infrared spectroscopy in pediatric congenital heart disease." *Journal of cardiothoracic and vascular anesthesia*, vol. 34, pp. 489–500, Feb. 2020. [Online]. Available: https://doi.org/10.1053/j.jvca.2019.08.048.

[218] F. F. Jöbsis, "Noninvasive, infrared monitoring of cerebral and myocardial oxygen sufficiency and circulatory parameters." *Science (New York, N.Y.)*, vol. 198, pp. 1264–1267, Dec. 1977. [Online]. Available: https://doi.org/10.1126/science.929199.

[219] P. Farzam, Z. Starkweather, and M. A. Franceschini, "Validation of a novel wearable, wireless technology to estimate oxygen levels and lactate threshold power in the exercising muscle." *Physiological reports*, vol. 6, Apr. 2018. [Online]. Available: https://doi.org/10.14814/phy2.13664.

[220] R. A. D. Blasi, M. Ferrari, A. Natali, G. Conti, A. Mega, and A. Gasparetto, "Noninvasive measurement of forearm blood flow and oxygen consumption by near-infrared spectroscopy." *Journal of Applied Physiolog*, vol. 76, pp. 1388–1393, Mar. 1994. [Online]. Available: https://doi.org/10.1152/jappl.1994.76.3.1388.

[221] V. Quaresima, S. Sacco, R. Totaro, and M. Ferrari, "Noninvasive measurement of cerebral hemoglobin oxygen saturation using two near infrared spectroscopy approaches." *Journal of Biomedical Optics*, vol. 5, pp. 201–205, Apr. 2000. [Online]. Available: https://doi.org/10.1117/1.429987.

[222] C. W. Yoxall and A. M. Weindling, "Measurement of venous oxyhaemoglobin saturation in the adult human forearm by near infrared spectroscopy with venous occlusion." *Medical and Biological Engineering and Computing*, vol. 35, pp. 331–336, Jul. 1997.

[223] B. Grassi, V. Quaresima, C. Marconi, M. Ferrari, and P. Cerretelli, "Blood lactate accumulation and muscle deoxygenation during incremental exercise." *Journal of applied physiology*, vol. 87, pp. 348–355, Jul. 1999. [Online]. Available: https://doi.org/10.1152/jappl.1999.87.1.348.

[224] L. Wang, T. Yoshikawa, T. Hara, H. Nakao, T. Suzuki, and S. Fujimoto, "Which common nirs variable reflects muscle estimated lactate threshold most closely?" *Applied physiology, nutrition, and metabolism = Physiologie appliquee,*

nutrition et metabolisme, vol. 31, pp. 612–620, Oct. 2006. [Online]. Available: https://doi.org/10.1139/h06-069.

[225] N. R. Borges and M. W. Driller, "Wearable lactate threshold predicting device is valid and reliable in runners." *Journal of strength and conditioning research*, vol. 30, pp. 2212–2218, Aug. 2016. [Online]. Available: https://doi.org/10.1519/JSC.0000000000001307.

[226] L. Heinemann and G. Schmelzeisen-Redeker, "Non-invasive continuous glucose monitoring in type i diabetic patients with optical glucose sensors. non-invasive task force (nitf)." *Diabetologia*, vol. 41, pp. 848–854, Jul. 1998. [Online]. Available: https://doi.org/10.1007/s001250050998.

[227] T. Kossowski, K. Kossowska, and R. Stasiński, "Non-invasive measurement of chemical compounds levels in human body." *Measurement Automation Monitoring*, vol. 63, no. 6, pp. 200–202, May 2017. [Online]. Available: http://yadda.icm.edu.pl/baztech/element/bwmeta1.element.baztech-3492a590-bb24-46b8-a730-0d36bdd78843.

[228] M. J. Martelo-Vidal and M. Vazquez, "Evaluation of ultraviolet, visible, and near infrared spectroscopy for the analysis of wine compounds," *Czech Journal of Food Sciences*, vol. 32, no. 1, pp. 37–47, 2014. [Online]. Available: https://doi.org/10.17221/167/2013-CJFS.

[229] A. J. Berger, Y. Wang, and M. S. Feld, "Rapid, noninvasive concentration measurements of aqueous biological analytes by near-infrared raman spectroscopy." *Applied optics*, vol. 35, pp. 209–212, Jan. 1996. [Online]. Available: https://doi.org/10.1364/AO.35.000209.

[230] H. Chung, M. A. Arnold, M. Rhiel, and D. W. Murhammer, "Simultaneous measurements of glucose, glutamine, ammonia, lactate, and glutamate in aqueous solutions by near-infrared spectroscopy." *Applied Spectroscopy*, vol. 50, pp. 270–276, Feb. 1996. [Online]. Available: https://doi.org/10.1366/0003702963906447.

[231] M. J. McShane and G. L. Coté, "Near-infrared spectroscopy for determination of glucose, lactate, and ammonia in cell culture media." *Applied Spectroscopy*, vol. 52, no. 8, pp. 1073–1078, Aug. 1998. [Online]. Available: https://doi.org/10.1366/0003702981944968.

[232] M. J. McShane, G. L. Coté, and C. H. Spiegelman, "Assessment of partial least-squares calibration and wavelength selection for complex near-infrared spectra." *Applied Spectroscopy*, vol. 52, pp. 878–884, Jun. 1998. [Online]. Available: https://doi.org/10.1366/0003702981944427.

[233] T. Yano, H. Matsushige, K.-I. Suehara, and Y. Nakano, "Measurement of the concentrations of glucose and lactic acid in peritoneal dialysis solutions using near-infrared spectroscopy." *Journal of Bioscience and Bioengineering*, vol. 90, pp. 540–544, Jan. 2002. [Online]. Available: https://doi.org/10.1016/s1389-1723(01)80037-2.

[234] M. R. Riley, C. D. Okeson, and B. L. Frazier, "Rapid calibration of near-infrared spectroscopic measurements of mammalian cell cultivations." *Biotechnology progress*, vol. 15, no. 6, pp. 1133–1141, Sept. 2008. [Online]. Available: https://doi.org/10.1021/bp990117v.

[235] M. Riley, "The effect of analyte concentration range on measurement errors obtained by nir spectroscopy." *Talanta*, vol. 52, pp. 473–484, Jun. 2000. [Online]. Available: https://doi.org/10.1016/s0039-9140(00)00403-3.

[236] M. R. Riley, H. M. Crider, M. E. Nite, R. A. Garcia, J. Woo, and R. M. Wegge, "Simultaneous measurement of 19 components in serum-containing animal cell culture media by fourier transform near-infrared spectroscopy." *Biotechnology Progress*, vol. 17, pp. 376–378, Sep. 2008. [Online]. Available: https://doi.org/10.1021/bp0100068.

[237] D. Lafrance, L. C. Lands, L. Hornby, and D. H. Burns, "Near-infrared spectroscopic measurement of lactate in human plasma." *Applied Spectroscopy*, vol. 54, no. 2, pp. 300–304, Feb. 2000. [Online]. Available: https://doi.org/10.1366/0003702001949267.

[238] D. Lafrance, "Measurement of lactate in whole human blood with near-infrared transmission spectroscopy." *Talanta*, vol. 60, pp. 635–641, Jul. 2003. [Online]. Available: https://doi.org/10.1016/s0039-9140(03)00042-0.

[239] D. Lafrance, L. C. Lands, and D. H. Burns, "In vivo lactate measurement in human tissue by near-infrared diffuse reflectance spectroscopy." *Vibrational Spectroscopy*, vol. 36, pp. 195–202, Dec. 2004. [Online]. Available: https://doi.org/10.1016/j.vibspec.2004.01.020.

[240] G. Cassanas, M. Morssli, E. Fabrègue, and L. Bardet, "Vibrational spectra of lactic acid and lactates." *Journal of Raman Spectroscopy*, vol. 22, pp. 409–413, Jul. 1991. [Online]. Available: https://doi.org/10.1002/jrs.1250220709.

[241] C. Petibois, G. Cazorla, A. Cassaigne, and G. Déléris, "Plasma protein contents determined by fourier-transform infrared spectrometry." *Clinical chemistry*, vol. 47, pp. 730–738, Apr. 2001. [Online]. Available: https://doi.org/10.1093/clinchem/47.4.730.

[242] C. Petibois, A.-M. Melin, A. Perromat, G. Cazorla, and G. Déléris, "Glucose and lactate concentration determination on single microsamples by fourier-transform infrared spectroscopy." *Journal of Laboratory and Clinical Medicine*, vol. 135, no. 2, pp. 210–215, Feb. 2000. [Online]. Available: https://doi.org/10.1067/mlc.2000.104460.

[243] B. R. Soller, R. H. Micheels, J. Coen, B. Parikh, L. Chu, and C. Hsi, "Feasibility of non-invasive measurement of tissue ph using near-infrared

reflectance spectroscopy." *Journal of clinical monitoring*, vol. 12, pp. 387–395, Sep. 1996. [Online]. Available: https://doi.org/10.1007/BF02077636.

[244] K. Alam, M. R. Rohrscheib, J. E. Franke, T. M. Niemczyk, J. D. Maynard, and M. R. Robinson, "Measurement of ph in whole blood by near-infrared spectroscopy." *Applied Spectroscopy*, vol. 53, no. 3, pp. 316–324, Mar. 1999. [Online]. Available: https://doi.org/10.1366/0003702991946523.

[245] N. A. Rosen, W. E. Charash, and E. F. Hirsch, "Near-infrared spectrometric determination of blood ph." *The Journal of surgical research*, vol. 106, pp. 282–286, Aug. 2002. [Online]. Available: https://doi.org/10.1006/jsre.2002.6377.

[246] T. Ube, Y. Yoneyama, and T. Ishiguro, "In situ measurement of the ph-dependent transmission infrared spectra of aqueous lactic acid solutions." *Analytical Sciences*, vol. 33, pp. 1395–1400, Dec. 2017. [Online]. Available: https://doi.org/10.2116/analsci.33.1395.

[247] H. Martens, J. P. Nielsen, and S. B. Engelsen, "Light scattering and light absorbance separated by extended multiplicative signal correction. application to near-infrared transmission analysis of powder mixtures." *Analytical Chemistry*, vol. 75, pp. 394–404, Jan. 2003. [Online]. Available: https://doi.org/10.1021/ac020194w.

[248] P. Geladi, D. MacDougall, and H. Martens, "Linearization and scatter-correction for near-infrared reflectance spectra of meat." *Applied Spectroscopy*, vol. 39, pp. 491–500, May 1985. [Online]. Available: https://doi.org/10.1366/0003702854248656.

[249] A. Savitzky and M. J. E. Golay, "Smoothing and differentiation of data by simplified least squares procedures." *Analytical Chemistry*, vol. 36, pp. 1627–1639, Jul. 1964. [Online]. Available: https://doi.org/10.1021/ac60214a047.

[250] K. Budidha, M. Mamouei, N. Baishya, P. Vadgama, and P. A. Kyriacou, "In vitro quantification of lactate in phosphate buffer saline (pbs) samples." in *41st Annual International Conference of the IEEE Engineering in Medicine and Biology Society (EMBC)*, Oct. 2019. [Online]. Available: https://doi.org/10.1109/embc.2019.8857756.

[251] N. Baishya, M. Mamouei, K. Budidha, M. Qassem, P. Vadgama, and P. A. Kyriacou, "Investigations into the effects of ph on quantitative measurements of lactate in biological media using atr-ftir spectroscopy." *Moelcules*, vol. 25, p. 3695, Aug. 2020. [Online]. Available: https://doi.org/10.3390/molecules25163695.

[252] L. J. Henderson, "Concerning the relationship between the strength of acids and their capacity to preserve neutrality." *American Journal of Physiology-Legacy Content*, vol. 21, no. 2, pp. 173–179, Mar. 1908. [Online]. Available: https://doi.org/10.1152/ajplegacy.1908.21.2.173.

[253] K. A. Hasselbalch, *Die Berechnung der Wasserstoffzahl des Blutes aus der freien und gebundenen Kohlensäure desselben, und die Sauerstoffbindung des Blutes als Funktion der Wasserstoffzahl.* Julius Springer, 1916.

[254] N. Baishya, M. Momouei, K. Budidha, M. Qassem, P. Vadgama, and P. A. Kyriacou, "Near infrared spectrometric investigation of lactate in a varying ph buffer." *Journal of Near Infrared Spectroscopy*, p. (available online), Mar. 2020. [Online]. Available: https://doi.org/10.1177/0967033520905374.

[255] G. Allison, P. R. Stevens, R. Jackman, and J. Moorby, "Normal ranges and temporal variation in plasma concentrations of l-lactate and free amino acids in adult sheep." *Research in veterinary science*, vol. 85, no. 1, pp. 22–25, Aug. 2008. [Online]. Available: https://doi.org/10.1016/j.rvsc.2007.08.005.

[256] N. Bosschaart, G. J. Edelman, M. C. Aalders, T. G. van Leeuwen, and D. J. Faber, "A literature review and novel theoretical approach on the optical properties of whole blood." *Lasers in medical science*, vol. 29, no. 2, pp. 453–479, Oct. 2014.

[257] D. B. Pyne, T. Boston, D. T. Martin, and A. Logan, "Evaluation of the lactate pro blood lactate analyser." *European journal of applied physiology*, vol. 82, pp. 112–116, May 2000. [Online]. Available: https://doi.org/10.1007/s004210050659.

[258] R. K. Tanner, K. L. Fuller, and M. L. R. Ross, "Evaluation of three portable blood lactate analysers: Lactate pro, lactate scout and lactate plus." *European journal of applied physiology*, vol. 109, pp. 551–559, Jun. 2010. [Online]. Available: https://doi.org/10.1007/s00421-010-1379-9.

[259] F. Shen, X. Niu, D. Yang, Y. Ying, B. Li, G. Zhu, and J. Wu, "Determination of amino acids in chinese rice wine by fourier transform near-infrared spectroscopy." *Journal of agricultural and food chemistry*, vol. 58, no. 17, pp. 9809–9816, Aug. 2010. [Online]. Available: https://doi.org/10.1021/jf1017912.

[260] E. Ferrari, G. Foca, M. Vignali, L. Tassi, and A. Ulrici, "Adulteration of the anthocyanin content of red wines: Perspectives for authentication by fourier transform-near infrared and 1h nmr spectroscopies." *Analytica Chimica Acta*, vol. 701, no. 2, pp. 139–151, Sep. 2011. [Online]. Available: https://doi.org/10.1016/j.aca.2011.05.053.

[261] D. Cozzolino, W. Cynkar, N. Shah, and P. Smith, "Can spectroscopy geographically classify sauvignon blanc wines from australia and new zealand?" *Food chemistry*, vol. 126, no. 2, pp. 673–678, May 2011. [Online]. Available: https://doi.org/10.1016/j.foodchem.2010.11.005.

[262] I. Murray, "The nir spectra of homologous series of organic compounds in near-infrared diffuse relfectance/transmittance spectroscopy." 1987.

[263] V. A. McGlone and S. Kawano, "Firmness, dry-matter and soluble-solids assessment of post harvest kiwi fruit by nir spectroscopy." *Postharvest Biology and Technology*, vol. 13, no. 2, pp. 131–141, Apr. 1998. [Online]. Available: https://doi.org/10.1016/S0925-5214(98)00007-6.

[264] F. Liu, Y. He, L. Wang, and G. Sun, "Detection of organic acids and ph of fruit vinegars using near-infrared spectroscopy and multivariate calibration." *Food and Bioprocess Technology*, vol. 4, no. 8, p. 1331, Nov. 2011. [Online]. Available: http://dx.doi.org/10.1007/s11947-009-0240-9.

[265] A. Sthoer, J. Hladílková, M. Lund, and E. Tyrode, "Molecular insight into carboxylic acid–alkali metal cations interactions: reversed affinities and ion-pair formation revealed by non-linear optics and simulations." *Physical Chemistry, Chemical Physics*, vol. 21, pp. 11 329–11 344, may 2019. [Online]. Available: https://doi.org/10.1039/c9cp00398c.

[266] J. Coates, "Designing the ideal process analyser or at least making the attempt (continued)." *NIR news*, vol. 5, pp. 7–9, Jun. 1994. [Online]. Available: https://doi.org/10.1255/nirn.250.

[267] A. Peirs, N. Scheerlinck, K. Touchant, and B. M. Nicolaï, "Ph—postharvest technology: Comparison of fourier transform and dispersive near-infrared reflectance spectroscopy for apple quality measurements." *Biosystems Engineering*, vol. 81, no. 3, pp. 305–311, Mar. 2002. [Online]. Available: https://doi.org/10.1006/bioe.2001.0040.

[268] P. Armstrong, E. Maghirang, F. Xie, and F. Dowell, "Comparison of dispersive and fourier-transform nir instruments for measuring grain and flour attributes." *Applied Engineering in Agriculture*, vol. 22, no. 3, pp. 453–457, Apr. 2006. [Online]. Available: https://doi.org/10.13031/2013.20448.

[269] N. Pérez-Hernández, C. Pérez, M. L. Rodríguez, C. Foces-Foces, P. M. Tolstoy, H. H. Limbach, E. Q. Morales, R. Pérez, and J. D. Martín, "Water molecules in hydroxy/acid networks as a competition between dynamics and bonding. synthesis of a wet hydrophobic pore." vol. 12, pp. 1305–1314, Mar. 2004. [Online]. Available: https://doi.org/10.1016/j.bmc.2003.06.006.

[270] J. Toffaletti and B. Abrams, "Effects of in vivo and in vitro production of lactic acid on ionized, protein-bound, and complex-bound calcium in blood." *Clinical chemistry*, vol. 35, no. 6, pp. 935–938, Jun. 1989. [Online]. Available: https://doi.org/10.1093/clinchem/35.6.935.

[271] P. Constable, F. M. Trefz, and H. Stämpfli, "Effects of ph and the plasma or serum concentrations of total calcium, chloride, magnesium, l-lactate, and albumin on the plasma ionized calcium concentration in calves." *Journal of veterinary internal medicine*, vol. 33, no. 4, pp. 1822–1832, Jul. 2019. [Online]. Available: https://doi.org/10.1111/jvim.15509.

[272] H. Schaer and U. Bachmann, "Ionized calcium in acidosis: Differential effect of hypercapnic and lactic acidosis." *British Journal of Anaesthesia*, vol. 46, pp. 842–848, 1974. [Online]. Available: https://doi.org/10.1093/bja/46.11.842.

[273] D. J. Cooper, K. R. Walley, P. M. Dodek, F. Rosenberg, and J. A. Russell, "Plasma ionized calcium and blood lactate concentrations are inversely associated in human lactic acidosis." vol. 18, pp. 286–289, May 1992. [Online]. Available: https://doi.org/10.1007/bf01706475.

[274] B. Chernow, G. Zaloga, E. McFadden, M. Clapper, M. Kotler, M. Barton, and T. G. Rainey, "Hypocalcemia in critically ill patients." *Critical Care Medicine*, vol. 10, no. 12, pp. 848–851, Dec. 1982. [Online]. Available: https://doi.org/10.1097/00003246-198212000-00008.

[275] T. K. Desai, R. W. Carlson, and M. A. Geheb, "Prevalence and clinical implications of hypocalcemia in acutely iii patients in a medical intensive care setting." *The American Journal of Medicine*, vol. 84, pp. 209–214, Feb. 1988. [Online]. Available: https://doi.org/10.1016/0002-9343(88)90415-9.

[276] P. S. Underwood and A. Lamba, "Parathormone and ionized calcium in critically ill patients with sepsis." *Canadian Journal of Surgery*, vol. 7, p. 136, Mar. 1979. [Online]. Available: https://doi.org/10.1097/00003246-197903000-00054.

[277] G. P. Zaloga and B. Chernow, "The multifactorial basis for hypocalcemia during sepsis. studies of the parathyroid hormone-vitamin d axis." *Annals of internal medicine*, vol. 107, pp. 36–41, Jul. 1987. [Online]. Available: https://doi.org/10.7326/0003-4819-107-1-36.

[278] M. K. Holowaychuk and L. G. Martin, "Review of hypocalcemia in septic patients." *Journal of Veterinary Emergency and Critical Care*, vol. 17, pp. 348–358, Nov. 2007. [Online]. Available: https://doi.org/10.1111/j.1476-4431.2007.00246.x.

[279] J. C. Chatham and J. R. Forder, "Lactic acid and protein interactions: implications for the nmr visibility of lactate in biological systems." *Biochimica et Biophysica Acta (BBA) - General Subjects*, vol. 1426, no. 1, pp. 177–184, Jun. 1999. [Online]. Available: https://doi.org/10.1016/s0304-4165(98)00154-8.

[280] P. Guesnon, C. Poyart, E. Bursaux, and B. Bohn, "The binding of lactate and chloride ions to human adult hemoglobin." *Respiration Physiology*, vol. 38, no. 2, pp. 115–129, Oct. 1979. [Online]. Available: https://doi.org/10.1016/0034-5687(79)90031-8.

[281] I. Carneiro, S. Carvalho, R. Henrique, L. Oliveira, and V. V. Tuchin, "Simple multimodal optical technique for evaluation of free/bound water and dispersion of human liver tissue." vol. 22, p. 1, Dec. 2017. [Online]. Available: https://doi.org/10.1117/1.jbo.22.12.125002.

[282] Q. Liu and S. Xiao, "Effects of spectral resolution and signal-to-noise ratio of hyperspectral sensors on retrieving atmospheric parameters." *Optics Letters*, vol. 39, p. 60, Dec. 2013. [Online]. Available: https://doi.org/10.1364/ol.39.000060.

[283] J. Wang, J. Kang, and T. Wang, "The spectral characterizations of the low and high resolution remote ftir emission spectroscopy." *Spectroscopy Letters*, vol. 28, pp. 839–848, Mar. 1995. [Online]. Available: https://doi.org/10.1080/00387019508009924.

[284] M. G. Sowa, J. Wang, C. P. Schultz, M. K. Ahmed, and H. H. Mantsch, "Infrared spectroscopic investigation of in vivo and ex vivo human nails." *Vibrational Spectroscopy*, vol. 10, no. 1, pp. 49–56, Nov. 1995. [Online]. Available: https://doi.org/10.1016/0924-2031(95)00027-R.

[285] R. R. Anderson and J. A. Parrish, "The optics of human skin." *The journal of Investigate Dermatology*, vol. 77, no. 1, pp. 13–19, jul 1981. [Online]. Available: https://doi.org/10.1111/1523-1747.ep12479191.

A

Appendices

City Research Ethics Committees
Application for Approval of Research Involving Human Participants

Please tick the box for which Committee you are submitting your application to

☒	Senate Research Ethics Committee
☐	Cass Business School
☐	Department of Computer Science
☐	Department of Sociology
☐	School of Health Sciences Research Ethics Committee
☐	The City Law School
☐	Department for Learning Enhancement and Development

For **Senate** applications: a single copy of the application form and all supporting documents should be emailed to researchethics@city.ac.uk

For **Cass Business School** applications: a single copy of the application form and all supporting documents should be emailed to: claire.molloy.1@city.ac.uk

For **Computer Science** applications: a single copy of the application form and all supporting documents should be emailed to J.Dykes@city.ac.uk

For the Department of Sociology, submit all forms in Word format in a single document electronically. For projects falling under Sociology, Media Studies, Criminology, Food Policy and Q-Step, please send to Simon.Susen@city.ac.uk; and for projects falling under CCI, to Diana.Yeh@city.ac.uk

For **School of Health Sciences** applications: submit all forms (including the Research Registration form) electronically (in Word format in a single document) to A.Welton@city.ac.uk

For **The City Law School** applications: submit all forms electronically (in Word format in a single document) to jesse.elvin.1@city.ac.uk

For **Department for Learning Enhancement and Development:** a single copy of the application form and all the supporting documentation should be emailed to P.M.Parker@city.ac.uk

Refer to the separate guidelines while completing this form.

PLEASE NOTE THE FOLLOWING:

- Ethical approval **MUST** be obtained before any research involving human participants is undertaken. Failure to do so may result in disciplinary procedures being instigated, and you will not be covered by City's indemnity if you do not have approval in place. It may also result in the degree not being awarded or the data not being published in a peer review journal.
- The Signature Sections **MUST** be completed by the Principal Investigator (the supervisor and the student if it is a student project).

Project Title:
In-vitro blood spectroscopy using optical and electrical spectroscopy methods to understand the properties of parameters emulating septic shock (eg: lactate, pH, oxygenation, etc.)
Short Project Title (no more than 80 characters):
In-vitro laboratory analysis of blood components
Name of Principal Investigator(s) (if this is a student project, please note that the Principal Investigator is the supervisor and all correspondence will be with the supervisor):
(1) Professor Panicos Kyriacou (Principal Investigator and Point of Contact) (2) Dr. Meha Qassem (3) Dr. Mohammad Hossein Mamouei

(4) Ms. Nystha Baishya
(5) Mr. Chadi El Hajj
(6) Dr. Karthik Budidha

Post Held (including staff/student number):

(1) Associate Dean for Postgraduate Studies, Director of Biomedical Engineering Research Group, Reg No.: 90096558
(2) Postdoctoral Research Associate, Reg No.: 888034786
(3) Postdoctoral Research Associate in Data Science and Modelling, Reg No.: 888100708
(4) PhD Student, under supervision of Prof Kyriacou, Reg No.: 170049512
(5) PhD Student, under supervision of Prof Kyriacou, Reg No.: 160047936
(6) Postdoctoral Research Associate , Reg No: 888078256

Department(s)/School(s) involved at City:

EEE/MCSE

If this is part of a degree please specify type of degree:

Some of the work completed under this Ethics Applications will contribute to the following degrees:

1. PhD, Nystha Baishya, 2017-2021
2. PhD, Chadi El Hajj, 2018-2022

Date of Submission of Application:

30th Aug, 2018 (amendment 5)

Tick this box if you do not grant City permission to use your application form for training purposes ☐

1. Applicant Details

This project involves:
(*tick as many as apply*)

☒	Staff Research	☒	Doctoral Student
☐	Undergraduate	☐	M-level Project
☐	Externally funded	☐	External investigators
☐	Other		
Provide details of external investigators and/or other			

Email address for the Principal Investigator (City email, not private)

p.kyriacou@city.ac.uk

Other staff members involved

Title, Name & Staff Number	*Post*	*Dept & School*	*Phone*	*Email*
Dr. Meha Qassem (Reg: 888034786)	Postdoctoral research associate	EEE/MCSE	020 7040 3878	meha.qassem@city.ac.uk
Dr. Mohammad Hossein Mamouei (Reg: 888100708)	Postdoctoral research associate	EEE/MCSE	020 7040 3878	mohammad.mamouei@city.ac.uk
Dr. Karthik Budidha (Reg: 888078256)	Postdoctoral research associate	EEE/MCSE	020 7040 3878	karthik.budidha.1@city.ac.uk

All students involved in carrying out the investigation

Name & Student Number	*Course / Year*	*Dept & School*	*Email*
Ms. Nystha Baishya (Reg: 170049512)	PhD Biomedical Engineering 1st year	EEE/MCSE	nystha.baishya@city.ac.uk
Mr. Chadi El Hajj (Reg: 160047936)	PhD Biomedical Engineering 1st year	EEE/MCSE	chadi.el-hajj@city.ac.uk

External co-investigators

Title & Name	*Post*	*Institution*	*Phone*	*Email*

Please describe the role(s) of all the investigators, including all student(s)/external co-investigator(s) in the project, especially with regards to interaction with study participants.

Professor Kyriacou is the supervisor of the project. Meha & Nystha will be involved in testing blood samples for various investigations on blood, its properties and blood component analysis. The invasive withdrawal of a blood sample will be carried out by a qualified and registered clinician/nurse/phlebotomist who will be hired for the date of the sampling. Mohammad and Chadi are the researchers who will conduct the studies under Prof Kyriacou's supervision and analyse the collected data. Karthik will also be involved in parts of the investigations on blood and more in building the instrumentation of the sensor.

If external investigators are involved, please provide details of their indemnity cover.

Application Details

1.1 Is this application or any part of this research project being submitted to another ethics committee, or has it previously been submitted to an ethics committee? *This includes an NHS local Research Ethics Committee or a City local Research Ethics Committee or any other institutional committee or collaborating partners or research site.* (See the guidelines for more information on research involving NHS patients.)

YES ☐ **NO** ☒

If yes, please give details and justification for going to separate committees, details of the Secretary of the relevant authority/committee, and, if appropriate, attach correspondence and details of the outcome of the application, including any conditions of approval or reasons for rejection.

NA

1.2 If any part of the investigation is being carried out under the auspices of an outside organisation, involves collaboration between institutions or individual external researchers, or institutions/organisations where interviews/fieldwork will take place please give details and address of organisation(s).

NA

1.3 Has permission to conduct research in, at or through another institution or organisation been obtained? **YES** ☐ **NO** ☒

If yes, please provide details and attach the supporting correspondence.

NA

1.4 Will personal data collected be shared with the outside organisation? If so, will the outside organisation be a joint data controller with City or a data processor on behalf of City?

NA

1.5 If yes, please detail any collaboration agreements, data sharing arrangements (joint data controller) or data processing contract (data processor on behalf of City) with the outside organisation. Please attach a copy of the data sharing agreement (joint data controller) or contract (data processor) with your application. The Information Compliance Team at dataprotection@city.ac.uk can provide further advice.

NA

1.6 Duration of Project

Start date: 1st July 2018 Estimated end date: 30th Jun 2021

Conflicts of interest

1.7 Do any of the investigators listed have any direct personal involvement (e.g. financial, share holding, personal relationship etc.) in the organisations sponsoring or funding the research that may give rise to a possible conflict of interest? YES ☐ **NO** ☒

If yes, please provide details and attach the supporting correspondence.

1.8 Will any of the investigators receive any personal benefits or incentives, including payment above normal salary, from undertaking the research or the results of the research above those normally associated with scholarly activity? YES ☐ **NO** ☒

If yes, please provide details and attach the supporting correspondence.

Funding Details

1.9 Is the project reliant on funding? If no, please go to the next section. **YES** ☐ **NO** ☒

If yes, please provide details of the source of financial support (e.g. funding body, charity etc.) for the proposed investigation.

NA

1.9a Has funding been applied for? **YES** ☐ **NO** ☐

1.9 b Has funding been approved? **YES** ☐ **NO** ☐

If no, please provide details of when the outcome can be expected

International Research

1.10 Is any part of the research taking place outside of England/Wales? (if not go to section 2) **YES ☐ NO ☒**

If yes, please provide details of where.

NA

1.11 Have you identified and complied with all local requirements concerning ethical approval & research governance and data protection*?

YES ☐ NO ☒

1.11a Please provide details of the local requirements, including contact information.

NA

1.11b Please give contact details of a local person identified to field initial complaints locally so the participants can complain without having to write to or telephone the UK.

NA

*Please note that many countries require local ethical approval or registration of research projects, further some require specific research visas. You must also ensure you are aware of and abide by the national data protection legislation including legal requirements around research using patient data and transfer of data to and from the UK. If you do not abide by the local rules of the host country, you will invalidate your ethical approval from City, and may run the risk of legal action within the host country.

2. Project Details

2.1 Provide the background (including the current state of the art in this field), aim(s) and objectives of the proposed research,

There remains a need for the provision of non-invasive medical sensors for the determination of blood components. Examples include monitoring blood glucose levels in diabetic patients, or blood lactate levels for patients admitted in the ICU or for pharmaceuticals such as lithium medication. Such sensors would provide alternatives to laboratory blood tests, which require the withdrawal of blood samples, are infrequent and not immediately available to the clinician. Non-invasive sensors would allow for regular or continuous monitoring by the patient at home, or at point-of-care sites such as in GP surgeries, as a result reducing the risk of unnecessary health complications.

The Research Centre for Biomedical Engineering (RCBE) has expertise in optical spectroscopy and in developing optical sensors for non-invasive measurements, particularly of blood oxygenation. Recently, that expertise has extended to the area of Electrical Impedance Spectroscopy (EIS). EIS has been investigated by other researchers as a method for determining cholesterol and sodium levels in blood. The RCBE has been expanding on these areas of expertise in order to provide new optical and/or electrical sensors for blood component analysis. In particular, new research is being undertaken to measure blood lactate levels and blood lithium levels non-invasively, and to provide new knowledge on the

behaviour of light absorption by red-blood cells orientation. These areas will be expanded in the future to incorporate the analysis of the properties of other blood components and parameters like blood pH.

In order to achieve sensors of high sensitivities and accuracy, in-vitro optical and electrical spectroscopic measurements need to be carried out in the laboratory. This will enable the determination of the optical and electrical “fingerprints” of important substances such as lactate in blood.

The proposed research covers investigations where biological samples of human blood and will be required to acquire optical and/or electrical spectroscopy measurements. The project involves studying components in blood by commercially purchasing animal blood and lactate and doing controlled experiments in the beginning. This will help us understand the behaviour of lactate solution in blood, do controlled experiments and build an intelligent model based on Artificial Intelligence and data analysis techniques. In order to, test and verify this model for clinical purposes, actual human blood samples will be obtained, and the experiments will be repeated. Human blood (serum, plasma or whole blood) from healthy volunteers will be obtained following informed written consent or purchased from a reliable source. The withdrawal of blood will be achieved by taking a finger-prick droplet of blood, or for investigations that require larger blood samples, an arterial/venous blood sample of no more than 10 mL in volume will be withdrawn by a qualified and registered clinician/nurse/phlebotomist, who will be hired for the occasion. More details are given in the following sections.

2.2 Please explain how this project will further existing knowledge.

Blood lactate concentration acts as an indicator for critically ill and has been studied by various groups for a variety of patients, particularly in the ICU and it has been linked with organ dysfunction and mortality. This project will enable us to understand the optical properties of lactate and give us a platform estimate and monitor the concentrations non-invasively, continuously and at point-of-care sights.

2.3 Provide a summary and brief explanation of the design, methodology and plan for analysis that you propose to use.

1: Methods

This research will use a range of analytical techniques on human blood samples in the laboratory. These analytical methods are as follows:

1. A commercial UV-NIRS Spectrophotometer from Perkin Elmer
2. A commercial HATR FTIR Spectrometer from Perkin Elmer
3. A commercial Blood Gas Analyser from Radiometer
4. A commercial Impedance Analyser from Tektronix
5. Custom made optical/electrical impedance systems developed at RCBE

2: Acquisition of blood

Human blood samples will be purchased from a reliable source or acquired from volunteers following informed, written consent. Two forms will be signed, so that the participant is provided with a signed copy to keep for their records. The blood will be acquired using two methods:

(a) Fingerprick Method: Volunteers will be asked to prick the top of their finger using a lancet with a sterile needle (as commonly used by Diabetes Type I patients). The sterile needle will be in retractable container and disposed after use. The sensation on the fingertip will be like a light scratch. The blood droplet that surfaces will be removed with a single use pipette for analysis.

(b) Blood sample withdrawal: An invasive blood sample (arterial or venous) will be withdrawn from the arm of the patient by a qualified and registered clinician/nurse/phlebotomist using a sterile, disposable needle and syringe. No more than 10mL of blood will be withdrawn.

Depending on the wish of the volunteer, as filled in the consent form, they will be allowed to choose from the one of the above methods.

On completion of the blood samples acquisition, the volunteers will be kept under monitoring for a few hours (arterial blood sample volunteers) to monitor any bleeding and/or damage at the sampling site. Depending on the judgement of the clinician/nurse/phlebotomist they will be allowed to go home.

The lancet prick volunteers will be allowed to go home right after the blood sample acquisition.

3: Blood handling and preparation

Following acquisition of the blood sample, the blood may need to be further modified by the researcher – depending on the specific investigation. In this case,

- The blood will be placed in a suitable glass container, whereby a controlled amount of a substance, such as lactate, will be added and mixed.
- For other investigations, it may be required to centrifuge the blood sample before analysis. This will involve adding the blood sample to a sample tube and placing it in a centrifuge for approx. 10 minutes.

Bloods will only be handled in a suitable, well-prepared area within the Biomedical Engineering Research Lab. The area will include all the measuring equipment, handling equipment etc. so that blood samples will not be removed outside of the dedicated space for bloods. The area will have smooth, easily sterilisable surfaces, a sink, first aid kit, sterilising agents and kit, sharps disposal bin, blood disposal bin, and suitable storage for bloods. The investigator handling blood will wear suitable attire, such as a white lab coat, disposable gloves etc. (see section 3.4 for more information).

All blood samples will be analysed within a maximum time of 24 hours and disposed of on the same day. Within this time the blood will be stored in a dedicated, padlocked refrigerator when not being analysed or prepared.

4: Measurements on blood samples

- Following preparation, the blood sample will be removed from the container and placed in a cuvette or other container suitable for measurement. The container will then be closed.
- The container with the sample will then be placed in the appropriate measuring apparatus (es) (eg. spectrophotometer, impedance analyser) where measurements will be made.
- The measurements will be saved on a computer.

5: Disposal and Sterilisation Issues

- All waste will be collected by a registered carrier.
- Directly following measurements, bloods will be disposed of in appropriate blood bins, and all items that came into contact with bloods will either be disposed on the same day or cleaned with a sterilising solution.
- Syringes and needles will be disposed through a dedicated yellow biohazard-marked sharps bin which will then be collected and incinerated by a registered carrier on the same day.
- Blood samples, blood products and disposable items (e.g. pipettes) that have come into contact with blood will be disposed through a dedicated yellow biohazard-marked bin which will then be collected by a registered carrier on the same day.
- Items such as expensive cuvettes, silicon tubes, the silver electrodes and the pump will be washed and sterilised. The water used to rinse the items and the sterilisation agent will be disposed of appropriately.

6: Analysis of data
All acquired data will be de-identified and analysed retrospectively. Various signal processing techniques will be applied to the obtained optical and electrical spectra in order to acquire further information of blood component concentration and behaviour. Artificial Intelligence and Data Analysis will be applied to results to look for trends in the data.

2.4 Please explain how/if participants will be provided with the findings or outcomes of the project.

Results from the investigations will be used for:
• MPhil transfer reports
• PhD Theses
• Publications in peer reviewed journals.
• Conference Proceedings

If they wish, the participants can ask to be provided with outcomes of the project. They will then be sent a lay summary of the results at the end of the project.

2.5 What do you consider are the ethical issues associated with conducting this research and how do you propose to address them?

Ethical Issues include:

1: Risk to the volunteer donating blood via lancet prick

- Discomfort: The sensation of pricking the finger will be like a light scratch and should cause minimal discomfort to the volunteer.
- Infection: As the lancet needle will be sterile, there will be no risk of infection.

2: Risk to the volunteer donating blood via arterial blood sample

- Discomfort: The blood sample will be withdrawn by a trained professional; therefore, discomfort or bruising will be minimal.
- Discomfort: Even after signing the consent form, the volunteer has the right to withdraw from having the blood sample taken if they feel uncomfortable/nervous.
- Arteriospasm or involuntary contraction of the artery: The volunteers will be positioned comfortably and explained the procedure beforehand which will help them relax during the procedure.
- Haematoma or excessive bleeding: The blood sample will be withdrawn by a trained professional; therefore, the risk of insertion of the needle in the wrong way can be avoided and pressure will be applied immediately for a longer time and monitored closely until the bleeding has ceased.
- Nerve damage: An appropriate sampling site will be chosen by performing an Allen test** (explained further at the end of the section) and the blood sample will be withdrawn by a trained professional; therefore, the risk to this is minimal.
- Fainting or a vasovagal response: The risk of this will be minimised by ensuring that the volunteer is supine (lying down on their back) with feet elevated before beginning the blood draw.
- Infection: Prior to the sampling, the identified site on the volunteer will be disinfected with 70% alcohol dried. Sterile needles and pre-heparinized syringes shall be used, and the volunteer will not be in contact with any other bloods, so there will be no risk of infection. Also, an appropriate bandage to cover the puncture site after collection will be provided to every volunteer.

3: Risk to the researchers preparing and analysing bloods

Infection: All researchers undertaken investigations on blood samples will:

- Have been immunised according to the schedule recommended by the Green Book: Immunisation against infectious diseases for laboratory workers/ clinical workers
- Wear protective clothing, disposable gloves, safety goggles and facemask.
- Will maintain the area in a safe and sterile manner.
- Will not allow any other person into the bloods area while bloods or unsterile containers etc. are exposed.
- Volunteers will be screened for blood-borne virus (BBV, HIV and Hep C which cannot

be immunized against) by asking appropriate questions in the Health Questionnaire which will be provided to each volunteer prior to the study.

4: Risk to other staff or persons within the University

- Infection: Blood samples, if not been analysed to prepared, will be stored in a padlocked fridge. Samples will be disposed of on the same day after they were obtained. Bloods and needles will be disposed of correctly in dedicated bins and collected for disposal by a qualified company.
- Injury: Syringes and other sharp items will be locked away so they cannot be accessed by unauthorised persons.

However, ALL measurements and procedures will be stopped immediately if subjects expressed any discomfort and asks for it to be stopped.
A first aider is available to the research centre.

**Allen Test:

Source:
http://fitsweb.uchc.edu/student/selectives/TimurGraham/Modified_Allen%27s_Test.html

Procedure for the qualified and registered clinician/nurse/phlebotomist. performing the sampling:

1. Instruct the patient to clench his or her fist; if the patient is unable to do this, close the person's hand tightly.
2. Using your fingers, apply occlusive pressure to both the ulnar and radial arteries, to obstruct blood flow to the hand.
3. While applying occlusive pressure to both arteries, have the patient relax his or her hand, and check whether the palm and fingers have blanched. If this is not the case, you have not completely occluded the arteries with your fingers.

2.6 How is the research intended to benefit the participants, third parties and/or the local community? Please consider both direct and long term benefits.

The Committee recognises this does not apply to all research projects.

It is unlikely that the research will benefit the volunteers directly. However, the knowledge gained during the studies will provide important insights and parameters to allow for the technology developed by RCBE to be optimised for sensitive, specific measurements of blood components non-invasively through the skin. In the long term, the results of this study will feed into the development of new sensors to assist clinicians in monitoring and assisting a range of pathologies and conditions.

2.7 Will invasive procedures (for example medical or surgical) be used?

YES ☒ **NO** ☐

2.7 a If yes, what precautions will you take to minimise any potential harm?

The withdrawal of blood samples will be an invasive procedure. Any potential harm will be reduced by:

- Using sterile lancet and syringe needles.
- Having a trained clinical collaborator take the blood sample

2.8 Will intrusive procedures (for example psychological or social) be used?

YES ☐ **NO** ☒

2.8 a If yes, what precautions will you take to minimise any potential harm?

NA

2.9 In the course of the investigation might pain, discomfort (including psychological discomfort), inconvenience or danger be caused? YES ☒ NO ☐

2.9a If yes, what precautions will you take to minimise any potential harm?

The withdrawal of blood may cause discomfort to the volunteer. To minimise any potential harm, the obtainment of a blood sample will be carried out by a qualified and registered clinician/nurse/phlebotomist.

The volunteers will be free to withdraw consent for the study at any time if they so wish.

3. Information about Participants

3.1 How many participants will be involved?

20-30 per investigation.

3.1a What is the age group and gender of the participants?

18-65, male and female.

3.1b Explain how the sample size has been determined. If statistical sampling is relevant to this application, please include details of how the sample size was calculated.

No formal power study has been performed to calculate the sample size. However, the sample size has been roughly estimated from the knowledge of previous studies in order to validate the results.

3.1 c Please specify inclusion and exclusion criteria. If exclusion of participants is made on the basis of age, gender, ethnicity, race, disability, sexuality, religion or any other factor, please justify this.

Inclusion Criteria

In order to be eligible for inclusion in the study the participants must meet the following criteria:

- Adult volunteers aged between 18–65 years who can give informed consent.
- Adult volunteers who are not taking any type of medication.
- Adult volunteers who do not suffer from any existing medical condition, including any heart condition, vascular or arterial disease, arthritis, lung disease, diabetes, Epilepsy, anaemia or thyroid disease.
- Adult volunteers who have not used recreational drugs during the last month.
- Adult volunteers who do not excessively consume alcohol (more than 14 units per week), and preferably do not smoke.
- Adult volunteers who have not used stimulating supplements, either natural or synthetic, at least 48 hrs prior to taking part in the study.
- Potential participants will only be enrolled if they have a good understanding of spoken English.

Exclusion Criteria

A set of criteria that determine whether the patient is ineligible to participate in the study. These include:

Any inclusion criteria not met.

- Persons who decline consent.
- Persons who cannot give consent.
- Persons with acute illness/cold on the day of the study.
- Participation in drug trials/studies in the last 6 months.
- Participant declaring a Blood Borne Virus in their Participant Information Sheet.

3.2 How are the participants to be identified, approached and recruited, and by whom?

Advertisement in the form of a poster which will be affixed around the University premises. Emails with the study advertisement may also be sent to official City group lists e.g. All Staff

list, but only after permission is granted from the Dean of each school. This email will be sent out by Professor Panicos Kyriacou, (p.kyriacou@city.ac.uk), the principal investigator in the project.

Evidence to the Ethics Committee will be provided that the Deans have agreed that staff and students can be recruited when submitting amendments for each investigation.

3.3 Describe the procedure that will be used when seeking and obtaining consent, including when consent will be obtained. Include details of (a) who will obtain the consent, (b) how you are intending to arrange for a copy of the signed consent form to be given to the participants, (c) when they will receive the participant information sheet, and (d) how long the participants have between receiving information about the study and giving consent. Please note that if you are relying on consent as the lawful basis for processing special category (sensitive) personal data, consent has to be freely given, specific, informed and unambiguous indication of the individual's wishes.

Volunteers will be identified following an expression of interest on seeing a poster/email regarding the study. A participant information sheet will be provided, explaining exactly the aims and objectives of the study, and, if they agree to take part, exactly what the experimental procedure will involve. All potential participants will be given at least 24 hours to think whether to take part or to consult relatives, etc.

Volunteers will be clearly informed that participation in the study is voluntary and that refusal to participate will not affect their role, study etc. within the University. Participants will be provided with a full explanation of the nature, purpose and requirements of the study including Participant Information Sheet and Informed Consent Form.

No participants will be recruited if they lack capacity and if it is deemed that capacity is lost during the trial period then the participant will be removed from the trial and all information relating to them will be destroyed. If the volunteer agrees to take part and signs a consent form, they will be recruited to the study.

3.4 How will the participant's physical and mental suitability for participation be assessed? Are there any issues related to the ability of participants to give informed consent themselves or are you relying on gatekeepers on their behalf?

Participants will complete a medical questionnaire prior to commencement of the study. The questionnaire will cover basic questions about the general health of the participant and ensure that they do not suffer from any of the conditions outlined in the study criteria. Volunteers who are deemed physically unsuitable (see exclusion criteria in section 3.1), will not proceed with the study. Participants will need to be able to read the information sheet by themselves. They must show the ability to give informed consent by themselves without any gatekeeper on their behalf.

3.5 Are there any special pressures that may make it difficult for participants to refuse to take part in the study? Are any of the potential participants in a dependent relationship with any of the investigators (for instance student, colleague or employee) particularly those involved in recruiting for or conducting the project?

Students or colleagues will have complete freedom to withdrawn from the study at any time with absolutely no direct or indirect pressure put upon them.

3.6 Will the participant's doctor be notified? **YES** ☐ **NO** ☒
(If so, provide a sample letter to the subject's GP.)

3.7 What procedures are in place for the appropriate referral of a study participant who discloses an emotional, psychological, health, education or other issue during the course of the research or is identified by the researcher to have such a need?

NA

3.8 Is there any risk (emotional, psychological, health or other issues) to the researcher(s)?

Potential BBV transmission when handling blood without appropriate controls or needle stick injury.

3.9 What steps will be taken to safeguard the participants from over-research (i.e. to ensure that the participants are not being used in multiple research projects including those of other researchers)? Please consider all research projects whatever their field, not just those performed by you.

Participants will be asked whether they are taking part in any other research (or whether they have recently taken part in any other research) and may be excluded if over-research is considered detrimental to the participant of or to the study.

3.10 Where will the research take place?

The study will take place in the Physiological Measurement room of the Biomedical Engineering Laboratory at City, University of London.

3.11 What health and safety issues, if any, are there to consider?

1. Risk to the volunteer donating blood via venous/ arterial blood sample
   - Discomfort: The blood sample will be withdrawn by a trained qualified professional; therefore, discomfort or bruising will be minimal.
   - Discomfort: Even after signing the consent form, the volunteer has the right to withdraw from having the blood sample taken if they feel uncomfortable/nervous.
   - Arteriospasm or involuntary contraction of the artery: The volunteers will be positioned comfortably and explained the procedure beforehand which will help them relax during the procedure.
   - Haematoma or excessive bleeding: The blood sample will be withdrawn by a trained professional; therefore, the risk of insertion of the needle in the wrong way can be avoided and pressure will be applied immediately for a longer time and monitored closely until the bleeding has ceased.
   - Nerve damage: An appropriate sampling site will be chosen by performing an Allen test and the blood sample will be withdrawn by a trained professional; therefore, the risk to this is minimal.
   - Fainting or a vasovagal response: The risk of this will be minimised by ensuring that the patient is supine (lying down on their back) with feet elevated before beginning the blood draw.
   - Infection: Prior to the sampling, the identified site on the patient will be disinfected with 70% alcohol dried. Sterile needles and pre-heparinized syringes shall be used, and the volunteer will not be in contact with any other bloods, so there will be no risk of infection. Also, an appropriate bandage to cover the puncture site after collection will be provided to every volunteer.

2. Risk to the researchers preparing and analysing bloods

Infection: All researchers undertaken investigations on blood samples will:
   - Have been immunized according to the schedule recommended by the Green Book: Immunization against infectious diseases for laboratory workers/ clinical workers
   - Wear protective clothing i.e. lab coat, disposable gloves and eye protection. Will maintain the area in a safe and sterile manner.
   - Will not allow any other person into the bloods area while bloods or unsterile containers etc. are exposed.
   - Volunteers will be screened for blood-borne virus (BBV, HIV and Hep C which cannot be immunized against) by asking appropriate questions in the Health Questionnaire which will be provided to each volunteer prior to the study.

3. Risk to other staff or persons within the University
   - Infection: Blood samples will be analyzed as soon as they are collected and will not be stored for future analysis. Sharps and other contaminated waste will be disposed of correctly in dedicated bins and collected for incineration by a licensed

waste carrier.
- Injury: Syringes and other sharp items will be locked away, so they cannot be accessed by unauthorized persons.

3.12 How have you addressed the health and safety concerns of the participants, researchers and any other people impacted by this study? (This includes research involving going into participants' homes.)

Health and safety issues are described in section 3.11. For this research there will be no need to visit the participants at their home.

3.13 It is a requirement that at least an initial assessment of risk be undertaken for all research and if necessary a more detailed risk assessment be carried out. Has a risk assessment been undertaken?* **YES ☒ NO ☐**

Please contact the Health & Safety Office (safetyoffice@city.ac.uk) for advice on risk assessments and/or how to complete it.

3.14 Are you offering any incentives or rewards for participating? **YES ☐ NO ☒**
If yes please give details

3.15 Does the research involve any of the following:

Children under the age of 5 years	**YES ☐ NO ☒**
Clinical trials / intervention testing?	**YES ☐ NO ☒**
Over 500 participants?	**YES ☐ NO ☒**
Are you specifically recruiting pregnant women	**YES ☐ NO ☒**
Excluding information collected via questionnaires (either paper based or online), is any part of the research taking place outside of the UK?	**YES ☐ NO ☒**

If you have answered 'yes' to any of the above questions you will need to check that the City's insurance will cover your research. You should do this by submitting this application to insurance@city.ac.uk before applying for ethics approval.

*Note that it is the Committee's prerogative to ask to view risk assessments.

4. Vulnerable Groups

4.1 Will persons from any of the following groups be participating in the study? (If not go to section 5.)

Adults without capacity to consent	☐
Children under the age of 18	☐
Those with learning disabilities	☐
Prisoners	☐
Adults at risk	☐
Young offenders (16-21 years)	☐
Those who would be considered to have a particular dependent relationship with the investigator (e.g. those in care homes, students, employees, colleagues)	☒

4.2 Will you be recruiting or have direct contact with any children under the age of 18? **YES ☐ NO ☒**

4.2a If yes, please give details of the child protection procedures you propose to adopt should there be any evidence of or suspicion of harm (physical, emotional or sexual) to a young person. Include a referral protocol identifying what to do and who should be contacted.

NA

4.2b Please indicate how you will comply with the data protection legislation for processing children's personal information?

NA

4.2 c Please give details of how you propose to ensure the well-being of the young person, particularly with respect to ensuring that they do not feel pressured to take part in the research and that they are free to withdraw from the study without any prejudice to themselves at any time.

NA

4.3 Will you be recruiting or have direct contact with adults at risk? YES ☐ NO ☒

4.3a If yes, please give details of the protection procedures you propose to adopt should there be any evidence of or suspicion of harm (physical, emotional or sexual) to a adults at risk. Include a referral protocol, identifying what to do and who should be contacted.

NA

4.3b Please give details of how you propose to ensure the well-being of adults at risk, particularly with respect to ensuring that they do not feel pressured to take part in the research and that they are free to withdraw from the study without any prejudice to themselves at anytime. You should indicate how you intend to ascertain that person's views and wishes.

NA

4.3c Please give details of any City staff or students who will have contact with adults at risk and/or will have contact with young people (under the age of 18) and details of current (within the last 3 years) City Disclosure and Barring check.

Name	*Dept & School*	*Student/Staff Number*	*Date of DBS*	*Type of disclosure*

4.3 d Please give details of any non-City staff or students who will have contact with adults at risk and/or will have contact with young people (under the age of 18) and details of current (within the last 3 years) Disclosure and Barring check.

Name	*Institution*	*Address of organisation that requested the disclosure*	*Date of DBS*	*Type of disclosure*

4.4 Will you be recruiting any participants who fall under the Mental Capacity Act 2005?
YES ☐ NO ☒

If so you MUST get approval from an HRA approved committee (see separate guidelines for more information).

5. Data Collection

5.1 Please indicate which of the following you will be using to collect your data
Please tick all that apply

Questionnaire	☒
Interviews	☐
Participant observation	☐
Focus groups	☐
Audio/digital-recording interviewees or events	☐
Video recording	☐
Physiological measurements	☒
Digital/computer data	☐
Other	☐
Please give details if you have ticked other	

5.1b What steps, if any, will be taken to safeguard the confidentiality of the participants (including companies)?

Data will be saved and categorized as “subject 1” to “subject n”. The questionnaires and consent forms will be placed in a file and locked in the Biomedical Engineering Laboratory.

If you are using interviews or focus groups, please attach a topic guide. If you are using questionnaire, please attach the questionnaire.

6. Confidentiality and Data Handling

6.1 Will the research involve:

• **complete anonymity of participants** (i.e. researchers will not meet, or know the identity of participants, as participants are a part of a random sample and are required to return responses with no form of personal identification)**?**	☐
• **anonymised sample or data** (i.e. an *irreversible* process whereby identifiers are removed from data and replaced by a code, with no record retained of how the code relates to the identifiers. It is then impossible to identify the individual to whom the sample of information relates)**?**	☐
de-identified samples or data (i.e. a *reversible* process whereby identifiers are replaced by a code, to which the researcher retains the key, in a secure location)? Please note that de-identified data may be treated as personal data under GDPR depending on how difficult it is to attribute a pseudonym to a particular individual.	☒
• **subjects being referred to by pseudonym in any publication arising from the research?**	☐
• **any other method of protecting the privacy of participants?** (e.g. use of direct quotes with specific permission only; use of real name with specific, written permission only)	☐
Please give details of ‘any other method of protecting the privacy of participants’ is used	

6.1a Which of the following methods of assuring confidentiality of data will be implemented?
Please tick all the options that apply

• data to be kept in a locked filing cabinet	☒

• data and identifiers to be kept in separate, locked filing cabinets	☐
• access to computer files to be available by password only	☒
• storage at City	☐
• stored on an encrypted device (e.g. laptop, hard drive, USB)	☐
• stored at other site	☐
If stored at another site, please give details.	

6.1 b Will the data be accessed by people other than the named researcher?
YES ☐ **NO** ☒

If yes, please explain by whom and for what purpose.

6.2 Is the data intended for reuse or to be shared as part of longitudinal research, or a different/wider research project now, or in the future? **YES** ☐ **NO** ☒

If yes, please provide details.

NA

6.2a If the project is funded, does the funding body (e.g. ESRC) require that the data be stored and made available for reuse/sharing? **YES** ☐ **NO** ☒

6.2 b If you have responded yes to any of the questions above, explain how you are intending to obtain explicit consent for the reuse and/or sharing of the data.

NA

6.3 Retention and Destruction of Data

6.3 a Does the funding body or your professional organisation/affiliation place obligations or recommendations on the retention and destruction of research data?
YES ☒ **NO**

If yes, what are your affiliations/funding and what are the requirements? (If no, please specify City guidelines on retention.)

City Guidelines on Retention

6.3b How long are you intending to keep the data?

Note that the institutional guidelines on retention state a minimum of 10 years but some funding bodies require a longer retention period.

10 years

6.3c Are you intending to destroy the data after this period?
Please find guidance here.

Paper records will be formally shredded and all electronically archived data will be erased.

7. Curriculum Vitae

CV OF APPLICANTS (**Please duplicate this page for each applicant, including external persons and students involved.)**

NAME:	Professor Panicos Kyriacou
Title of Post:	Professor of Biomedical Engineering
Department:	SMCSE
Is your post funded for the duration of this proposal?	Yes
Funding source (if not City)	NA
Please give a summary of your training/experience that is relevant to this research project	
Prof Kyriacou received a BESc degree in Electrical Engineering from the Engineering Department of the University of Western Ontario, Canada in 1994 and an MSc degree in Medical Electronics and Physics from St. Bartholomew's Medical College, University of London in 1995. During 1995 -1996 Prof Kyriacou worked as a Senior Biomedical Engineer and application specialist in the medical devices industry. He received his PhD from St. Bartholomew's Medical College, University of London in 2001 where he engaged in research in the field of medical instrumentation and electro-optical sensors for monitoring critically ill patients. He is currently a Professor of Biomedical Engineering and Associate Dean for Postgraduate studies at the School of Engineering and Mathematical Sciences at City University London. He is also the Director of the undergraduate programme in Biomedical Engineering and Director of the Biomedical Engineering Research Group. Prof Kyriacou is an Honorary Professor in the Department of Anaesthesia at St. Andrews Centre for Plastic Surgery and Burns, Broomfield Hospital, Mid Essex Hospital Services NHS Trust. He is also an Honorary Senior Research Fellow at Great Ormond Street Hospital for Children and St. Bartholomew's Hospital and a Visiting Research Fellow at Yale Medical School, Yale University. Professor Kyriacou' s main research activities are primarily focused upon the understanding, development and applications of instrumentation, sensors and physiological measurement to facilitate the prognosis, diagnosis and treatment of disease or the rehabilitation of patients. His research pushes the frontiers of current optical and electronic technologies and demonstrates how such technologies can be used as medical "tools". His research is nationally and internationally recognised and this is evident by the number of organisations he is collaborating with and also from the wide spread of high impact factor scientific and clinical journals that he has published. He has authored and co-authored over 100 publications in peer reviewed journals, invited chapters in books and conference proceedings. He is also the holder of five patents with inventions in the area of Biomedical Instrumentation and Optical Biomedical Sensors. He is currently the Principle Investigator (PI) of more than nine research projects and has attracted funding from a variety of sources such as research councils, charities, NHS, and industry. Prof Kyriacou is the Chairman of the Instrument Science and Technology Group at the Institute of Physics and the Chair of the Engineering Advisory Group at the Institute of Physics and Engineering in Medicine. He is also a member of the Healthcare Science Advisory Group at NHS London.	

NAME:	Dr Meha Qassem
Title of Post:	Postdoctoral Research Associate
Department:	SMCSE
Is your post funded for the duration of this proposal?	Yes
Funding source (if not City University London)	EPSRC
Please give a summary of your training/experience that is relevant to this research project	
Dr Meha Qassem graduated with a BEng degree in Biomedical Engineering from City University in 2008, then went on to complete her PhD 2010 at City University, after working as a medical engineer for two years. During her PhD, she worked extensively in the areas of optical spectroscopy, spectral analysis and optical sensing. She had successfully completed multiple studies on animal and human skin, looking at the properties of skin and the effect of certain applicants on skin parameters using NIR spectroscopy. Her work has been published in several conferences and internationally recognised peer-reviewed journals. She is currently working as a postdoctoral researcher in the Research Centre for Biomedical Engineering	

(RCBE) at City, University of London.

NAME:	Dr Mohammad Hossein Mamouei
Title of Post:	Postdoctoral Research Associate
Department:	SMCSE
Is your post funded for the duration of this proposal?	Yes
Funding source (if not City University London)	EPSRC
Please give a summary of your training/experience that is relevant to this research project	
Dr Mohammad Mamouei graduated with a BSc in Electrical Engineering from Iran University of Science and Technology. He then went on to complete an MSc in Telecommunications and Networks from City, University of London. In 2013, he was awarded a full scholarship to start his PhD studies on applied Mathematics-Systems and Modelling at City, University of London. During his PhD, the focus of his work was on the applications of advanced mathematics, data analysis, and machine learning techniques on the control of semi- and fully automated vehicles. Dr Mamouei has recently joined the Research Centre for Biomedical Engineering at City, University of London as a postdoctoral researcher in data science. His current work as a postdoctoral researcher at RCBE involves processing biological signals and performing advanced analysis on optical spectra. He works closely with a group of three to ensure that the quality of signals and the data acquisition process is in line with relevant statistical requirements and modelling-related aspects of the project.	

NAME:	Ms Nystha Baishya
Title of Post:	PhD Student
Department:	SMCSE
Is your post funded for the duration of this proposal?	Yes
Funding source (if not City University London)	
Please give a summary of your training/experience that is relevant to this research project	
Nystha obtained her Bachelor of Engineering in Mechatronics at Manipal Institute of Technology, India in 2012. She then went to Italy to continue her studies at Politecnico di Milano where she received her Master of Science in Materials Engineering & Nanotechnology. She then went back to India and worked in Indian Institute of Technology Guwahati for a year in the field of Organic Electronics in bio-sensing applications. Since October 2017, she has been enrolled for a full time PhD at the Research Centre for Biomedical Engineering at City, University of London. Her research focuses on Spectroscopic studies for monitoring parameters in haemodynamic shock.	

NAME:	Mr Chadi El-Hajj
Title of Post:	PhD Student
Department:	SMCSE
Is your post funded for the duration of this proposal?	Yes
Funding source (if not City University London)	
Please give a summary of your training/experience that is relevant to this research project	
Chadi El Hajj graduated with a degree in Computer Science from the American University of Beirut in 2013. He worked as a software developer for a few years in different sectors as such web development, online publishing systems and banking. Recently, he completed his MSc. in Data Science at City, University of London. During his studies he worked on various projects involving Artificial Intelligence and machine learning techniques for a variety of tasks. His MSc. research project was focused on neural networks, where he worked on extending a neural network model to improve its accuracy/precision and provide solutions for new domains. He is starting his PhD in Feb 2018 in the Research Centre for Biomedical Engineering at City, University of London. In his PhD he will be working on developing a novel non-invasive sensor by applying neural networks for continuous monitoring for patients in haemodynamic shocks.	

NAME:	Dr K Budidha
Title of Post:	Postdoctoral Research Associate
Department:	SMCSE
Is your post funded for the duration of this proposal?	Yes
Funding source (if not City University London)	EPSRC
Please give a summary of your training/experience that is relevant to this research project	

Dr Karthik Budidha first came to City, University of London in 2006 to pursue his undergraduate degree (BEng) in Biomedical Engineering. Following his undergraduate degree, he acquired an MSc in biomedical engineering from Imperial College London in 2010. He then worked as a Biomedical Engineer in Hillingdon hospital for a year before returning to the Research Centre for Biomedical Engineering (RCBE), at City, University of London in 2011 to pursue his PhD. During his PhD he developed a novel In-ear oximeter to monitor arterial oxygen saturation and heart rate in patients with compromised peripheral perfusion.

Dr Budidha's primary interests lie in the design of novel wearable non-invasive sensors, and development of bio-electronic instrumentation to continuously monitor physiological and behavioural variables. Being named the primary researcher in the Wellcome Trust's Pathfinder Award, he is currently working towards the development of a novel intra-luminal sensor for monitoring intestinal viability in colorectal cancer surgery.

8.1 Supervisor's statement on the student's skills and ability to carry out the proposed research, as well as the merits of the research topic (up to 500 words)

NA

I confirm that I have discussed the project with the student to my satisfaction.	
Supervisor's Signature	
Print Name	Prof Panayiotis Kyriacou

8. Additional documents

You are expected to provide copies of relevant documents including all letters to be sent to participants and other individuals (such as GPs) and organisations involved in the research. Please follow the guidelines and templates which can be found at http://www.city.ac.uk/research/research-and-enterprise/research-ethics

Document Checklist

Please place an 'X' in all appropriate spaces for all documents you are submitting

	Attached	**Not applicable**
Copy of study advertisement (including recruitment emails/letters)	X	
Participant information sheet	X	
Participant consent form	X	
Questionnaire(s)	X	
Topic guide(s)		
Confirmation letter(s) from / correspondence with external organisations		
Confirmation that insurance is in place		
Product information		

GP Letter		
Data sharing agreement (with partner organisations)		
Contract with data processor (e.g. transcribing service)		
Other (Draft email to the Deans of the Schools for recruitment)	X	

9. Additional Information

10. Declarations by Investigator(s)

- I certify that to the best of my knowledge the information given above, together with any accompanying information, is complete and correct.
- I have read City's guidelines on human research ethics and accept the responsibility for the conduct of the procedures set out in the attached application.
- I have attempted to identify all risks related to the research that may arise in conducting the project.
- I have read and will comply with City's Data Protection and Information Security policies.
- I understand that **no** research work involving human participants or data can commence until **full** ethical approval has been given

	Print Name	Signature
Principal Investigator(s) (student and supervisor if student project)	Prof Panayiotis Kyriacou	
Date	30-Aug-2018	

B

Appendices

Multi-parametric optical sensing for monitoring haemodynamic shock

City Research Ethics Committees
Application for Approval of Research Involving Human Participants

Please tick the box for which Committee you are submitting your application to

☒	Senate Research Ethics Committee
☐	Cass Business School
☐	Department of Computer Science
☐	Department of Sociology
☐	School of Health Sciences Research Ethics Committee
☐	Department for Learning Enhancement and Development

For **Senate** applications: a single copy of the application form and all supporting documents should be emailed to Anna.Ramberg.1@city.ac.uk

For **Computer Science** applications: a single copy of the application form and all supporting documents should be emailed to S.M.Wilson@city.ac.uk

For the Department of Sociology, submit all forms in Word format in a single document electronically. For projects falling under Sociology, Media Studies, Criminology, Food Policy and Q-Step, please send to Simon.Susen@city.ac.uk; and for projects falling under CCI, to Diana.Yeh@city.ac.uk

For **School of Health Sciences** applications: submit all forms (including the Research Registration form) electronically (in Word format in a single document) to A.Welton@city.ac.uk

For **Department for Learning Enhancement and Development:** a single copy of the application form and all the supporting documentation should be emailed to P.M.Parker@city.ac.uk

Refer to the separate guidelines while completing this form.

PLEASE NOTE THE FOLLOWING:

- Ethical approval **MUST** be obtained before any research involving human participants is undertaken. Failure to do so may result in disciplinary procedures being instigated, and you will not be covered by City's indemnity if you do not have approval in place. It may also result in the degree not being awarded or the data not being published in a peer review journal.
- The Signature Sections **MUST** be completed by the Principal Investigator (the supervisor and the student if it is a student project).

Project Title:
Applications of direct spectrophotometric techniques in the visible and near infrared region to monitor shock by determining blood lactate and haemodynamic parameters in *in vitro* and *in vivo* studies on human volunteers.
Short Project Title (no more than 80 characters):
Multi-parametric optical sensing for monitoring haemodynamic shock
Name of Principal Investigator(s) (if this is a student project, please note that the Principal Investigator is the supervisor and all correspondence will be with the supervisor):
Prof Panayiotis Kyriacou; Dr Meha Qassem, Dr. Karthik Budidha
Post Held (including staff/student number):

Professor of Biomedical Engineering; Postdoctoral research associate (Reg No: 888034786); Postdoctoral research associate (Reg No: 888078256)
Department(s)/School(s) involved at City:
Research Centre for Biomedical Engineering, MCSE
If this is part of a degree please specify type of degree:
Date of Submission of Application:
20th Sep 2017

Tick this box if you do not grant City permission to use your application form for training purposes ☐

1. Applicant Details

This project involves:
(*tick as many as apply*)

☒	Staff Research	☒	Doctoral Student
☐	Undergraduate	☐	M-level Project
☐	Externally funded	☐	External investigators
☐	Other		
Provide details of external investigators and/or other			

Contact details for the Principal Investigator (including email address and telephone number)

City, University of London, Northampton square, London EC1V 0HB
p.kyriacou@city.ac.uk
0207 040 8131

Other staff members involved

Title, Name & Staff Number	*Post*	*Dept & School*	*Phone*	*Email*
Dr Meha Qassem (Reg no. 888034786)	Postdoctoral research associate	RCBE, MCSE	02070403878	Meha.qassem.1@city.ac.uk
Dr Mohammad Mamouei (Reg.: 110038889)	Postdoctoral research associate	RCBE, MCSE	02070403878	Mohammad.Mamouei.1@city.ac.uk
Dr. Karthik Budidha (Reg: 888078256)	Postdoctoral research associate	EEE/MCSE	02070403878	karthik.budidha.1@city.ac.uk

All students involved in carrying out the investigation

Name & Student Number	*Course / Year*	*Dept & School*	*Email*
Miss Nystha Baishya (Reg: 170049512)	Phd (year 1)	RCBE, MCSE	Nystha.Baishya@city.ac.uk
Mr Chadi.El-Hajj (Reg: 160047936)	Phd (year 1)	RCBE, MCSE	Chadi.El-Hajj@city.ac.uk

External co-investigators

Title & Name	*Post*	*Institution*	*Phone*	*Email*
Dr Gerrard Rafferty	Reader in Human & Translational Physiology	King's College London	02032992082	Gerrard.rafferty@kcl.ac.uk

Please describe the role(s) of all the investigators, including all student(s)/external co-investigator(s) in the project, especially with regards to interaction with study participants.

Professor Kyriacou is the supervisor of the project. Meha, Karthik, Mohammad, Chadi and Nystha are the researchers who will conduct the studies under Prof Kyriacou's supervision, and analyse the collected data. Dr. Rafferty will act as an advisor and will be directly involved in the experimental and medical device set up, data collection and also data analysis.

If external investigators are involved, please provide details of their indemnity cover.

Application Details

1.1 Is this application or any part of this research project being submitted to another ethics committee, or has it previously been submitted to an ethics committee? *This includes an NHS local Research Ethics Committee or a City local Research Ethics Committee or any other institutional committee or collaborating partners or research site.* (See the guidelines for more information on research involving NHS patients.)

YES ☐ NO ☒

If yes, please give details and justification for going to separate committees, details of the Secretary of the relevant authority/committee, and, if appropriate, attach correspondence and details of the outcome of the application, including any conditions of approval or reasons for rejection.

n/a

1.2 If any part of the investigation is being carried out under the auspices of an outside organisation, involves collaboration between institutions or individual external researchers, or institutions/organisations where interviews/fieldwork will take place please give details and address of organisation(s).

n/a

1.3 Has permission to conduct research in, at or through another institution or organisation been obtained? **YES ☐ NO ☒**

If yes, please provide details and attach the supporting correspondence.

n/a

1.4 Duration of Project

Start date: 8th Jan 2018 Estimated end date: 7th Jan 2021

Funding Details

1.5 Is the project reliant on funding? If no, please go to the next section. **YES** ☒ **NO** ☐

If yes, please provide details of the source of financial support (e.g. funding body, charity etc.) for the proposed investigation.

EPSRC (Research council)

1.5a Has funding been applied for? **YES** ☒ **NO** ☐

1.5b Has funding been approved? **YES** ☒ **NO** ☐

If no, please provide details of when the outcome can be expected

International Research

1.6 Is any part of the research taking place outside of England/Wales? (if not go to section 2) **YES** ☐ **NO** ☒

If yes, please provide details of where.

n/a

1.7 Have you identified and complied with all local requirements concerning ethical approval & research governance*? **YES** ☒ **NO** ☐

1.7a Please provide details of the local requirements, including contact information.

n/a

1.7b Please give contact details of a local person identified to field initial complaints locally so the participants can complain without having to write to or telephone the UK.

n/a

*Please note that many countries require local ethical approval or registration of research projects, further some require specific research visas. If you do not abide by the local rules of the host country, you will invalidate your ethical approval from City, and may run the risk of legal action within the host country.

2. Project Details

2.1 Provide the background (including the current state of the art in this field), aim(s) and objectives of the proposed research,

The primary function of blood circulation is to provide oxygen and substrates to the tissues. Failure to do this results in a clinical condition known as shock. Up to one-third of patients admitted to intensive care units (ICUs) are in circulatory shock, and early recognition of the condition is vital to avoiding subsequent tissue injuries.

The level of lactate in blood is an important indicator when assessing response to therapy and guiding treatment in patients with life-threatening shock. For this reason, lactate measurements are routinely carried out in critically ill patients. Patients with elevated

lactate concentration have a higher mortality rate and are at greater risk of developing multiple organ failure.

At present, lactate measurements are performed using invasive techniques where blood sample are needed to perform each measurement. These invasive procedures are time consuming and inhibit continuous monitoring of lactate. There is demand for a rapid use non-invasive medical device that allows continuous measurements of blood lactate levels in real time. Such a device is currently unavailable.

In addition, many experimental studies have confirmed the relationship between inadequate tissue oxygenation and blood lactate. Increased blood lactate levels have also been linked to metabolic processes not related to tissue oxygenation. This complexity makes it difficult to interpret lactate readings directly. A better understanding of the link between tissue oxygenation and blood lactate levels is necessary to improve the use of important lactate data and enable better interpretation and diagnosis.

The aim of this project is to address this demand by developing a novel non-invasive sensor that can continuously monitor blood lactate levels in real time. The device will be based on light sensing technology, consisting of a light source and a processing system that contains smart data analysis software to process light reflected from the skin. In principal, this is possible because the lactate chemical is sensitive to near infrared light, and together with the appropriate analysis, this property can be used to measure lactate levels from light reflected from the body.

It is also the aim of this project to conduct rigorous research and acquire new understanding of the relationship between tissue oxygenation and blood lactate levels through exercise studies of varying intensities. Exercise alters levels of blood lactate and perfusion levels, and hence this property can be used to investigate the relationship between these parameters and to calibrate the technology which will be developed during the project.

2.2 Please explain how this project will further existing knowledge.

The engineering aspect of the project aims to develop novel optical technology that can detect multiple parameters noninvasively and in real-time. This will contribute to solving the problem of multi-parametric measurement of dynamic processes, which is one of the central problems in biomedical sensor research. The project will also develop new computational models that capture haemodynamic variations. The development of these models from a physically informed basis with empirical coefficients will be of great interest to the scientific community.

In addition, the project will improve understanding of haemodynamic response to hyperlactatemia and its relationship with tissue oxygenation. The project combines numerical/computational with experimental measurements, which will give information of greater depth and quality than anything currently available.

2.3 Provide a summary and brief explanation of the design, methodology and plan for analysis that you propose to use.

Once a participant has expressed an interest in enrolling into the study, they will be asked to fast 2hrs before coming to the Biomedical Engineering laboratory. An investigator will then discuss the protocol with the participant and perform trial runs, to ensure that the participant is confident with the experimental protocol and how to dismount safely from the treadmill/bicycle ergometer.

Once signed consent is obtained, the participant will be asked to complete a general health questionnaire, then a trained phlebotomist/nurse will insert a cannula into their arm. This is to allow multiple blood samples to be acquired without multiple punctures. A baseline blood sample will be taken, and additional non-invasive sensors will be placed on the arm, shoulders, hips, finger, and mouth and ear.

Following baseline measurements, the subject will undertake an incremental exercise test on a cycle ergometer, standard exercise bike, Wattbike. After an initial rest period with the subject seated on the cycle ergometer, the incremental cycle exercise protocol will commence with 3 min unloaded cycling a constant speed of 60 rpm followed subsequently by 25 watt increases in workload every 3 minutes until either volitional exhaustion or reaching approximately 90% predicted maximal heart rate (derived using the equation max heart rate = 220 – age in years). Blood sample will be taken from the indwelling cannula at the end of every 3 minute increment to analyse lactate concentration for comparative purposes. At the end of exercise, blood samples will continue to be taken every 3 minutes for a further 12 mins, starting immediately at the end of exercise. Ventilatory parameters (respiratory flow and volume, 0_2 consumption and CO_2 production) will also be measured breath by breath using a Metamax cardiopulmonary exercise testing system via a facemask worn by the subject during testing.

Employing an incremental exercise protocol in this way would produce approximately 6-8 exercise increments for healthy subjects (ie 0 ~ 200 Watts) plus those obtained during recovery during which lactate levels return towards baseline. Overall, this approach provides a greater number of comparative measures of blood lactate from the non-invasive sensors and from direct blood sampling across a range of lactate concentrations.

The collected blood samples will be analysed on the same day of collection, and then disposed of through incineration by a licensed waste carrier.

The collected blood samples will be analysed for:

- blood gases, lactate and electrolytes using a blood gas analyser.
- Optical absorption in the range 380-25,000nm.

Results from this will be combined with data acquired from non-invasive sensors, and more advanced analysis techniques will then be applied.

Non-invasive sensors

The non-invasive sensors placed on participants will range from custom-made to commercial medical devices. All custom-made devices will be battery operated and approved for use on human subjects. A description of these and the data they will collect is given below:

(1) Spectrophotometer: both commercial and custom-made (CE marked) types of this device will be used. They will collect light reflectance spectra in Visible and Near Infrared regions (380-2,500 nm). The commercial spectrophotometer will be used whilst connected to a fibre optic probe to allow *in vivo* measurements on humans. The custom-made version will also incorporate an optical probe, connected to a customised system developed in the Research Centre for Biomedical Engineering (RCBE) at City. The probes from both versions of this device will be placed on the arm and are completely non-invasive. The commercial device will be used as reference.

(2) Photoplethysmographic sensors: these are custom-made, CE-marked, non-invasive optical sensors developed in RCBE. They utilise light in the visible and near infrared range to derive important parameters. The will provide data on; (1) Red and Infrared Photoplethysmographs (PPGs), Heart Rate, ECG (Electrocardiogram graphs of heart activity) and Blood Oxygen Saturation. The sensors will be connected to a processing system device, also developed by the group.

(3) Pulse oximeter: this is a commercial medical device that measures blood oxygen saturation and heart rate continuously over time. The device has a probe that will be placed on the finger.

(4) Temperature sensor: commercial and custom-made temperature sensors will be place inside the ear canal at specific points during the study in order to record the core temperature of the participant.

(5) Near Infrared Spectroscopy (NIRS): This commercial device will be used to evaluate Tissue Oxygenation Index and Haemoglobin concentrations from the arms. The device will provide a continuous graph showing Haemoglobin levels and Tissue Oxygenation Index.

(6) Laser Doppler Flowmetry: A commercial LDF sensor will assess blood flow. This sensor will be attached to the arm, and provides continuous readings of blood flow in arbitrary unit.

(7) Ultrasound Doppler: A commercial ultrasound Doppler sensor will be used for assessing blood flow. This will be placed on the arm and will record ultrasound waves of blood flowing through an artery.

(8) Metamax cardiopulmonary exercise testing system: A facemask to be worn by the subject during testing to measure the ventilatory parameters (respiratory flow and volume, 02 consumption and CO2 production).

Measurements from all sensors will be acquired simultaneously and displayed on a laptop computer. The data will be saved on the computer's hard drive and no volunteers' personal information will be stored except for age and gender.

2.4 Please explain how/if participants will be provided with the findings or outcomes of the project.

If they wish, the participants can ask to be provided with outcomes of the project. They will then be sent a lay summary of the results at the end of the project.

2.5 What do you consider are the ethical issues associated with conducting this research and how do you propose to address them?

Ethical issues include:

Performing physical exercises

- Discomfort or pain: Only healthy volunteers who can withstand the required exercise i.e. have good balance and upper body strength, will be recruited.
- Cramps or Injuries: Participants will be informed that they can stop at any time if they feel too tired.
- Injuries, trips or falls: Researchers will engage in several trial runs explaining best ways to lift one's feet off the treadmill i.e. using both hands/arms and lifting the feet from the revolving surface. Only when the participant is completely comfortable with the technique then experimentation can begin.

Donation of blood via arterial blood sample

- Discomfort: The blood sample will be withdrawn by a trained qualified professional; therefore, discomfort or bruising will be minimal.
- Discomfort: Even after signing the consent form, the volunteer has the right to withdraw from having the blood sample taken if they feel uncomfortable/nervous.
- Arteriospasm or involuntary contraction of the artery: The volunteers will be positioned comfortably and explained the procedure beforehand which will help them relax during the procedure.
- Haematoma or excessive bleeding: The blood sample will be withdrawn by a trained professional; therefore, the risk of insertion of the needle in the wrong way can be avoided and pressure will be applied immediately for a longer time and monitored closely until the bleeding has ceased.
- Nerve damage: An appropriate sampling site will be chosen by performing an Allen test** (explained at the end of this section, for the trained nurse/doctor, hired for the blood collection) and the blood sample will be withdrawn by a trained professional; therefore, the risk to this is minimal.

- Fainting or a vasovagal response: The risk of this will be minimised by ensuring that the patient is supine (lying down on their back) with feet elevated before beginning the blood draw.
- Infection: Prior to the sampling, the identified site on the patient will be disinfected with 70% alcohol dried. Sterile needles and pre-heparinized syringes shall be used, and the volunteer will not be in contact with any other bloods, so there will be no risk of infection. Also, an appropriate bandage to cover the puncture site after collection will be provided to every volunteer. Handling of biological samples by researchers

Infection. All researchers undertaken investigations on blood samples will:

- Have received vaccinations against Hep B and are up to date with their routine immunisations: tetanus, polio, diphtheria, measles, mumps and rubella.
- Wear protective clothing, disposable gloves, safety goggles and facemask.
- Will maintain the area in a safe and sterile manner.
- Will not allow any other person into the study area while bloods or unsterile containers etc are exposed. Used syringes will be disposed safely in appropriate sharps bins.
- Volunteers will be screened for blood-borne virus (BBV, HIV and Hep C which cannot be immunized against) by asking appropriate questions in the Health Questionnaire which will be provided to each volunteer prior to the study.

Exposure of hazards to other staff or persons within the University

- Infection: Blood samples will not be stored for future analysis, and all tests will be carried out on the same day of the study. Bloods and needles will be disposed of correctly in dedicated bins and collected for disposal by a qualified company.
- Injury: Syringes and other sharp items will be locked away so they cannot be accessed by unauthorised persons.

**Allen Test:
Source:
http://fitsweb.uchc.edu/student/selectives/TimurGraham/Modified_Allen%27sTest.html
Procedure for the qualified and registered clinician/nurse/phlebotomist. performing the sampling:

1. Instruct the patient to clench his or her fist; if the patient is unable to do this, close the person's hand tightly.
2. Using your fingers, apply occlusive pressure to both the ulnar and radial arteries, to obstruct blood flow to the hand.
3. While applying occlusive pressure to both arteries, have the patient relax his or her hand, and check whether the palm and fingers have blanched. If this is not the case, you have not completely occluded the arteries with your fingers.

2.6 How is the research intended to benefit the participants, third parties and/or the local community? Please consider both direct and long-term benefits.
The Committee recognises this does not apply to all research projects.

Participants are unlikely to benefit directly from the experiments, but the knowledge gained during the project will provide important insights and parameters to allow for the technology developed by the Research Centre of Biomedical Engineering (RCBE) to be optimised for sensitive, specific measurements of blood lactate and perfusion parameters simultaneously and in a non-invasive manner. In the long term, the results of this study will contribute towards the development and calibration of sensors that will enhance patient monitoring in critical care settings.

2.7 Will invasive procedures (for example medical or surgical) be used?
YES ☒ NO ☐

2.7a If yes, what precautions will you take to minimise any potential harm?

The withdrawal of blood samples will be an invasive procedure. Any potential harm will be reduced by:

- Having a trained qualified healthcare worker i.e. nurse/clinician hired from a UK registered organisation, take the blood samples.
- Using sterile syringe needles.
- Inserting a cannula to avoid multiple punctures.

2.8 Will intrusive procedures (for example psychological or social) be used?
YES ☐ NO ☒

2.8a If yes, what precautions will you take to minimise any potential harm?

n/a

2.9 In the course of the investigation might pain, discomfort (including psychological discomfort), inconvenience or danger be caused? YES ☒ NO ☐

2.9a If yes, what precautions will you take to minimise any potential harm?

Exhaustion and discomfort due to intense exercises

- Participants will be advised that they are free to stop at any point during experiments.
- Several trial runs will be performed with each participant to provide full understanding of the protocol prior to giving consent.

Safety of using treadmill/cycle ergometer

- Researcher will ensure that all risk assessments and H&S requirements are in place prior to performing any experimentation.
- Trial runs with each participant will be carried out explaining safe ways of lifting the feet off the treadmill i.e. using both hands/arms and lifting the feet from the revolving surface. Only when the participant is completely comfortable with the technique then experimentation can begin.

3. Information about Participants

3.1 How many participants will be involved?

85-200

3.1a What is the age group and gender of the participants?

18-40, male and female.

3.1b Explain how the sample size has been determined. If statistical sampling is relevant to this application, please include details of how the sample size was calculated.

No formal power study has been carried out to estimate the sample size, as this is considered preliminary work and may serve to inform the design of future studies and/or technology.

Instead, the sample size has been estimated based on knowledge from previous similar studies, and on pre-determined table of cumulative distribution function which are designed to aid selection of appropriate sample sizes for hypothesis tests.

3.1c Please specify inclusion and exclusion criteria. If exclusion of participants is made on the basis of age, gender, ethnicity, race, disability, sexuality, religion or any other factor, please justify this.

Inclusion Criteria

In order to be eligible for inclusion in the study the participants must meet the following criteria:

- Adult volunteers aged between 18–40 years who can give informed consent.
- Adult volunteers who are not taking any type of medication.
- Adult volunteers who do not suffer from any existing medical condition, including any heart condition, vascular or arterial disease, arthritis, lung disease, diabetes, Epilepsy, anaemia or thyroid disease.
- Adult volunteers with good balance and upper body strength to handle performing exercises and using a treadmill/bicycle ergometer.
- Adult volunteers who have not used recreational drugs during the last month.
- Adult volunteers who do not excessively consume alcohol (more than 14 units per week), and preferably do not smoke.
- Adult volunteers who have not used stimulating supplements, both natural or synthetic, at least 48 hrs prior to taking part in the study.
- Potential participants will only be enrolled if they have a good understanding of spoken English.

Exclusion Criteria

A set of criteria that determine whether the patient is ineligible to participate in the study. These include:

- Any inclusion criteria not met.
- Persons who decline consent.
- Persons who cannot give consent.
- Persons with acute illness/cold on the day of the study.
- Participation in drug trials/studies in the last 6 months.

3.2 How are the participants to be identified, approached and recruited, and by whom?

Advertisement in the form of a poster which will be affixed around the University premises, and emails, with the advertisement attached, will be sent to City staff and students from our contact list (not using any official City lists), asking them to contact the investigator(s) if they are interested in participating in the study and if they wish to be contacted in the future with similar adverts. The latter will be used to build a list of contacts that can be used in future volunteer studies.

Students and official City group lists e.g. All Staff list, will not be used unless permission is granted from the Dean of each school.

3.3 Describe the procedure that will be used when seeking and obtaining consent, including when consent will be obtained. Include details of (a) who will obtain the consent, (b) how you are intending to arrange for a copy of the signed consent form to be given to the participants, (c) when they will receive the participant information sheet, and (d) how long the participants have between receiving information about the study and giving consent.

Volunteers will be identified following an expression of interest on seeing a poster/email regarding the study. A participant information sheet will be provided, explaining exactly the aims and objectives of the study, and, if they agree to take part, exactly what the experimental procedure will involve. All potential participants will be given at least 24 hours to think whether to take part or to consult relatives, etc.

Volunteers will be clearly informed that participation in the study is voluntary and that refusal to participate will not affect their role, study etc within the University.

Participants will be provided with a full explanation of the nature, purpose and requirements of the study including Participant Information Sheet and Informed Consent Form.

The participant will then be asked to sign the consent form. Before starting the study, trial runs will be carried out using the exercise equipment (treadmill/bicycle ergometer) and the Borg scale. The researcher will explain best ways to lift one’s feet off the equipment i.e.

using both hands/arms and lifting the feet from the revolving surface. The investigators will continue with the study only when satisfied that the participant has understood the information sheet, the experimental procedure, and that they understand that it is their right to withdraw from the study at any time without the need to explain their reason for doing so and without any prejudice for future treatment.

No participants will be recruited if they lack capacity and if it is deemed that capacity is lost during the trial period then the participant will be removed from the trial and all information relating to them will be destroyed.

If the volunteer agrees to take part and signs a consent form, they will be recruited to the study.

3.4 How will the participant's physical and mental suitability for participation be assessed? Are there any issues related to the ability of participants to give informed consent themselves or are you relying on gatekeepers on their behalf?

Participants will complete a medical questionnaire to prior to commencement of the study. The questionnaire will cover basic questions about the general health of the participant and ensure that they do not suffer from any of the conditions outlined in the study criteria. volunteers who are deemed physically unsuitable (see exclusion criteria in section 3.1), will not proceed with the study.

Participants will need to be able to read the information sheet by themselves. They must show the ability to give informed consent by themselves without any gatekeeper on their behalf.

3.5 Are there any special pressures that may make it difficult for participants to refuse to take part in the study? Are any of the potential participants in a dependent relationship with any of the investigators (for instance student, colleague or employee) particularly those involved in recruiting for or conducting the project?

Students or colleagues will have complete freedom to withdrawn from the study at any time with absolutely no direct or indirect pressure put upon them.

3.6 Will the participant's doctor be notified? **YES ☐ NO ☒**
(If so, provide a sample letter to the subject's GP.)

3.7 What procedures are in place for the appropriate referral of a study participant who discloses an emotional, psychological, health, education or other issue during the course of the research or is identified by the researcher to have such a need?

In the case of a study participant disclosing emotional, psychological, health, education or other issues during the course of the research then they will be advised to visit their GP.

A trained first aider will be present in the Research Centre for Biomedical Engineering (RCBE) at all times during the study, who will deal with any adverse health issues, and ensure that the participant is referred to the appropriate service.

3.8 Is there any risk (emotional, psychological, health or other issues) to the researcher(s)?

No.

3.9 What steps will be taken to safeguard the participants from over-research (i.e. to ensure that the participants are not being used in multiple research projects including those of other researchers)? Please consider all research projects whatever their field, not just those performed by you.

Participants will be asked whether they are taking part in any other research (or whether they have recently taken part in any other research) and may be excluded if over-research is considered detrimental to the participant of or to the study.

3.10 Where will the research take place?

The study will take place in the Physiological Measurement room of the Biomedical Engineering Laboratory at City, University of London.

3.11 What health and safety issues, if any, are there to consider?

Risk of using exercise equipment i.e. treadmill or bicycle ergometer

Volunteers will be required to perform exercises of varying intense and this can cause pain or discomfort from cramps. There is also risk of injury by falling off the exercise equipment. To minimise this risk

- Equipment will be inspected prior to use to ensure that all mechanical parts are intact and functioning.
- Regular maintenance of the equipment, including electrical safety testing will be kept.
- Persons unfamiliar with the equipment will be supervised by trained staff.
- All users will be checked for suitable footwear (no flipflops, high heels or trailing laces), and to ensure that there is no loose or trailing clothing which could become caught in the treadmill belt or other moving parts.

Risk of donating blood via venous blood sample

To prevent discomfort or bruising, sample withdraw will be performed by a trained qualified professional, and even after signing the consent form, volunteers will have the right to withdraw from giving a blood sample if they feel uncomfortable/nervous.

Moreover, sterile needles and syringes shall be used to eliminate the risk of infection and the volunteer will not be in contact with any other bloods.

Risk of light application to skin

All the optical modalities do not cause overheating of the tissue for the limited time of their application on the skin. Furthermore, the light sources used do not emit sufficient power as to cause any tissue damage.

Risk of electric shock

All the commercial devices are CE marked meeting the requirements of European Regulations for Medical Devices. Custom-made optical sensors and instrumentations will be electrically safe as they will involve no direct electrical contact with the volunteer. Custom-made ECG and temperature sensors will be battery operated or run through an isolation transformer.

Risk of Infection from re-using non-invasive sensors

Some of the non-invasive sensors that will be used have disposable attachments e.g. temperature sensor and ECG electrodes, which reduces the risk of infection.

The remainder of sensors will be cleaned with alcohol wipes after each use.

Risks of handling blood samples

- Infection: All researchers undertaken investigations on blood samples will:
- Have received vaccinations against Hep B, and are up to date with their routine immunisations: tetanus, polio, diphtheria, measles, mumps and rubella.
- Wear protective clothing, disposable gloves, safety goggles and facemask.
- Will maintain the area in a safe and sterile state.

- Will not allow any other person into the bloods area while bloods or unsterile containers etc are exposed.

Risk to other staff or persons within the University

- Infection: Blood samples will be analysed as soon as they are collected, and will not be stored for future analysis. Bloods and needles will be disposed of correctly in dedicated bins and collected for disposal by a qualified company.
- Injury: Syringes and other sharp items will be locked away so they cannot be accessed by unauthorised persons.

3.12 How have you addressed the health and safety concerns of the participants, researchers and any other people impacted by this study? (This includes research involving going into participants' homes.)

Health and safety issues are described in section 3.11. For this research, there will be no need to visit the participants at their home.

3.13 It is a requirement that at least an initial assessment of risk be undertaken for all research and if necessary a more detailed risk assessment be carried out. Has a risk assessment been undertaken?* **YES ☒ NO ☐**

Please contact the Health & Safety Office (safetyoffice@city.ac.uk) for advice on risk assessments and/or how to complete it.

3.14 Are you offering any incentives or rewards for participating? **YES ☐ NO ☒**
If yes please give details

3.15 Does the research involve any of the following:

Children under the age of 5 years	**YES ☐ NO ☒**
Clinical trials / intervention testing?	**YES ☐ NO ☒**
Over 500 participants?	**YES ☐ NO ☒**
Are you specifically recruiting pregnant women	**YES ☐ NO ☒**
Excluding information collected via questionnaires (either paper based or online), is any part of the research taking place outside of the UK?	**YES ☐ NO ☒**

If you have answered 'yes' to any of the above questions you will need to check that the City's insurance will cover your research. You should do this by submitting this application to insurance@city.ac.uk before applying for ethics approval.

*Note that it is the Committee's prerogative to ask to view risk assessments.

4. Vulnerable Groups

4.1 Will persons from any of the following groups be participating in the study? (If not go to section 5.)

Adults without capacity to consent	☐
Children under the age of 18	☐
Those with learning disabilities	☐
Prisoners	☐
Vulnerable adults	☐
Young offenders (16-21 years)	☐
Those who would be considered to have a particular dependent relationship with the investigator (e.g. those in care homes, students, employees, colleagues)	☒

4.2 Will you be recruiting or have direct contact with any children under the age of 18? **YES ☐ NO ☒**

4.2a If yes, please give details of the child protection procedures you propose to adopt should there be any evidence of or suspicion of harm (physical, emotional or sexual) to a young person. Include a referral protocol identifying what to do and who should be contacted.

n/a

4.2b Please give details of how you propose to ensure the well-being of the young person, particularly with respect to ensuring that they do not feel pressured to take part in the research and that they are free to withdraw from the study without any prejudice to themselves at any time.

n/a

4.3 Will you be recruiting or have direct contact with vulnerable adults? YES ☐ NO ☒

4.3a If yes, please give details of the protection procedures you propose to adopt should there be any evidence of or suspicion of harm (physical, emotional or sexual) to a vulnerable adult. Include a referral protocol, identifying what to do and who should be contacted.

n/a

4.3b Please give details of how you propose to ensure the well-being of vulnerable adults, particularly with respect to ensuring that they do not feel pressured to take part in the research and that they are free to withdraw from the study without any prejudice to themselves at anytime. You should indicate how you intend to ascertain that person's views and wishes.

n/a

4.3c Please give details of any City staff or students who will have contact with vulnerable adults and/or will have contact with young people (under the age of 18) and details of current (within the last 3 years) City Disclosure and Barring check.

Name	*Dept & School*	*Student/Staff Number*	*Date of DBS*	*Type of disclosure*

4.3d Please give details of any non-City staff or students who will have contact with vulnerable adults and/or will have contact with young people (under the age of 18) and details of current (within the last 3 years) Disclosure and Barring check.

Name	*Institution*	*Address of organisation that requested the disclosure*	*Date of DBS*	*Type of disclosure*

4.4 Will you be recruiting any participants who fall under the Mental Capacity Act 2005? YES ☐ NO ☒

If so you MUST get approval from an HRA approved committee (see separate guidelines for more information).

5. Data Collection

5.1 Please indicate which of the following you will be using to collect your data

Please tick all that apply

Questionnaire	☒
Interviews	☐
Participant observation	☐
Focus groups	☐
Audio/digital-recording interviewees or events	☐
Video recording	☐
Physiological measurements	☒
Digital/computer data	☐
Other	☐
Please give details if you have ticked other	

5.1b What steps, if any, will be taken to safeguard the confidentiality of the participants (including companies)?

Data will be saved and categorized as “subject 1” to “subject n”. The questionnaires and consent forms will be placed in a file and locked in the Biomedical Engineering Laboratory.

If you are using interviews or focus groups, please attach a topic guide. If you are using questionnaire, please attach the questionnaire.

6. Confidentiality and Data Handling

6.1 Will the research involve:

• **complete anonymity of participants** (i.e. researchers will not meet, or know the identity of participants, as participants are a part of a random sample and are required to return responses with no form of personal identification)**?**	☐
• **anonymised sample or data** (i.e. an *irreversible* process whereby identifiers are removed from data and replaced by a code, with no record retained of how the code relates to the identifiers. It is then impossible to identify the individual to whom the sample of information relates)**?**	☐
• **de-identified samples or data** (i.e. a *reversible* process whereby identifiers are replaced by a code, to which the researcher retains the key, in a secure location)?	☒
• **subjects being referred to by pseudonym in any publication arising from the research?**	☐
• **any other method of protecting the privacy of participants?** (e.g. use of direct quotes with specific permission only; use of real name with specific, written permission only)	☐
Please give details of ‘any other method of protecting the privacy of participants’ is used	

6.1a Which of the following methods of assuring confidentiality of data will be implemented?
Please tick all the options that apply

• data to be kept in a locked filing cabinet	☒
• data and identifiers to be kept in separate, locked filing cabinets	☐
• access to computer files to be available by password only	☒
• storage at City	☐
• stored on an encrypted device (e.g. laptop, hard drive, USB)	☐
• stored at other site	☐
If stored at another site, please give details.	

6.1b Will the data be accessed by people other than the named researcher?

YES ☒ NO ☐

If yes, please explain by whom and for what purpose.

The data may also be accessed by researchers within the School of Mathematics, Computer Science and Engineering (MCSE) at City, and possibly future collaborators with expertise in data analysis and statistics. However, the researchers will access the data which has been de-identified, and will not be given access to the file which identifies the volunteers.

6.2 Is the data intended for reuse or to be shared as part of longitudinal research, or a different/wider research project now, or in the future? YES ☒ NO ☐

If yes, please provide details.

It is the aim of the researchers working on this project to continuously pursue developments in *in vivo* sensing of haemodynamic parameters. Therefore, although there aren't any immediate plans to reuse the data, it is possible that the data will be used in future research relating to this work and/or to seek funding.

6.2a If the project is funded, does the funding body (e.g. ESRC) require that the data be stored and made available for reuse/sharing? YES ☐ NO ☒

6.2b If you have responded yes to any of the questions above, explain how you are intending to obtain explicit consent for the reuse and/or sharing of the data.

n/a

6.3 Retention and Destruction of Data

6.3a Does the funding body or your professional organisation/affiliation place obligations or recommendations on the retention and destruction of research data? YES ☐ NO ☒

If yes, what are your affiliations/funding and what are the requirements? (If no, please specify City guidelines on retention.)

n/a

6.3b How long are you intending to keep the data?

Note that the institutional guidelines on retention state a minimum of 10 years.

10 yrs.

6.3c How are you intending to destroy the data after this period?

Please find guidance here.

Paper records will be formally shredded and all electronically archived data will be erased.

7. Curriculum Vitae

CV OF APPLICANTS (**Please duplicate this page for each applicant, including external persons and students involved.)**

NAME:	Professor Panicos Kyriacou
Title of Post:	Professor of Biomedical Engineering
Department:	SMCSE
Is your post funded for the duration of this proposal?	Yes
Funding source (if not City)	n/a
Please give a summary of your training/experience that is relevant to this research project	

Prof Kyriacou received a BESc degree in Electrical Engineering from the Engineering Department of the University of Western Ontario, Canada in 1994 and an MSc degree in Medical Electronics and Physics from St. Bartholomew's Medical College, University of London in 1995. During 1995 -1996 Prof Kyriacou worked as a Senior Biomedical Engineer and application specialist in the medical devices industry. He received his PhD from St. Bartholomew's Medical College, University of London in 2001 where he engaged in research in the field of medical instrumentation and electro-optical sensors for monitoring critically ill patients. He is currently a Professor of Biomedical Engineering and Associate Dean for Postgraduate studies at the School of Engineering and Mathematical Sciences at City University London. He is also the Director of the undergraduate programme in Biomedical Engineering and Director of the Biomedical Engineering Research Group. Prof Kyriacou is an Honorary Professor in the Department of Anaesthesia at St. Andrews Centre for Plastic Surgery and Burns, Broomfield Hospital, Mid Essex Hospital Services NHS Trust. He is also an Honorary Senior Research Fellow at Great Ormond Street Hospital for Children and St. Bartholomew's Hospital and a Visiting Research Fellow at Yale Medical School, Yale University. Professor Kyriacou' s main research activities are primarily focused upon the understanding, development and applications of instrumentation, sensors and physiological measurement to facilitate the prognosis, diagnosis and treatment of disease or the rehabilitation of patients. His research pushes the frontiers of current optical and electronic technologies and demonstrates how such technologies can be used as medical "tools".

His research is nationally and internationally recognised and this is evident by the number of organisations he is collaborating with and also from the wide spread of high impact factor scientific and clinical journals that he has published. He has authored and co-authored over 100 publications in peer reviewed journals, invited chapters in books and conference proceedings. He is also the holder of five patents with inventions in the area of Biomedical Instrumentation and Optical Biomedical Sensors. He is currently the Principle Investigator (PI) of more than nine research projects and has attracted funding from a variety of sources such as research councils, charities, NHS, and industry. Prof Kyriacou is the Chairman of the Instrument Science and Technology Group at the Institute of Physics and the Chair of the Engineering Advisory Group at the Institute of Physics and Engineering in Medicine. He is also a member of the Healthcare Science Advisory Group at NHS London.

NAME:	Dr Gerrard Rafferty
Title of Post:	Reader in Human & Translational Physiology
Department:	King's College London
Is your post funded for the duration of this proposal?	Yes
Funding source (if not City)	N/A
Please give a summary of your training/experience that is relevant to this research project	

Dr Gerrard Rafferty – Reader in Human & Translational Physiology at King's College London. He is based in the Respiratory Muscle Laboratory in the Centre for Human and Applied Physiological Sciences on the Denmark Hill Campus (King's College Hospital). Dr Rafferty received a BSc in Physiology from the University of Leeds in 1989 and subsequently gained his PhD in King's College London (University of London) in 1994 in the field of respiratory control in healthy humans. He continued his research in respiratory control while working at the Defence Research Agency, Centre for Human Sciences, (Institute of Aviation Medicine) Farnborough prior to returning to King's College London as a Non-Clinical Lecturer in Clinical Physiology in 1995 with promotion to Senior Lecturer in 2005 and Reader in 2016.

His primary research interests are respiratory and musculoskeletal physiology with a specific interest in respiratory and peripheral muscle physiology in infants, children and adults in both health and disease. Dr Rafferty has substantial experience of basic, mechanistic and applied research, both in healthy human subjects and patients with acute illness and chronic disease. Working at the interface between basic and clinical physiological research, much of his work has been translational, involving the development and further refinement of physiological measurement techniques to allow understanding of basic physiological processes and the effect of disease pathology and treatment interventions. Dr Rafferty's research is nationally and internationally recognised, and he has published over 150 articles in high impact factor, peer reviewed scientific and clinical journals and invited chapters in books. His research has attracted funding from the Wellcome Trust, research charities, NHS, and industry and is member of a number of learned and professional societies.

NAME:	Dr Meha Qassem
Title of Post:	Postdoctoral Research Associate
Department:	SMCSE
Is your post funded for the duration of this proposal?	Yes
Funding source (if not City)	EPSRC
Please give a summary of your training/experience that is relevant to this research project	

Dr Meha Qassem graduated with a BEng degree in Biomedical Engineering from City University in 2008, then went on to complete her PhD 2010 at City University, after working as a medical engineer for two years. During her PhD, she worked extensively in the areas of optical spectroscopy, spectral analysis and optical sensing. She had successfully completed multiple studies on animal and human skin, looking at the properties of skin and the effect of certain applicants on skin parameters using NIR spectroscopy. Her work has been published in several conferences and internationally recognised peer-reviewed journals. She is currently working as a postdoctoral researcher in the Research Centre for Biomedical Engineering (RCBE) at City, University of London.

NAME:	Dr. Karthik Budidha
Title of Post:	Postdoctoral Research Associate
Department:	SMCSE
Is your post funded for the duration of this proposal?	Yes
Funding source (if not City)	EPSRC
Please give a summary of your training/experience that is relevant to this research project	

Dr Karthik Budidha first came to City, University of London in 2006 to pursue his undergraduate degree (BEng) in Biomedical Engineering. Following his undergraduate degree, he acquired an MSc in biomedical engineering from Imperial College London in 2010. He then worked as a Biomedical Engineer in Hillingdon hospital for a year before returning to the Research Centre for Biomedical Engineering (RCBE), at City, University of London in 2011 to pursue his PhD. During his PhD he developed a novel In-ear oximeter to monitor arterial oxygen saturation and heart rate in patients with compromised peripheral perfusion. Dr Budidha's primary interests lie in the design of novel wearable non-invasive sensors, and development of bio-electronic instrumentation to continuously monitor physiological and behavioural variables. Being named the primary researcher in the Wellcome Trust's Pathfinder Award, he is currently working towards the development of a novel intra-luminal sensor for monitoring intestinal viability in colorectal cancer surgery.

NAME:	Dr Mohammad Hossein Mamouei
Title of Post:	Postdoctoral Research Associate
Department:	SMCSE
Is your post funded for the duration of this proposal?	Yes
Funding source (if not City)	EPSRC
Please give a summary of your training/experience that is relevant to this research project	
Dr Mohammad Mamouei graduated with a BSc in Electrical Engineering from Iran University of Science and Technology. He then went on to complete an MSc in Telecommunications and Networks from City, University of London. In 2013, he was awarded a full scholarship to start his PhD studies on applied Mathematics-Systems and Modelling at City, University of London. During his PhD, the focus of his work was on the applications of advanced mathematics, data analysis, and machine learning techniques on the control of semi- and fully automated vehicles. Dr Mamouei has recently joined the Research Centre for Biomedical Engineering at City, University of London as a postdoctoral researcher in data science.	

NAME:	Miss Nystha Baishya
Title of Post:	PhD Student
Department:	SMCSE
Is your post funded for the duration of this proposal?	Yes
Funding source (if not City)	
Please give a summary of your training/experience that is relevant to this research project	
Nystha obtained her Bachelor of Engineering in Mechatronics at Manipal Institute of Technology, India in 2012. She then went to Italy to continue her studies at Politecnico di Milano where she received her Master of Science in Materials Engineering & Nanotechnology. She then went back to India and worked in Indian Institute of Technology Guwahati for a year in the field of Organic Electronics in bio-sensing applications. Since October 2017, she has been enrolled for a full time PhD at the Research Centre for Biomedical Engineering at City, University of London. Her research focuses on Spectroscopic studies for monitoring parameters in haemodynamic shock.	

NAME:	Mr Chadi El-Hajj
Title of Post:	PhD Student
Department:	SMCSE
Is your post funded for the duration of this proposal?	Yes
Funding source (if not City)	
Please give a summary of your training/experience that is relevant to this research project	
Chadi El Hajj graduated with a degree in Computer Science from the American University of Beirut in 2013. He worked as a software developer for a few years in different sectors as such web development, online publishing systems and banking. Recently, he completed his MSc. in Data Science at City, University of London. During his studies he worked on various projects involving Artificial Intelligence and machine learning techniques for a variety of tasks. His MSc. research project was focused on neural networks, where he worked on extending a neural network model to improve its accuracy/precision and provide solutions for new	

domains. He is starting his PhD in Feb 2018 in the Research Centre for Biomedical Engineering at City, University of London. In his PhD he will be working on developing a novel non-invasive sensor by applying neural networks for continuous monitoring for patients in haemodynamic shocks.

8.1 Supervisor's statement on the student's skills and ability to carry out the proposed research, as well as the merits of the research topic (up to 500 words)

n/a

I confirm that I have discussed the project with the student to my satisfaction.	
Supervisor's Signature	
Print Name	

8. Additional documents

You are expected to provide copies of relevant documents including all letters to be sent to participants and other individuals (such as GPs) and organisations involved in the research. Please follow the guidelines and templates which can be found at http://www.city.ac.uk/research/research-and-enterprise/research-ethics

Document Checklist		
Please place an 'X' in all appropriate spaces for all documents you are submitting		
	Attached	**Not applicable**
Copy of study advertisement (including recruitment emails/letters)	**X**	
Participant information sheet	**X**	
Participant consent form	**X**	
Questionnaire(s)	**X**	
Topic guide(s)		
Confirmation letter(s) from / correspondence with external organisations		
Confirmation that insurance is in place		
Product information		
GP Letter		
Other (please provide details)		

9. Additional Information

10. Declarations by Investigator(s)

- I certify that to the best of my knowledge the information given above, together with any accompanying information, is complete and correct.
- I have read City's guidelines on human research ethics, and accept the responsibility for the conduct of the procedures set out in the attached application.
- I have attempted to identify all risks related to the research that may arise in conducting the project.
- I understand that **no** research work involving human participants or data can commence until **full** ethical approval has been given

	Print Name	Signature
Principal Investigator(s) (student and supervisor if student project)	Prof Panayiotis Kyriacou	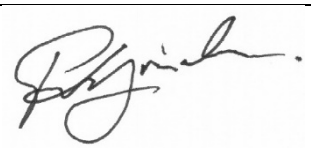
Principal Investigator(s) (student and supervisor if student project)	Dr Meha Qassem	
Associate Dean for Research (or equivalent) or authorised signatory	Prof Chris Atkin	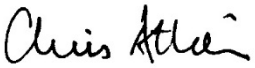
Date	23/11/2018	